Functional and structural characterizationof LysM proteins in interactions between fungi and plants

Hui Tian

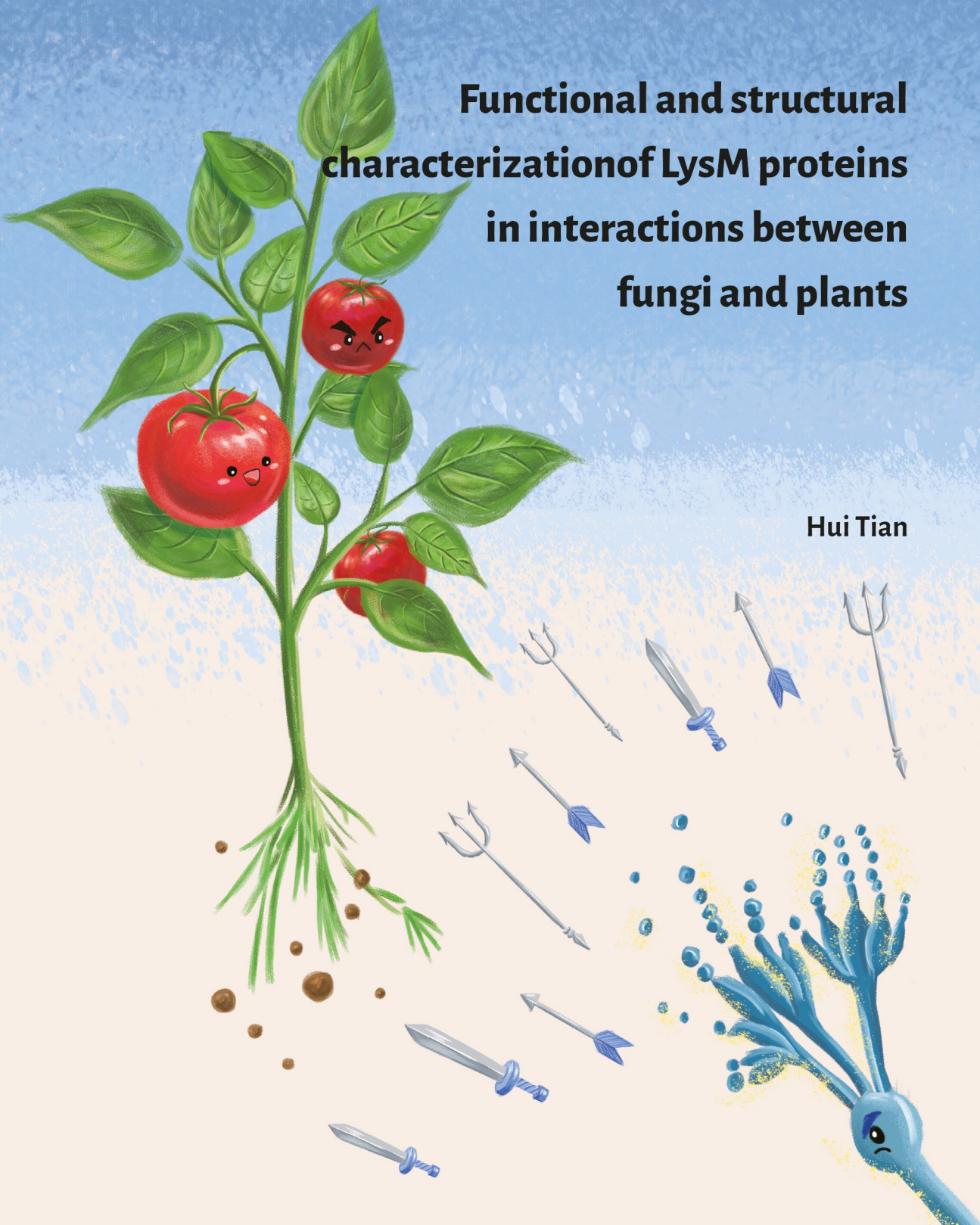

Propositions

1. Plant-associated fungi employ lysin motif effectors to perturb host chitin receptor complexes.
   (this thesis)

2. Fungal effectors composed of two lysin motifs bind chitin through intermolecular dimerization.
   (this thesis)

3. Nature can deal with any human footprint.

4. Genetic modification will be used to restore human genetic disorders in future.

5. Quasi-scientific opinions of public figures greatly damage trust of the general public in science.

6. Performing a PhD project is like selecting a partner for life, one has to compromise between security and adventure.

7. Although our understanding of life on earth is rapidly increasing, we may still go extinct because of a simple microbe.

Propositions belonging to the thesis, entitled
Functional and structural characterization of LysM proteins in interactions between fungi and plants
Hui Tian
Wageningen, 14 September, 2020

Functional and structural characterization of LysM proteins in interactions between fungi and plants

Hui Tian

Thesis committee

Promotor
Prof. Dr Bart P.H.J. Thomma
Professor of Phytopathology
Wageningen University & Research

Co-promotor
Dr Jeroen R. Mesters
Senior Researcher in Institut für Biochemie
Universität zu Lübeck, DE

Other members
Prof. Dr Mark J. Banfield, John Innes Centre (JIC, UK)
Prof. Dr Vivianne G.A.A. Vleeshouwers, Wageningen University & Research
Prof. Dr Bas J. Zwaan, Wageningen University & Research
Dr Erik H.M. Limpens, Wageningen University & Research

This research was conducted under the auspices of the Graduate School of Experimental Plant Science

Functional and structural characterization of LysM proteins in interactions between fungi and plants

Hui Tian

Thesis
submitted in fulfilment of the requirement for the degree of doctor
at Wageningen University
by the authorship of the Rector Magnificus,
Prof. Dr A.P.J. Mol
in the presence of the
Thesis Committee appointed by the Academic Board
to be defended in public
on Monday 14 September 2020
at 4 p.m. in the Aula.

Hui Tian
Functional and structural characterization of LysM proteins in interactions between fungi and plants, 170 pages.

PhD thesis, Wageningen University, Wageningen, the Netherlands (2020)
With references, with summary in English

DOI: https://doi.org/10.18174/525407
ISBN: 978-94-6395-442-6

TABLE OF CONTENTS

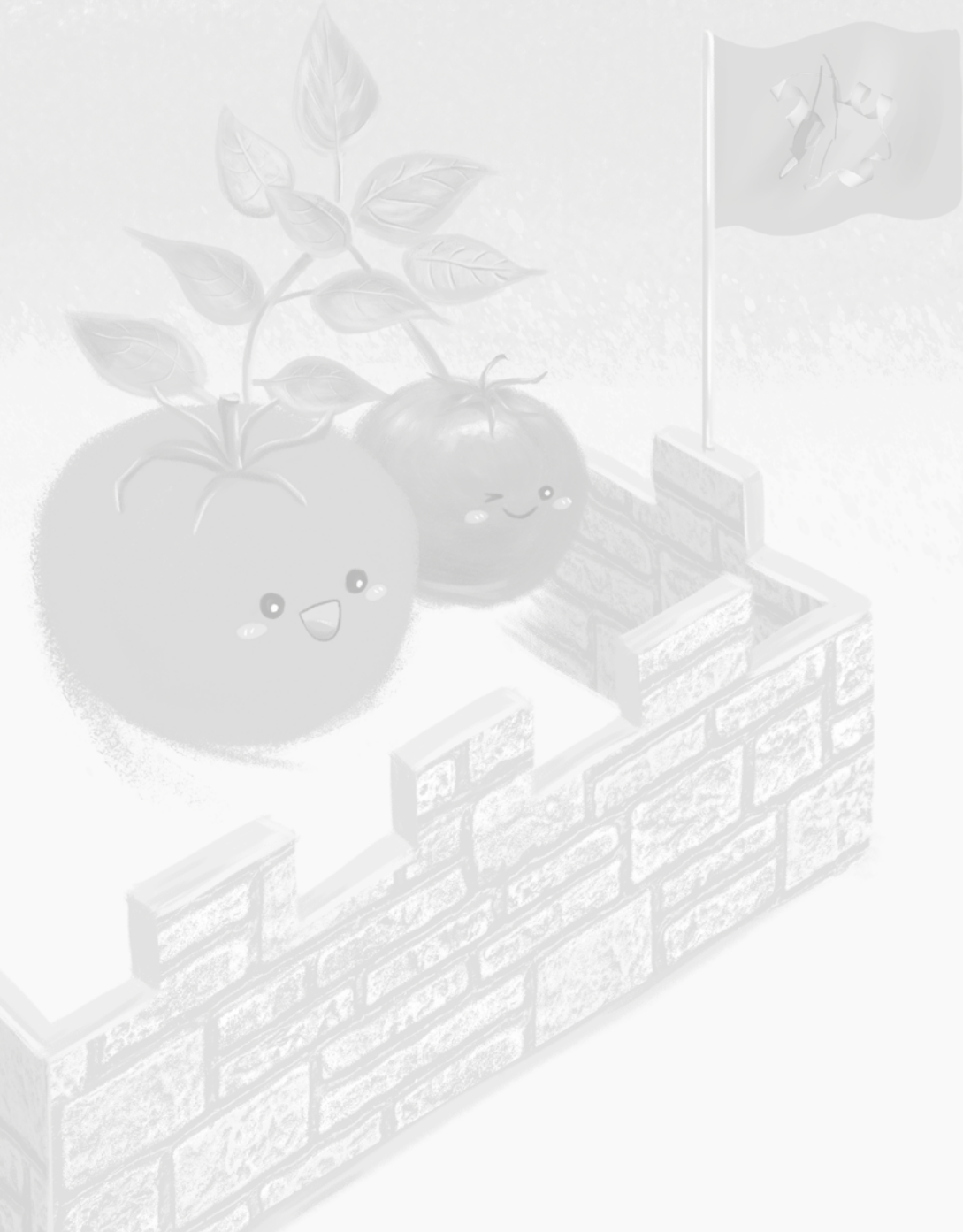

Chapter 1

General introduction

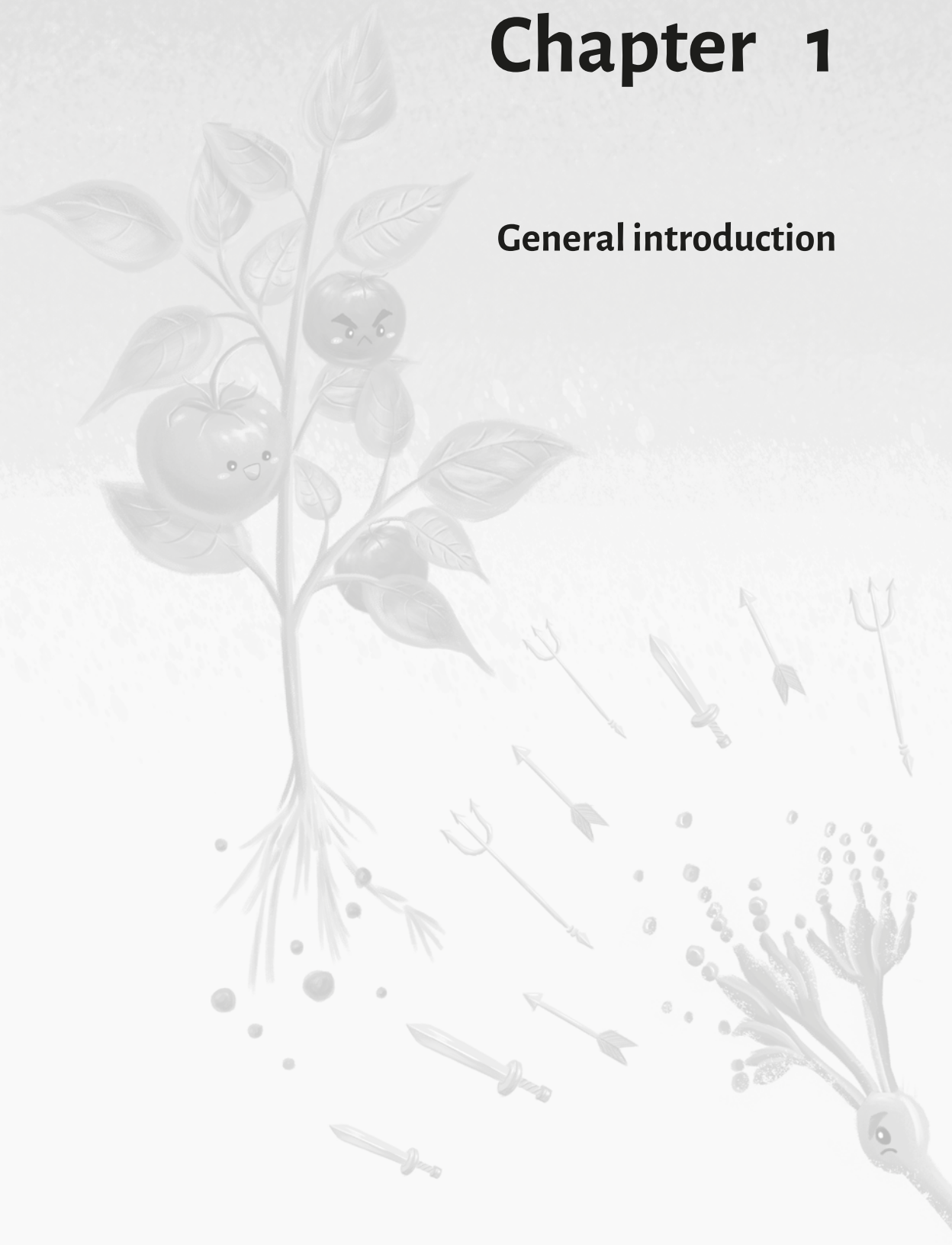

Plants are extremely important for all lifes on our planet. Not only because they generate a considerable part of the oxygen that is essential for life of aerobic organisms, but also because they form the basis of our food chain. Thus, mankind has relied on plants since its existence, and has developed the practice to cultivate plant species as agricultural crops for thousands of years. However, other organisms thrive on plants as their major food source too. Therefore, the yield of crops can be heavily reduced by biotic constraints such as pests, including insects and nematodes, and pathogenic microbes, including viruses, bacteria, fungi and oomycetes (Teng et al, 1984; Hammond-Kosack and Jones, 1996; Strange and Scott, 2005; Fisher et al., 2012). In extreme cases, epidemic disease outbreaks on major crops have led to severe economic losses and even to millions of deaths due to starvation. For instance, the Great French Wine Blight in the mid-19th century caused by the *Phylloxera* aphid resulted in an enormous economic loss since over 40% of French grape vines and vineyards were devastated over a period of 15 years. Another notorious example concerns the Irish potato famine of the 1840s caused by the oomycete *Phytophthora infestans* that led to the death of a million people while another million people immigrated to the USA (Bourke, 1964; Ristaino, 2002; Sorensen et al., 2008). Presently it is recognized that plant pathogens are still major threats for agricultural production and food security worldwide. For example, the rice blast disease caused by *Magnaporthe oryzae*, the wheat rust caused by *Puccinia graminis* and the soybean rust caused by *Phakospora pachyrizi* lead to huge yield losses annually (Strange and Scott, 2005; Pennisi, 2010; Fisher et al., 2012).

A widespread strategy to protect crop plants from diseases is the application of synthetic chemicals such as pesticides and fungicides. The extensive use of crop protection chemicals makes agricultural production largely dependent on these chemicals to secure yields (Damalas and Eleftherohorinos, 2011). Nonetheless, many of these chemicals have adverse effects on human health and on the environment. Additionally, pest and pathogen populations are often capable of evolving new genotypes that overcome the crop protection chemicals that are used (Hawkins et al., 2018). Therefore, alternatives that enable durable crop protection are needed that, besides for instance the use of bio-control and improved agronomic practices, concern the use of resistant crop varieties, in which resistance genes or quantitative trait loci (QTLs) are incorporated into a plant genotype with high yield potential (Carolan et al., 2017). To this end, more research is needed to understand resistance mechanisms of plants as well as mechanisms of microbial pathogenicity to provide novel strategies to breed resistant crop varieties.

The plant immune system

Plants possess an effective innate immune system to recognize microbial invasions (Jones and Dangl, 2006; Thomma et al., 2011; Cook et al., 2015). Microbe- and damage-associated molecular patterns (MAMPs and DAMPs, respectively) are recognized as invasion patterns by plant cell surface-localized pattern recognition receptors (PRRs) to activate so-called invasion pattern-triggered plant immunity (PTI) that includes a broad range of immune responses such as reactive oxygen species (ROS) production, ion fluxes, callose deposition and defence-related

gene expression (Jones and Dangl, 2006; Altenbach and Robatzek, 2007; Boller and Felix., 2009). To overcome PTI, successful microbes employ effectors to disarm immune responses. However, to re-establish host immunity, plants in turn evolved receptors to recognize such microbe-secreted effectors, often by nucleotide binding-leucine rich repeat (NB-LRR) type of intracellular receptors that are known as resistance (R) proteins. In response, microbes again evolved novel strategies to deregulate host immunity by either discarding or mutating recognized effectors, or evolving new ones to perturb the immune response that is activated upon effector recognition (Jones and Dangl, 2006). This co-evolutionary interaction between pathogens and their plant hosts is thought to continue in an ever-lasting arms race.

The Lysin motif (LysM)

The lysin motif (LysM; Pfam PF01476) was first identified in a *Bacillus* phage lysozyme that degrades peptidoglycan, a critical structural component of bacterial cell walls, through glycosidic bond hydrolysis (Garvey et al., 1986). A similar motif was characterized in the peptidoglycan hydrolase of *Enterococcus faecalis* (Béliveau et al., 1991) and various other prokaryotic proteins such as bacteriophage proteins, and bacterial lysins, peptidases, chitinases and nucleotidases (Buist et al., 1995; Buist et al., 2008). The LysM was characterized as a carbohydrate-binding protein module, recognizing polysaccharides containing *N*-acetylglucosamine (GlcNAc) homo- or heteropolymers. A LysM comprises 44 to 65 amino acid residues, displaying a βααβ secondary structure with the two α-helices packed onto the same side of the two β-sheets (Bateman and Bycroft, 2000; Bielnicki et al., 2006). Particularly the N-terminal 16 residues, but also the C-terminal 10 residues, are typically more conserved than the central part of a LysM (Buist et al., 2008; de Jonge and Thomma, 2009). If multiple LysMs are present in a single protein, a flexible region that often consists of Ser, Thr and Asp or Pro residues is found between the LysMs (Radutoiu et al., 2003; de Jonge and Thomma, 2009). In addition to prokaryotic proteins, LysM domains are found in eukaryotic organisms as well, including proteins from animals, plants and fungi (Buist et al., 2008).

LysM-containing receptors in plants

Plants detect microbe-derived molecular patterns, such as bacterial peptidoglycan and lipopolysaccharides, oomycete glucans, and fungal chitin, by deploying a broad range of PRRs (Ayers et al., 1976; Felix et al., 1993; Dow et al., 2000; Erbs et al., 2008; Boller and Felix, 2009; Gust et al., 2012; Mesnage et al., 2014; Tang et al., 2017). These PRRs can be further classified into receptor-like kinases (RLKs) and receptor-like proteins (RLPs) based on whether a kinase domain is coupled to their transmembrane domain or not, respectively (Altenbach and Robatzek, 2007; Gust et al., 2012). While the largest group of PRRs contain extracellular leucine-rich repeats, PRRs with extracellular LysMs have been characterized as well. LysM-containing receptor-like kinases (LysM-RLKs) are mostly composed of one to three extracellular LysMs, a single-pass transmembrane domain and an intracellular kinase domain and were first identified in legume

plants as receptors for nodulation (Nod) factors (Madsen et al., 2003; Gough, 2003). These factors are lipochitin oligosaccharide signal molecules secreted by Rhizobium bacteria to initiate a symbiosis with legume plants to develop nitrogen-fixing root nodules that accommodate the bacteria (Radutoiu et al., 2007). For example, in the model legume *Lotus japonicus*, the LysM receptors NFR1 and NFR5 form a protein complex that is essential for Nod factor recognition during the interaction with *Mesorhizobium loti* bacteria (Madsen et al., 2003; Radutoiu et al., 2003; Broghammer et al., 2012). Similarly, in *Medicago truncatula* the NFR5 ortholog MtNFP is responsible for symbiosis signal transduction by functioning together with the NFR1 ortholog MtLYK3 (Amor et al., 2003; Arrighi et al., 2006; Pietraszewska-Bogiel et al., 2013). Interestingly, LjNFR5 and MtNFP possess no active intracellular kinase domain, suggesting that LjNFR1 and MtLYK3 confer downstream signalling (Limpens et al., 2015).

In non-legume plants, LysM-containing receptors have been characterized to act in defence responses against pathogens. Fungal cell wall chitin is a long chain polymer of β-(1,4)-linked *N*-acetylglucosamine (GlcNAc) which is recognized by plant receptors containing extracellular LysM motifs (Sanchez-Vallet et al., 2015; Rovenich et al., 2016; Zipfel and Oldroyd, 2017). The genome of the model plant *Arabidopsis thaliana* (Arabidopsis) comprises five genes that encode LysM-receptor like kinases, *AtLYK1* to *AtLYK5*. Of these, AtLYK1, which is also known as AtCERK1, contains three LysMs and was found to be essential for chitin signalling as *AtCERK1* mutants are compromised in immune responses to chitin elicitation, such as reactive oxygen species (ROS) production and mitogen-activated protein kinase (MAPK) activation (Miya et al., 2007; Wan et al., 2008; Petutschnig et al., 2010; Liu et al., 2012b). However, despite initial claims that AtCERK1 is the chitin receptor of Arabidopsis (Miya et al., 2007; Petutschnig et al., 2010), AtLYK5 was proposed as primary chitin receptor since its chitin binding affinity is significantly higher than that of AtCERK1 (Cao et al., 2014). Upon chitin recognition, two AtLYK5 molecules form a homodimer that recruits two AtCERK1 molecules to form protein complex for chitin signal transduction (Fig. 1). Intriguingly, only a double mutant of *AtLYK4*/*AtLYK5* leads to fully abolished chitin-induced immunity, indicating partially overlapping functions between AtLYK4 and AtLYK5 (Wan et al., 2012; Cao et al., 2014). In fact, it has recently been shown that AtLYK4 functions as a AtLYK5-associated co-receptor protein, stablizing the assembled AtLYK5-AtCERK1 receptor complex and thus enhancing chitin-induced signaling in Arabidopsis (Xue et al., 2019). Additionally, a glycosylphosphatidylinositol (GPI)-anchored RLP, AtLYM2, was identified in the Arabidopsis proteome of plasmodesmata. This LysM-containing protein binds chitin oligosaccharides and mediates plasmodesmal fluxes between cells in the presence of chitin (Fernandez-Calvino et al., 2011; Shinya et al., 2012; Faulkner et al., 2013). Moreover, it was recently demonstrated that chitin-induced closure of plasmodesmata requires LYK4 and LYK5 in addition to LYM2, and chitin induces dynamic changes in the localization, association, and mobility of these receptors at distinct membrane domains (Cheval et al., 2020).

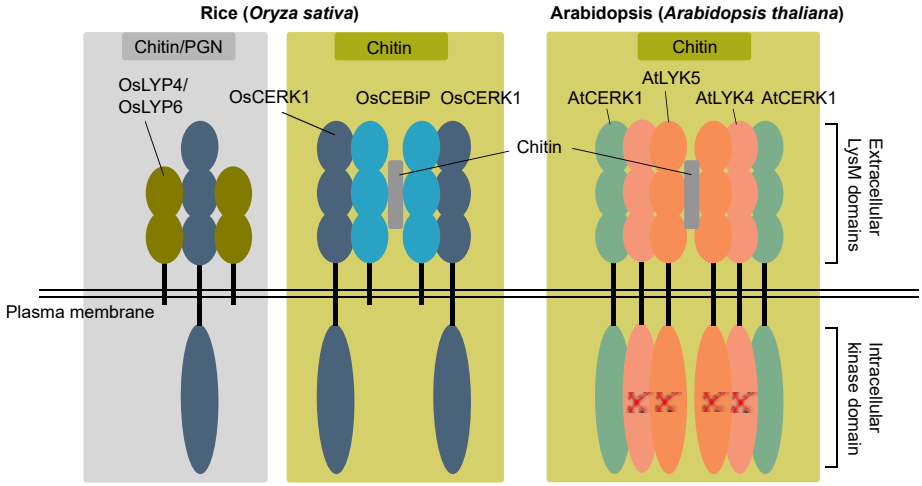

FIGURE 1 | Chitin perception systems in rice (*Oryza sativa*) and Arabidopsis (*Arabidopsis thaliana*). Rice OsCEBiP, which carries three extracellular LysM domains (M1-M3) and lacks a kinase domain, undergoes homodimerization upon chitin binding, followed by the recruitment of two OsCERK1 molecules that possess three extracellular LysM domains (M1-M3) and active kinase domains to form a receptor complex in a sandwich-like manner. In parallel, the two LysM-containing receptor-like proteins OsLYP4 and OsLYP6 function together with OsCERK1 to respond to chitin and PGN signals. In Arabidopsis two AtLYK5 monomers that carry three extracellular LysMs bind chitin and then form a tetrameric receptor complex by the recruitment of two AtCERK1 molecules that similarly carry three LysMs. All these Arabidopsis proteins carry intracellular kinase domains and red cross indicates an inactive kinase domain.

In contrast to Arabidopsis, in rice (*Oryza sativa*) the main chitin receptor is an RLP known as OsCEBiP, a GPI-anchored LysM-receptor-like protein with three extracellular LysM domains and a short membrane spanning domain (Kaku et al., 2006). OsCEBiP forms a tetrameric protein complex with the rice ortholog of AtCERK1, OsCERK1 (chitin elicitor receptor kinase 1), to initiate chitin immune signalling (Shimizu et al., 2010; Akamatsu et al., 2013; Hayafune et al., 2014) (Fig. 1). Two further LysM-RLPs, OsLYP4 and OsLYP6, have been implicated in chitin-induced rice immune responses as well (Fig. 1). Interestingly, by forming a ligand-induced protein complex with OsCERK1, these two receptor proteins furthermore respond to bacterial cell-wall peptidoglycan (PGN), suggesting a dual role of OsCERK1 as an adaptor protein in both chitin and PGN signaling (Liu et al., 2012a; Ao et al., 2014; Miyata et al., 2014).

Besides Arabidopsis and rice, no *bona fide* chitin receptors have yet been cloned from other plant species, although LysM receptors were implicated in chitin signaling in some species. For instance, in wheat (*Triticum* spp.), orthologs of AtCERK1 and OsCEBiP were implicated in arresting colonization by mutants of the fungal pathogen *Zymoseptoria tritici* that are no longer able to suppress chitin-triggered immunity and that are not pathogenic on wild-type wheat plants (Lee et al., 2014). In upland cotton (*Gossypium hirsutum*), the LysM-RLKs GhLYK1 and GhLYK2 are transcriptionally induced by chitin and contribute to resistance against the pathogenic fungus *Verticillium dahliae* (Gu et al., 2017). In tomato (*Solanum lycopersicum*), four LysM-RLKs with

relatively high identity to AtCERK1 were identified, namely SlLYK1, and SlLYK11 to SlLYK13 (Liao et al., 2018). While SlLYK12 was found to regulate arbuscular mycorrhizal (AM) symbiosis, SlLYK1 was implicated in chitin responses (Buendia et al., 2016; Liao et al., 2018).

LysM-containing effectors from plant pathogenic fungi

Chitinases secreted by plants aim to not only disrupt cell wall integrity but also liberate more chitin molecules from fungal cell walls for perception (Fig. 2A). To overcome plant immune responses activated by fungal cell wall chitin, successful pathogens evolved various strategies, such as chemical modification of cell wall chitin such that it is no longer recognized (Fujikawa et al., 2009; Fujikawa et al., 2012; Sanchez-Vallet et al., 2015; Rövenich et al., 2016; Gao et al., 2019) and the secretion of effector proteins to either protect fungal cell walls (van den Burg et al., 2006; Marshall et al., 2016) (Fig. 2C) or perturb the activation of chitin-triggered immunity (de Jonge et al., 2010; Mentlak et al., 2012; Takahara et al., 2016) (Fig. 2B). Among the effectors that target chitin-triggered immunity are so-called LysM effectors, fungal secreted proteins that contain no other annotated protein modules than LysM domains. These effectors are widely distributed in the fungal kingdom and occur in pathogenic and non-pathogenic fungi (de Jonge and Thomma, 2009). Previously, publicly available sequence data of 70 fungal species were investigated and 403 putatively secreted LysM-containing proteins were identified that could be grouped into five types, with the largest group comprising LysM effectors; a group of 302 proteins with one to seven LysMs (de Jonge and Thomma, 2009). Although the biological roles of the majority of these LysM effectors remain to be demonstrated, several of them have been functionally characterized in fungal symbionts of plants.

The LysM effector Ecp6 from *Cladosporium fulvum*

The biotrophic fungus *Cladosporium fulvum* is the causal agent of the tomato leaf mould disease. It secretes Ecp6 (extracellular protein 6), a LysM effector that carries three lysin motifs (LysMs). Ecp6 is a critical virulence factor since compromised expression in a silenced mutant led to significantly reduced disease symptoms in tomato when compared with the wild-type *C. fulvum* strain (Bolton et al., 2008). The mechanism underlying the virulence function of Ecp6 is that the effector protein has the ability to sequester fungal cell wall-derived chitin to disarm chitin-induced host immunity (Fig. 2B; de Jonge et al., 2010). A crystal structure of Ecp6 revealed that two of its three LysM domains, namely LysM1 and LysM3, undergo ligand-induced intermolecular dimerization, thus establishing a chitin binding groove with picomolar affinity. This affinity is sufficient to outcompete host receptors for chitin binding, as these bind chitin in the nanomolar range at best (Iizasa et al., 2010; Liu et al., 2012b; Cao et al., 2014). The remaining LysM domain of Ecp6 (LysM2) can also bind chitin, albeit with significantly lower (μM) affinity (Sanchez-Vallet et al., 2013). Because of this relatively low affinity, it is speculated that LysM2 suppresses chitin-triggered immunity through another mechanism than outcompeting host receptors for chitin binding (Sanchez-Vallet et al., 2013). However, it remains unclear whether this relatively low-affinity chitin binding site actually contributes to the virulence function of Ecp6 during host colonization by *C. fulvum*.

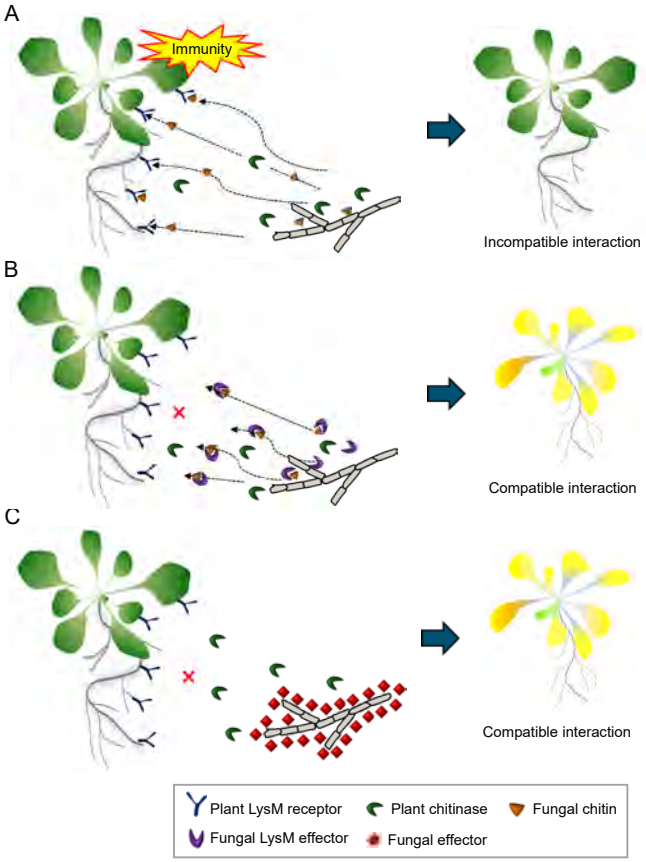

FIGURE 2 | Graphic representation of the interaction between plants and pathogenic fungi. (A) Plants secrete hydrolytic enzymes to target the fungal cell wall, including chitinases that hydrolyse fungal cell wall chitin. Released chitin molecules are recognized by plant lysin motif (LysM)-containing receptors that activate immunity to halt fungal invasion. (B) Some fungal pathogens were demonstrated to secrete LysM effectors to outcompete plant LysM receptors for chitin binding, thus preventing the activation of chitin-induced plant immunity, leading to a compatible interaction. (C) Furthermore, some fungal pathogens secrete effectors that bind to fungal cell walls to protect them, resulting in inaccessibility towards hydrolytic enzymes such as chitinases and glucanases.

LysM effectors from *Zymoseptoria tritici*

The hemibiotrophic fungus *Zymoseptoria tritici* (formerly *Mycosphaerella graminicola*) causes *Septoria tritici* blotch (STB) disease of wheat (Eyal, 1999). Upon infection, wheat plants display an extended period of symptomless host colonization, followed by the death of host tissues coincided by a rapid invasive growth and asexual reproduction of the fungus. Three LysM effector genes were identified in *Z. tritici*; *Mg1LysM* and *MgxLysM* encoding proteins with one LysM and *Mg3LysM* encoding an effector carrying three LysMs (Marshall et al., 2011). However, only Mg1LysM and Mg3LysM were believed to be transcriptionally induced during wheat infection, and both LysM effectors were shown to bind chitin. However, only Mg3LysM was found to be

able to suppress chitin-induced plant immune responses (Marshall et al., 2011). Surprisingly, and in contrast to *C. fulvum* Ecp6, both Mg1LysM and Mg3LysM were found to protect fungal hyphae against hydrolytic enzymes that plants secrete as a defence response against fungal invasion, including chitinases. The analysis of deletion strains suggested that Mg3LysM, but not Mg1LysM, is required for full virulence of *Z. tritici*, although the inability to demonstrate a contribution of Mg1LysM to virulence may be obscured by the redundancy in protection against hydrolytic activity with Mg3LysM (Marshall et al., 2011).

LysM effectors of various other plant-associated fungi

Various LysM effectors were identified from other plant pathogenic fungi as well, besides those from *C. fulvum* and *Z. tritici* described above. Slp1 (secreted LysM-protein 1) is a secreted effector protein carrying two LysMs from *Magnaporthe oryzae*. It binds chitin and competes with the rice chitin receptor OsCEBiP to suppresses chitin-triggered immune responses such as ROS production and expression of defence-related genes (Mentlak et al., 2012). Similarly, Elp1 and Elp2 of the Brassicaceae antracnose fungus *Colletotrichum higginsianum* that carry two LysM domains bind chitin and are able to suppress the activation chitin-triggered immunity in Arabidopsis (Takahara et al., 2016). *M. oryzae* Slp1, and *C. higginsianum* Elp1 and Elp2 do not protect hyphae from plant chitinases (Mentlak et al., 2012; Takahara et al., 2016). Vd2LysM is a lineage-specific effector with two LysM domains from the broad host-range vascular wilt fungus *Verticillium dahliae* that binds chitin with high affinity, suppresses chitin-triggered immunity and contributes to fungal virulence in tomato (Kombrink et al., 2017). Interestingly, like Mg1LysM and Mg3LysM, and unlike Ecp6, Slp1, Elp1 and Elp2, Vd2LysM additionally has the ability to protect fungal hyphae against chitinase hydrolysis (Kombrink et al., 2017). Also the first identified LysM effector from a Basidiomycete, namely RsLysM from *Rhizoctonia solani,* binds chitin and suppresses chitin-triggered immunity but cannot protect hyphae against hydrolysis (Dolfors et al., 2019).

Besides pathogenic fungi, mutualistic fungi employ LysM effectors as well. It was recently demonstrated that the AM fungus *Rhizophagus irregularis* secretes the LysM effector RiSLM to bind chitin and to interfere with chitin-induced immune responses during symbiosis established on the legume plant *M. truncatula* (Zeng et al., 2019). Like Mg1LysM, Mg3LysM and Vd2LysM, RiSLM protects hyphal growth against plant hydrolytic chitinases as well (Zeng et al., 2019). While it is anticipated that the ability to suppress chitin-triggered immunity is conferred by sufficiently high chitin-binding affinity of a LysM effector (de Jonge et al., 2010; Sanchez-Vallet et al., 2013), it is presently not yet understood what confers the capability to only some LysM effectors to protect fungal cell wall chitin to chitinase hydrolysis.

Thesis outline

Plants deploy cell surface-localized LysM-containing receptors to recognize fungal cell wall chitin to activate a broad range of immune responses. In turn, successful pathogenic fungi evolved various strategies to overcome chitin-triggered plant immunity, such as the secretion of LysM effectors to

disarm the activation of chitin-triggered immunity and to protect fungal cell walls. The aim of the studies described in this thesis is to functionally characterize LysM-containing proteins that act in the interaction of fungal pathogens with plant hosts to further our understanding of the LysM domain in immune responses that revolve around fungal cell wall chitin.

Arguably, the best characterized LysM effector is Ecp6 of the tomato pathogenic fungus *Cladosporium fulvum*. However, while the chitin perception system has been extensively studied in Arabidopsis and rice, chitin receptors from tomato (*Solanum lycopersicum*) remain to be identified. Previous research identified tomato chitin receptor candidates through a proteomic approach combined with gene silencing experiments. In **Chapter 2**, we describe tomato mutants for each of the previously identified chitin receptor candidates that were generated with CRISPR-Cas9 and the investigation of their sensitivity to chitin elicitation by testing ROS production and gene expression analysis, as well as their resistance against fungal infection.

It has previously been demonstrated that Ecp6 sequesters fungal cell wall-derived chitin molecules from plant receptors with picomolar affinity, because two of its three LysM domains (LysM1 and LysM3) undergo ligand-induced intermolecular dimerization, resulting in an ultrahigh-affinity substrate binding groove. The remaining LysM2 domain can bind chitin as well, albeit with a relatively low affinity. **Chapter 3** investigates whether this relatively low-affinity chitin binding site also contributes to the virulence function of Ecp6 or not, as well as the molecular mechanism underlying its activity.

Besides *C. fulvum*, various other pathogenic fungi employ LysM effectors to perturb chitin-induced host immunity. Despite the fact that *C. fulvum* Ecp6 contains three LysM domains, most other pathogens employ LysM effectors with two LysM motifs, such as *M. oryzae* Slp1, *C. higginsianum* Elp1 and Elp2 and *V. dahliae* Vd2LysM. **Chapter 4** describes our attempts to reveal the mechanism of chitin-binding by LysM effectors that are composed of two LysM domains via attempts to obtain crystals and a structure.

In the hemibiotrophic fungus *Z. tritici*, three LysM effector genes were identified, namely *Mg3LysM* encoding a protein containing three LysMs, *Mg1LysM* and *MgxLysM* encoding proteins with only one LysM motif. *MgxLysM* was reported not to be transcriptionally induced during wheat infection. However, more recent expression analysis revealed significant induction in *Z. tritici* during transition from the biotrophic to necrotrophic phase. In **Chapter 5**, we study the biological function of Mgx1LysM, renamed from MgxLysM, during the interaction of *Z. tritici* with wheat plants.

While *Z. tritici* Mg3LysM suppresses chitin-induced plant immunity, both Mg3LysM and Mg1LysM protect fungal hyphae against plant hydrolytic enzymes. **Chapter 6** investigates the mechanism underlying the protective role of Mg1LysM as a single LysM-containing effector through determination of a crystal structure in combination with biochemical and functional assays.

Finally, **Chapter 7** summarizes the major findings that are presented in this thesis and discusses the broader view of mechanisms employed by LysM-containing receptors and effectors during the interaction between pathogenic fungi and their host plants.

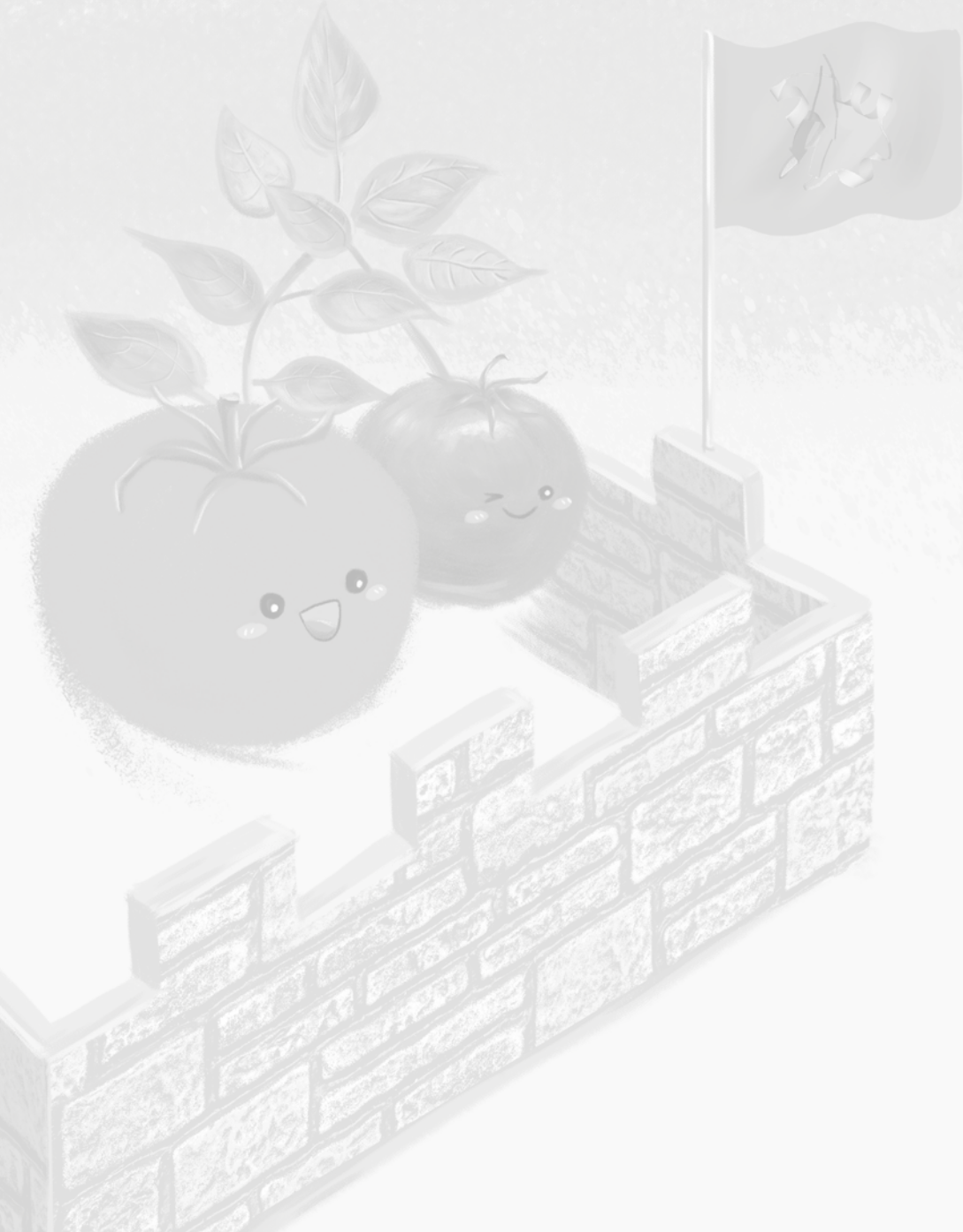

Chapter 2

Characterization of a LysM-containing receptor kinase that mediates chitin-triggered immune responses in tomato

Hui Tian[1,#], Hanna Rövenich[1,#], Valentina Bracuto[2,$], Katharina Hanika[1,2,$], Elena K. Petutschnig[3], Oliver Valerius[4], Malaika K. Ebert[1], Grardy C.M. van den Berg[1], Yuling Bai[2], Bart P.H.J. Thomma[1,5]

[1] Laboratory of Phytopathology, Wageningen University and Research, Droevendaalsesteeg 1, 6708PB Wageningen, The Netherlands;
[2] Laboratory of Plant Breeding, Wageningen University and Research, Droevendaalsesteeg 1, 6708PB Wageningen, The Netherlands;
[3] Department of Plant Cell Biology, Schwann-Schleiden Centre, Georg-August-University Göttingen, 37077 Göttingen, Germany;
[4] Department of Molecular Microbiology and Genetics, Institute of Microbiology and Genetics, Georg-August-University Göttingen, 37077 Göttingen, Germany;
[5] University of Cologne, Institute for Plant Sciences, Cluster of Excellence on Plant Sciences (CEPLAS), 50674 Cologne, Germany.

[#]These authors contributed equally
[$]These authors contributed equally

ABSTRACT

Plants detect the presence of potential fungal pathogens by sensing the conserved cell wall component chitin. To date, all chitin receptors identified in plants belong to the class of cell surface-exposed lysin motif (LysM)-containing receptor proteins. In Arabidopsis, the LysM-RLK AtLYK5 binds chitin with high affinity and forms a tripartite receptor complex with the other two LysM-RLKs AtLYK4 and AtCERK1 to initiate chitin signaling. In rice, OsCERK1 is required for chitin perception upon ligand-induced association with the LysM-RLP OsCEBiP. However, thus far, a chitin perception system of tomato remains elusive. In this study, we identified two chitin-binding LysM receptors of tomato using affinity purification that were named SlLYK4 and SlCEBiP, respectively. Silencing of either of the genes resulted in impaired responsiveness to chitin. Furthermore, *SlLYK4* mutants generated with CRISPR-Cas9 revealed greatly compromised chitin-induced immunity as well as enhanced susceptibility to infection by the leaf mould fungus *Cladosporium fulvum*. Thus, SlLYK4 mediates chitin signaling in tomato and may be a crucial component of the chitin receptor complex.

INTRODUCTION

Plants detect the presence of invading microbes through cell surface-localized receptor molecules, which recognize either microbe-derived or modified-self molecules that indicate invasion (Boller and Felix., 2009; Cook et al., 2015). This recognition leads to a series of cellular events that either promote or restrict microbial colonization (Zipfel and Oldroyd, 2017). The activation of immune responses, which include the generation of extracellular reactive oxygen species (ROS), an increase in cytosolic calcium concentrations, the activation of mitogen-activated protein kinases (MAPKs) and calcium-dependent protein kinase (CDPK) cascades as well as changes in gene expression, protect the plant from invasion by potential pathogens (Boller and Felix, 2009; Cook et al., 2015).

Bacterial molecules that are recognized by plant receptors include flagellin, elongation factor Tu (EF-Tu), peptidoglycan or lipopolysaccharide (Boller and Felix, 2009). Filamentous microbes that include fungi and oomycetes are generally perceived due to the presence of their major cell wall components β-glucan or chitin (Sánchez-Vallet et al., 2015; Fesel and Zuccaro, 2016). Although β-glucan is the most abundant fungal cell wall polysaccharide, the mechanism of its recognition in plants remains largely unknown. In contrast, the activity of the β-1,4-linked *N*-acetylglucosamine (GlcNAc) homopolymer chitin as a stimulator of host immune responses and its perception by host cells has been well characterized in several plant species (Felix et al., 1998; Bowman and Free, 2006; Lenardon et al., 2010; Sanchez-Vallet et al., 2015). Interestingly, bacterial peptidoglycan as well as lipochitooligosaccharides (LCOs) produced by beneficial rhizobacteria and arbuscular mycorrhizal (AM) fungi, respectively, are chitin derivatives. Until now, the receptor molecules that have been implicated in the recognition of GlcNAc-containing molecules belong to the group of cell surface-localized lysin motif (LysM) receptors, which are further classified into LysM receptor-like kinases (LysM-RLKs) and LysM receptor-like proteins (LysM-RLPs) based on whether a kinase domain is coupled to their single pass transmembrane domain (Altenbach and Robatzek, 2007; Gust et al., 2012). LysM-RLPs are generally membrane-bound via a glycosyl phosphatidylinositol (GPI) anchor.

Signal transduction requires the presence of receptor complexes containing RLK receptor molecules, which relay the signal via their intracellular kinase domain. Over the past years several chitin receptors have been characterized in plants (Kaku et al., 2006; Miya et al., 2007; Sanchez-Vallet et al., 2015; Zipfel and Oldroyd, 2017). For example, in *Arabidopsis thaliana* (hereafter referred to as Arabidopsis), the LysM-RLK AtLYK5 binds chitin with high affinity and forms a heteromeric complex with the receptor kinase AtCERK1 to initiate chitin signaling (Liu et al., 2012b; Cao et al., 2014). While AtLYK5 has been proposed as the main chitin receptor in Arabidopsis, its paralogue AtLYK4 has also been implicated in chitin recognition and only *lyk4lyk5* double mutants show a complete loss of chitin responsiveness (Wan et al., 2012; Cao et al., 2014; Erwig et al., 2017). It was recently proposed that AtLYK4 acts as a third partner in the AtLYK5-AtCERK1 receptor complex to stabilize the assembly, thus enhancing chitin-induced plant immunity (Xue et al., 2019). As in Arabidopsis, rice (*Oryza sativa*) CERK1 is required for chitin signaling following its ligand-induced association with the LysM-RLP OsCEBiP (Kaku et

al., 2006; Hayafune et al., 2014; Miyata et al., 2014; Shimizu et al., 2010). Two further LysM-RLPs, OsLYP4 and OsLYP6, have been implicated in chitin-induced rice immune responses as well. Interestingly, these two receptor proteins also form a ligand-induced protein complex with OsCERK1 in response to bacterial cell wall peptidoglycan (PGN) (Liu et al., 2012a; Ao et al., 2014; Miyata et al., 2014). One of the three OsCEBiP orthologues in Arabidopsis, AtLYM2, controls the chitin-induced molecular fluxes across plasmodesmata and resistance to fungal pathogens independent of AtCERK1 (Faulkner et al., 2013; Narusaka et al., 2013; Cheval et al., 2020). Like OsCERK1, AtCERK1 has been shown to be required for peptidoglycan-triggered immunity (Willmann et al., 2011). In addition to its role in immunity, OsCERK1 has also been implicated in AM symbiosis that is established upon perception of fungal LCOs in combination with COs (Miyata et al., 2014; Zhang et al., 2015; Feng et al., 2019). These findings suggest that CERK1 likely acts as a co-receptor in different receptor complexes (Sánchez-Vallet et al., 2015). Similar to fungal LCOs, also bacterial LCOs are recognized by LysM receptor pairs in leguminous plant species during the establishment of symbiosis with rhizobacteria (Limpens and Bisseling, 2003; Radutoiu et al., 2003; op den Camp et al., 2011; Limpens et al., 2015).

Based on the findings in rice and Arabidopsis, it is likely that also in tomato LysM receptors are required for the perception of GlcNAc-containing molecules. However, to date, little is known about chitin perception and signaling in this plant species. Of the four tomato LysM-RLKs with relatively high identity to AtCERK1, namely SlLYK1, SlLYK11, SlLYK12, and SlLYK13, only SlLYK1 was implicated in chitin responsiveness, whereas SlLYK12 was found to be involved in symbiosis with the arbuscular mycorrhizal (AM) fungus *Rhizophagus irregularis* (Liao et al., 2018). Similarly, SlLYK10 has been shown to act in this symbiosis (Buendia et al., 2016). Nonetheless, none of these LysM-RLKs, or any other LysM receptor encoded in the tomato genome, has been characterized as a true chitin receptor. In this study, we identified potential chitin receptor candidates through a proteomics approach. Subsequently, we verified their potential role as chitin receptor with transient virus-induced gene silencing experiments, as well as through the analysis of stable tomato mutants that were generated with CRISPR-Cas9.

RESULTS

Mass spectrometry identifies two LysM receptors as candidate chitin receptors

To identify receptor protein(s) involved in chitin perception in tomato, we isolated microsomal proteins from tomato cv. Heinz 1706 leaf tissue for affinity purification with magnetic chitin beads (Petutschnig et al., 2010). Specifically bound proteins were eluted either with chitohexaose ($(GlcNAc)_6$ or GN6) or chitosan. In order to elute the remaining proteins, chitin beads were boiled in sample buffer. Following separation by SDS-PAGE, proteins in the range of 50-100 kDa were subjected to trypsin digestion. Subsequent mass spectrometric analysis yielded several unique peptides in both GN6 and chitosan eluents for only two LysM-containing receptors encoded by

Solyc02g089900 and *Solyc01g112080* (Table 1; Fig. S1). Unique peptides for the same receptors were also detected in the on-bead fractions, suggesting that the elution with GN6 and chitosan had been incomplete. Moreover, only 0 and 1 unique peptide were found in the supernatant following affinity purification (unbound fraction) for Solyc02g089900 and Solyc01g112080, respectively, demonstrating that the majority of both proteins present in the whole leaf extracts bound to chitin beads (Table 1).

TABLE 1 | Identification of chitin-binding LysM proteins of tomato (*Solanum lycopersicum* Heinz 1706). Chitin-binding proteins identified from microsomal fractions. Numbers represent unique peptides identified by Sequest and/or Mascot analyses.

Gene ID	Name	Subfamily	ΣCoverage (%)	Size (aa)	MW (kDa)	pI	Unbound	GN_6 eluent	GN_6-treated beads	Chitosan eluent	Chitosan -treated beads
Solyc02g089900	SlLYK4	RLK	17.2	645	70	5.3	0	3	4	4	4
Solyc01g112080	SlCEBiP	RLP	18	345	37	5.4	1	4	4	3	3

Solyc02g089900 codes for a membrane-bound LYR with three surface-exposed LysM domains that is closely related to Arabidopsis LYK4, and is therefore referred to as SlLYK4 (Fig. 1; Fig. 2) (Buendia et al., 2016). Phylogenetic analysis of full-length LysM receptor protein sequences showed that, in addition to AtLYK4, SlLYK4 forms a clade together with AtLYK5, SlLYK6, SlLYK7, and SlLYK15 on a longer branch, as was shown previously (Buendia et al., 2016). *Solyc01g112080* encodes a receptor protein with extracellular LysM domains that are membrane-bound via a GPI anchor (Fig. 2). Sequence analysis with the domain prediction algorithm InterPro (http://www.ebi.ac.uk/interpro/) suggested the presence of two LysM domains in SlCEBiP. However, an amino acid sequence alignment with its orthologue OsCEBiP suggests that SlCEBiP, like OsCEBiP, *Medicago truncatula* LYM2 and Arabidopsis LYM2, contains three instead of two LysMs (Fig. 1; Fig. 2; Fig. S2) (Fliegmann et al., 2011; Hayafune et al., 2014; Shinya et al., 2015; Liu et al., 2016). Considering the implication of their orthologues in chitin signaling in Arabidopsis, rice and *M. truncatula*, we further investigated the role of SlLYK4 and SlCEBiP in chitin recognition of tomato.

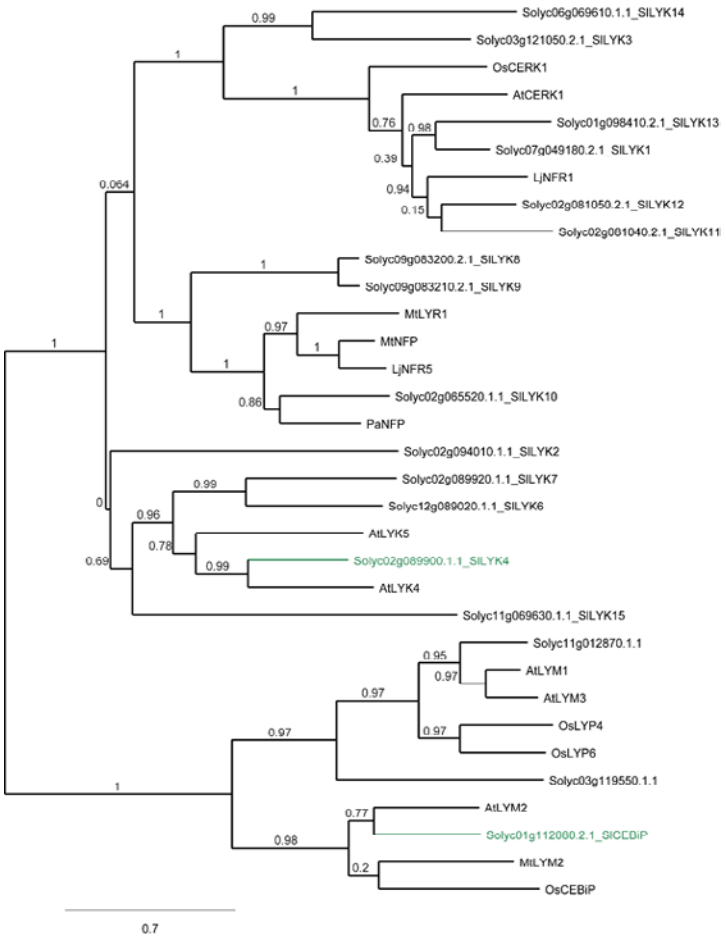

FIGURE 1 | Phylogenetic analysis of LysM receptor proteins. Tomato LysM proteins were selected based on the presence of an extracellular domain containing LysM motifs as well as their predicted localization to the plasma membrane due to the presence of a predicted transmembrane domain or a GPI anchor. Their phylogenetic relationship to LysM receptor proteins of rice, Arabidopsis, *Lotus japonicas*, and *Medicago truncatula* was inferred based on the maximum likelihood method. SlLYK4 and SlCEBiP are represented in green.

Expression of *SlLYK4* and *SlCEBiP* is induced upon chitin elicitation and fungal infection

To assess whether the expression of *SlLYK4* and *SlCEBiP* is induced upon chitin elicitation, leaf discs were collected from tomato plants and treated with either water or GN6. Subsequent real-time PCR analysis revealed that both genes are strongly induced by chitin (Fig. 3A). To further analyze whether the expression of *SlLYK4* and *SlCEBiP* changes upon fungal infection, tomato plants were inoculated with the vascular wilt fungus *Verticillium dahliae* and stem tissue was collected at 4, 8, and 12 days after inoculation. Real-time PCR analysis showed that transcript accumulation of both genes was enhanced during pathogen infection when compared with mock-inoculated plants (Fig.

3B). Whereas *SlCEBiP* expression levels peaked at around 8 days post inoculation (dpi), *SlLYK4* expression was the highest at 4 dpi and then gradually decreased. Collectively, these data suggest that both *SlLYK4* and *SlCEBiP* can be implicated in chitin signaling during fungal invasion.

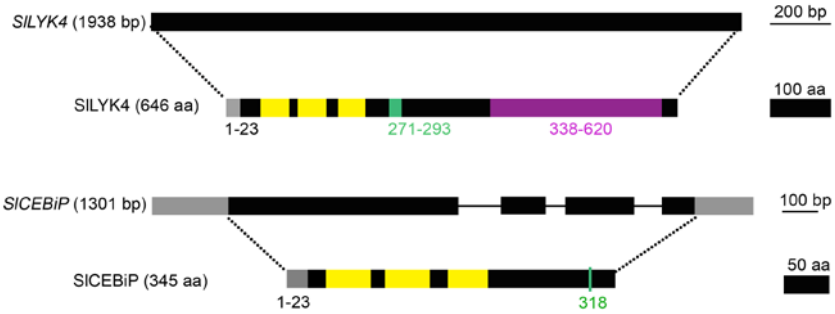

FIGURE 2 | Schematic representation of putative tomato chitin receptor genes and their encoded protein structures. Genes are represented by black boxes (exons), black lines (introns) and grey boxes (5/ and 3/UTR). The protein structures include signal peptides (grey), LysM domains predicted by InterPro (yellow), the intracellular kinase domain of SlLYK4 (Purple) and predicted transmembrane domains in SlLYK4 and GPI anchor in SlCEBiP (green).

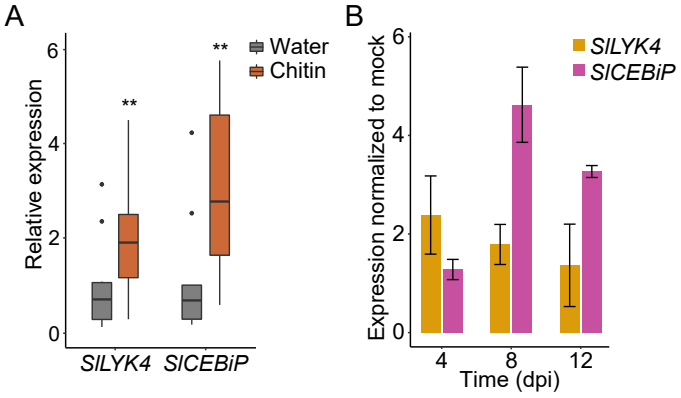

FIGURE 3 | Expression of *SlLYK4* and *SlCEBiP* is induced upon chitin elicitation and fungal infection. (A) Expression of *SlLYK4* and *SlCEBiP* of ten independent tomato leaf samples treated with water or GN6 determined with real-time PCR, normalized to *SlRUB* and calculated with the $E^{-\Delta t}$ method. The expression analysis was repeated twice with similar results and asterisks indicate statistically significant differences between water and GN6 treatment, calculated with IBM SPSS 25 according to an independent sample T test (**p value < 0.01). (B) Tomato stem tissue was harvested at 4, 8 and 12 days post inoculation with *Verticillium dahliae*. Gene expression of *SlLYK4* and *SlCEBiP* was determined with real-time PCR with gene specific primers and primers targeting tomato tubulin gene (*SlTUB*) for calibration. Expression values were normalized to mock-treated tomato samples. The standard deviation of the mean (SD) is indicated. Graphs were made with RStudio using the package of ggplot2.

Silencing of *SlLYK4* and *SlCEBiP* impairs chitin-triggered immune responses

Chitin perception triggers the activation of multiple downstream responses in plants, including the generation of reactive oxygen species (ROS) and changes in gene expression. In order to determine whether *SlLYK4* and *SlCEBiP* contribute to chitin-triggered immunity, we generated tobacco rattle virus (TRV)-based constructs to silence the genes individually. Tomato plants were treated with TRV:*SlLYK4*, TRV:*SlCEBiP*, or with TRV:*GUS* as negative control. Three weeks later, two of the youngest fully expanded leaves were collected from each plant and tested for their ability to respond to chitin. The silencing efficiency and specificity were confirmed with real-time PCR in water-treated leaf samples (Fig. S3). As expected, treatment with GN6 resulted in the induction of *SlLYK4* and *SlCEBiP* in *GUS*-silenced plants, while transcript levels of the receptor genes were not affected in *SlLYK4*- and *SlCEBiP*-silenced plants (Fig. 4AB). The expression of *SlCAL-like* and *SlERF5*, which are homologs of chitin-responsive Arabidopsis genes (Wan et al., 2008; de Jonge et al., 2010), was analyzed in these plants as well, showing severely compromised expression in *SlLYK4*- and *SlCEBiP*-silenced plants in response to GN6, but not in *GUS*-silenced plants (Fig. 4CD). Collectively, these gene silencing data further confirm that both *SlLYK4* and *SlCEBiP* act in chitin signaling in tomato.

Generation of *SlLYK4* and *SlCEBiP* mutant lines

The generation of stable mutant lines was pursued to further assess the functional role of SlLYK4 and SlCEBiP. To this end, we employed clustered regularly interspaced short palindromic repeats/CRISPR-associated protein 9 (CRISPR/Cas9) mutagenesis on the tomato cultivar MoneyMaker (MM) (Brooks et al., 2014). Two guide RNAs (sgRNAs) were designed to induce mutations at the start of *SlLYK4* gene (Table S1; Fig. 5A). After the transformation and initial selection of T0 plants, three lines (TV1203, TV1013 and TV1017) were selected for further evaluation. PCR analysis demonstrated that TV1017 carries a homozygous deletion in *SlLYK4*, whereas TV1203 and TV1013 delivered PCR fragments of the same size as the parental MM line (Fig. 5B). Sequence analysis revealed a 170 bp deletion in TV1017, resulting in an altered sequence from amino acid position 67 onwards and a truncation of SlLYK4 after 70 amino acids within the first part of the coding region for the first LysM domain, strongly suggesting that this is a loss-of-function mutant (Fig. S4). Sequence analysis furthermore revealed that line TV1013 carries a homozygous 1 bp insertion near the sgRNA1 target site, leading to a frame shift in *SlLYK4* that alters the amino acid sequence after 67 amino acids and leads to a premature stop after 79 amino acids, suggesting that this line also produces a loss-of-function mutant (Fig. S4). Finally, line TV1203 was shown to contain a homozygous wild-type *SlLYK4* allele and was used as control in our further assays.

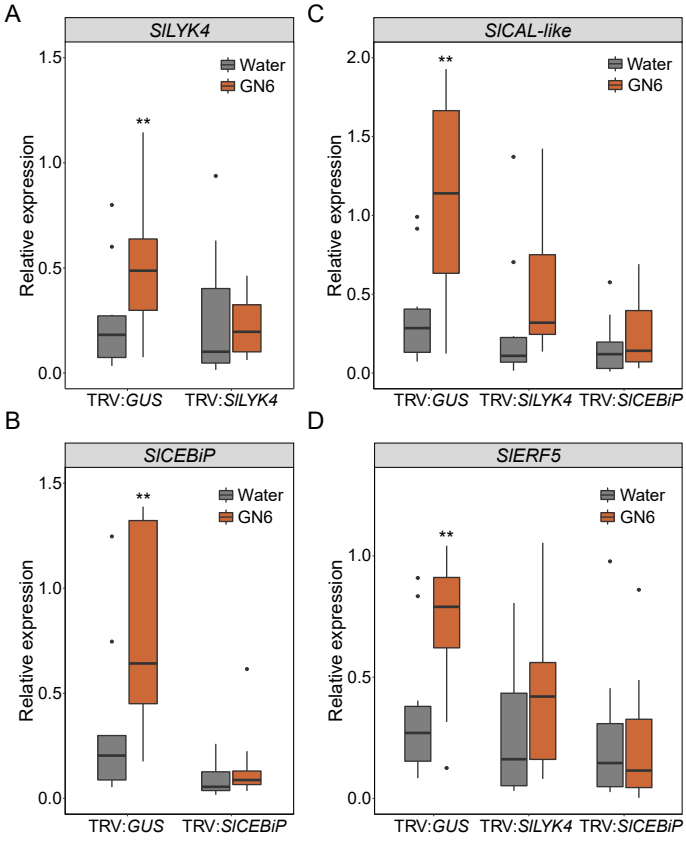

FIGURE 4 | Transient silencing of the putative chitin receptors *SlLYK4* and *SlCEBiP* abolishes chitin responsiveness. Leaf discs were harvested from *GUS*-, *SlLYK4*- and *SlCEBiP*-silenced tomato plants and incubated with either 10 μM chitohexaose (GN6) or water as negative control for one hour, and gene expression was monitored by real-time PCR using gene-specific primers, normalized to expression of the tomato rubisco (*SlRUB*) gene and calculated with the $E^{-\Delta t}$ method. The expression analysis was conducted in ten plants for each gene and repeated three times. (A) *SlLYK4* expression in *SlLYK4*-silenced plants. (B) *SlCEBiP* expression in *SlCEBiP*-silenced plants. (C) Expression of the chitin responsive *SlCAL-like* gene in *SlLYK4*- and *SlCEBiP*-silenced plants. (D) Expression of the chitin responsive *SlERF5* gene in *SlLYK4*- and *SlCEBiP*-silenced plants. Boxplots were made with RStudio and asterisks indicate statistically significant differences between water and GN6 treatment, calculated with IBM SPSS 25 (Independent sample T test, **p value < 0.01).

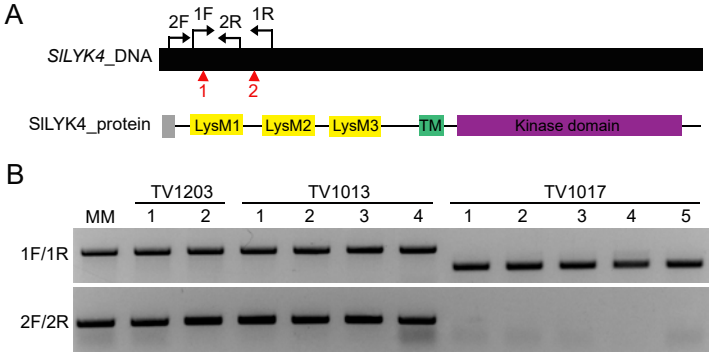

FIGURE 5 | Transgenic tomato lines TV1013 and TV1017 generated with CRISPR/Cas9 carry different *SlLYK4* mutations. (A) Schematic drawing illustrating the position of two guide RNAs (sgRNAs, red arrowhead) used for CRISPR/Cas9 mutagenesis targeting the *SlLYK4* coding sequence, and the primer pairs (black arrows) used for evaluation. The signal peptide (grey), LysM domains (yellow), transmembrane domain (green), and kinase domain (purple) are shown on the protein structure. (B) PCR genotyping of tomato plants of TV1203, TV1013 and TV1017 as well as the parental MoneyMaker (MM) plant. Numbers represent independent tomato plants.

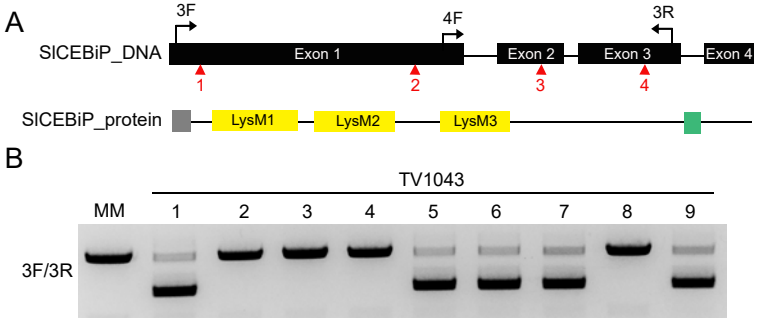

FIGURE 6 | Transgenic tomato line TV1043 generated with CRISPR/Cas9 carries a heterozygous *SlCEBiP* mutation. (A) Schematic drawing illustrating the position of four guide RNAs (sgRNAs, red arrowhead) used for CRISPR/Cas9 mutagenesis targeting the *SlCEBiP* coding sequence, and the primer pairs (black arrows) used for evaluation. The signal peptide (grey), LysM domains (yellow) and GPI anchor (green) are shown on the protein structure. (B) PCR genotyping of nine tomato plants of TV1043 as well as the parental MoneyMaker (MM) plant.

For *SlCEBiP*, four sgRNAs were designed (Table S1; Fig. 6A). Unfortunately, this mutagenesis delivered only a single line; TV1043. The analysis of nine TV1043 plants revealed a heterozygous nature with two *SlCEBiP* alleles carrying different mutations (Fig. 6B; Fig. S5). One allele carries a 1 bp insertion within the sgRNA3 target area, within exon 2 between the sequences encoding the three extracellular LysMs and the transmembrane domain, which results in a frame shift and an altered protein sequence after 225 amino acids. Thus, it cannot be excluded that this allele still encodes a functional SlCEBiP variant. The second *SlCEBiP* allele carries a 539 bp deletion from 20

bp downstream of the sgRNA2 target sequence to 17 bp upstream of that of sgRNA4, resulting in an altered protein sequence from amino acid position 167 onwards between the second and third LysM domains, suggesting that also this allele may still encode a functional SlCEBiP variant (Fig. S5). However, as TV1043 was the only mutant obtained, heterozygous seeds of this line was included in our further analyses.

A *SlLYK4* mutant line displays enhanced susceptibility to fungal infection

To assess whether *SlLYK4* or *SlCEBiP* mutant lines possess altered susceptibility to fungal infection, the tomato leaf mould pathogen *Cladosporium fulvum* was inoculated onto leaves of control line TV1203, *SlLYK4* mutants TV1013, TV1017 and *SlCEBiP* mutant TV1043. At 18 days post inoculation, typical leaf mould symptoms emerged on all lines. Interestingly, *SlLYK4* mutant TV1017 developed evidently more infection symptoms when compared with control line TV1203. However, in contrast, the other *SlLYK4* mutant TV1013 did not developed more symptoms than line TV1203, similar to *SlCEBiP* mutant TV1043 (Fig. 7A). Determinations of fungal biomass with real-time PCR mirrored these phenotypic observations (Fig. 7B).

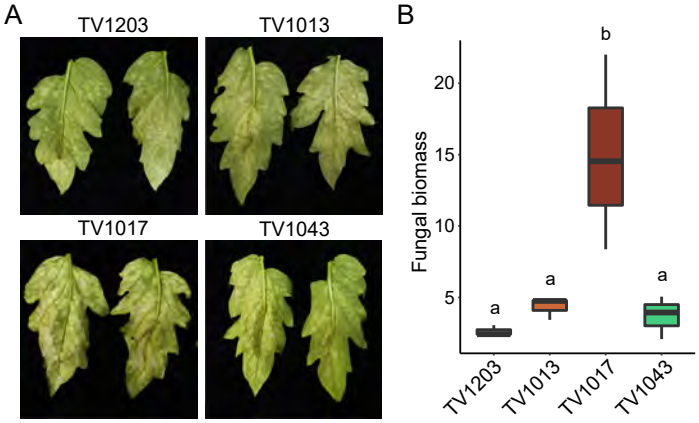

FIGURE 7 | *SlLYK4* mutant line displays enhanced susceptibility to *Cladosporium fulvum* infection. (A) Representative phenotype of tomato leaves of *SlLYK4* and *SlCEBiP* mutant lines inoculated with the wild-type *C. fulvum* strain race 0. Pictures were taken at 18 dpi. (B) *C. fulvum* biomass determined by real time PCR at 18 dpi with the expression of *C. fulvum tublin* (*CfTUB*) normalized to tomato *rubisco* (*SlRUB*) and calculated with the $E^{-\Delta t}$ method. Different letters represent statistically significant differences calculated with IBM statistics 25 (One-way ANOVA; $P < 0.05$).

SlLYK4 mutant lines are compromised in chitin-triggered immunity

To analyse whether the expression of *SlLYK4* or *SlCEBiP* responds to chitin elicitation in the mutant lines, leaf discs of control line TV1203, *SlLYK4* mutants TV1013 and TV1017, and *SlCEBiP* mutant TV1043 were harvested and incubated with GN6 or water as control. As expected, *SlLYK4* expression was significantly induced in TV1203 treated with GN6. However, *SlLYK4* no longer responded to chitin elicitation in *SlLYK4* mutants TV1013 and TV1017 (Fig.

8A), confirming the involvement of SlLYK4 in chitin signalling. Similarly, *SlCEBiP* expression cannot be induced by chitin treatment in TV1043 (Fig 8D). Surprisingly, however, whereas *SlCEBiP* expression was compromised in the *SlLYK4* mutants TV1013 and TV1017 (Fig. 8B), *SlLYK4* expression was not compromised in the *SlCEBiP* mutant TV1043 (Fig. 8C).

To further evaluate the role of SlLYK4 and SlCEBiP in chitin signalling, we assessed the responsiveness of the mutant lines to chitin elicitation by means of assessment of the reactive oxygen species (ROS) burst, one of the fastest immune responses in plants upon chitin recognition (Boller and Felix, 2009; Cook et al., 2015). Treatment with 10 μM GN6 induced a ROS burst in tomato line TV1203 within 4 min, whereas *SlLYK4* mutants TV1013 and TV1017 displayed greatly impaired ROS production (Fig. 9). Consistent with the gene expression analysis described above, *SlCEBiP* mutant TV1043 showed no compromised ROS burst when compared with control line TV1203 (Fig. 9).

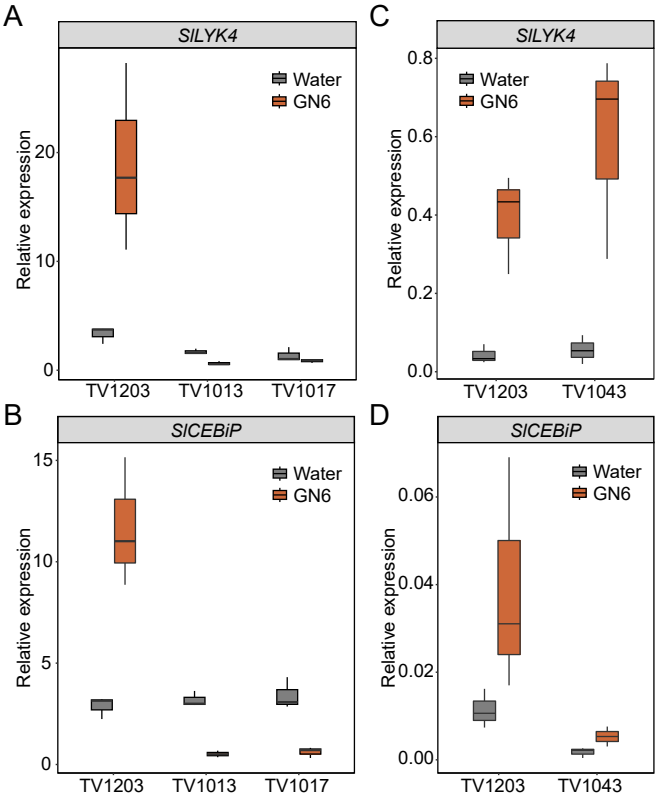

FIGURE 8 | Chitin responsiveness of *SlLYK4* and *SlCEBiP* are abolished in tomato mutant lines TV1013 and TV1017, whereas the expression of *SlLYK4* but not *SlCEBiP* is still induced by chitin elicitation in TV1043. Leaf samples were harvested and incubated with 10 μM chitohexaose (GN6) or water as negative control for one hour. Gene expression was monitored by real-time PCR using gene-specific primers and normalized to expression of the tomato rubisco (*SlRUB*) gene and calculated with the $E^{-\Delta t}$ method. Expression of *SlLYK4* (A) and *SlCEBiP* (B) in transgenic lines TV1203, TV1013 and TV1017. Expression of *SlLYK4* (C) and *SlCEBiP* (D) in transgenic line TV1043 in comparison with TV1203. Boxplots were made with RStudio using the package ggplot2.

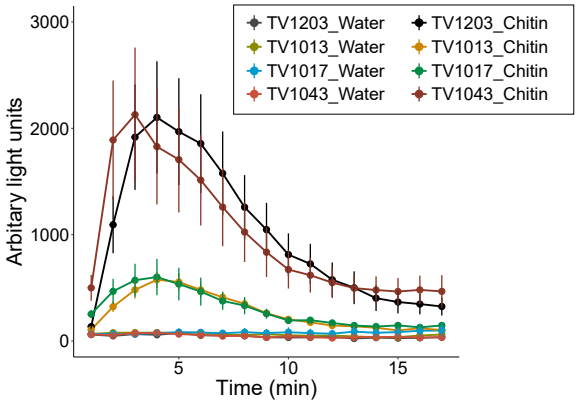

FIGURE 9 | Chitin-induced ROS production is severely compromised in *SlLYK4* mutant lines TV1013 and TV1017, but not in *SlCEBiP* mutant line TV1043. Leaf discs of tomato lines were harvested and incubated with 10 μM chitohexaose (chitin) or water as negative control. Standard error of the mean (SEM) is indicated.

To further confirm the involvement of SlLYK4 in chitin signalling, we assessed the induction of the chitin-responsive genes *SlCAL-like* and *SlERF5* in *SlLYK4* mutants TV1013 and TV1017, revealing dramatically compromised expression of both genes in *SlLYK4* mutant lines TV1013 and TV1017 upon chitin treatment when compared with control line TV1203 (Fig. 10).

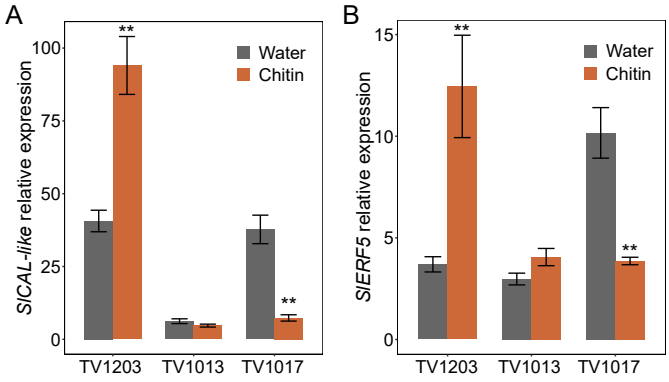

FIGURE 10 | Two tomato chitin-responsive genes no longer respond to chitin elicitation in *SlLYK4* mutant lines. Expression of *SlCAL-like* (A) and *SlERF5* (B) was determined with real-time PCR, normalized to expression of tomato rubisco (*SlRUB*) as calculated with $E^{-\Delta Ct}$ method. Barplots were made with RStudio with the package of ggplot2 and standard error of the mean (SEM) is indicated. Asterisks indicate statistically significant differences calculated with IBM statistics 25 (Independent sample T-test; **p value < 0.01).

DISCUSSION

Extracellular LysM domain-containing receptor proteins have been demonstrated to mediate recognition of microbe-derived structural patterns, including bacterial peptidoglycan, fungal chitin and its derivatives, in several plant species (Antolín-Llovera et al., 2014; Sánchez-Vallet et al., 2015; Zipfel and Oldroyd, 2017). The perception of such patterns triggers plant responses that either lead to the establishment of a mutually beneficial plant-microbe interaction, or to the activation of plant immunity that restricts microbial colonization (Zipfel and Oldroyd, 2017). Here we identified two chitin-binding LysM receptors from tomato, SlLYK4 and SlCEBiP, and investigated their role in the activation of chitin-triggered immunity.

Transient silencing of either of the two genes resulted in compromised induction of chitin responsive genes, suggesting that they are critical for the activation of chitin-triggered immune responses (Fig. 4). In order to further evaluate the role of SlLYK4 and SlCEBiP in chitin-triggered immune signaling, stable mutant lines were generated with CRISPR/Cas9 mutagenesis (Zhang et al., 2014; Pan et al., 2016). However, the *SlCEBiP* mutant still showed chitin-induced *SlLYK4* expression, and furthermore displayed neither a reduction of chitin-induced ROS generation (Fig. 8), nor enhanced susceptibility to fungal infection (Fig. 10), which may suggest that SlCEBiP is not required for chitin-triggered immune signaling transduction in tomato. If this is the case, phenotypes that were obtained upon transient silencing of *SlCEBiP* should be attributed to off-target silencing of a critical component of chitin-triggered immune signaling. However, the data for the CRISPR/Cas9 mutant of SlCEBiP should be interpreted with caution, as it is important to note that functional SlCEBiP may still be formed in the *SlCEBiP* mutant. After all, the mutations occurred relatively far downstream into the coding sequence such that one allele may still encode a protein with two LysMs while the other allele may encode a variant with all three LysMs intact. To resolve this inconsistency, ultimately, additional *SlCEBiP* mutants should be generated and analyzed to determine whether *SlCEBiP* is required for chitin-triggered immune signaling.

In contrast to *SlCEBiP*, *SlLYK4* was found to be required not only for chitin-triggered ROS generation (Fig. 8), but also for the induction of chitin-responsive genes (Fig. 9). Thus, these data confirm the initial observations based on the transient silencing data that SlLYK4 is required for chitin-triggered immune signaling in tomato. With this observation, it was expected that the mutants would also display enhanced susceptibility towards fungal pathogens. Indeed, one of the two *SlLYK4* mutants showed enhanced susceptibility to *C. fulvum* infection (Fig. 10). Unfortunately, the second mutant did not support this observation (Fig. 10). However, it has previously been demonstrated that the contribution of individual chitin receptors to resistance against fungal defense is difficult to visualize. Although Arabidopsis *LYK4* mutants were reported to display enhanced susceptibility to *Alternaria brassicicola* (Wan et al., 2012), inactivation of *CERK1* or *LYK5* in Arabidopsis Col-0 plants only led to a marginal increase in lesion size induced by this fungus (Miya et al., 2007; Wan et al., 2008; Cao et al., 2014). However, whereas *cerk1* mutants displayed moderately enhanced susceptibility towards *Erysiphe cichoracearum*, no significant difference in symptom development was observed between *cerk1* mutants and the

wild-type plants upon inoculation with *Colletotrichum higginsianum* (Miya et al., 2007; Wan et al., 2008). Furthermore, whereas no pathogen phenotypes have been reported for mutants in *CEBiP* or *CERK1* in rice (Kaku et al., 2006; Shimizu et al., 2010), silencing of the *CEBiP* homolog of barley, *HvCEBiP*, only resulted in a slight increase in symptoms caused by *Magnaporthe oryzae*, and *CERK1*- and *CEBiP*-silenced wheat plant displayed similar disease severity when inoculated with *Zymoseptoria tritici* as control plants (Tanaka et al., 2010; Lee et al., 2014). Thus, to provide further support for a role of SlLYK4 in defense against fungal infection, a more meticulous phenotyping of *C. fulvum* infections should be performed, preferably in a detailed time course, but also additional fungal pathogens may be tested.

Considering that SlLYK4 is required for chitin-triggered immune signaling, the question arises whether SlLYK4 is a genuine chitin receptor and part of a receptor complex, or rather a downstream signaling component. Although the identification through affinity purification with chitin beads is a first line of evidence for a role as chitin receptor, as its identification relied on direct chitin binding, further evidence is needed such as the determination of the chitin binding affinity of the ectodomain of the protein molecule.

Phylogenetic analysis demonstrated that SlLYK4 is closely related to the Arabidopsis receptor kinases AtLYK4 and AtLYK5 (Fig. 1). Like its Arabidopsis orthologues, SlLYK4 belongs to the group of LYR receptor kinases that lack a glycine-rich loop and display a degenerated HRD motif in their catalytic loop, rendering their kinase domains inactive (Arrighi et al., 2006; Cao et al., 2014; Buendia et al., 2016). Since its kinase lacks the important structural features for functionality, it is likely that SlLYK4 associates with a co-receptor that contains a functional kinase domain upon ligand perception like other LYR receptors (Zipfel and Oldroyd, 2017). However, in our affinity purification approach with chitin beads we did not identify a LysM receptor protein with an active kinase domain, suggesting that this co-receptor may not bind chitin directly, or only with significantly lower affinity. It has been demonstrated that Arabidopsis AtLYK4/AtLYK5 forms a receptor complex with AtCERK1 that contains a functional kinase domain to initiate chitin signaling (Miya et al., 2007; Liu et al., 2012b; Cao et al., 2014; Erwig et al., 2017). Similarly, OsCEBiP interacts with OsCERK1 to activate chitin-induced immune responses in rice (Shimizu et al., 2010; Hayafune et al., 2014). Thus, it is possible that the tomato CERK1 homolog acts together with SlLYK4 to initiate chitin signalling. Interestingly, the tomato homolog of CERK1 was recently characterized as SlLYK1 and shown to mediate chitin responsiveness (Liao et al., 2018). However, future experiments should reveal whether SlLYK4 is able to interact with SlLYK1 in a chitin-dependent manner, like AtLYK4 and AtLYK5 with AtCERK1 and like OsCEBiP with OsCERK1 (Shimizu et al., 2010; Cao et al., 2014; Hayafune et al., 2014).

Thus far, it has been demonstrated that different receptor complexes for chitin perception can occur within the same plant species that encompass LysM-RLKs and LysM-RLPs. For instance, in Arabidopsis, the LysM-RLK AtLYK5 forms a heteromeric complex with the receptor kinase AtCERK1 to initiate chitin signaling (Liu et al., 2012b; Cao et al., 2014). Meanwhile, AtLYK4 seems to share some degree of functional redundancy with AtLYK5 as only *lyk4lyk5* double

mutants display complete loss of chitin responsiveness (Wan et al., 2012; Cao et al., 2014; Erwig et al., 2017). Additionally, it has previously been shown that chitin perception in plasmodesmata, which leads to the inhibition of molecular fluxes, occurs in an AtCERK1-independent manner (Faulkner et al., 2013). Rather, this response relies on the OsCEBiP orthologue AtLYM2 (Faulkner et al., 2013). Recently, it was demonstrated that, besides AlLYM2, these responses in the plasmodesmal plasma membrane require AtLYK4 and AtLYK5 as well, although only AtLYM2 and AtLYK4 could be detected in the plasmodesmal plasma membrane (Faulkner et al., 2013; Narusaka et al., 2013; Cheval et al., 2020). Collectively, these observations point towards the existence of dynamic changes in the localization, association, or mobility of these receptors in chitin perception complexes, and furthermore that different receptor complexes may exist at different subcellular localizations. Similarly, it has been reported for rice that not only OsCEBiP associates with OsCERK1, but also the two LysM-RLPs OsLYP4 and OsLYP6, mediating chitin-induced immunity (Shimizu et al., 2010; Liu et al., 2012a; Hayafune et al., 2014). Consequently, different receptor complexes for chitin recognition that involve multiple LysM-RLKs and LysM-RLPs may occur in tomato as well, suggesting that not only SlLYK4, but also SlCEBiP and/or SlLYK1 could be involved in chitin-induced immunity.

MATERIALS & METHODS

Receptor candidate purification

Microsomal fractions were prepared from tomato (*Solanum lycopersicum*) cv. Heinz 1706 leaf tissue and used for chitin or chitosan affinity enrichment as described previously (Petutschnig et al., 2010). Proteins from unbound, eluent and bead fractions were separated by SDS-PAGE. Gel slices containing proteins of 50-100 kDa were utilized for tryptic digestion and purification for liquid chromatography-mass spectrometry (LC-MS/MS).

Candidate identification by liquid chromatography-mass spectrometry

LC-MS analysis was performed with an Orbitrap Velos Pro™ Hybrid Ion Trap-Orbitrap mass spectrometer. 1-5 µl of peptide solutions were loaded and washed on an Acclaim® PepMAP 100 pre-column (#164564, 100 µm x 2 cm, C18, 3µm, 100 Å, Thermo Fisher Scientific) with 100% loading solvent A (98% H_2O, 2% acetonitrile, 0.07% TFA) at a flow rate of 25 µl/min for 6 min. Peptides were separated by reverse phase chromatography on an Acclaim® PepMAP RSLC column (#164540, 75 µm x 50 cm, C18, 3 µm, 100 Å, Thermo Fisher Scientific) with a gradient from 98% solvent A (H_2O, 0.1% formic acid) and 2% solvent B (80% acetonitrile, 20% H_2O, 0.1% formic acid) to 42% solvent B for 95 min and to 65% solvent B for the following 26 min at a flow rate of 300 nl/min. Peptides eluting from the chromatographic column were on-line ionized by nano-electro-spray at 2.4 kV with the Nanospray Flex Ion Source (Thermo Fisher Scientific). Full scans of the ionized peptides were recorded within the Orbitrap FT analyzer of the mass spectrometer

within a mass range of 300-1850 m/z at a resolution of 30.000. Collision-induced dissociation fragmentation of data-dependent top-fifteen peptides was performed with the LTQ Velos Pro linear ion trap. Data acquisition and programming were carried out with the XCalibur *2.2* software (Thermo Fisher Scientific). A UniProt-derived *Solanum lycopersicum*-specific database (http://www.uniprot.org, Proteome ID UP000004994, 33952 entries) was used for database searches with SequestHT and Mascot search engines. Proteins were identified with the Proteome Discoverer™ 1.4 software. The digestion mode was set to trypsin and the maximum of missed cleavage sites to two. Carbamidomethylation of cysteins was set as fixed modification, oxidation of methionines, and biotinylation of lysines were set as variable modifications (if required). The mass tolerance was 10 ppm for precursor ions and 0.6 Da for fragment ions. The decoy mode was revert with a false discovery rate of 0.01.

Phylogeny of LysM receptors and protein sequence analyses

Selected sequences of LysM domain-containing protein sequences were retrieved from the solgenomics network (http://solgenomics.net) for tomato (ITAG3.0), from TAIR (http://arabidopsis.org) for Arabidopsis, from Phytozome 12 (http://phytozome.jgi.doe.gov) for rice (v7) and *Medicago truncatula* (Mt4.0v1), and UniProt (http://uniprot.org) for *Lotus japonicus*. The sequences were loaded into the "one click" phylogeny.fr server for phylogenetic analysis, ignoring alignment curation by Gblocks (Dereeper et al., 2008).

The sequences of SlLYK4 and SlCEBiP were further analyzed with SignalP 4.1 and TargetP 1.1 (http://www.cbs.dtu.dk/services/) to predict the presence of signal peptides and extracellular localization of both candidates. The localization of the LysM domains in the extracellular region of SlLYK4 was adopted from a previous study (Buendia et al., 2016), whereas the LysM domains of SlCEBiP were predicted with InterPro (http://www.ebi.ac.uk/interpro/). The GPI modification site in SlCEBiP was predicted with the big-PI plant server (http://mendel.imp.ac.at/gpi/plant_server.html).

Gene expression analysis

To assess the expression of LysM receptor genes, shoot tissue was collected from nine tomato *cv*. Moneymaker (MM) plants inoculated with *Verticillium dahliae* strain JR2 (Faino et al., 2015) at 4, 8 and 12 days post inoculation (dpi). Tissues from three plants were pooled for RNA isolation using the TRIzol reagent (Ambion, Connecticut, USA) according to manufacturer's instructions. Expression of *SlLYK4*, *SlCEBiP*, and tomato tubulin (*SlTUB*) was analysed with real-time PCR as described previously (Livak and Schmittgen, 2001) using primer pairs shown in Table S2. Expression levels were calculated relative to *SlTUB* using the $E^{-\Delta Ct}$ method (Livak and Schmittgen, 2001) and normalized to mock-inoculated plants.

To assess gene expression upon chitin elicitation, leaf discs of tomato plants were collected, placed into a 96-well microtiter plate and incubated in 200 µL water overnight. The next day, water was replaced with either 10 µM chitohexaose or water in a total volume of 150 µL and incubated

for one hour. Leaf samples were subsequently harvested and snap-frozen in liquid nitrogen for RNA extraction as described above. Gene expression assays were conducted with gene-specific primers listed in table S2, normalized to tomato rubisco (*SlRUB*) and calculated with the $E^{-\Delta Ct}$ method. All gene expression assays were conducted using SYBR™ green master mix kit (Bioline, Luckenwalde, Germany) in a C1000 Touch™ Thermal Cycler (Bio-Rad, California, USA).

Virus-induced gene silencing of receptor candidates

SlLYK4 and *SlCEBiP* fragments were amplified from tomato cv. Moneymaker cDNA and cloned into the pTRV2 vector (Liu et a., 2002) using Gateway® technology (primers are listed in Table S2). Constructs were evaluated by sequencing and transformed into *Agrobacterium tumefaciens* strain GV3101 by electroporation. Control TRV:*GUS* and TRV:*PDS* vectors were previously generated and transformed into *A. tumefaciens* (Liebrand et al., 2012). To silence *SlLYK4* and *SlCEBiP*, cotyledons of ten-day-old tomato cv. Moneymaker seedlings were infiltrated with 1:1 mixtures of pTRV1 and pTRV2 constructs (Liu et al., 2002). Photobleaching was observed about two weeks after agroinfiltration of TRV:*PDS*. At 21 dpi leaf tissue was harvested for physiological assays.

Oxidative burst and chitin-responsive gene expression assays

Reactive oxygen species (ROS) measurements were performed on tomato leaf discs (ø 5 mm) using a luminol-based chemiluminescence assay as previously described (Gimenez-Ibanez et al., 2009; de Jonge et al., 2010). Three leaf discs were placed into one well of a 96-well microtiter plate and incubated in 200 µl demineralized water overnight. The next day, water was replaced with 100 µL of assay solution containing 100 µM L-012 substrate (FUJIFILM, Neuss, Germany) and 20 µg/mL horseradish peroxidase (Sigma-Aldrich, Missouri, USA) in presence or absence of 10 µM chitohexaose (IsoSep AB, Tullinge, Sweden). Luminescence was measured using a CLARIOstar® microplate reader (BMG LABTECH, Ortenberg, Germany). Leaf discs were kept in elicitor solutions for an additional 30 min and then harvested and snap-frozen in liquid nitrogen for RNA extraction as described above. Chitin-responsive gene expression was tested as described previously (De Jonge et al., 2010).

CRISPR/Cas9 construct design and tomato transformation

The 'CCTop-CRISPR/Cas9 target online predictor' (https://crispr.cos.uni-heidelberg.de/; Stemmer et al. 2015) was used to design sgRNAs with tomato as reference genome for sgRNA target site evaluation. Any sgRNA with more than one exonic off-target site was discarded. To evaluate the predicted sgRNAs, G/C content was checked (http://www.endmemo.com/bio/gc.php) and the secondary sgRNA structures were predicted (http://unafold.rna.albany.edu/?q=mfold/RNA-Folding-Form; Zuker, 2003) and assessed (Liang et al., 2016). Different

scoring tools (https://sgrnascorer.cancer.gov/, Chari et al., 2017; https://portals.broadinstitute.org/gpp/public/analysis-tools/sgrna-design, Doench et al., 2016, Sanson et al., 2018; http://crispr.wustl.edu/) were used to select sgRNAs fulfilling most of the criteria and with no off-targets.

Golden Gate Cloning (Engler et al., 2008) method was used and the following plasmids were obtained from Addgene (https://www.addgene.org/): pICH86966 (level 0 plasmid for amplification), pICSL01009 (level 0 plasmid containing AtU6), pICH47751 (level 1 position 1), pICH47761 (level 1 position 2), pICH47772 (level 1 position 3), pICH47781 (level 1 position 4), pICH47732 (level 1 containing NPTII), pICH47742 (level 1 containing Cas9), pICH41822 (linker) and pAGM4723 (level 2 binary vector) (Weber et al,. 2011). Amplification of sgRNAs was conducted using Phusion High-Fidelity DNA Polymerase (Thermo Scientific, Bleiswijk, The Netherlands). Level 1 plasmids were digested using *Bsa*I/*Eco*31I and ligated using T4 DNA ligase (Thermo Scientific, Bleiswijk, The Netherlands) and level 2 plasmids were digested using *Bpi*I/*Bps*I and ligated using T4 DNA ligase (Thermo Scientific, Bleiswijk, The Netherlands). The final constructs were introduced into *Agrobacterium tumefaciens* strain AGL1. Tomato transformation was carried out as described previously (Huibers et al., 2013).

Cladosporium fulvum inoculation onto tomato

Conidiospores of the wild-type *C. fulvum* strain race 0 were harvested from half-strength potato dextrose agar (PDA) and adjusted to a concentration of 5×10^6 conidiospores/mL with milli-Q water and 0.02% Tween20 was added. Four-week-old tomato plants were inoculated by spray inoculation onto the lower side of the leaves until droplet run-off and positioned in a closed, transparent plastic tent for two days to maintain high humidity. Regular inspections for the occurrence of disease symptoms were carried out from 10 dpi onwards, and pictures and leaf samples were taken at 18 dpi.

Three representative tomato leaves of each inoculation were harvested and subjected to genomic DNA extraction using the CTAB-based extraction buffer (100 mM Tris-HCl PH 8.0, 20 mM EDTA, 2 M NaCl, 3 % CTAB). DNA concentrations were adjusted to 50 ng/µL and 2 µL was used as template for real-time PCR that was performed using SYBR™ green master mix kit (Bioline, London, UK) on a C1000 Touch™ Thermal Cycler (Bio-Rad, California, USA). Relative expression of the *C. fulvum* tubulin gene (*CfTub)* was normalized to the tomato rubisco gene (*SlRUB*) and calculated with the $E^{-\Delta Ct}$ method. The biomass graph was made with RStudio using the package ggplot2 (Wickham, 2009; R Core Team, 2014).

ACKNOWLEDGEMENT

H. Tian acknowledges receipt of a PhD fellowship from the China Scholarship Council (CSC). The authors thank Bert Essenstam (Unifarm) for the excellent plant care. Work in the laboratory of B.P.H.J. Thomma is supported by the Research Council Earth and Life Sciences (ALW) of the Netherlands Organization of Scientific Research (NWO) and by the Deutsche Forschungsgemeinschaft (DFG, German Research Foundation) under Germany´s Excellence Strategy – EXC 2048/1 – Project ID: 390686111.

SUPPLEMENTARY DATA


```
>Solyc02g089900.1.1 | mature SlLYK4
QQPYFGTGTNDCSSQDTSTSAFGYLCNGVNRTCQSYLTFRSQPPFNTVSSISSLLGANPSQLSQLNSV
SQNATFNTNQMVLVPVTCSCSGQFYQSNASYVIRRDDSFLNIAMNTLQGLSTCQAINAENSEQANNLV
VGSRINVPLRCACPTQNQTNNGTNYLLTYLIASGEFVSFISDKFGVDFRATLAANSIPEDAPTVFPNT
TLLVPLSTPPLSSQVAGPSPPPPPATTPTPPAVPVSESSSSNKTWIYVVAGVVGGLVALCILGVVVFFL
FFRKKEKKADPQFVSESFEAVEKPSNKKVEEESEEFLESLSSIAQSVKVYKFEEVKAATENFSPTCLI
KGSVYRGTINGDFAAIKKMSGDVSKEINLLSKINHFNLISLSGICFHDGHWYLVYEYAANGPLSDWIC
HHNGEQKSLSWAQRVQISFDVATGLNYLHSYTSPPHVHKDLNGDNILLDGDLRAKIANFGLARSADGQ
EGEFALTRHIVGTQGYMAPEYLENGLVSPKLDVYALGVLLLEILTGKEVSALYEGSNTNLAELLIPVL
NDDNAKESLSNFVDPSLQGKYPVELAFAMVRLIDNCLMKDPSHRPNTDEIVQSVSRIMTATHSWETSF
STSVSPHRLP

>Solyc01g112080.2.1 | mature SlCEBiP
SFSCTSPGTCDAIIDYTLPNATTFNAVKKLFNVKNLRSLLGVNNLPVNTPADEKLPANQTIKIPFPCL
CRNGTGIANKRPIYTVVAGDFLSHIVTDIFAGLFTVEELQRVNNISNPNLIQPGDKLWIPLPCSCDDV
DGEKVVHYGRLVSSGNSIEAIAQQYNVSQETLLRLNGLASPRELLAGAVLDVPLKACQSRVSNASLDY
PLLVPNDTYIFTAANCVTCKCDAASNWTLQCQPSQIKSSLWKTCPSMQCQGLDNLYIGNVTDCNSTSC
AYAGYSNQTIFTTNTQLTCPASDNSAFGMRPGTWIWNVILVAVSSMVIVF
```

FIGURE S1 | Coverage map of SlLYK4 and SlCEBiP peptides identified by mass spectrometry. Peptides identified by LC-MS and mapping to SlLYK4 or SlCEBiP protein sequences are highlighted in grey. The first amino acid residue of the transmembrane domain of SlLYK4 is underlined (W248).

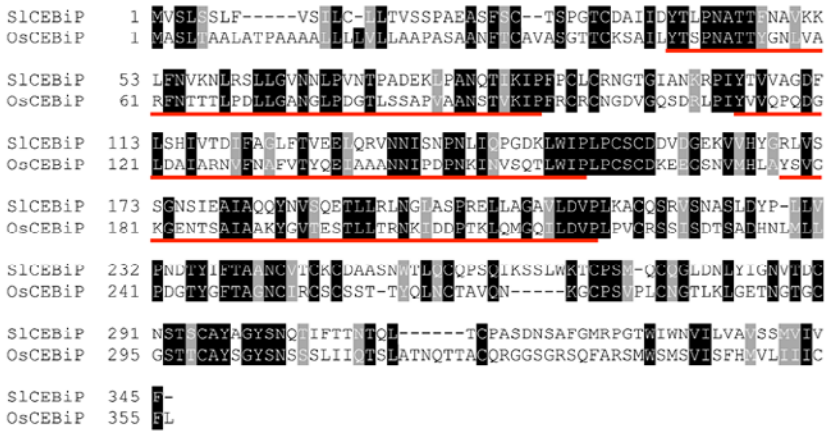

FIGURE S2 | Pairwise alignment of rice and tomato CEBiP protein sequences. Full-length protein sequences of SlCEBiP and OsCEBiP were aligned with Clustal Omega (http://www.ebi.ac.uk/Tools/msa/clustalo/). LysM domains as annotated for OsCEBiP are underlined in red. Sequence conservation between the two receptors suggests that SlCEBiP contains three LysM domains.

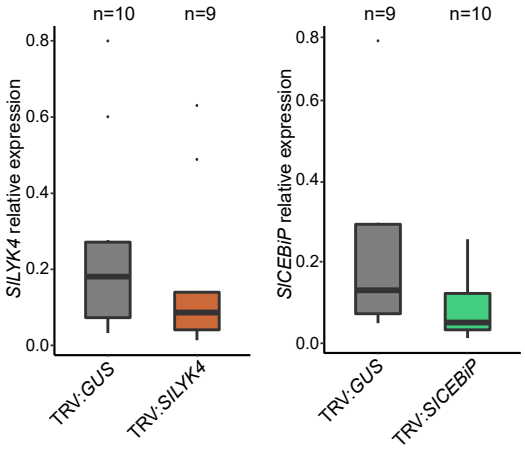

FIGURE S3 | Silencing efficiency of TRV:*SlLYK4*- and TRV:*SlCEBiP*-treated tomato plants as determined with real-time PCR. Gene expression analysis was conducted using primers targeting *SlLYK4* and *SlCEBiP* and normalized to the expression of tomato rubisco (*SlRUB*). Boxplots are made with RStudio.

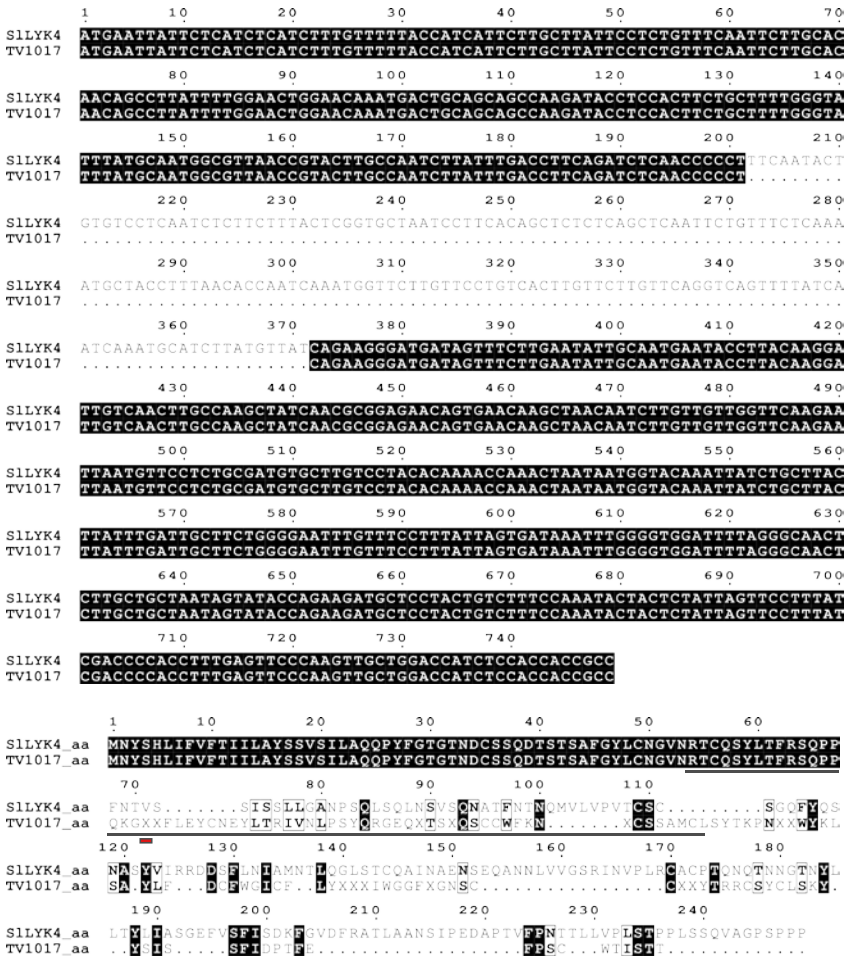

FIGURE S4 | DNA and protein sequence alignments of *SlLYK4* amplified from tomato cultivar MoneyMaker (MM) and transgenic tomato lines TV1013 and TV1017. The alignments were conducted with ClustalX and the figures were made using ESPript 3 (http://espript.ibcp.fr/ESPript/ESPript/index.php; Robert and Gouet, 2014). The first extracellular LysM domain is underlined and the first premature stop is indicated in red.

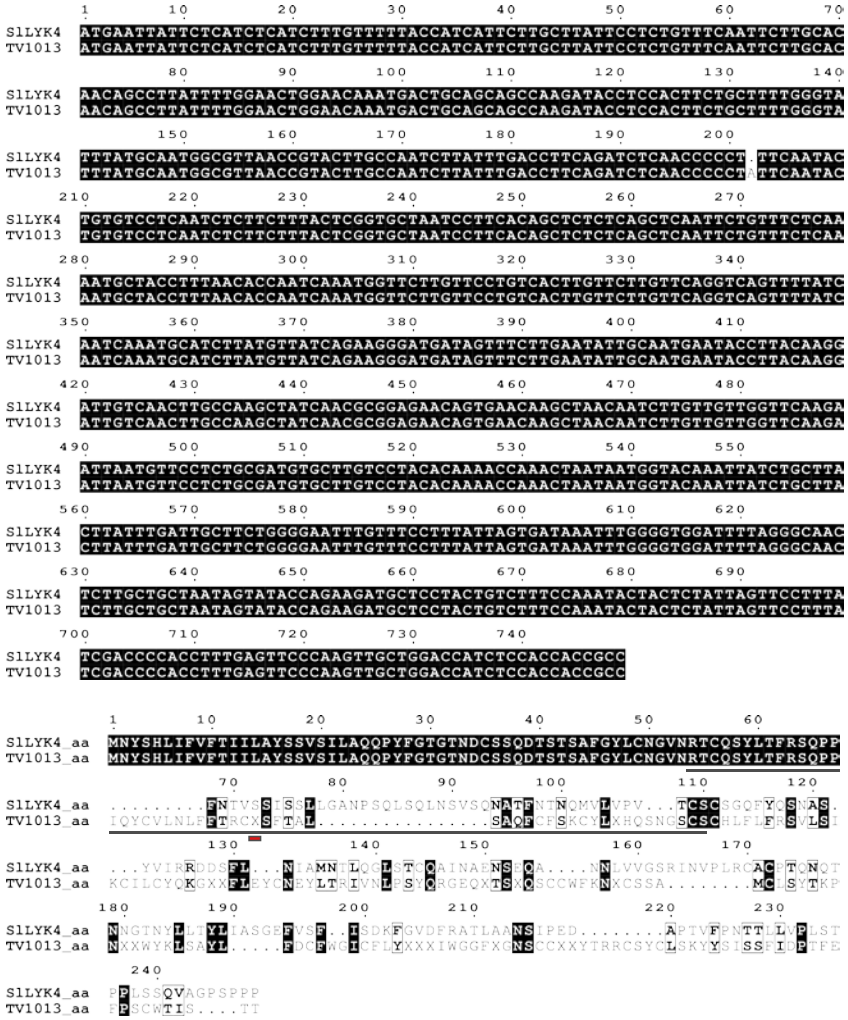

FIGURE S4 | Continued.

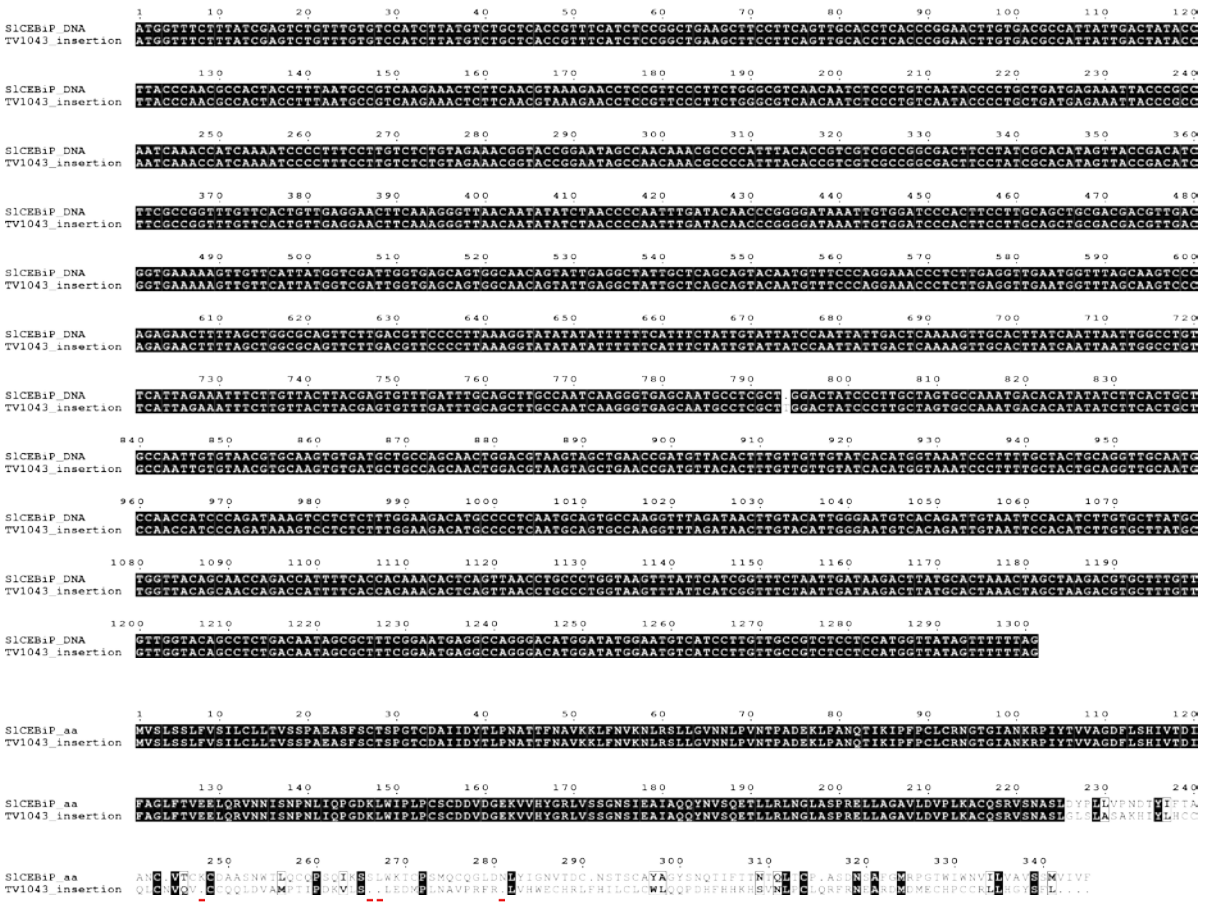

FIGURE S5 | DNA and protein sequence alignments of *SlCEBiP* amplified from the tomato cultivar MM and transgenic tomato line TV1043. The alignments were conducted with ClustalX and the figures were made using ESPript 3 (http://espript.ibcp.fr/ESPript/ESPript/index.php; Robert and Gouet, 2014). Three LysM domains are underlined.

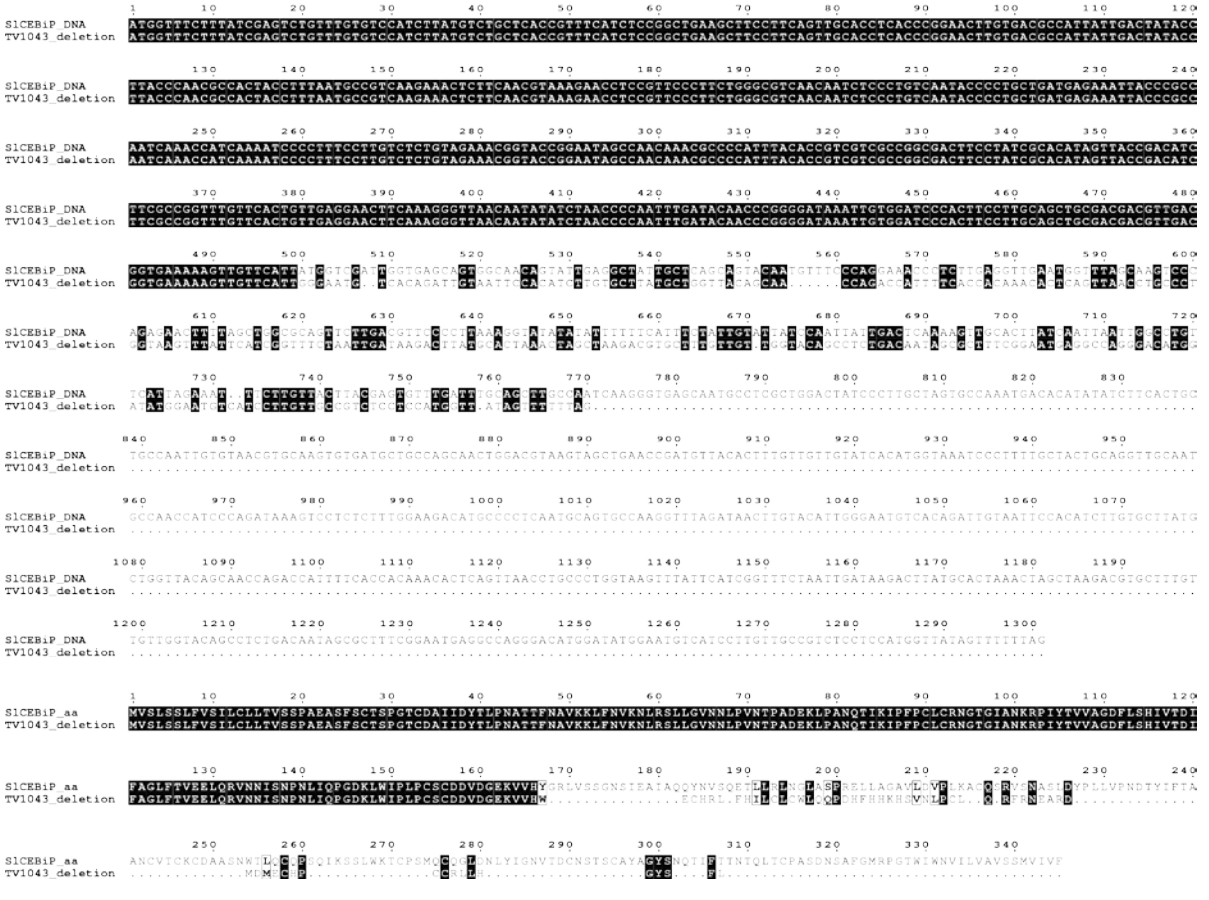

FIGURE S5 | Continued.

TABLE S1 | Guide RNAs used for *SlLYK4* and *SlCEBiP* mutant generation with CRISPR/Cas9.

sgRNA	Target gene	Sequence	Starting position in gene
sgRNA1	*SlLYK4*	CCTTTCAATACTGTGTCCT	199
sgRNA2	*SlLYK4*	ATGCATCTTATGTTATCAGA	355
sgRNA1	*SlCEBiP*	AACGGTGAGCAGACATAAGA	32
sgRNA2	*SlCEBiP*	TCAACGTCGTCGCAGCTGCA	478
sgRNA3	*SlCEBiP*	TAGCAAGGGATAGTCCAGCG	790
sgRNA4	*SlCEBiP*	AACCTTGGCACTGCATTGAG	1002

TABLE S2 | Primers used in this study.

Primers	Sequences
1F	CCTCCACTTCTGCTTTTGGG
1R	GTTAGCTTGTTCACTGTTCTCC
2F	GACTGCAGCAGCCAAGATACCT
2R	GATAAAACTGACCTGAACAAGAACAAGT
3F	ATGGTTTCTTTATCGAGTCTGTTTGTGTCCA
3R	CAGGGCAGGTTAACTGAGTGTTT
SlTUB-F	AACCTCCATTCAGGAGATGTTT
SlTUB-R	TCTGCTGTAGCATCCTGGTATT
SlRUB-F	GAACAGTTTCTCACTGTTGAC
SlRUB-R	CGTGAGAACCATAAGTCACC
CfTUB-F	CCTTCAGAGCTGTAACTGTCC
CfTUB-R	CCTCCTTCATAGATACCTT
SlLYK4-qPCR-F	TCAACGCGGAGAACAGTGAA
SlLYK4-qPCR-R	GCCCTAAAATCCACCCCAAA
SlCEBiP-qPCR-F	CTTGCCAATCAAGGGTGAGC
SlCEBiP-qPCR-R	ATCTGGGATGGTTGGCATTG
SlCAL-like-qPCR-F	TGAGATAACGGTGGAGGAGG
SlCAL-like-qPCR-R	ACATTCCAAATGCTCCCATC
SlERF5-qPCR-F	ACTTGAGAGAACGGAAGCCA
SlERF5-qPCR-R	ACCAAACTCGAGTCCCCTTT
SlLYK4-ecto-F	ATGAATTATTCTCATCTCATCTTTGTTTT
SlLYK4-ecto-R	AGTTTTGTTCGAGCTGCTCTC
SlLYK4-His-FLAG-F	CGGTATGAATTCATGCATCATCATCATCATCATCCCGACTACAAGGACGAC GATGACAAGCAACAGCCTTATTTTGGAACTGG
SlLYK4-His-FLAG-R	CGGTATGCGGCCGCAGTTTTGTTCGAGCTGCTCTC
SlLYK4-HA-F	CGGTATGAATTCATGGCTACCCGTACGATGTGCCGGATTACGCGACAA CAGCCTTATTTTGGAACTGG
AtLYK5-ecto-F	CAGCAACCGTACGTCAACAACCACCA
AtLYK5-HA-F	CGGTATGAATTCATGGCTACCCGTACGATGTGCCGGATTACGCGACAGCAAC CGTACGTCAACAACCACCA
AtLYK5-ecto-R	CGGTATGCGGCCGCTTAAGCCTTAGTAGACAACGGAATAGA
AtLYK5-His-FLAG-F	CGGTATGAATTCATGCATCATCATCATCATCATCCCGACTACAAGGACGAC GATGACAAGCAGCAACCGTACGTCAACAACCACCA

His-tag, green font; FLAG-tag, blue font; HA-tag, double underline; Restriction enzyme recognition sites, red font.

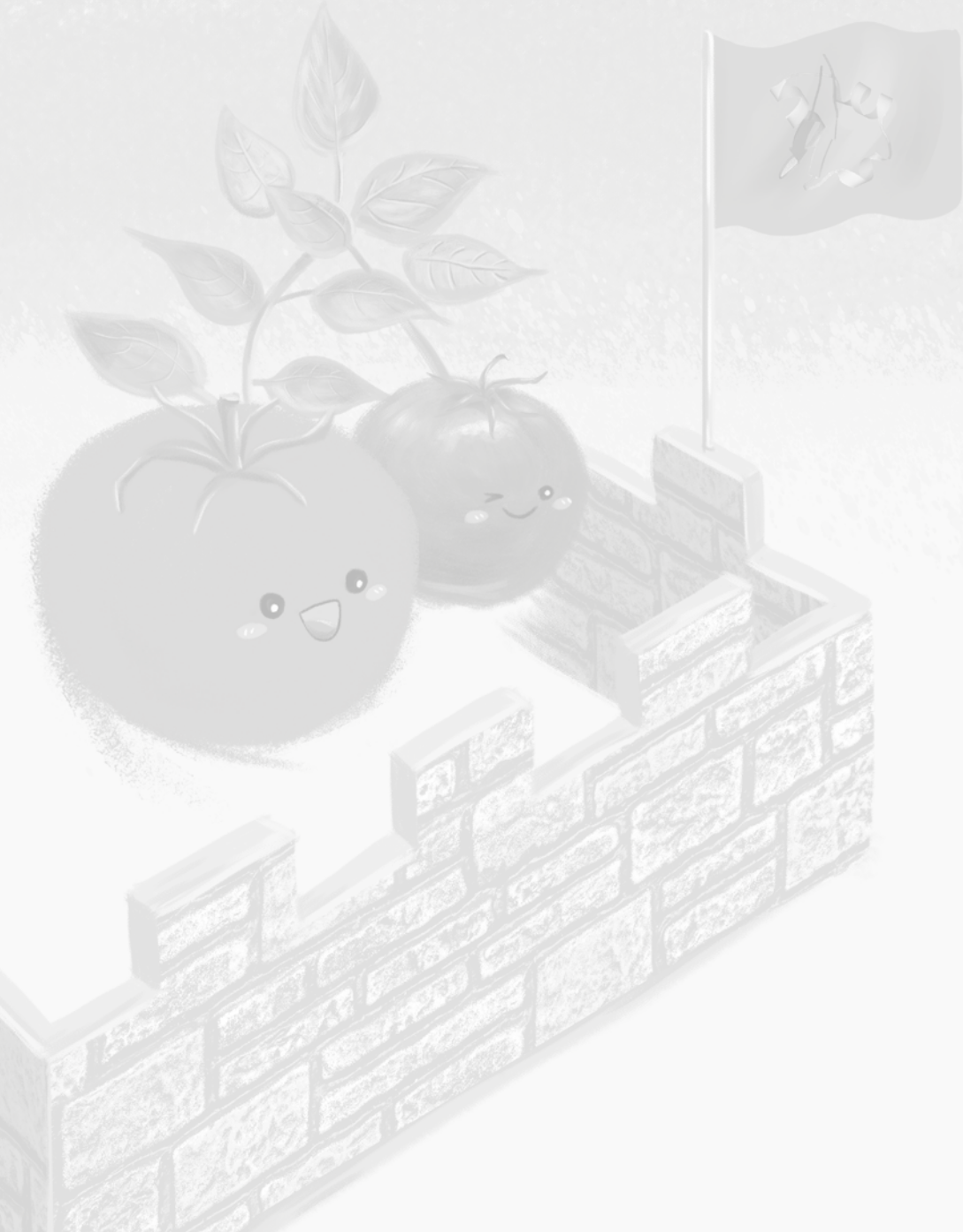

Chapter 3

LysM2 of the *Cladosporium fulvum* effector Ecp6 may contribute to virulence through interference in chitin receptor complex assembly

Hui Tian[1], Hanna Rövenich[1], Jeroen R. Mesters[2], Bart P.H.J. Thomma[1,3]

[1] Laboratory of Phytopathology, Wageningen University and Research, Droevendaalsesteeg 1, 6708PB Wageningen, The Netherlands; [2]Institute of Biochemistry, University of Lübeck, Ratzeburger Allee 160, 23538 Lübeck, Germany; [3]Botanical Institute, Cologne Biocenter, University of Cologne, Zülpicher Straße 47b, 50674 Cologne, Germany

ABSTRACT

The conserved fungal cell wall component chitin acts as a microbe-associated molecular pattern (MAMP) that can be recognized by plant receptors to activate immune signalling. Successful fungal pathogens overcome this host plant recognition through the secretion of effectors that protect their cell walls and deregulate host immunity. For example, the tomato leaf mould fungal pathogen *Cladosporium fulvum* employs the LysM-containing effector Ecp6 to outcompete plant receptors for chitin binding. Two of the three LysM domains of Ecp6 compose a chitin-binding groove with ultra-high substrate affinity that goes beyond the affinity of host receptors. However, while the remaining singular LysM domain of Ecp6, LysM2, displays the capability to bind chitin, it only has a relatively low affinity that falls in the range of host immune receptors and that, therefore, does not permit to outcompete these receptors. Hence, whether LysM2 contributes to fungal virulence remains elusive thus far. In this study, we show that LysM2 of Ecp6 contributes to fungal virulence as mutation of this chitin-binding site leads to a marked decrease in aggressiveness of *C. fulvum* on tomato. More specifically, LysM2 contributes to the suppression of chitin-responsive gene expression in tomato. Interestingly, we demonstrate the occurrence of physical interactions between Ecp6 and previously characterized chitin receptors, where LysM2 seems to confer an interaction in a chitin-independent manner, whereas the composite LysM1-LysM3 binding site contributes in a chitin-dependent manner. Thus, we propose that, besides in competition with plant immune receptors for chitin binding, Ecp6 perturbs the assembly of a receptor complex that is crucial for activation of chitin-induced immunity.

INTRODUCTION

Chitin, a long-chain polymer of *N*-acetylglucosamine (NAc), is a conserved structural cell wall component of fungal organisms, including pathogens and other fungi that engage in intimate host interactions such as endophytes and mutualists. Together with another major structural constituent, β-(1,3)-glucan, chains of chitin form a basic constituent of fungal cell walls. Importantly, chitin acts as a microbe-associated molecular pattern (MAMP) that is recognized by most higher plants and animals as a non-self signal to activate immune signalling (Felix et al., 1993; Shibuya et al., 1993; Sanchez-Vallet., 2015). In plants, cell surface-localized receptors containing lysin motifs (LysMs) recognize chitin molecules that are released from fungal cell walls to activate immune responses to try and halt fungal invasion (Kaku et al., 2006; Miya et al., 2007; Shinya et al., 2015). These immune responses include the production of reactive oxygen species (ROS), the activation of mitogen-activated protein kinases (MAPKs) and transcriptional regulation of other defence-related genes including pathogenesis-related (*PR*) genes (Boller and Felix., 2009).

The first identified chitin receptor was the chitin elicitor binding protein (CEBiP) of rice (*Oryza sativa*), a cell surface-localized glycoprotein containing three extracellular LysM domains and a transmembrane domain (Kaku et al., 2006). Knockdown of CEBiP caused a suppression of chitin-triggered defence responses, such as significantly decreased ROS production (Kaku et al., 2006). Since CEBiP does not carry an intracellular kinase domain, it was anticipated that other proteins are involved in the activation of downstream cellular signalling. Indeed, the transmembrane *Oryza sativa* chitin elicitor receptor kinase 1 (OsCERK1) that carries three extracellular LysM domains and an intracellular Ser/Thr kinase domain was demonstrated to play a critical role in chitin signalling (Shimizu et al., 2010). Moreover, it was proposed that two OsCEBiP and two OsCERK1 molecules form a hetero-tetramer in a ligand-dependent manner to perceive chitin and activate immunity (Akamatsu et al., 2013; Hayafune et al., 2014).

In Arabidopsis, mutants of AtCERK1 exhibit clear loss of ROS production, MAPK activation and *PR* gene expression upon chitin elicitation, implying an important role in chitin signalling (Miya et al., 2007; Wan et al., 2008). Moreover, the Arabidopsis genome possesses four other genes encoding LysM-containing receptor-like kinases (LYKs), namely AtLYK2 to AtLYK5. The expression of *AtLYK4* and *AtLYK5* can be greatly induced by chitin elicitation and AtLYK5 was proposed as the primary chitin receptor in Arabidopsis, since *lyk5* mutant plants displayed a significant suppression of chitin-induced plant responses, and AtLYK5 displays significantly higher binding affinity to chitin when compared with AtCERK1 (Wan et al., 2012; Cao et al., 2014). Though AtLYK5 serves as the main chitin receptor in Arabidopsis, only the double mutant of *Atlyk4*/*Atlyk5* displays fully abolished chitin-induced plant immunity, suggesting at least partially overlapping functions that are shared between AtLYK4 and AtLYK5 in chitin perception (Cao et al., 2014). It has recently been demonstrated that AtLYK4 acts as a scaffold protein that stablizes the AtLYK5-AtCERK1 receptor complex, thus enhancing the chitin-induced immunity in Arabidopsis (Xue et al., 2019).

Successful fungal plant pathogens evolved various mechanisms to overcome chitin-triggered plant immunity (Rövenich et al., 2014; Sanchez-Vallet et al., 2015). These include chemical modification of cell wall chitin and the secretion of so-called effector proteins to either protect cell walls (van den Burg et al., 2006; Marshall et al., 2011; Fujikawa et al., 2012) or perturb the activation of plant immunity (de Jonge et al., 2010; Mentlak et al., 2012; Takahara et al., 2016; Fiorin et al., 2018). For example, the LysM domain-containing effector protein Ecp6 (extracellular protein 6) of the tomato leaf mould pathogen *Cladosporium fulvum* was demonstrated to play a critical role in suppression of chitin recognition by the host because of its ultra-high chitin-binding affinity, allowing to sequester chitin molecules from host receptors (Bolton et al., 2008; de Jonge et al., 2010). Interestingly, homologs of the LysM effector Ecp6 from various fungal pathogens were found to similarly suppress chitin-triggered immunity in their hosts, including LysM effectors of the wheat pathogen *Zymoseptoria tritici* (Marshall et al., 2011), the rice blast fungus *Magnaporthe oryzae* (Mentlak et al., 2012), the Brassicaceae antracnose fungus *Colletotrichum higginsianum* (Takahara et al., 2016), and the broad host range vascular wilt fungus *Verticillium dahliae* (Kombrink et al., 2017). However, not only fungal pathogens employ LysM effectors to suppress host immunity, as the mutualistic fungus *Rhizophagus irregularis* was shown to secrete the LysM effector RiSLM to facilitate the establishment of arbuscular mycorrhizal symbiosis (Zeng et al., 2020).

A crystal structure of the *C. fulvum* Ecp6 molecule revealed that Ecp6 typically occur as a dimer, and that two of the three LysM domains (LysM1 and LysM3) of a single Ecp6 molecule undergo intramolecular dimerization in a chitin-dependent manner, thus establishing a chitin binding groove with picomolar affinity. The remaining LysM domain (LysM2) of Ecp6 can also bind chitin, albeit with a significantly lower (μM) affinity (Sanchez-Vallet et al., 2013). Until now, it has remained unclear whether this relatively low-affinity chitin binding site of Ecp6 contributes to its virulence function as well. In this study, we performed a series of functional assays to investigate the contribution of LysM2 to the functionality of Ecp6 in *C. fulvum* virulence.

RESULTS

LysM2 contributes to the virulence function of *Cladosporium fulvum* LysM effector Ecp6

To determine whether LysM2 of Ecp6 contributes to *C. fulvum* virulence, an *Ecp6* deletion strain of *C. fulvum* was complemented with either of three different *Ecp6* mutant variants carrying a mutation in the chitin-binding domain of LysM2 (T95R; threonine at position 95 substituted by arginine), or in LysM3 (L152R; leucine at position 152 substituted by arginine), or in both LysM2 and LysM3 (T95R-L152R), based on their previously determined importance for chitin-binding (Sánchez-Vallet et al, 2013). As a control, the deletion mutant was complemented with the wild-type *Ecp6* gene. Transformants were collected, subjected to genomic DNA extraction, and the presence of the correct Ecp6 variant was confirmed by PCR (Fig. S1) and sequencing (Fig. S2).

To assess the contribution of LysM2 to *C. fulvum* virulence, the *C. fulvum* wild-type strain, the *Ecp6* deletion strain, and the four complementation strains were inoculated onto four-week-old tomato plants. Similar to previous observations (Bolton et al., 2008; de Jonge et al., 2010), typical leaf mould symptoms emerged on tomato leaves at around 16 days after inoculation with the wild-type strain, whereas the *Ecp6* deletion strain hardly caused any disease symptoms and only showed a few infection sites on the infected leaves, whereas typical leaf mould symptoms emerged on tomato leaves at around 16 days after inoculation with the wild-type strain (Fig. 1A). As expected, the transformants that were complemented with the wild-type *Ecp6* sequence were equally virulent as the wild-type strain (Fig. 1). As anticipated based on the previously determined importance of the chitin binding groove that is composed by LysM domains 1 and 3, the transformant carrying the LysM3 mutant L152R was severely compromised in virulence, although the inoculated leaves developed slightly more symptoms than the *Ecp6* deletion mutant (Fig. 1A). This finding suggests that LysM2 contributes to fungal virulence. This suggestion

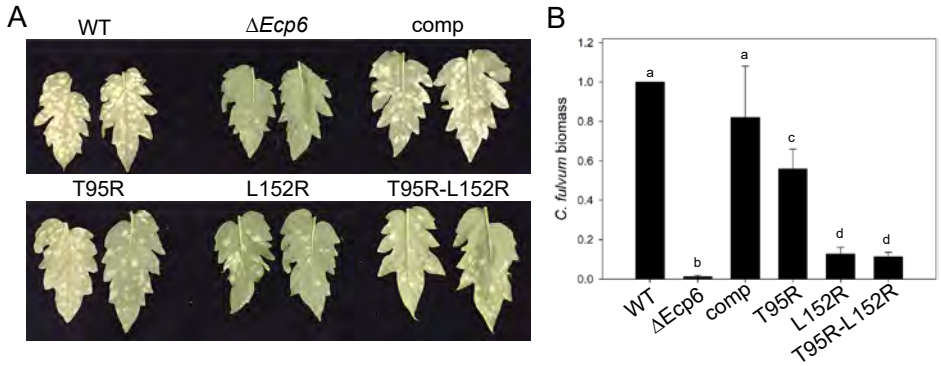

FIGURE 1 | LysM2 of Ecp6 contributes to *C. fulvum* virulence. (A) Representative phenotype of tomato leaves inoculated with the wild-type *C. fulvum* strain race 0 (WT), an *Ecp6* deletion mutant (*ΔEcp6*), and *ΔEcp6* complemented with wild-type *Ecp6* (comp), with the LysM2 mutant (T95R), with the LysM3 mutant (L152R), and with the LysM2-LysM3 double mutant (T95R-L152R), respectively. Pictures were taken at 16 dpi. (B) *C. fulvum* biomass as determined with quantitative RT-PCR at 16 dpi. Bars display the expression levels of *C. fulvum CfTUB* (*Tubulin*) normalized to tomato *SlRUB* (*Rubisco*) with standard deviation as determined for three independent leaves. The biomass of tomato leaves infected with the wild-type *C. fulvum* strain WT was set to 1.0 and the relative fungal biomass in other samples was calculated with the $E^{-\Delta\Delta t}$ method. Different letter labels indicate statistically significant differences between inoculations, calculated with IBM SPSS Statistic 25 (One-way ANOVA; $P < 0.05$).

was further substantiated by the observation that the transformant carrying the LysM2 mutant T95R was able to infect and cause leaf mould symptoms on tomato, albeit with significantly compromised virulence when compared with the wild-type strain and the deletion strain that was complemented with wild-type *Ecp6*. However, the strain was markedly more aggressive than the transformant carrying the LysM3 mutant L152R in which the ultra-high affinity chitin binding site was disrupted. Intriguingly, the transformant carrying both LysM2 and LysM3 mutants T95R-L152R was equally virulent as the transformant carrying the LysM3 mutant L152R,

and more aggressive than the *Ecp6* deletion mutant, which can be explained by the remaining functionality of LysM1 as a singular LysM domain. We previously showed that mutation of LysM1 leads to improper protein folding, so further mutation of this domain was not pursued (Sanchez-Vallet et al., 2013). All visual observations of disease development were mirrored by real-time PCR determinations of fungal biomass, showing that the symptom display positively correlates with the amount of fungal biomass (Fig. 1B). Collectively, our data show that LysM2 of Ecp6 contributes to *C. fulvum* virulence, albeit with a significantly smaller contribution than the ultra-high affinity chitin-binding groove composed by LysM1 and LysM3.

LysM2 of Ecp6 contributes to virulence through suppression of chitin-responsive gene expression in tomato

To investigate how the LysM2 domain contributes to the virulence function of Ecp6, tomato leaves infected with the wild type *C. fulvum* and the various *Ecp6* mutants were harvested at 16 dpi and subjected to RNA isolation. The expression of tomato homologs of various previously characterized chitin-responsive Arabidopsis and rice genes was assessed, including *SlLYK4* (Solyc02g089900), *SlCEBiP* (Solyc01g112080), *SlMPK1* (Solyc12g019460), *SlCHI9* (Solyc10g074440), *PR1A2* (Solyc09g007020) and *PR5* (Solyc08g080660). Indeed, real-time PCR analysis demonstrated that the expression of these tomato genes is induced by chitin treatment (Fig. S3). Interestingly, for each of these genes a similar expression level was recorded upon inoculation with the *Ecp6* deletion strain when compared with the wild-type strain or the complementation strain in which the wild-type *Ecp6* sequence was re-introduced (Fig. 2). Furthermore, a similar expression level was recorded upon inoculation with the complementation line encoding the LysM3 mutant L152R. Intriguingly, however, expression of each of the genes was strongly induced upon inoculation with the complementation line encoding the LysM2 mutant T95R when compared with the wild-type strain (Fig. 2). Collectively, these data point towards a significant contribution of LysM2, but not of the chitin binding groove composed by LysM1 and LysM3, to the suppression of chitin-responsive gene expression during *C. fulvum* colonization by Ecp6. However, expression of chitin responsive genes was not induced upon infection with the transformants carrying the LysM2-LysM3 double mutant T95R-L152R, except for *SlMPK1* and *SlPR1A2* for which an intermediate level of induction was recorded when compared with the induction by the *C. fulvum* LysM2 mutant T95R. Possibly, this observation is due to LysM1 acting as a singular LysM domain that complements LysM2 activity after disruption of the LysM1-LysM3 chitin binding groove.

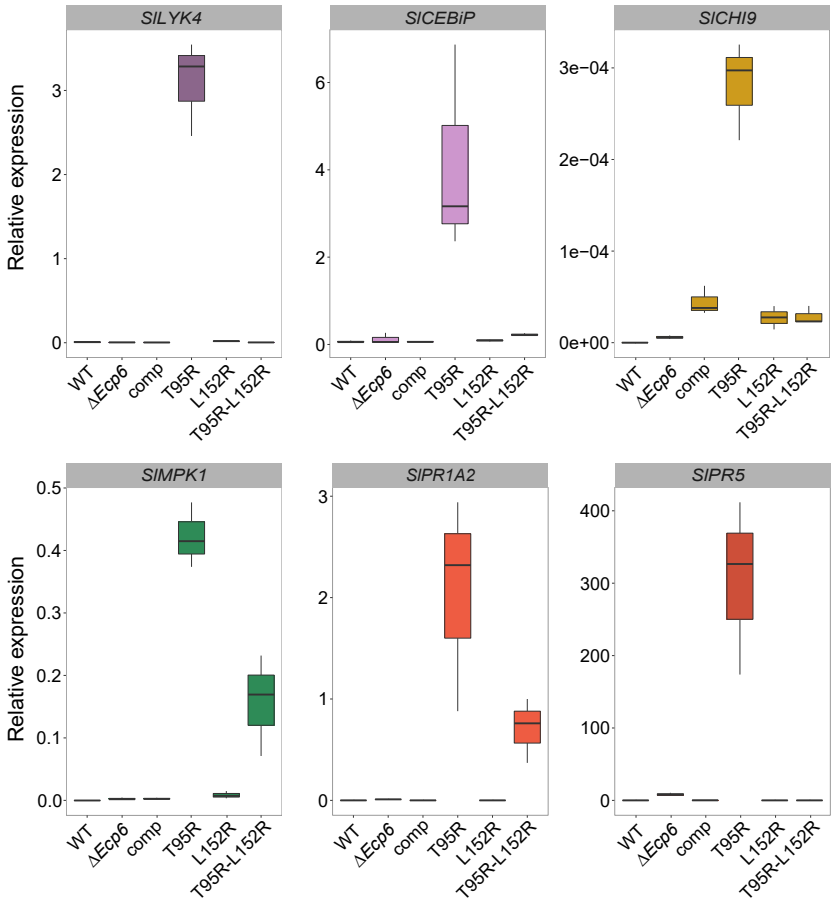

FIGURE 2 | The expression induction of chitin-responsive tomato genes *SlLYK4*, *SlCEBiP*, *SlCHI9*, *SlMPK1*, Sl*PR1A2* and Sl*PR5* at 16 days post inoculation with various *C. fulvum* genotypes. Gene expression was analysed using gene-specific primers in tomato leaves inoculated with wild-type *C. fulvum* (WT), an *Ecp6* deletion mutant (*ΔEcp6*), and *ΔEcp6* complemented with wild-type *Ecp6* (comp), with the LysM2 mutant (T95R), with the LysM3 mutant (L152R), and with the LysM2-LysM3 double mutant (T95R-L152R), respectively. All expression was normalized to tomato *rubisco* (*SlRUB*) and calculated with the $E^{-\Delta t}$ method. Boxplot graphs are made with RStudio with the package of ggplot2.

Ecp6 can interact with plant chitin receptors

Based on the chitin-binding affinity of LysM2, it is highly unlikely that this domain contributes to the suppression of chitin-responsive gene expression through substrate sequestration (Fig. 3 hypothesis I). Therefore, we hypothesized that Ecp6 LysM2 may contribute to suppression of chitin-triggered immunity through perturbation of host receptor complex formation or functioning (Fig. 3 hypothesis II). To address this hypothesis, we assessed whether Ecp6 can interact with the extracellular domain of characterized chitin receptor proteins in the presence and absence of chitin. To this end, we produced FLAG-tagged Ecp6 as well as the LysM2 mutant

T95R on the one hand, and HA-tagged extracellular domains of the Arabidopsis chitin receptor AtLYK5 (Cao et al., 2014) and the tomato LysM receptor kinase SlLYK4 (Chapter 2) on the other hand. Subsequently, co-immunoprecipitation (co-IP) experiments were conducted by incubating *C. fulvum* Ecp6 with these receptors in the presence or absence of chitin. After pull-down with anti-HA magnetic beads, pellets were analysed with western blotting using anti-FLAG and anti-HA antibodies. Indeed, this analysis revealed that Ecp6 is able to interact with AtLYK5 as well as with SlLYK4 in the presence and absence of chitin, because in incubations of Ecp6 with AtLYK5 or SlLYK4 anti-FLAG signal was detected at ~30 kDa, which is the expected molecular size of Ecp6 monomers (Fig. 4). Although the LysM2 mutant T95R was also detected after the incubation with AtLYK5 or SlLYK4 in the presence of chitin, the signals were considerably reduced (Fig. 4), suggesting not only that LysM2 makes a major contribution to the interaction with the receptor proteins, but also that the LysM1-LysM3 groove of Ecp6 contributes to the interaction. Interestingly, the T95R mutant was not detected after the incubation with receptor proteins in the absence of chitin (Fig. 4), suggesting that the interaction of the LysM1-LysM3 binding groove with the receptors is chitin-dependent, while the interaction between LysM2 and the receptors appears to be chitin-independent.

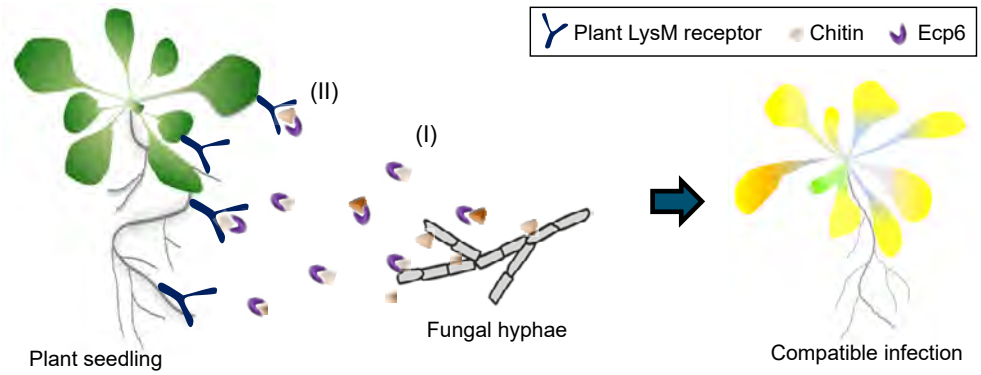

FIGURE 3 | Dual functionality of *C. fulvum* Ecp6. To prevent the recognition of fungal cell wall chitin molecules that are released by plant chitinase hydrolysis, on one hand, i) Ecp6 sequesters chitin from plant receptors with ultra-high affinity, on the other hand, ii) Ecp6 interact with plant receptor in a chitin-dependent manner in order to perturb the formation of receptor complex, thus deregulating the chitin-induced plant immunity.

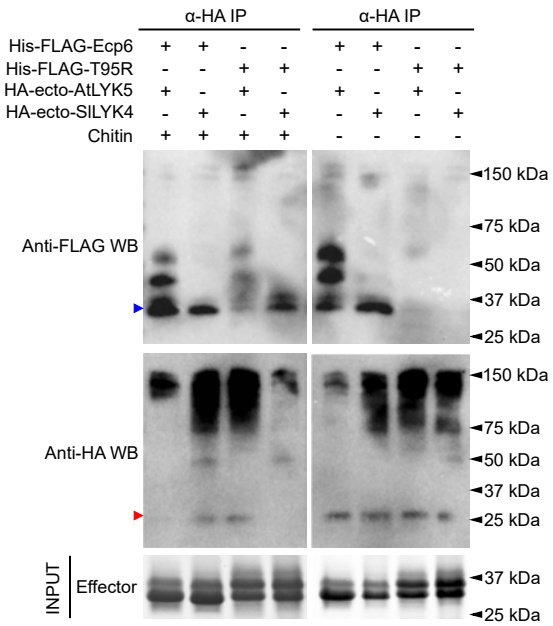

FIGURE 4 | *Cladosporium fulvum* Ecp6 interacts with plant chitin receptors *in vitro*. *Pichia pastoris*-produced FLAG-tagged Ecp6 and the LysM2 mutant T95R (monomer ~30 kDa) were incubated with HA-tagged extracellular domains of Arabidopsis AtLYK5 or tomato SlLYK4 in the presence and absence of chitohexaose (chitin) and pull-down was conducted using anti-HA magnetic beads. Pellets were analysed by western blot analysis with anti-FLAG or anti-HA antibody. Equal effector protein loading was confirmed by protein polyacrylamide gel electrophoresis followed by Coomassie brilliant blue (CBB) staining. Blue and red arrowheads indicate expected molecular sizes of effector and receptor protein monomers, respectively.

DISCUSSION

It has been well established that the *C. fulvum* LysM effector Ecp6 is able to outcompete plant receptors for chitin binding because two of its three LysM domains compose a composite chitin-binding groove that possesses ultra-high substrate binding affinity that goes far beyond the affinity of receptors of plant hosts (de Jonge et al., 2010; Sanchez-Vallet et al., 2013; Rövenich et al., 2014). It was previously determined that the remaining LysM domain of Ecp6, LysM2, binds chitin as well, albeit with a considerably lower affinity that is in the range of that of host chitin receptors (Sanchez-Vallet et al., 2013). This observation suggested that if LysM2 contributes to the virulence function of Ecp6, it is unlikely to operate through competition with host receptors for chitin binding. In this study, we demonstrated that LysM2 indeed contributes to the virulence function of Ecp6 based on two independent observations. Firstly, the virulence of *C. fulvum* carrying a mutation in the coding region of LysM3 that disrupts the ultra-high affinity binding site is not compromised as severely as the virulence of an *Ecp6* deletion mutant of *C. fulvum*. This difference in fungal aggressiveness can only be attributed to a functional LysM2 domain.

Secondly, we observed that the virulence of the *C. fulvum* genotype expressing the LysM2 mutant T95R was significantly compromised when compared with that of the wild-type strain. Thus, we provide unambiguous evidence that LysM2 contributes to the virulence function of Ecp6 during the infection of *C. fulvum* on tomato.

The finding that LysM2 contributes to the virulence function of Ecp6 led to the further question how this domain contributes to fungal virulence. In our study, we demonstrate that LysM2 of Ecp6 acts through the suppression of chitin-responsive tomato genes upon *C. fulvum* infection. Furthermore, we provided evidence for physical interaction between Ecp6 and the extracellular domains of Arabidopsis AtLYK5, a previously established chitin receptor (Cao et al., 2014), and SlLYK4, which was identified as a chitin receptor of tomato in this thesis (Chapter 2) by means of co-IP (Fig. 2; Fig. 4). This finding may suggest that Ecp6 can bind to chitin receptors, possibly to disrupt the homo- or heteromeric dimerization of receptor monomers into receptor complex assemblies that is required for the activation of chitin-triggered immunity (Liu et al., 2012; Hayafune et al., 2014). Interestingly, this interaction between Ecp6 and the chitin receptors could not only be attributed to LysM2 in a chitin-independent manner, but partially also to the cooperative LysM1-LysM3 binding groove in a chitin-dependent manner. Thus, it appears that Ecp6 possesses a dual functionality that comprises i) sequestration of fungal cell wall-derived chitin from plant receptors by competition for chitin binding, and ii) chitin-dependent and -independent interaction with plant receptors, possibly to perturb assembly of the receptor complex that is crucial for the activation of chitin-induced plant immunity (Fig. 3). Arguably, although we have provided evidence for the capability of Ecp6 to physically associate with host chitin receptors, we have not yet provided evidence for such associations to occur *in planta*, nor for detrimental effects on correct chitin receptor complex assembly, or for inhibition of chitin signaling though this interaction. Future efforts should, therefore, be devoted to provide further evidence for this mechanism. However, intuitively, perturbation of host receptor complex functionality rather than scavenging of MAMP molecules would be a more effective manner to disarm host immunity and promote host invasion, as this strategy may be more efficient: once sufficient host receptors are disarmed, the amount of MAMP molecules that are available in the host no longer matters. In any case, if further evidence can be provided for a role of Ecp6 in the obstruction of correct chitin receptor complex formation, it is likely that other LysM effectors that suppress chitin-triggered immunity could display such an activity as well.

MATERIALS AND METHODS

Generation of complementation constructs and *Cladosporium fulvum* mutants

The full length *Ecp6* gene with its native promotor was amplified from genomic DNA of a *C. fulvum* race 0 wild-type strain using primer pair Ecp6-BP-F/R (Table. S1). The PCR product was cloned into the binary vector pCG that was re-constructed based on the vector pCOM but

with an inserted gateway element *ccdB* in the *Kpn* I cleavage site (Zhou et al, 2013) and designated as pCG-Ecp6-WT. The Ecp6 mutants T95R (threonine in amino acid position 95 substituted by arginine) and L152R (leucine in amino acid position 152 substituted by arginine) in which the chitin binding sites of LysM2 and LysM3, respectively, are disrupted were generated by fusion-PCR using primers Ecp6-BP-F/T95R-R, T95R-F/Ecp6-BP-R and Ecp6-BP-F/L152R-R, L152R-F/Ecp6-BP-R (Table. S1). Subsequently, the Ecp6 mutants were cloned into binary vector pCG as pCG-Ecp6-T95R and pCG-Ecp6-L152R. Finally, a mutant in which the two mutations were combined was generated by fusion PCR as well and cloned into pCG as pCG-Ecp6-T95R/L152R. All constructs were introduced into *Agrobacterium tumefaciens* strain AGL-1.

A. tumefaciens-mediated transformation (ATMT) was performed as described previously (Ökmen et al, 2013) with minor modifications. *A. tumefaciens* was first grown in 5 mL minimal medium (MM) supplemented with 50 μg/mL kanamycin at 28°C for two days. After centrifugation at 3,000 g for 5 min, cells were resuspended in 5 mL induction medium (IM) supplemented with 50 μg/mL kanamycin, adjusted to OD_{600} 0.15 and grown at 28°C for at least 6 h until OD_{600} reached 0.5. Meanwhile, conidiospores of the *C. fulvum Ecp6* deletion strain were harvested after two weeks of cultivation on half-strength PDA plates with water, rinsed, and adjusted to a final concentration of 5×10^6 conidiospores/mL. The *A. tumefaciens* suspension was mixed with *C. fulvum* conidiophores in a volume ratio of 1:1 and 200 μL of the mixture was spread onto PVDF membranes that were placed in the centre of IM agar plates. After incubation at 25°C for two days, membranes were transferred onto fresh half-strength PDA plates supplemented with 20 μg/mL geneticin (G418) and 200 μM cefotaxime. All plates were incubated at 25°C for approximately three weeks until *C. fulvum* colonies emerged. Putative transformants were transferred to fresh half-strength PDA supplemented with 20 μg/mL G418 twice, and transformation was confirmed by PCR and DNA sequencing.

C. fulvum virulence assays on tomato

Conidiospores were harvested from three-week-old *C. fulvum* cultures on half-strength PDA plates with water, rinsed, and the spore concentrations were adjusted to 5×10^6 conidiospores/mL with milli-Q water and 0.02% Tween20 was added. Four-week-old tomato cultivar MoneyMaker plants were inoculated with the conidial suspensions by means of spray inoculation onto the lower side of the leaves until droplet run-off. The inoculated plants were placed in a plastic tent for 2 days, after which the tent was opened. Regular inspections for the occurrence of disease symptoms were carried out from 10 dpi onwards, pictures and leaf samples were taken at 16 dpi.

For each inoculation, three tomato leaves with representative disease symptoms were harvested after pictures were taken and subjected to genomic DNA extraction using a CTAB-based extraction buffer (100 mM Tris-HCl PH 8.0, 20 mM EDTA, 2 M NaCl, 3 % CTAB). DNA concentrations were adjusted to 50 ng/μL and 2 μL was used as template for real-time PCR that was performed using SYBR™ green master mix kit (Bioline, London, UK) on a C1000 Touch™ Thermal Cycler (Bio-Rad, California, USA). Relative expression of the *C. fulvum* tubulin gene

(*CfTub)* was normalized to the tomato rubisco gene (*SlRUB*) using primer pairs *CfTub*-F/R and *SlRUB*-F/R, respectively (Table. S1). Ct values were analysed with the $E^{-\Delta\Delta Ct}$ method and the biomass figure was made with SigmaPlot 13.

Gene expression assays

C. fulvum-inoculated tomato leaves were subjected to RNA extraction using TRIzol (Ambion, Texas, USA). The RNA samples were cleaned with the DNA-*free*™ DNA Removal Kit (Invitrogen, California, USA) and 2 ug of each sample was used for cDNA synthesis with M-MLV Reverse Transcriptase (Promega, Wisconsin, USA). Real-time quantitative PCR was conducted in a C1000 Touch™ Thermal Cycler (Bio-Rad, California, USA) using a SYBR™ green master mix kit (Bioline, London, UK). All gene expression was normalized to *SlRUB* and primer pairs are shown in Table 1. Ct values were analysed with the $E^{-\Delta Ct}$ method and the boxplot figures were made with RStudio using the package ggplot2 (Wickham, 2009; R Core Team, 2014).

Heterologous protein production in *Pichia pastoris*

Coding sequences of mature fungal effector proteins without signal peptide and the extracellular domain of plant receptor proteins were amplified, fused with N-terminal 6×His-FLAG- or HA-tag using primers listed in Table S1, respectively, and cloned into the expression vector pPIC9. The primer pairs used for cloning are listed in Table 1. The resulting constructs were checked with DNA sequencing and introduced into *Pichia pastoris* strain GS115. Fermentation of *P. pastoris* was conducted in a BioFlo120 (Eppendorf, Hamburg, Germany) bioreactor at 30°C for a total of 5 days including 3 days of methanol induction.

Yeast cells were collected by centrifugation at 3800 g, 4°C for 50 min. Approximately 3 L of yeast culture was harvested from the bioreactor, centrifuged at 3,800 g for one hour and the supernatant was concentrated to 200 mL using a Vivaflow 200 Cross Flow Cassette (5000NWCO; Sartorius, Göttingen, Germany) at 4°C for approximately 20 h. The resulting concentrated supernatant was purified using His60 Ni Superflow resin (TaKaRa, California, USA) on a BioLogic LP system (Bio-Rad, California, USA). Purified protein was tested on polyacrylamide protein gels and dialyzed against 5 L of 50 mM Tris, 100 mM NaCl to remove imidazole. Finally, proteins were concentrated using Amicon Ultra-15 Centrifugal Filter Units (MERCK, Carrigtohill, Ireland) and stored at -20°C.

Co-immunoprecipitation (co-IP) assays

Pichia pastoris-produced N terminal HA-tagged receptor protein was incubated with 40 μM FLAG-tagged Ecp6 or T95R (final concentration) in 1.5 mL Eppendorf tubes in the presence or absence of 40 μM chitohexaose (final concentration) at 4°C for six hours. Subsequently, 80 μL of Pierce™ Anti-HA magnetic beads (Thermo Fisher Scientific, Massachusetts, USA) was added and incubated overnight at 4°C. The next day, magnetic beads were pulled down using a magnetic stand, washed three times with water and resuspended in 80 μL water. 30 μL of 4x

protein loading buffer (200 mM Tris-HCl, pH 6.5, 0.4 M dithiothreitol, 8% sodium dodecyl sulfate, 6 mM bromophenol blue, 40% glycerol) was added, incubated at 95°C for 10 min and 10 µL was used for a protein polyacrylamide gel followed by immunoblotting that was performed with monoclonal anti-FLAG antibody (MERCK, Darmstadt, Germany) or monoclonal anti-HA antibody (MERCK, Massachusetts, USA).

ACKNOWLEDGEMENTS

H. Tian acknowledges receipt of a PhD fellowship from the China Scholarship Council (CSC). The authors thank Bert Essenstam (Unifarm) for excellent plant care. Work in the laboratory of B.P.H.J. Thomma is supported by the Research Council for Earth and Life Science (ALW) of the Netherlands Organization for Scientific Research (NWO) and by the Deutsche Forschungsgemeinschaft (DFG, German Research Foundation) under Germany´s Excellence Strategy – EXC 2048/1 – Project ID: 390686111.

SUPPLEMENTARY DATA

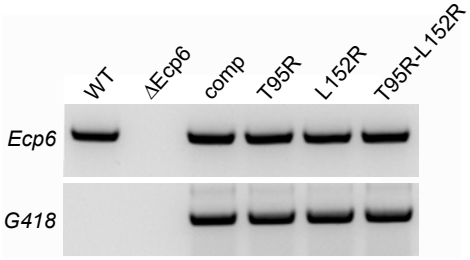

FIGURE S1 | Agrose gel electrophoresis of the PCR products amplified from genomic DNA of the wild-type *C. fulvum* strain (WT), an *Ecp6* deletion mutant (*ΔEcp6*), and *ΔEcp6* complemented with wild-type *Ecp6* (comp), with the LysM2 mutant (T95R), with the LysM3 mutant (L152R), and with the LysM2-LysM3 double mutant (T95R-L152R), respectively. Gene-specific primers for *Ecp6* and the selection marker gene *G418* were used to detect gene presence.

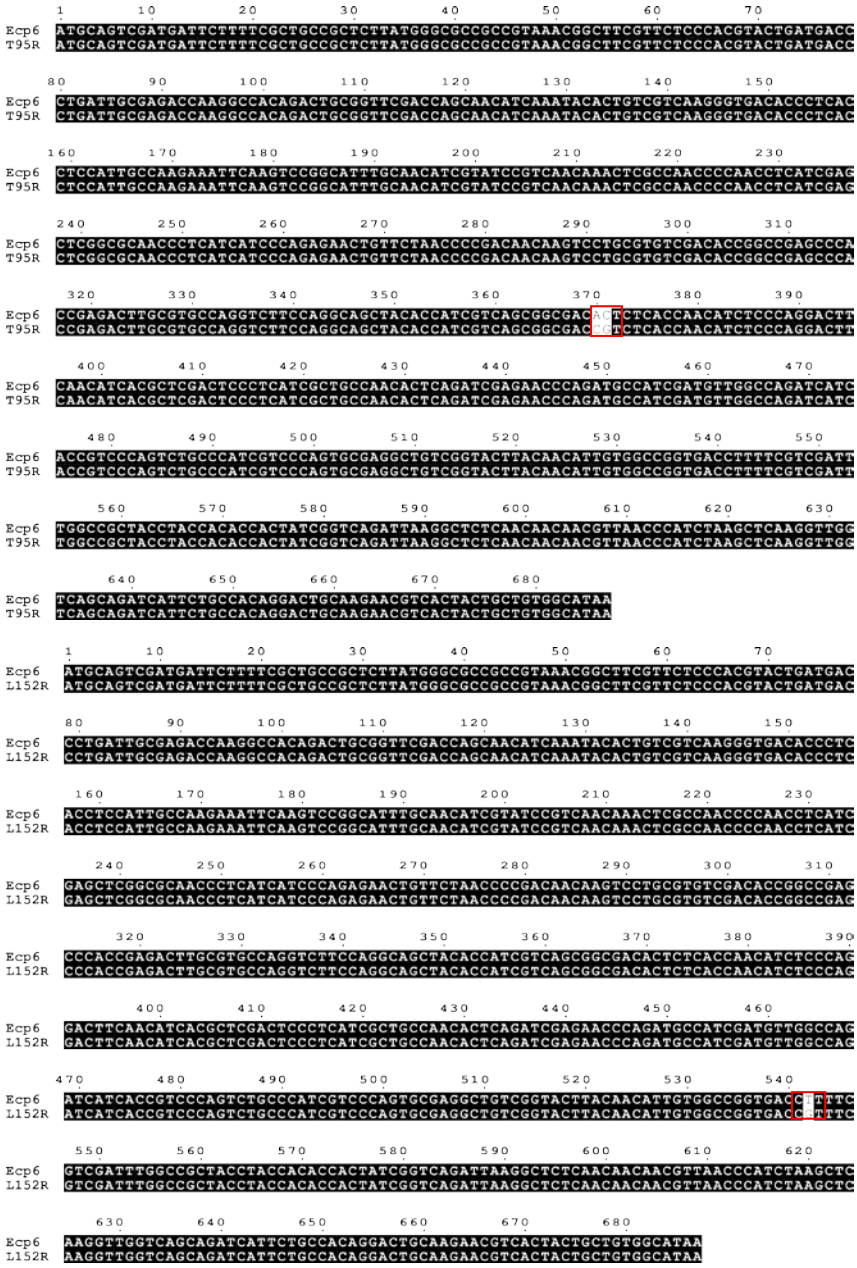

FIGURE S2 | Gene sequence alignments of wild-type *Ecp6* with the fragments amplified from the *Ecp6* deletion mutant (*ΔEcp6*), and *ΔEcp6* complemented with wild-type *Ecp6* (comp), with the LysM2 mutant (T95R), with the LysM3 mutant (L152R), and with the LysM2-LysM3 double mutant (T95R-L152R), respectively, using specific primers targeting full length *Ecp6*. The nucleotide replacements are indicated in red boxes and the alignments were made with Clustal X and ESPript 3.0.

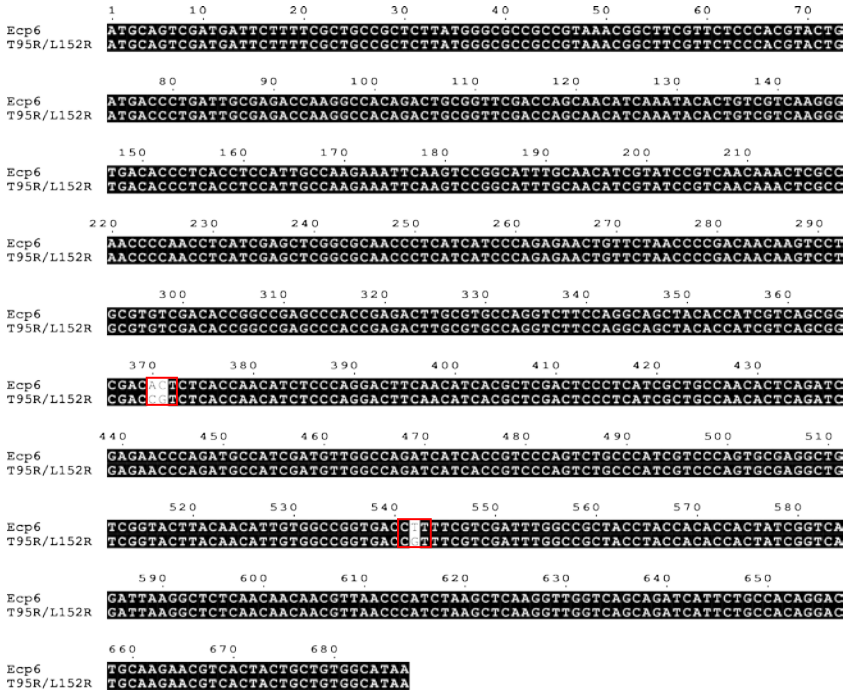

FIGURE S2 | Continued.

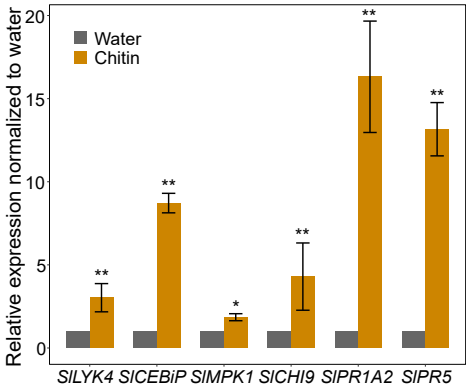

FIGURE S3 | Chitin-inducibility of selected tomato genes. Leaf samples were harvested and incubated in 10 μM chitohexaose or water as negative control. Expression analysis was determined with real-time PCR, normalized to tomato *Rubisco* (*SlRUB*) and calculated with the $E^{-\Delta\Delta t}$ method. The graph is made with RStudio using ggplot2 package. Asterisks indicate significant differences when compared with to water-treated plants and calculated with IBM SPSS statistics with independent sample T-test (* P<0.05; ** P<0.01).

TABLE S1 | Primers used in this study.

Primers	Sequences
Ecp6-BP-F	GGGGACAGCTTTCTTGTACAAAGTGGGTGATGATACCTAATCCCAGTC
Ecp6-BP-R	GGGGACAACTTTGTATAATAAAGTTGTTATGCCACAGCAGTAGTGACG
T95R-F	CACCATCGTCAGCGGCGAC**CGT**CTCACCAACATCTCCCAG
T95R-R	CTGGGAGATGTTGGTGAG**ACG**GTCGCCGCTGACGATGGTG
L152R-F	ACTTACAACATTGTGGCCGGTGAC**CGT**TTCGTCGATTTGG
L152R-R	CCAAATCGACGAA**ACG**GTCACCGGCCACAATGTTGTAAGT
SIRUB-F	GAACAGTTTCTCACTGTTGAC
SIRUB-R	CGTGAGAACCATAAGTCACC
CfTub-F	CCTTCAGAGCTGTAACTGTCC
CfTub-R	CCTCCTTCATAGATACCTT
SlLYK4-Q-F	TCAACGCGGAGAACAGTGAA
SlLYK4-Q-R	GCCCTAAAATCCACCCCAAA
SlCERK1-Q-F	AGGAATCATTTCTCCAAGGGTCATCT
SlCERK1-Q-R	GACCAATCTTATTTTCCATGCTGAAG
SlCEBiP-Q-F	CTTGCCAATCAAGGGTGAGC
SlCEBiP-Q-R	ATCTGGGATGGTTGGCATTG
SlBAP2-Q-F	GGTTTTCCAAAGTGGAACGA
SlBAP2-Q-R	GCAAATAATCTTCGGGCAAA
SlERF5-Q-F	ACTTGAGAGAACGGAAGCCA
SlERF5-Q-R	ACCAAACTCGAGTCCCCTTT
SlCAL-like-Q-F	TGAGATAACGGTGGAGGAGG
SlCAL-like-Q-R	ACATTCCAAATGCTCCCATC
MPK1-Q-F	ATCTTCATGGAGTTGATGGACAGA
MPK1-Q-R	ATGCAAATGGGCTCGTCACTGAT
SlCHI9-Q-F	GCAAATTCGGGTGGTGCGGTA
SlCHI9-Q-R	GAAGGCCATCCTCCAGTAGTT
SlCHI14-Q-F	AACAAAATGAGGCTTTTAGTATTGG
SlCHI14-Q-R	TTTGTAGCAATATCCCCATGAATAT
PR1A2-Q-F	GAGTCGGGCCAATGTCTTGGGA
PR1A2-Q-R	CTAGTCGAACTGAGTCACGCC
PR5-Q-F	GTTCCGGTGTATTTGAGGTCCAT
PR5-Q-F	GTATTCAGCTAAGGTGTTTGGTGG
PR5x-Q-F	CTACACCGTTTGGGCAG
PR5x-Q-R	CAACCAAAGAAATGTCCCAG
SlLYK4-extra-F	CGGTATGAATTCATGGCTACCCGTACGATGTGCCGGATTACGCGACAACAGCCT TATTTTGGAACTGG
SlLYK4-extra-R	CGGTATGCGGCCGCAGTTTTGTTCGAGCTGCTCTC
AtLYK5-extra-F	CGGTATGAATTCATGGCTACCCGTACGATGTGCCGGATTACGCGACAGCAACCG TACGTCAACAACCACCA
AtLYK5-extra-R	CGGTATGCGGCCGCTTAAGAAGAAGAAGATCCCGGAGGATCAA

*The sequence required for Gateway cloning is indicated with blue font. Restriction enzyme recognition sites are indicated with red font, while coding sequences for the HA-tag are indicated with red font and underlining.

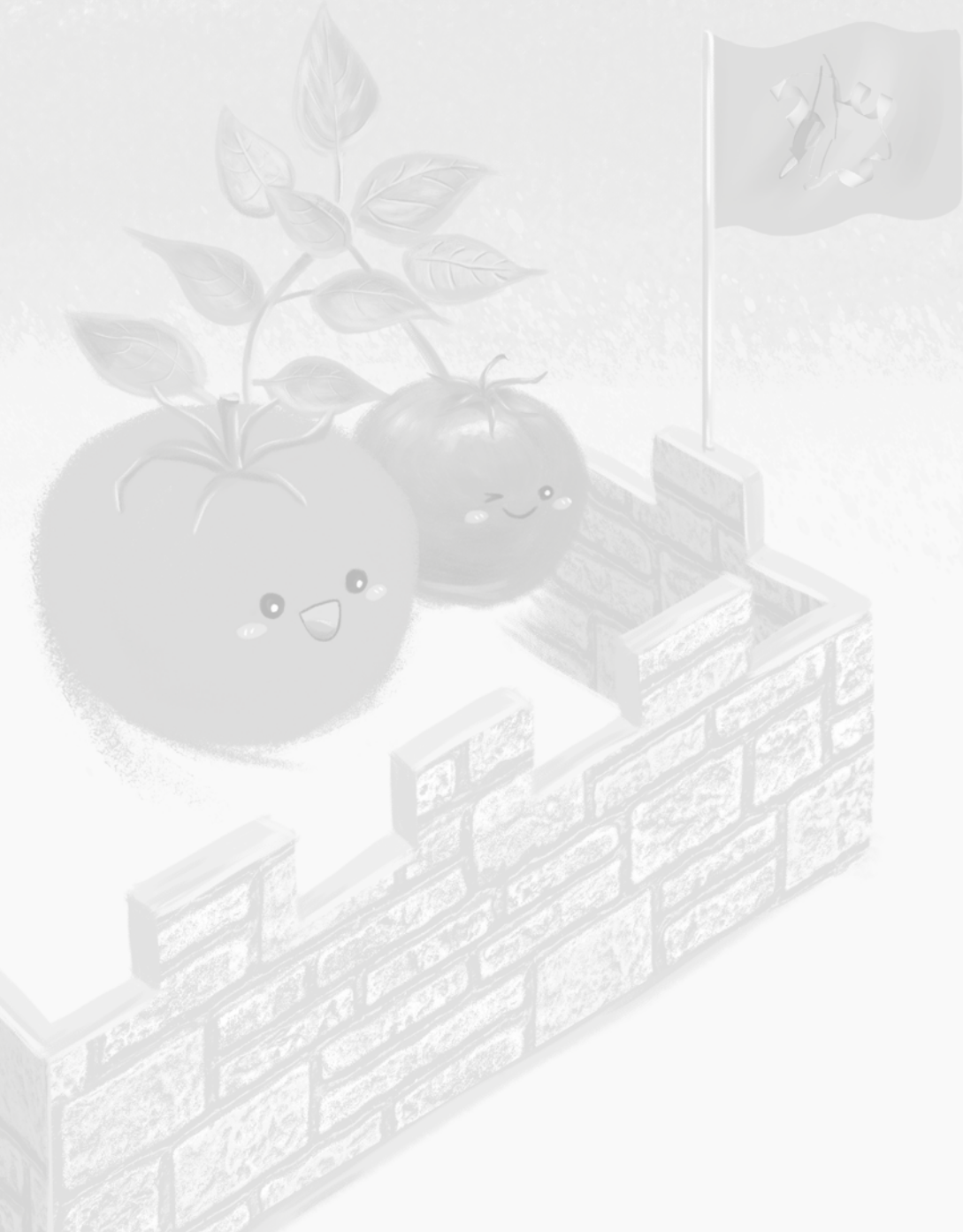

Chapter 4

Fungal LysM effectors that comprise two LysM domains bind chitin through intermolecular dimerization

Hui Tian[1], Gabriel L. Fiorin[1], Anja Kombrink[1], Jeroen R. Mesters[2,*], Bart P.H.J. Thomma[1,3,*]

[1] Laboratory of Phytopathology, Wageningen University and Research, Droevendaalsesteeg 1, 6708PB Wageningen, The Netherlands; [2]Institute of Biochemistry, University of Lübeck, Ratzeburger Allee 160, 23538 Lübeck, Germany; [3]University of Cologne, Institute for Plant Sciences, Cluster of Excellence on Plant Sciences (CEPLAS), 50674 Cologne, Germany.

A modified version has been submitted to Plant Physiology

ABSTRACT

Chitin is a polymer of β-(1,4)-linked *N*-acetyl-D-glucosamine (GlcNAc) and a major structural component of fungal cell walls that acts as a microbe-associated molecular pattern (MAMP) that can be recognized by plant cell surface-localized pattern recognition receptors (PRRs) to activate a wide range of immune responses. In order to deregulate chitin-induced plant immunity and successfully establish their infection, many fungal pathogens secrete effector proteins with LysM domains. We previously determined that two of the three LysM domains of the LysM effector Ecp6 from the tomato leaf mould fungus *Cladosporium fulvum* cooperate to form a chitin-binding groove that binds chitin with ultra-high affinity, allowing to outcompete host PRRs for chitin binding. In this study, we describe functional and structural analyses aimed to investigate whether LysM effectors that contain two LysM domains bind chitin through intramolecular or intermolecular LysM dimerization. To this end, we focus on MoSlp1 from the rice blast fungus *Magnaporthe oryzae*, Vd2LysM from the broad host range vascular wilt fungus *Verticillium dahliae*, and ChElp1 and ChElp2 from the Brassicaceae anthracnose fungus *Colletotrichum higginsianum*. We show that these LysM effectors likely bind chitin through intermolecular LysM dimerization, allowing the formation of polymeric complexes that may precipitate in order to eliminate the presence of chitin oligomers at infection sites to suppress activation of chitin-induced plant immunity.

INTRODUCTION

Chitin is a homopolymer of β-(1,4)-linked *N*-acetyl-D-glucosamine (GlcNAc) and a major structural component of fungal cell walls (Free, 2013; Lenardon et al., 2010). Additionally, chitin has been characterized as a fungal microbe-associated molecular pattern (MAMP) that can be recognized by plant cell surface-localized pattern recognition receptors that contain extracellular LysM domains (LysM-PRRs) (Zhang et al., 2007; Zipfel, 2008; Sanchez-Vallet et al., 2015; Rövenich et al., 2016). Upon recognition of chitin by such receptors, plants evoke a broad range of immune responses including the production of reactive oxygen species (ROS), the activation of mitogen-associated protein kinases (MAPKs), the generation of ion fluxes and the expression of defence-related genes that include those encoding hydrolytic enzymes such as chitinases in order to halt fungal invasion (Felix et al., 1993; Jones and Dangl, 2006; Altenbach and Robatzek, 2007; Boller and Felix., 2009; Sanchez-Vallet et al., 2015). LysM-PRRs have been functionally characterized in several plants, including the model plant Arabidopsis (*Arabidopsis thaliana*) in which the LysM receptor AtLYK5 binds chitin with high affinity (1.72 μM) and recruits AtLYK4 and AtCERK1 upon chitin elicitation to form a tripartite receptor complex to initiate chitin signalling (Cao et al., 2014). AtCERK1 was found to bind chitin directly as well, albeit with approximately 200-fold lower affinity than AtLYK5 (Miya et al, 2007; Petutschnig et al, 2010; Cao et al., 2014). Moreover, a crystal structure of the ectodomain of AtCERK1 revealed that only one out of its three LysMs (LysM2) binds chitin (Liu et al., 2012).

To avoid chitin-induced immune responses, successful fungal pathogens evolved various strategies to either protect fungal cell wall chitin against hydrolysis by host enzymes, or prevent the activation of plant immunity by fungal cell wall-derived chitin oligomers (de Jonge et al, 2011; Thomma et al, 2011; Rövenich et al., 2014; Sanchez-Vallet et al., 2015). A well-studied fungus for which several strategies to deal with chitin-triggered immunity have been characterized is *Cladosporium fulvum*, the fungus that causes leaf mould disease of tomato. *C. fulvum* secretes the Ecp6 effector protein during host colonization, which contains three LysMs and binds chitin oligosaccharides with ultra-high affinity, to prevent the activation of chitin-induced plant immune responses (Bolton et al, 2008; de Jonge et al, 2010). A crystal structure of Ecp6 revealed that two of its three LysMs cooperate to form a composite chitin-binding groove that binds chitin through intrachain LysM dimerization (Sanchez-Vallet et al, 2013). The genome of another host-specific fungus, *Zymoseptoria tritici*, the causal agent of Septoria tritici blotch (STB) of wheat, encodes a close homolog of Ecp6 known as Mg3LysM that similarly suppresses chitin-triggered immunity (Marshall et al., 2011). Additionally, the *Z. tritici* genome encodes two secreted effectors that carry a single LysM only. Of these, Mg1LysM was characterized to protect hyphae against hydrolysis by plant chitinases (Marshall et al., 2011). An Mg1LysM crystal structure showed that two Mg1LysM monomers form a chitin-independent homodimer via the β-sheet that is present in the *N*-terminus of Mg1LysM (Chapter 6). Furthermore, Mg1LysM homodimers undergo ligand-induced polymerization in the presence of chitin, leading to a polymeric structure that is able to protect fungal cell walls (Chapter 6). In contrast to Ecp6 and Mg3LysM, Mg1LysM cannot suppress chitin-triggered immune responses in host plants (Marshall et al., 2011).

Suppression of chitin-triggered immunity by secreted fungal effectors that only carry LysM domains, collectively referred to as LysM effectors, has been demonstrated for various phytopathogenic fungi by now. For instance, *Magnaporthe oryzae*, the causal agent of rice blast disease, secretes the LysM effector Slp1 to bind chitin and suppresses chitin-triggered immune responses (Mentlak et al., 2012). Similarly, the Brassicaceae anthracnose fungus *Colletotrichum higginsianum* secretes Elp1 and Elp2, while the broad host-range vascular wilt fungus *Verticillium dahliae* secretes Vd2LysM (Takahara et al., 2016; Kombrink et al., 2017). While these examples are from plant-associated Ascomycete fungi, also plant-associated fungi that belong to other phyla utilize LysM effectors to suppress chitin-triggered immunity. For instance, the Basidiomycota soil-borne broad host-range pathogen *Rhizoctonia solani* secretes RsLysM, while the Glomeromycota arbuscular mycorrhizal fungus *Rhizophagus irregularis* secretes RiSLM to suppress chitin-triggered immunity (Dolfors et al., 2019; Zeng et al., 2019). The latter example demonstrates that also non-pathogenic fungi utilize LysM effectors in their interaction with host plants. Moreover, the finding that LysM effectors contribute to the virulence of the Ascomycete fungus *Beauveria bassiana* by evasion of immune responses in insect hosts demonstrates that LysM effectors play roles in fungal interactions beyond plant hosts (Cen et al., 2017; Kombrink and Thomma, 2013). Intriguingly, almost all characterized LysM effectors that were shown to suppress chitin-triggered immunity in plant hosts contain two LysM domains, except for Ecp6 and Mg3LysM that possess three LysMs, and RiSLM that possesses only one LysM.

Based on the functional analysis of *C. fulvum* Ecp6, it has been proposed that the ability to suppress chitin-triggered immunity resides in the ability to bind chitin with ultrahigh affinity, such that host chitin receptors can be outcompeted for substrate binding (Sanchez-Vallet et al, 2013; Sanchez-Vallet et al., 2015). In Ecp6, and most likely also in Mg3LysM, the ultrahigh affinity is mediated by intramolecular LysM dimerization of two of the three LysM domains. However, it remains unclear whether LysM effectors that comprise two LysMs are able to similarly undergo intramolecular LysM dimerization, which then would allow for ultrahigh chitin-binding affinity. Thus, in order to understand how these LysM effectors suppress chitin-triggered immunity, we performed functional and structural analysis using several representatives of this group of LysM effectors, namely MoSlp1 from *M. oryzae*, Vd2LysM from *V. dahliae*, ChElp1 and ChElp2 from *C. higginsianum*.

RESULTS

Three-dimensional structure prediction of LysM effectors with two LysM domains

It has previously been determined that MoSlp1 from *M. oryzae*, Vd2LysM from *V. dahliae*, and ChElp1 and ChElp2 from *C. higginsianum* contain two LysM domains, bind chitin and suppress chitin-induced host immunity (Mentlak et al., 2012; Takahara et al., 2016; Kombrink et al., 2017). Their length varies from a minimum of 145 aa (Vd2LysM) to a maximum of 176 aa (ChElp2), with the molecular weight of the mature proteins ranging from 14.24 to 16.14 kDa (Fig. 1A). An amino acid sequence alignment of the LysM domains of the LysM effectors with two LysM domains with those of *C. fulvum* Ecp6 displayed a significant conservation of the domains, and of the residues involved in chitin binding in particular (Fig. S1). Structural analysis of Ecp6 has previously revealed that the first and third LysM domain cooperate to form a composite ultra-high affinity chitin-binding groove, enabled by a long and flexible linker between these domains (Sánchez-Vallet et al., 2013). To assess whether intramolecular LysM dimerization could also occur in MoSlp1, Vd2LysM, ChElp1 and ChElp2, their overall three-dimensional structure was predicted using two software packages, I-TASSER and Phyre2 (Roy et al., 2010; Yang and Zhang, 2015; Kelley et al., 2015). Interestingly, the predicted three-dimensional structures by the different methods resulted in protein models with different substrate-binding possibilities (Fig. 2). The four structures modelled by I-TASSER are predicted to have confidence (C) scores of -0.92, -0.86, -0.99 and -0.91 for MoSlp1, Vd2LysM, ChElp1 and ChElp2, respectively on a scale between -5 and 2, where models with C-scores > -1.5 are considered reliable (Roy et al., 2010). It is important to note that the surface-areas with amino-acid residues involved in chitin binding are facing outward in these structures (Fig. 2), and that the linker regions between the two LysM domains are much more tightly packed and thus do not straightforward permit for a structural reorganisation of the two domains to enable intramolecular LysM dimerization. In contrast, Phyre2 presents a model where the two LysM domains of MoSlp1 are facing inward and intramolecular LysM dimerization is possible by maximally stretching the linker in between the two LysM domains. However, for the three additional LysM effectors Phyre2 is only able to allow intramolecular LysM dimerization by interrupting this linker domain, suggesting that intramolecular LysM dimerization is normally not possible. Thus, except for MoSlp1 for which the two software tools disagree, both tools agree that chitin binding through intramolecular dimerization is highly unlikely. Based on these predictions, we decided to further pursue investigations into the substrate-binding mechanisms of fungal effectors that contain two LysM domains.

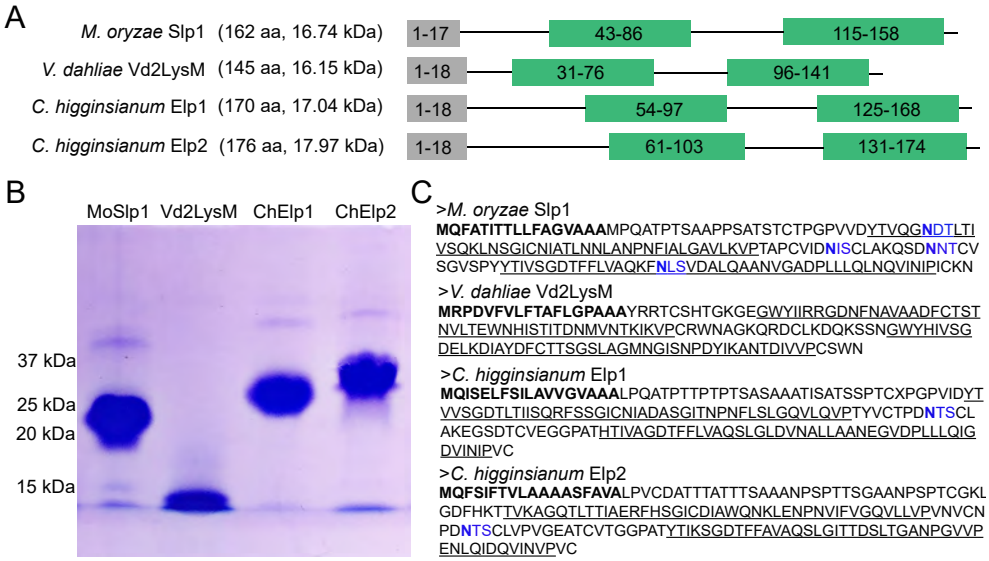

FIGURE 1 | Characteristics and heterologous production of four LysM effectors. (A) Schematic representation of four fungal LysM effectors that contain two LysM domains. Signal peptides (grey boxes) were predicted with SignalP 4.0 (http://www.cbs.dtu.dk/services/SignalP-4.0/) and LysM domains (green boxes) with InterPro (https://www.ebi.ac.uk/interpro/). The numbers in the boxes indicate the amino acids that compose the motif. (B) Protein polyacrylamide gel electrophoresis of 1 µl of purified and concentrated preparation of the effectors produced in *Pichia pastoris* followed by CBB staining. (C) Primary amino acid sequence of the four LysM effectors with signal peptides in bold, LysMs underlined, and putative *N*-glycosylation sites as predicted with the NetNGlyc 1.0 Server (http://www.cbs.dtu.dk/services/NetNGlyc/) in blue. *N*-glycosylation sites are composed of asparagine-X-Serine/Threonine (N-X-S/T) triads, with the asparagines that may be *N*-glycosylated in bold.

Heterologous LysM effector production

The most direct method to reveal the chitin-binding mechanism of a LysM effector is by determination of a three-dimensional protein structure in the presence of chitin, for instance by X-ray crystallography. This strategy requires a protein crystal of sufficient size and quality to be used in an X-ray diffraction experiment, which in turn requires highly pure protein of a sufficiently high concentration. To this end, heterologous production of each of the LysM effectors as *N*-terminally 6×His-FLAG-tagged fusion protein was performed using *Pichia pastoris* as a yeast expression system. After purification from the culture filtrate, the LysM effectors were subjected to protein polyacrylamide gel analysis, revealing that only Vd2LysM migrated as expected based on its predicted molecular weight (Fig. 1A, B). Interestingly, the three other proteins (MoSlp1, ChElp1 and ChElp2) migrated slower than expected based on their calculated molecular weights (Fig. 1A, B), suggesting the presence of post-translational modifications, such as glycan decorations, on these proteins (Haltiwanger and Lowe, 2004; Moremen et al., 2012; Xu and Ng., 2015; Nagashima et al., 2018). On the one hand, however, glycans can greatly hamper crystal packing since they may prevent or reduce favourable molecular contacts between protein molecules. Moreover, glycosylation may

cause microheterogeneity in protein solutions that affects protein ordering as well (Davis et al., 1993; Baker et al., 1994; Tang et al., 2019). On the other hand, glycosylation may be explicitly required for proper protein folding and/or aid in crystal growth by forming critical intermolecular contacts and thus, does not *a priori* hinder crystallization (Mesters et al, 2007).

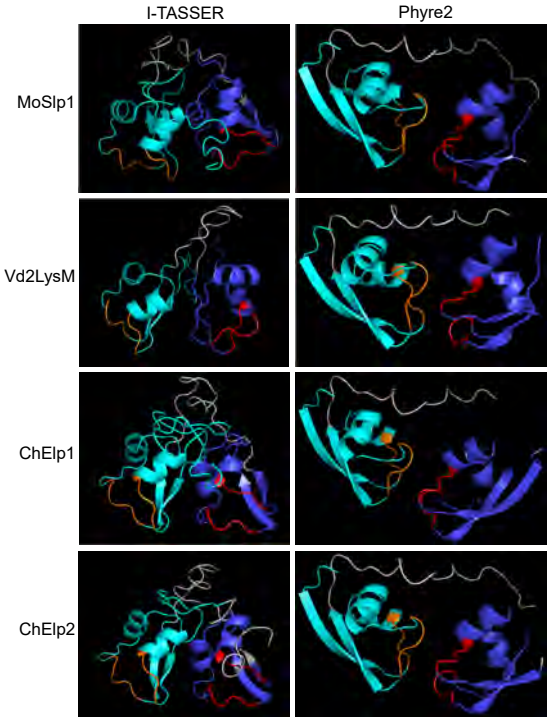

FIGURE 2 | *In-silico* prediction of the three-dimensional structures of four LysM effectors with two LysM domains with I-TASSER and Phyre2 software. Residues proposed to be involved in chitin binding are indicated in orange and red. Structures were visualized using the PyMOL molecular graphics system (Schrodinger, LLC).

To assess the potential for posttranslational modifications to occur on LysMs, we performed *N*-linked protein glycosylation site prediction. MoSlp1 was predicted to possess four potential glycosylation sites (**N**^{48}DT, **N**^{94}IS, **N**^{130}LS and **N**^{104}NT) on four asparagine residues (Asn, N) that match the glycosylation consensus sequence Asn-Xaa-Ser/Thr (N-X-S/T), where X can be any amino acid except proline (Pro, P) or glutamate (Glu, E) (Fig. 1C). ChElp1 as well as ChElp2 contains only a single potential glycosylation site, namely **N**^{105}TS and **N**^{111}TS, respectively (Fig. 1C). Consistent with our protein polyacrylamide gel electrophoresis observation, Vd2LysM is not predicted to possess any glycosylation site (Fig. 1C). These predictions were matched by a glycoprotein staining assay, revealing that Vd2LysM is the only one out of the four proteins that does not react with the dye (Fig. S2), and confirming that MoSlp1, ChElp1 and ChElp2 were indeed glycosylated during yeast production.

In an attempt to increase protein homogeneity and possibly promote crystallization success, enzymatic deglycosylation was pursued based on mannosidase treatment. However, treatment of MoSlp1 and ChElp2 with mannosidase failed to decrease the observed molecular weights of the proteins in polyacrylamide gel analysis (Fig. 3), suggesting that high-mannose-type N-glycans do not form the most important glycan decorations on these proteins. To further pursue enzymatic deglycosylation of the LysM proteins, the peptide:N-glycosidase F (PNGase F) amidase that cleaves between the innermost GlcNAc and asparagine residues of high mannose, hybrid, and complex oligosaccharides from N-linked glycoproteins was used on MoSlp1 and ChElp2. Unfortunately, also this treatment did not decrease the observed molecular weights (Fig. 3).

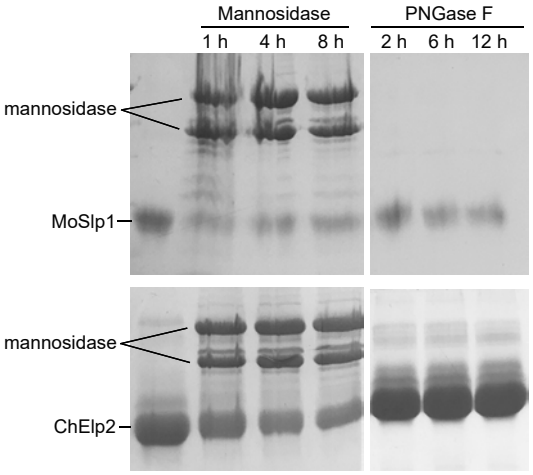

FIGURE 3 | Treatment of the *P. pastoris*-produced LysM effectors MoSlp1 and ChElp2 with mannosidase and PNGase F in an attempt to remove putative *N*-glycans. Polyacrylamide gel electrophoresis of the LysM effectors MoSlp1 (top panels) and ChElp2 (bottom panels) after incubation with mannosidase (left panels) and PNGase F (right panels). Protein samples were collected at different time points after incubation and subjected to gel electrophoresis followed by CBB staining.

As an alternative strategy to reduce glycosylation of the protein preparations, site-directed mutagenesis was conducted on *ChElp1* and *ChElp2* such that the asparagines in the single potential glycosylation sites, $\mathbf{N}^{105}$ and $\mathbf{N}^{111}$ respectively, were replaced by glutamines (Gln, Q). Unfortunately, however, production of the mutated proteins failed repeatedly due to protein instability. As we have previously successfully crystallized Ecp6 protein that was produced in the same manner despite containing two spatially close glycosylation sites that were indeed found to be glycosylated in the crystal structure (Sanchez-Vallet et al., 2013), we decided to arrest our efforts to prevent glycosylation of the proteins.

Solubility and homogeneity of the LysM protein preparations

Since the isoelectric point (pI) is an important indicator of protein solubility, the pI of the four proteins was calculated. Whereas MoSlp1, ChElp1 and ChElp2 were determined to be acidic proteins with pI of 4.48, 3.73 and 4.64, respectively, Vd2LysM was calculated to have a rather neutral pI of 7.76. Based on the pIs, all four LysM proteins were dissolved in a buffer with pH 8.5 (20 mM Tris, 150 mM NaCl, 5% glycerol), and concentrated (>7 mg/mL) without occurrence of visible precipitation (Table S1).

Next, dynamic light scattering (DLS) was employed to determine the molecular homogeneity of the protein solutions (Bergfors, 1999; McPherson, 1999; Proteau and Cygler, 2010; Dessau and Modis, 2011). The DLS heatmaps exhibited extremely heterogenous particle size distributions for each of the LysM proteins. In particular, the particle size distribution for MoSlp1 and ChElp2 was quite heterogenous and ranged from 10 nm to 100 nm (Fig. 4A), which is significantly larger than the expected size of 1-3 nm for a protein with a molecular weight of approximately 16 kDa. Although less heterogenous, ChElp1 mostly occurred as particles of around at 100 nm, which again points towards a significant degree of aggregation (Fig. 4A). Finally, Vd2LysM occurred as a heterogenous population of particles of 100 nm and larger. The heterogeneity of the four protein preparations together with the relatively large particle size is likely to negatively impact crystal formation (Niesen et al., 2008; Price et al., 2009).

In order to improve protein solubility and particle size distribution, gel filtration and mild detergent treatment were pursued for all four LysM effectors. However, eventually, we only successfully improved the homogeneity of Vd2LysM and ChElp2 by gel filtration combined with the treatment with the nonionic detergent decyl β-D-maltopyranoside (DM). These protein samples were tested by DLS, which revealed uniform particle distributions for both proteins with main molecular populations at around 10 nm (Fig. 4B). Therefore, both protein preparations were used for crystallization screenings.

Attempts to obtain protein crystals failed for all four LysM effectors

Primary protein crystallization is a screening experiment where a concentrated solution of target protein is subjected to a variety of conditions that cover a wide range of buffers, salts, precipitating agents, pH, additives and even ligands (Chayen and Saridakis, 2008; Bergfors, 2009; Skarina et al., 2014). The ultimate aim is to reach a protein's supersaturation state, where protein molecules may self-assemble into a periodically repeating pattern that extends in three dimensions, yielding protein crystals. For protein crystallization, there is no systematic analysis or comprehensive theory to guide efforts to directions that can increase the success rate. Consequently, macromolecular crystal growth largely remains empirical (McPherson and Gavira, 2014). Both structures of *C. fulvum* Ecp6 and *Z. tritici* Mg1LysM were determined using protein crystals obtained from *P. pastoris*-produced protein preparations without additional chitin treatment. However, chitin molecules were found to be already present in the Ecp6 and Mg1LysM crystals, suggesting that they were derived from the cell wall of yeast. In this study, four *P. pastoris*-produced LysM proteins

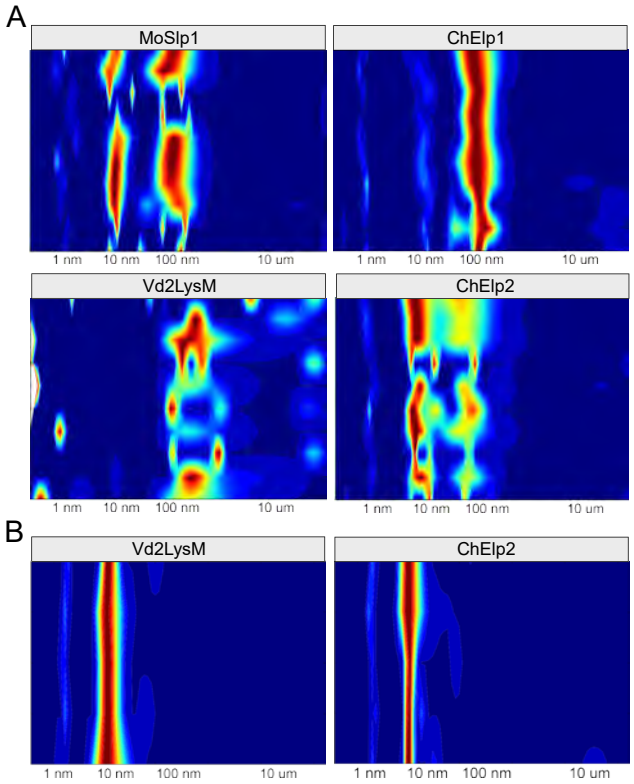

FIGURE 4 | Particle size distribution of four LysM effectors as measured by dynamic light scattering (DLS). The particle size distribution is shown as a colour scale heat map ranging from blue (lowest abundance) to red (highest abundance) for a particle size range of 1 nm to 100 µm. (A) Heat maps of the four *Pichia pastoris*-produced LysM effectors after initial purification and concentration. (B) Heat maps of Vd2LysM and ChElp2 after gel filtration and decyl β-D-maltopyranoside (DM) treatment.

were directly subjected to initial screening using commercial crystallization kits PACT premier™, Salt^{RX}, Index™, PEG^{RX} and PEG/Ion screen (96 conditions/kit) with the original concentrations (Table S1). Because we observed instant heavy precipitations in more than half of the conditions, the four LysM protein preparations were diluted to half the original concentrations and subjected to the initial screening again. Unfortunately, none of these attempts yielded any genuine protein crystals. Subsequently, we pre-incubated the LysM proteins with chitinhexaose in molar ratios of 3:1 and 1:1 (protein:chitin) and subjected them to the initial crystallization screening again. However, even after one year, none of the conditions developed genuine protein crystals.

To promote crystallization, active small molecules, traditionally referred to as "additives", can be added to promote the formation of favourable lattice contacts (McPherson and Cudney, 2006; McPherson et al., 2011). Therefore, we conducted further screenings by adding 96 additives into two different buffers, namely i) 0.1 M HEPES, 30% PEG 3350, pH 7.0; ii) 50%Tacsimate, which is a mixture of organic acids with pH 7.0, for all four LysM proteins at their original concentrations

as well as at half-diluted concentrations. Unfortunately, none of these attempts yielded any genuine protein crystals.

Finally, Vd2LysM and ChElp2 were produced in *E. coli* and subjected to an initial screening in the absence of exogenously added chitin and after pre-treatment with chitinhexaose in molar ratios of 3:1 and 1:1 (protein:chitin) using the five commercial kits, and also subjected to the additive screen kit in the two different buffers. Unfortunately, also these attempts were in vain.

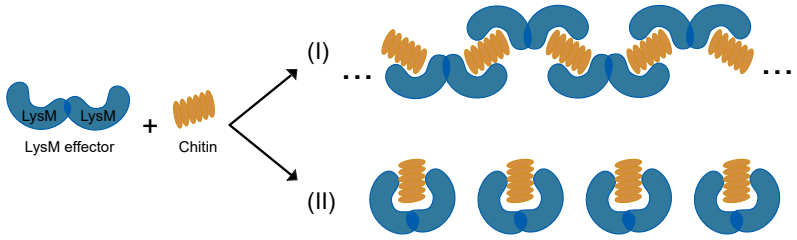

FIGURE 5 | Two hypotheses for chitin binding by fungal effectors containing two LysM domains. LysM effectors that contain two LysMs may bing chitin through (I) intermolecular dimerization, in which LysM effectors may undergo ligand-induced polymerization, or through (II) Intramolecular dimerization, which should not lead to polymerization.

Chitin-induced polymerisation suggests intermolecular LysM dimerization

As all our crystallization attempts for the four different LysM effectors failed, we pursued other strategies to provide evidence for the occurrence of either inter- or intramolecular LysM dimerization. We reasoned that treatment with chitin oligomers would lead to higher order oligomeric or polymeric protein complexes if intermolecular LysM dimerization occurs (Fig. 5, hypothesis I), while such complexes will not be formed in case of intramolecular LysM dimerization (Fig. 5, hypothesis II). To address these hypotheses, ChElp2 was selected as a representative and was expressed in *Escherichia coli* to obtain protein that is devoid of chitin. After purification and concentration, the aggregation status of the two protein preparations was tested with DLS. Interestingly, the addition of chitin resulted in a clear shift in particle size distribution in a concentration-dependent manner. Whereas a 3:1 protein:chitin molecular ratio shifted the particle size distribution of ChElp2 towards larger complexes of 10 nm to 100 nm (Fig. 6), further addition of chitin to a protein:chitin ratio of 1:1 fully shifted the dominant ChElp2 particle size towards 100 nm (Fig. 6). This finding strongly suggests that chitin addition mediates intermolecular LysM dimerization, leading to the formation of polymeric protein complexes.

As a second, independent line of evidence for polymerization, we hypothesized that if ChElp2 undergoes chitin-induced polymerization, we should be able to precipitate polymeric complexes during centrifugation. Thus, with Ecp6 as a negative control, we incubated ChElp2 overnight with chitohexaose and subsequently centrifuged the samples at 20,000 g in the presence of 0.002% methylene blue to visualize the protein. Indeed, a clear protein pellet appeared when ChElp2 was incubated with chitin, but not in the control treatment without chitin, nor in the Ecp6 samples

(Fig. 7). Next, we assessed whether a similar precipitation in the presence of chitin, as evidence for polymerisation, could be obtained for MoSlp1 and Vd2LysM as well. Indeed, this appeared to be the case (Fig. 7). Collectively, these data confirm the occurrence of chitin-induced polymerisation of LysM effectors that comprise two LysMs, and prove that intermolecular dimerization (Fig. 5, hypothesis I) rather than intramolecular dimerization (Fig. 5, hypothesis II) occurs in the presence of chitin.

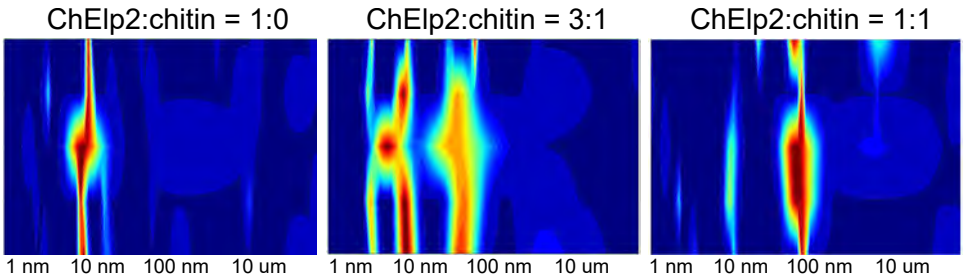

FIGURE 6 | Particle size distribution of ChElp2 in absence and presence of chitin as measured by dynamic light scattering (DLS). The particle size distribution is shown as a colour scale heat map ranging from blue (lowest abundance) to red (highest abundance) for a particle size range of 1 nm to 100 μm.

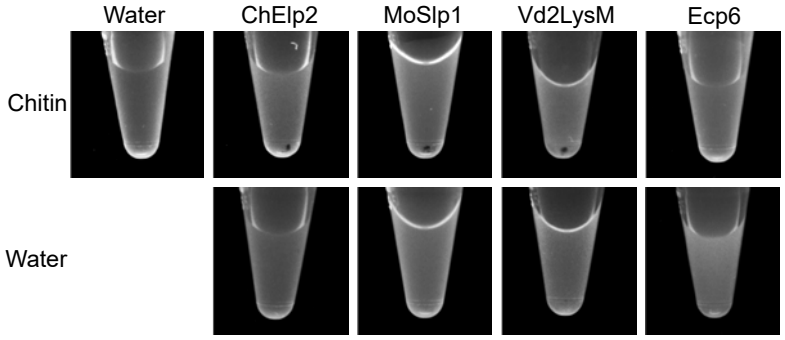

FIGURE 7 | Chitin-induced polymerization of LysM effectors with two LysM domains. The LysM effector proteins ChElp2, MoSlp1 and Vd2LysM, together with Ecp6 as negative control, were incubated with chitohexaose (chitin) or water. After overnight incubation, methylene blue was added and protein solutions were centrifuged, resulting in protein pellets (red arrowheads) as a consequence of polymerization for ChElp2, MoSlp1 and Vd2LysM, but not for Ecp6.

DISCUSSION

To address the question whether LysM effectors that comprise two LysM domains bind chitin through inter- or intramolecular dimerization, we heterologously expressed four such LysM proteins and pursued the determination of 3D-protein structures based on X-ray crystallography. We screened the four *P. pastoris*-produced LysM effectors in two different concentrations with five different commercial kits that amount to a total of 480 conditions, in absence and presence of chitin in two different ratios, as well as with an additive screening in two different buffers with a total of 192 conditions. Moreover, for Vd2LysM and ChElp2, *E. coli*-produced protein was screened under the above-mentioned conditions as well. Although we tested this large amount of conditions on four homologous proteins, no protein crystals developed. Generally, if crystallization of a protein fails, it can be attributed to many factors, ranging from insufficient purity and homogeneity of the protein, to the fact that some proteins are simply naturally or biologically unable to crystalize (Dessau and Modis, 2011; Wlodawer et al., 2017). In this study, we tried to address as many factors with respect to protein quality as possible, but our attempts to obtain protein crystals failed nonetheless.

Obviously, absence of crystal formation does not prove that crystal formation is impossible. However, the lack of crystal formation inspired our further thoughts about LysM effector chitin binding. Theoretically, we anticipated that two possible substrate-binding mechanisms may occur for our LysM effectors (Fig. 5): chitin binding through inter- (hypothesis I) or intramolecular (hypothesis II) chitin binding. If intramolecular chitin binding would occur, it can be expected that chitin molecules reduce protein flexibility and promote protein homogeneity in solution, theoretically promoting crystal formation. However, arguably, if intermolecular chitin binding is prevalent, polymerization is likely to occur, which may involve chains of polymers of variable lengths. As a consequence, homogeneity in protein solution may be severely compromised, leading to precipitation rather than to crystallization. The finding that exogenously added chitin can induce the formation of oligomeric complexes of ChElp2 as determined in DLS experiments (Fig. 6) suggested that oligomers indeed occur, pointing towards the occurrence of intermolecular dimerization as proposed in hypothesis I (Fig. 5). However, solid proof was subsequently obtained by performing centrifugation experiments upon incubation with chitin hexamers, revealing that protein pellets as a consequence of chitin-induced polymerisation were obtained not only for ChElp2, but also for MoSlp1 and VdLysM2 (Fig. 7). The finding that such pellets were not obtained with Ecp6 is important, as it demonstrates that the pellets are associated with intermolecular dimerization of LysM effector molecules, a process that is not supposed to occur with Ecp6 that undergoes intramolecular LysM dimerization (Sánchez-Vallet et al., 2013).

The initial prediction of the three-dimensional protein structures with I-TASSER as well as with Phyre2 could not support the occurrence of intramolecular dimerization of LysMs to mechanistically explain chitin binding by LysM effectors that comprise two LysMs. Our experimental evidence further supports this notion. Taken together, we propose that fungal LysM effectors that comprise two LysM domains bind chitin through intermolecular dimerization,

contributing to fungal virulence through formation of polymeric complexes that have the propensity to precipitate in order to eliminate the presence of chitin oligomers at infection sites that may otherwise alarm the host immune system.

MATERIALS AND METHODS

Sequence alignment and three-dimensional protein structure prediction

LysM domains of proteins were predicted by InterPro (https://www.ebi.ac.uk/interpro/; Finn et al., 2017) and the alignment of amino acid sequences was performed by ClustalX2. Protein structures were predicted with I-TASSER (https://zhanglab.ccmb.med.umich.edu/I-TASSER/; Roy et al., 2010) and with Phyre2 (http://www.sbg.bio.ic.ac.uk/~phyre2/html/page.cgi?id=index; Kelley et al., 2015). Structures were viewed by the PyMOL molecular graphics system, version 2 (DeLano, 2004).

Heterologous protein production in *Pichia pastoris*

Protein sequences were analysed using SignalP4.0 (http://www.cbs.dtu.dk/services/SignalP; Petersen et al., 2011) and the coding sequences of mature proteins without signal peptide were amplified with primers listed in Table S2, fused with an N-terminal 6×His-tag and cloned into expression vector pPIC9 (Thermo Fisher Scientific, California, USA). Correctness of the resulting constructs was confirmed by DNA sequencing prior to introduction into *Pichia pastoris* strain GS115 (Thermo Fisher Scientific, California, USA). Fermentation was conducted in approximately 3 L of culture in a bioreactor BioFlo120 (Eppendorf, Hamburg, Germany) at 30°C for 5 days, including 3 days of methanol induction. Next, *P. pastoris* cells were pelleted by centrifugation at 3800 g at 4°C for 50 min and the supernatant was concentrated to 200 ml using a Vivaflow 200 Cross Flow Cassette (5000NWCO; Sartorius, Göttingen, Germany) at 4°C for approximately 20 h. The concentrated supernatant was purified using His60 Ni Superflow resin (TaKaRa, California, USA) on a BioLogic LP system (Bio-Rad, California, USA). Purified protein was analysed by protein polyacrylamide gel electrophoresis followed by staining with Coomassie Brilliant Blue (CBB) and dialyzed against 5 L of 50 mM Tris, 150 mM NaCl to remove imidazole. Finally, proteins were further concentrated using Amicon Ultra-15 Centrifugal Filter Units (MERCK, Carrigtohill, Ireland) and stored at -20°C.

Heterologous protein production in *E. coli*

Coding sequences of mature proteins without signal peptide were amplified with primers listed in Table S2 and cloned into expression vector pETSUMO (Thermo Fisher Scientific, Massachusetts, USA). Correctness of the resulting constructs pETSUMO-ChElp2 and pETSUMO-Vd2LysM were confirmed by DNA sequencing and introduced into *E. coli* strains BL21 and Origami, respectively. Both proteins were produced at 28°C with 0.2 mM IPTG. Cell culture was pelleted

by centrifugation at 4000 g for 40 min at 4°C, and the pellet was resuspended in 20 mL lysis buffer (Table S2), shaken at 4°C for at least two hours and centrifuged at 10,000 g for 1 h. The supernatant was collected and purified using His60 Ni Superflow resin (TaKaRa, California, USA) on a BioLogic LP system (Bio-Rad, California, USA). The resulting protein was dialyzed 3 L of 20 mM Tris, 150 mM NaCl, 5% glycerol, pH 8.0 while 5 μL of cleavage protein ULP1 was added into the dialysis membrane to cleave-off the 6×His-SUMO tag. Next day, protein solution was collected and subjected to purification using His60 Ni Superflow resin (TaKaRa, California, USA) to remove 6×His-SUMO tag from the protein preparations. Eventually, LysM proteins were dissolved in 20 mM Tris, 150 mM NaCl, 5% glycerol, pH 8.0 and concentrated to a high concentration.

Glycoprotein staining assay

1 μL of concentrated LysM protein solution was tested using a protein polyacrylamide gel followed by CBB and glycoprotein staining with the Pierce Glycoprotein Staining Kit (Thermo Fisher Scientific, California, USA) according to the manufacturer's instructions, including the addition of horseradish peroxidase and soybean trypsin inhibitor as positive and negative control, respectively.

Mannosidase and PNGase F treatments

Deglycosylation was conducted with α-Mannosidase from *Canavalia ensiformis* (MERCK, New Jersey, USA) and PNGase F (MERCK, New Jersey, USA) according to the manufacturer's instructions. 5 μl of concentrated LysM protein solution was treated with 10 μl of α-mannosidase (1 mg/ml, pH 4.5) at 25°C or 1 μl PNGase F (one unit, pH 7.5) at 37°C. Protein samples were collected after 1, 4 and 8 h of incubation for α-mannosidase treatment, and after 2, 6 and 12 h of incubation for PNGase F treatment. Subsequently, protein samples were analysed using protein polyacrylamide gel electrophoresis followed by CBB staining.

Crystallization conditions

Commercial kits PACT premier™ (Molecular dimensions, Sheffield, UK) and Salt^{RX}, Index^{TM}, Shotgun, PEG^{RX}, PEG/Ion screen (Hampton Research, California, USA) were used for initial screening. 96-well protein crystallization plates were prepared using a Crystal Phoenix robot (Art Robbins Instruments, California, USA). Chitohexaose (Megazyme, Wicklow, Ireland) was added in molar ratios of 3:1 and 1:1. The additive screening was conducted using the Additive Screen HR2-428 (Hampton Research, California, USA) and Tacsimate pH 7.0 (Hampton Research, California, USA) according to the manufacturer's instructions.

Dynamic light scattering (DLS) measurements

LysM proteins were dialyzed overnight against 100 mM NaCl and used for particle size distribution measurement using a SpectroSize 300 machine (Xtal Concepts, Hamburg, Germany). For the chitin-induced polymerization measurements, proteins were dissolved in 20 mM Tris, 150 mM

NaCl, pH 8.0 and treated with 0.1 % Triton X-100. Chitohexaose (Megazyme, Wicklow, Ireland) was added in molar ratios of 1:1 and 1:2 (protein:chitin) and incubated for 4 hours.

Polymerization assay

LysM effector proteins were adjusted to a concentration of 200 μM and 200 μL of each protein was incubated with 200 μL of 2 mM chitohexaose (Megazyme, Wicklow, Ireland), or 200 μL water as control, at room temperature overnight. The next day, 2 μL of 0.2% methylene blue (Sigma-Aldrich, Missouri, USA) was added and incubated for 30 min after which protein solutions were centrifuged at 20,000 g for 15 min. Photos were taken with a ChemiDoc MP system (Bio-Rad, California, USA) with custom setting for RFP.

ACKNOWLEDGEMENT

H. Tian acknowledges receipt of a PhD fellowship from the China Scholarship Council (CSC). The authors thank Bert Essenstam (Unifarm) for excellent plant care. Work in the laboratory of B.P.H.J. Thomma is supported by the Research Council for Earth and Life Science (ALW) of the Netherlands Organization for Scientific Research (NWO) and by the Deutsche Forschungsgemeinschaft (DFG, German Research Foundation) under Germany's Excellence Strategy – EXC 2048/1 – Project ID: 390686111.

SUPPLEMENTARY DATA

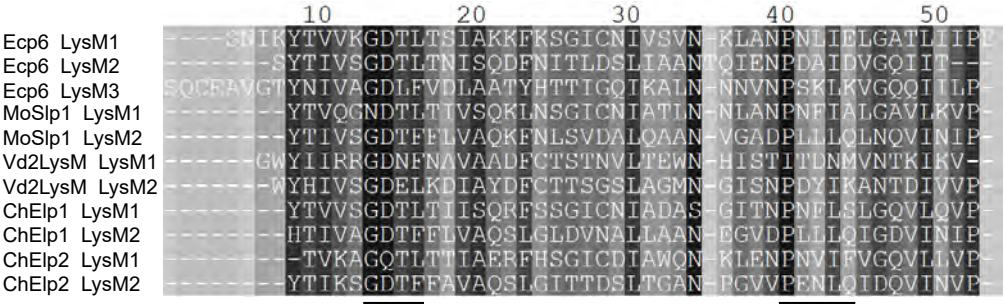

FIGURE S1 | Amino acid sequence alignment of the LysM domains of four LysM effector proteins with two LysM domains in comparison with those of Ecp6. Residues that are predicted to be involved in chitin-binding are indicated with black underlining.

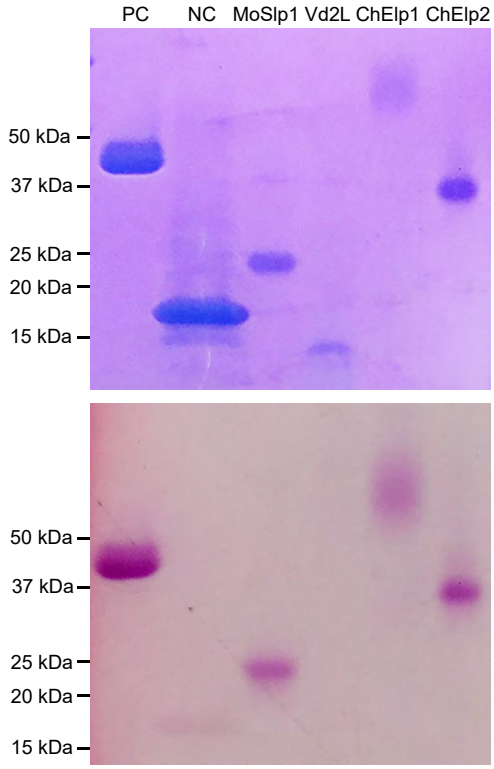

FIGURE S2 | Coomassie brilliant blue (top panel) and glycoprotein staining (lower panel) of polyacrylamide gels with four LysM proteins produced by *Pichia pastoris*. PC and NC are positive (horseradish peroxidase) and negative (soybean trypsin inhibitor) control, respectively.

TABLE S1 | Final concentrations of the four LysM effectors heterologously produced by *P. pastoris*.

Protein	Concentration
MoSlp1	10 mg/ml
Vd2LysM	7.35 mg/ml
ChElp1	9.0 mg/ml
ChElp2	14 mg/ml

TABLE S2 | The recipe for 20 mL of lysis buffer.

Amount	Reagent	Company
18 mL	50 mM Tris, 150 μM NaCl, pH 8.5	
2 mL	Glycerol	VWR, Ohio, USA
120 mg	Lysozyme from chicken egg white	Sigma-Aldrich, Missouri, USA
80 mg	Sodium deoxycholate	Sigma-Aldrich, Missouri, USA
1.25 mg	Deoxyribonuclease I	Sigma-Aldrich, Missouri, USA
1 pill	Protease inhibitor cocktail	Roche, Mannheim, Germany

TABLE S3 | Primers used in this study.

Primers	Sequences
His-Flag-MoSlp1-F	CGGTATGAATTCATGCATCATCATCATCATCAT CCCGACTACAAGGACGACGATGACAAGGCCATGCCTCAGGCAAC
His-Flag-MoSlp1-R	CGGTATGCGGCCGCCTAGTTCTTGCAGATGGGGATGTTG
His-Flag-Vd2L-F	CGGTATGAATTCATGCATCATCATCATCATCAT CCCGACTACAAGGACGACGATGACAAGTACCGAAGGACATGCAGTCATACC
His-Flag-Vd2L-R	CGGTATGCGGCCGCTTAGTTCCAGCTGCACGGC
His-Flag-ChElp1-F	CGGTATGAATTCATGCATCATCATCATCATCAT CCCGACTACAAGGACGACGATGACAAGCTCCCTCAGGCTACCCCGACCACG
His-Flag-ChElp1-R	CGGTATGCGGCCGCTTAACAGACGGGGATGTTGATGACATCGC
His-Flag-ChElp2-F	CGGTATGAATTCATGCATCATCATCATCATCAT CCCGACTACAAGGACGACGATGACAAGCTCCCTGTCTGTGACGCCACTAC
His-Flag-ChElp2-R	CGGTATGCGGCCGCCTAACACACAGGGACGTTGATGACC
MoSlp1-F	CGGTATGAATTCGCCATGCCTCAGGCAAC
MoSlp1-R	CGGTATGCGGCCGCTTATTACTAGTTCTTGCAGATGGGGATGTTG
Vd2L-F	CGGTATGAATTCTACCGAAGGACATGCAGTCATACC
Vd2L-R	CGGTATGCGGCCGCTTATTATTAGTTCCAGCTGCACGGC
ChElp1-F	CGGTATGAATTCCTCCCTCAGGCTACCCCGACCACG
ChElp1-R	CGGTATGCGGCCGCTTATTATTAACAGACGGGGATGTTGATGACATCGC
ChElp2-F	CGGTATGAATTCCTCCCTGTCTGTGACGCCACTAC
ChElp2-R	CGGTATGCGGCCGCTTATTACTAACACACAGGGACGTTGATGACC

*The coding sequence of the 6×His-tag is indicated with blue font, the coding sequence of the FLAG-tag is indicated with green font, and restriction enzyme recognition sites are indicated as with red font.

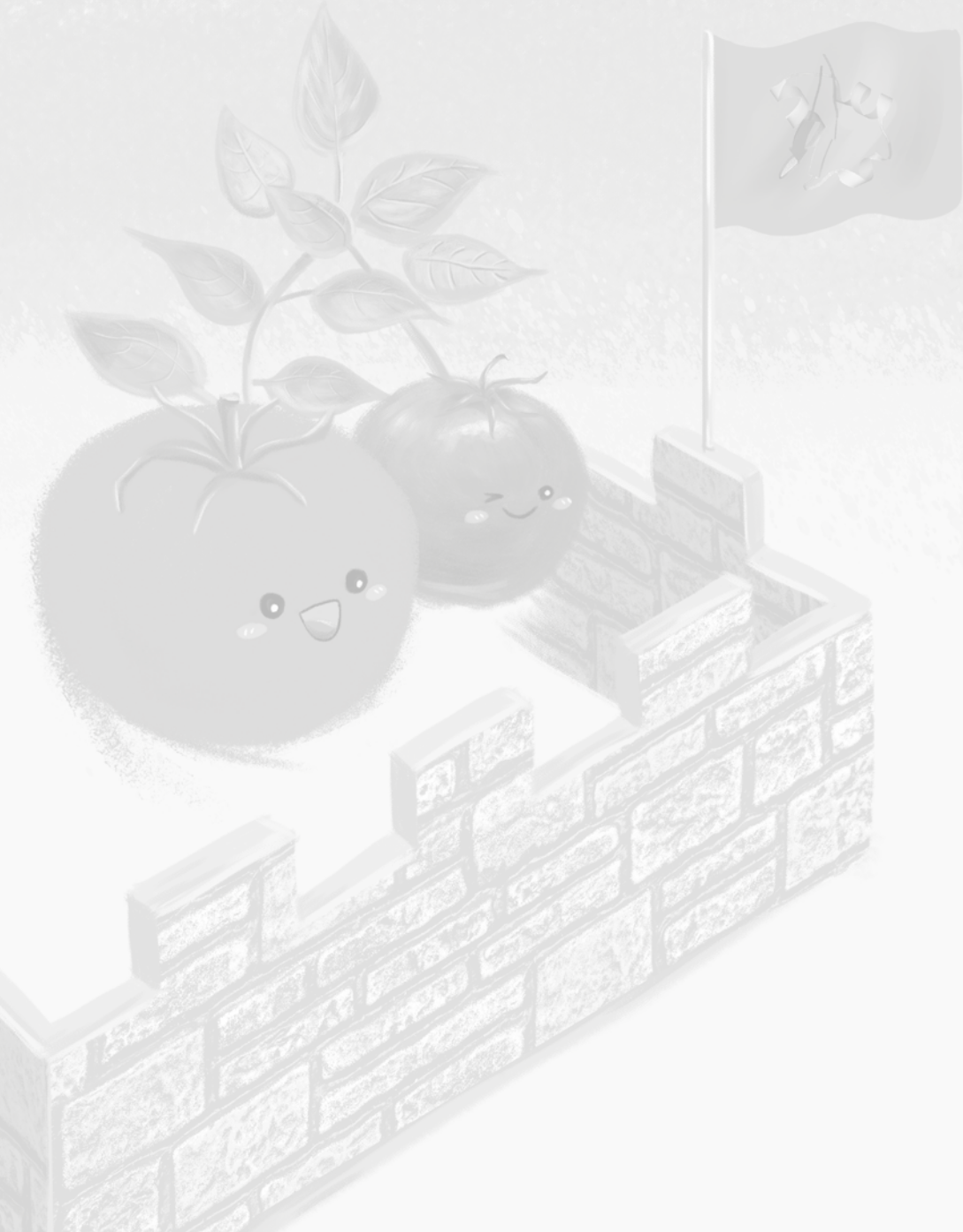

Chapter 5

Three LysM effectors of *Zymoseptoria tritici* collectively disarm chitin-triggered plant immunity

Hui Tian[1], Craig I. MacKenzie[1,‡], Luis Rodriguez-Moreno[1,#,‡], Grardy C.M. van den Berg[1], Hongxin Chen[2], Jason J. Rudd[2], Jeroen R. Mesters[3], Bart P.H.J. Thomma[1,4,*]

[1] Laboratory of Phytopathology, Wageningen University and Research, Droevendaalsesteeg 1, 6708PB Wageningen, The Netherlands; [2]Department of Plant Biology and Crop Science, Rothamsted Research, Harpenden, AL5 2JQ, UK; [3]Institute of Biochemistry, University of Lübeck, Ratzeburger Allee 160, 23538 Lübeck, Germany; [4]University of Cologne, Institute for Plant Sciences, Cluster of Excellence on Plant Sciences (CEPLAS), 50674 Cologne, Germany.

[‡]These authors contributed equally

A modified version has been submitted to Molecular Plant Pathology

ABSTRACT

Chitin is a major structural component of fungal cell walls and acts as a microbe-associated molecular pattern (MAMP) that, upon recognition by a plant host, triggers the activation of immune responses. In order to avoid the activation of these responses, the Septoria tritici blotch (STB) pathogen of wheat, *Zymoseptoria tritici*, secretes LysM effector proteins. Previously, the LysM effectors Mg1LysM and Mg3LysM were shown to protect fungal hyphae against host chitinases. Furthermore, Mg3LysM, but not Mg1LysM, was shown to suppress chitin-induced reactive oxygen species (ROS) production. Whereas initially a third LysM effector was disregarded as a presumed pseudogene, we now provide functional data to show that also this LysM effector, named Mgx1LysM, is functional during wheat colonization. We show that Mgx1LysM binds chitin, protects fungal hyphae against chitinase hydrolysis and is able to suppress chitin-induced ROS burst. Finally, we demonstrate that while Mg3LysM confers a major contribution to *Z. tritici* virulence, also Mg1LysM and Mgx1LysM contribute to virulence, albeit with smaller contributions, and that all LysM effectors displays partial functional redundancy. Collectively, our data show that *Zymoseptoria tritici* utilizes three LysM effectors to disarm chitin-triggered wheat immunity.

INTRODUCTION

Plants deploy an effective innate immune system to recognize and appropriately respond to microbial invaders. An important part of this immune system involves the recognition of conserved microbe-associated molecular patterns (MAMPs) that are recognized by cell surface-localized pattern recognition receptors (PRRs) to activate pattern-triggered immunity (PTI) (Jones and Dangl, 2006; Thomma et al., 2001; Cook et al., 2015). PTI includes a broad range of immune responses, such as the production of reactive oxygen species (ROS), ion fluxes, callose deposition and defence-related gene expression (Jones and Dangl, 2006; Altenbach and Robatzek, 2007; Boller and Felix., 2009).

Chitin, a homopolymer of β-(1,4)-linked *N*-acetylglucosamine (GlcNAc), is an abundant polysaccharide in nature and a major structural component of fungal cell walls (Free, 2013). Plants secrete hydrolytic enzymes, such as chitinases, as an immune response to target fungal cell wall chitin in order to disrupt cell wall integrity, but also to release chitin molecules that act as a MAMP that can be recognized by PRRs that carry extracellular lysin motifs (LysMs) to activate further immune responses against fungal invasion (Felix et al., 1993; Kombrink and Thomma, 2013; Sanchez-Vallet et al., 2015). Presently, chitin receptor complexes that comprise LysM-containing receptors have been characterized in Arabidopsis and rice (Miya et al., 2007; Wan et al., 2012; Shimizu et al., 2010; Cao et al., 2014). Homologs of the crucial components of these complexes have also been identified in wheat (Lee et al., 2014).

In order to successfully establish an infection, fungal pathogens evolved various strategies to overcome chitin-triggered plant immunity, such as alternation of cell wall chitin in such way that it is no longer recognized (Fujikawa et al., 2009; Fujikawa et al., 2012), but also the secretion of effector proteins to either protect fungal cell walls against hydrolytic host enzymes or to prevent the activation of chitin-induced immunity (van den Burg et al., 2006; Marshall et al., 2016; Kombrink et al., 2011; Mentlak et al., 2012; Rövenich et al., 2014; Takahara et al., 2016). For example, some fungi can convert the surface-exposed chitin in fungal cell walls to chitosan, which is a poor substrate for chitinases, thus avoiding the activation of chitin-triggered immune responses during host invasion (Ride and Barber, 1990; El Gueddari et al., 2002). Furthermore, from the soil-borne fungus *Verticillium dahliae* a secreted polysaccharide deacetylase was characterized to facilitate fungal virulence through direct deacetylation of chitin oligomers, converting them to chitosan that is a relatively poor inducer of immune responses (Gao et al., 2019). The use of effector molecules to successfully target chitin-triggered plant immunity has been well-studied for the tomato leaf mould fungus *Cladosporium fulvum*. This fungus secretes the invertebrate chitin-binding domain (CBM14)-containing effector protein Avr4 to bind fungal cell wall chitin, resulting in the protection of its hyphae against hydrolysis by tomato chitinases (van den Burg et al., 2006; van Esse et al., 2007). Additionally, *C. fulvum* secretes the effector protein Ecp6 (extracellular protein 6) that carries three LysMs, binds chitin and suppresses chitin-induced plant immunity. A crystal structure of Ecp6 revealed that two of its three LysM domains undergo ligand-induced intramolecular dimerization, thus establishing a groove with ultrahigh (pM) chitin

binding-affinity that enables Ecp6 to outcompete plant receptors for chitin binding (Sanchez-Vallet et al., 2013). Whereas Avr4 cannot suppress chitin-triggered immunity, Ecp6 does not possess the ability to protect fungal hyphae against chitinases (Bolton et al., 2008; de Jonge et al., 2010). Homologs of Ecp6, coined LysM effectors, have been found in many fungi (de Jonge and Thomma 2009). In contrast, homologs of Avr4 are less widespread (Stergiopoulos et al., 2010).

Zymoseptoria tritici (formerly *Mycosphaerella graminicola*) is a host-specific hemibiotrophic fungus and the causal agent of Septoria tritici blotch (STB) of wheat (*Triticum* spp.) (Eyal, 1999). Upon infection, wheat plants undergo an extended period of symptomless colonization of approximately one week, followed by the death of host tissues coinciding with rapid invasive growth and asexual reproduction of the fungus (Kema et al., 1996; Pnini-Cohenet al., 2000; Glazebrook, 2005). This transition from biotrophic to necrotrophic growth of *Z. tritici* is associated with the induction of host immune processes such as a hypersensitive response (HR)-like programmed cell death and differential expression of wheat mitogen-activated protein kinase (MAPK) genes (Rudd et al., 2008). Three LysM effector genes were previously identified in the *Z. tritici* genome (Marshall et al., 2011). These comprise *Mg1LysM* and *MgxLysM* that encode LysM effector proteins that carry a single LysM only, and *Mg3LysM* encoding an effector with three LysMs (Marshall et al., 2011). Whereas *Mg1LysM* and *Mg3LysM* were subjected to functional analysis, *MgxLysM* was disregarded because this gene lacked EST support and was believed to contain an intronic repeat insertion, rendering it a pseudogene. Both *Mg1LysM* and *Mg3LysM* were found to be induced during wheat infection, and both proteins were found to bind chitin. However, only Mg3LysM was found to suppress chitin-induced plant immunity (Marshall et al., 2011). Surprisingly, and in contrast to Ecp6, both Mg1LysM and Mg3LysM were found to protect fungal hyphae against plant chitinase activity. However, thus far the mechanism underlying the protection of cell walls by the *Z. tritici* LysM effectors remains unclear. In this study, we revisited the previously discarded *MgxLysM* gene and characterize its role during *Z. tritici* colonization of wheat plants.

RESULTS

Mgx1LysM is expressed during wheat colonization

Although *MgxLysM* was previously reported to be a pseudogene and found not to be induced upon wheat infection (Marshall et al., 2011), a more recent transcriptome profiling study on wheat demonstrated *MgxLysM* expression during host colonization, demonstrating that the initial assessment was incorrect (Rudd et al., 2015). Thus, we propose to rename MgxLysM to Mgx1LysM, according to the single LysM domain in the protein, similar to the previously described Mg1LysM effector (Marshall et al., 2011).

To confirm the expression of *Mgx1LysM* in *Z. tritici* upon host colonization, we inoculated the wild-type strain IPO323 onto wheat leaves and sampled leaves at 0, 4, 8, 10 and 14 days post

inoculation (dpi). In addition, IPO323 growing *in vitro* in Czapek-Dox broth (CDB) and in potato dextrose broth (PDB) was subjected to expression analysis. This analysis confirmed that *Mgx1LysM* is not expressed upon growth *in vitro*, but only during host colonization at all tested time points (Fig. 1). More specifically, *Mgx1LysM* expression was strongly induced at 4 dpi, peaked at 8 dpi and dramatically decreased by 10 dpi. Interestingly, the peak of expression at 8 dpi is around the transition time when the infection switches from asymptomatic to symptomatic with the appearance of lesions on wheat leaves (Marshall et al., 2011).

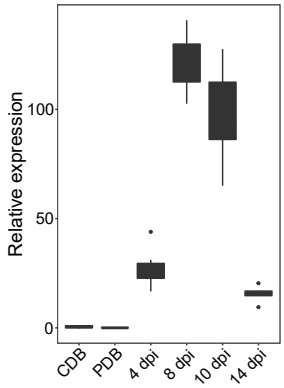

FIGURE 1 | Expression of *Mgx1LysM* is induced in *Zymoseptoria tritici* upon inoculation on wheat plants. Relative expression of *Mgx1LysM* at 4, 8, 10 and 14 days post inoculation on wheat plants and upon growth *in vitro* in Czapek-dox (CDB) or potato dextrose broth (PDB) when normalized to *Z. tritici* β-tublin. The boxplot was made with RStudio using the package ggplot2.

Mgx1LysM binds chitin and suppresses the chitin-induced ROS burst

In order to investigate the substrate-binding characteristics of Mgx1LysM, the protein was heterologously expressed in *E. coli* and subjected to a polysaccharide precipitation assay. Mgx1LysM was incubated with chitin beads and shrimp shell chitin, but also with plant-derived cellulose and xylan, revealing that Mgx1LysM binds chitin beads and shrimp shell chitin but not cellulose or xylan (Fig. 2). Thus, Mgx1LysM resembles Mg1LysM that similarly binds chitin but not cellulose or xylan (Fig. 2).

To test whether Mgx1LysM can prevent chitin-triggered immunity in plants, the occurrence of a chitin-induced reactive oxygen species (ROS) burst was assessed in *Nicotiana benthamiana* leaf discs upon treatment with 10 μM chitohexaose (chitin) in the presence or absence of the effector protein. As previously demonstrated (de Jonge et al., 2010), *C. fulvum* Ecp6 suppresses ROS production in this assay (Fig. 3). Remarkably, pre-incubation of 10 μM chitin with 50 μM Mgx1LysM prior to the addition to leaf discs led to a significant reduction of the ROS burst (Fig. 3), demonstrating its ability to suppress chitin-induced plant immune responses. This finding was unexpected because we previously found that its close homolog Mg1LysM does not possess this ability (Marshall et al., 2011), albeit that we used Mg1LysM that was heterologously produced in the yeast *Pichia pastoris* rather than in *E. coli* in that study. To revisit this initial observation, we now tested whether *E. coli*-produced Mg1LysM is able to suppress the chitin-induced ROS burst. Indeed, similar to the results obtained for Mgx1LysM, we now observed that pre-incubation with

of 10 μM chitin with 50 μM Mg1LysM prior to the addition to leaf discs led to a significantly compromised ROS burst. Thus, both LysM effectors have the ability to suppress chitin-triggered host immunity.

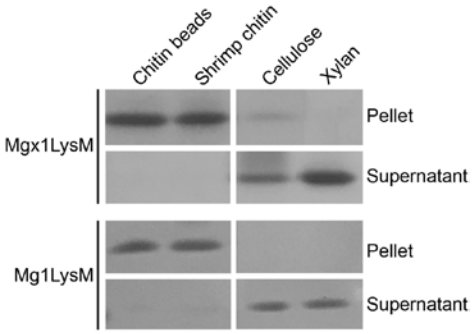

FIGURE 2 | Mgx1LysM binds chitin. *E. coli*-produced Mgx1LysM and Mg1LysM were incubated with four chitin products for 6 hours and, after centrifugation, pellets and supernatants were analysed using polyacrylamide gel electrophoresis followed by CBB staining.

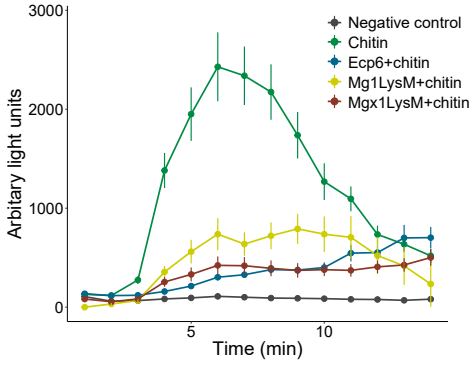

FIGURE 3 | Mgx1LysM suppresses the chitin-induced reactive oxygen species (ROS) burst. Leaf discs of *Nicotiana benthamiana* were treated with chitohexaose (chitin) to induce ROS production. Chitin was pre-incubated with Ecp6, Mg1LysM or Mgx1LysM for two hours and subsequently added to the leaf discs. Error bars represent standard errors from five biological replicates.

Mgx1LysM protects *Trichoderma viride* hyphae against chitinases

We previously demonstrated that Mg1LysM can protect fungal hyphae against chitinase hydrolysis (Marshall et al., 2011). To evaluate a possible role in hyphal protection, the ability of Mgx1LysM to protect hyphae of *Trichoderma viride*, a fungus that exposes its cell wall chitin *in vitro*, against chitinases was tested (Mauch et al., 1988). *C. fulvum* effector protein Avr4 and Mg1LysM were used as positive controls because of their previously demonstrated ability to protect fungal hyphae (van den Burg et al., 2006; Marshall et al., 2011). As expected, while the addition of chitinase drastically inhibited *T. viride* hyphal growth, Avr4 as well as Mg1LysM protected the hyphae against chitinase hydrolysis (Fig. 4). Furthermore, the assay revealed that pre-incubation with Mgx1LysM similarly protected the hyphae against chitinases (Fig. 4).

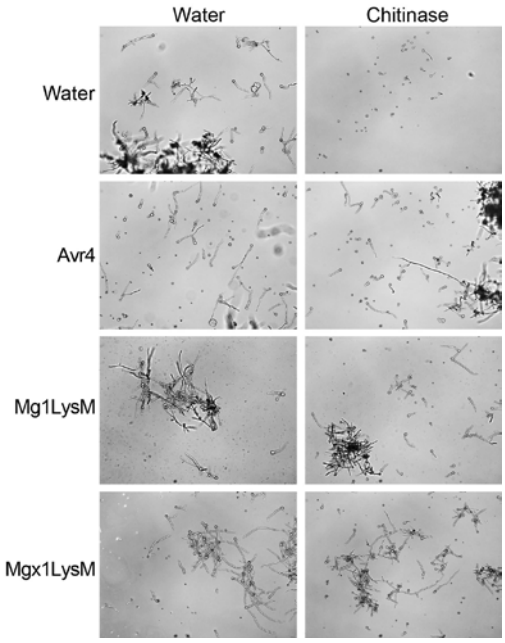

FIGURE 4 | Mgx1LysM protects hyphal growth of *Trichoderma viride* against chitinase hydrolysis. Microscopic pictures of *T. viride* grown *in vitro* with or without two hours of preincubation with *C. fulvum* Avr4, or *Z. tritici* Mg1LysM or Mgx1LysM, followed by the addition of chitinase or water. Pictures were taken ~4 hours after the addition of chitinase.

Mgx1LysM contributes to *Z. tritici* virulence on wheat but displays functional redundancy with Mg1LysM and Mg3LysM

Collectively, our data above suggest that Mg1LysM, Mgx1LysM and Mg3LysM display redundant activities as all three proteins display the ability to suppress chitin-triggered host immunity and to protect fungal hyphae against chitinase hydrolysis. However, previously only a contribution of Mg3LysM to virulence could be demonstrated (Marshall et al., 2011). To assess the contribution of the three *Z. tritici* LysM effector proteins to virulence on wheat plants, the single-gene deletion mutants *ΔMg1, ΔMgx1* and *ΔMg3*, the double-gene deletion mutants *ΔMg1-ΔMgx1*, *ΔMgx1 -ΔMg3* and *ΔMg1-ΔMg3*, and the triple-gene deletion mutant *ΔMg1-ΔMgx1 -ΔMg3*, that were generated in a *Δku70* strain that permits non-homologous recombination (Bowler et al., 2010), were inoculated onto wheat plants. By 17 days post inoculation (dpi), the *Δku70* strain developed typical necrosis symptom on the wheat leaves, while the *ΔMg3* strain caused much less necrosis symptoms (Fig. 5AB) as previously reported (Marshall et al., 2011). Furthermore, like previously reported, the *ΔMg1* strain developed similar necrosis as the *Δku70* strain. We now show that not only the *ΔMgx1* strain developed similar levels of necrosis as the *Δku70* strain and the *ΔMg1* strain, but also that the *ΔMg1-ΔMgx1* double mutant shows no apparent decrease in disease development, suggesting that these two LysM effectors are dispensable for full virulence of

Z. tritici. In line with these observations, the *ΔMgx1 -ΔMg3* and *ΔMg1-ΔMg3* double mutants induced similar symptoms as the *ΔMg3* strain (Fig. 5AB). Nevertheless, the necrosis symptoms caused by inoculation with the triple mutant *ΔMg1-ΔMgx1 -ΔMg3* were drastically reduced when compared with those caused by the *ΔMg3* strain. Collectively, these findings suggest that Mg3LysM is the most important LysM effector for *Z. tritici* disease development, and that Mgx1LysM and Mg1LysM contribute to disease development through redundant functionality.

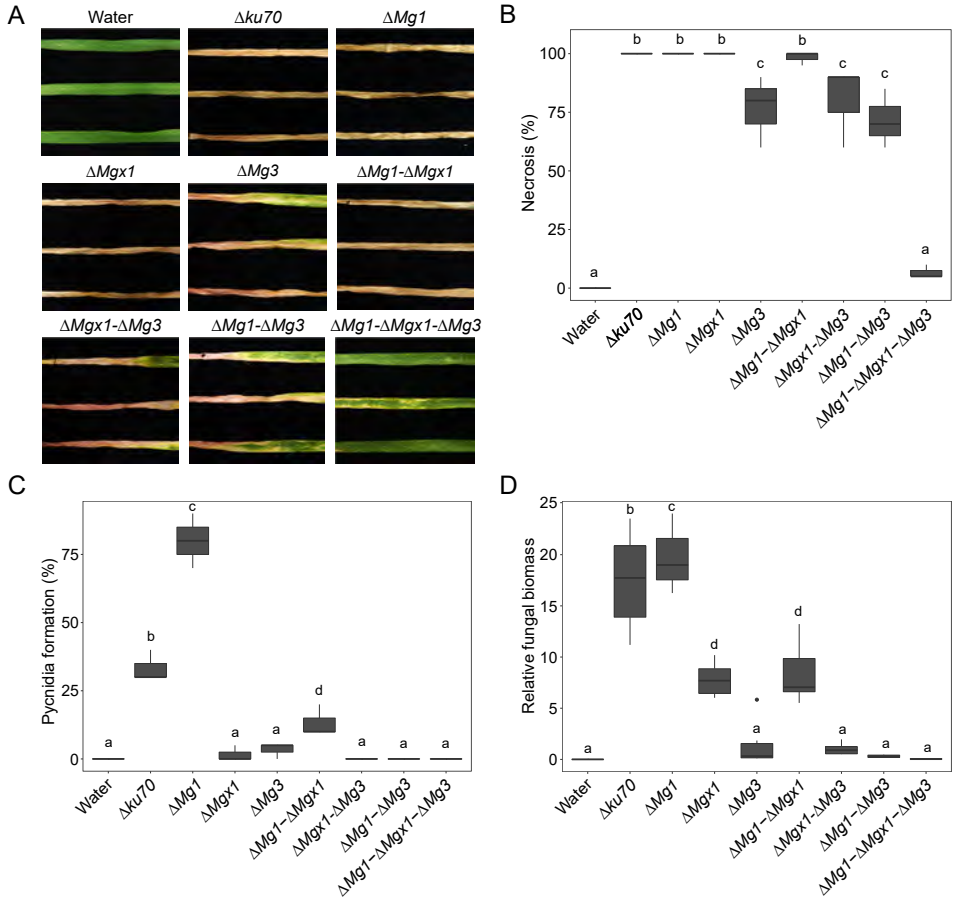

FIGURE 5 | Mgx1LysM contributes to *Z. tritici* virulence on wheat and displays functional redundancy with Mg1LysM and Mg3LysM. (A) Disease symptoms on wheat leaves at 17 days post inoculation (dpi) with Δ*ku70* and LysM effector gene deletion strains. Quantification of the necrotic area (B) and of the area displaying the formation of asexual fruiting bodies (pycnidia) (C) on wheat leaves inoculated with Δ*ku70* and LysM effector gene deletion strains at 17 dpi. (D) Fungal biomass determined with real-time PCR on *Z. tritici* β-tubulin relative to the wheat cell division control gene, on wheat leaf samples harvested at 17 dpi. Graphs were made with RStudio using the package of ggplot2 and different letters indicating significant differences between each inoculation were calculated with IBM Statistics 25 with One-way ANOVA (Duncan; $P<0.05$). Fungal inoculation experiments were conducted on six plants with six first-primary leaves per inoculation and repeated three times with similar results.

To further substantiate our findings, we also determined the formation of asexual fruiting bodies (pycnidia) as a measure for fungal colonization on the wheat leaves at 17 dpi. To this end, we determined the percentage of leaf surface displaying pycnidia. Surprisingly, repeated assays revealed that the *ΔMg1* mutant developed significantly more pycnidia than the *Δku70* strain, whereas the *ΔMgx1* mutant, like the *ΔMg3* mutant, produced no to only a few pycnidia (Fig. 5C). Accordingly, whereas the *ΔMg1-ΔMgx1* double mutant developed an intermediate amount of pycnidia, all mutants that involved *ΔMg3* were devoid of conidia formation (Fig. 5C). These data first of all suggest that symptom development does not correlate with fungal colonization levels as measured by pycnidia formation and, furthermore, that the three LysM effectors display differential roles in fungal colonization.

To further substantiate the fungal colonization assessments, we measured fungal biomass with real-time PCR. While the *ΔMg1* mutant developed a similar amount of fungal biomass as the *Δku70* strain, the *ΔMgx1* mutant displayed significantly compromised colonization at a similar level as the *ΔMg1-ΔMgx1* double mutant, but not as compromised as the *ΔMg3* mutant or the double mutants and triple mutant that carry *ΔMg3* (Fig. 5D). These observations confirm the discrepancy between fungal colonization and symptom development, and also confirm the differential contribution of the LysM effectors to fungal colonization. Consequently, our data reveal that the three LysM effectors make differential contributions to symptom display, that again differ from the differential contributions to fungal colonization. Thus, our findings present evidence for partially redundant, but also partially divergent, contributions of the three LysM effectors to *Z. tritici* virulence.

DISCUSSION

In this study, we demonstrate that the previously disregarded LysM effector gene as presumed pseudogene of the fungal wheat pathogen *Z. tritici*, *Mgx1LysM*, is a functional LysM effector gene that plays a role in *Z. tritici* virulence during infection of wheat plants. Like the previously characterized *Z. tritici* LysM effectors Mg1LysM and Mg3LysM, Mgx1LysM binds chitin (Fig. 2), suppresses chitin-induced ROS production (Fig. 3) and has the ability to protect fungal hyphae against chitinase hydrolysis (Fig. 4). Through these activities, Mgx1LysM makes a noticeable contribution to *Z. tritici* virulence on wheat plants (Fig. 5).

Based on the expression profile as well as on the biological activities, the three genes seem to behave in an identical fashion and complete redundancy could be expected, However, this is not what we observed in the mutant analyses, as these revealed that Mg3LysM confers the largest contribution as targeted deletion of *Mg3LysM*, but not of Mg1LysM or Mgx1LysM, results in a noticeable difference in symptomatology. Moreover, even the simultaneous deletion of *Mgx1LysM* and *Mg1LysM* did not lead to compromised necrosis development, although deletion of these two genes from the *Mg3LysM* deletion strain in the triple mutant resulted in a further

decrease of virulence. Thus, in can be concluded that all three LysM effectors contribute to fungal virulence. Moreover, these findings are suggestive of partially redundant and partially additive activities. This suggestion is further reinforced when assessing pycnidia development and fungal colonization data that demonstrate that single LysM effector deletions have significant effects on these traits. However, it presently remains unknown through which functional divergence these differential phenotypes are established.

The ability to protect fungal hyphae against chitinase hydrolysis that is shared by the three *Z. tritici* LysM effectors (Fig. 4) has previously been recorded for some, but not all, LysM effectors from other fungal species as well. For example, although *Verticillium dahliae* Vd2LysM and *Rhizophagus irregularis* RiSLM can protect hyphae as well (Kombrink et al., 2017; Zeng et al., 2019), *C. fulvum* Ecp6, *Colletotrichum higginsianum* ChElp1 and ChElp2, and *Magnaporthe oryzae* MoSlp1 do not possess such activity (de Jonge et al., 2010; Mentlak et al., 2012; Takahara et al., 2016). Intriguingly, all LysM effectors that contain a single LysM characterized to date (Mg1LysM, Mgx1LysM, RiSLM) were found to protect fungal hyphae. However among the ones with two LysM domains members are found that do (Vd2LysM) and that do not (ChElp1, ChElp2, MoSlp1) protect, which is also true for members with three LysMs (Mg3LysM versus Ecp6, respectively), suggesting that the ability to protect hyphae is not determined by the amount of LysMs in the effector protein. Further research will have to reveal how the ability to protect hyphae is conferred by some of these LysM effectors. Previously, a mechanistic explanation for the ability to protect fungal cell wall chitin has been provided for the *C. fulvum* effector protein Avr4 that acts as a functional homolog of LysM effectors that protect fungal hyphae, but that binds chitin through an invertebrate chitin-binding domain (CBM14) rather than through LysMs (van den Burg et al., 2006). Intriguingly, Avr4 strictly interacts with chitotriose, but binding of additional Avr4 molecules to chitin occurs through cooperative interactions between Avr4 monomers, which can explain the effective shielding of cell wall chitin (van den Burg, 2004). Despite being a close relative of *C. fulvum* in the Dothidiomycete class of Ascomycete fungi, *Z. tritici* lacks an Avr4 homolog (Stergiopoulos et al., 2010). This may explain why the *Z. tritici* LysM effectors, in contrast to *C. fulvum* Ecp6, evolved the ability to protect fungal cell wall chitin.

It was previously reported that Mg1LysM was incapable of suppressing chitin-induced ROS production (Marshall et al., 2011), in contrast to the immune-suppressive activity of Mg3LysM. A mechanistic explanation for this observation was found in the observation that Ecp6, being a close homolog of Mg3LysM, was able to efficiently sequester chitin oligomers from host receptors through intramolecular LysM dimerization, leading to a binding groove with ultra-high chitin-binding affinity. As a single LysM-containing effector protein, Mg1LysM lacks the ability to undergo intramolecular LysM dimerization, and thus to form an ultra-high affinity groove for chitin binding, which could explain the inability to suppress immune responses by out-competition of host receptor molecules for chitin binding. However, this mechanistic explanation was recently challenged by data showing that the *R. irregulars* RiSLM is able to suppress chitin-triggered immunity as well (Zeng et al., 2019). In the present study we show that not only Mgx1LysM can suppress chitin-triggered immunity, but also that Mg1LysM possesses this activity (Fig. 4).

However, it needs to be acknowledged that whereas we used *P. pastoris*-produced protein in our initial analyses (Marshall et al., 2011), we used *E. coli*-produced protein in the current study. More recent insights after the publication of our initial study have revealed that LysM effector proteins may bind chitin fragments that are released from the *P. pastoris* cell walls during protein production, which may compromise the activity of the protein preparation in subsequent assays (Sánchez-Vallet et al., 2013; Kombrink et al., 2016). As the *E. coli* cell wall is devoid of chitin, partially or fully inactive protein preparations due to occupation of the substrate binding site are unlikely to occur. However, since Mg1LysM, Mgx1LysM and RiSLM are likely to suppress chitin-triggered immunity, a mechanistic explanation needs to be provided for the suppressive activity that does not involve substrate sequestration. Possibly, these LysM effectors are able to perturb the formation of active chitin receptor complexes by binding to receptor monomers in a similar fashion as we have shown for LysM2 of Ecp6 in chapter 3, thus preventing the activation of chitin-triggered immune responses.

MATERIALS AND METHODS

Gene expression analysis

Total RNA was isolated using the RNeasy Plant Mini Kit (Qiagen, Maryland, USA). For each sample, 2 μg RNA was used for cDNA synthesis with M-MLV Reverse Transcriptase (Promega, Madison, USA) and 1 μL of the obtained cDNA was used for real-time PCR with SYBR™ green master mix (Bioline, Luckenwalde, Germany) on a C1000 Touch™ Thermal Cycler (Bio-Rad, California, USA). Expression of *Mgx1LysM* was normalized to the *Z. tritici* housekeeping gene *β-tubulin* using primer pairs *Mgx1LysM*-F/*Mgx1LysM*-R and *Ztβtubulin*-F/R, respectively (Table S1). Relative expression was calculated with the $E^{-\Delta Ct}$ method and the boxplot was made with RStudio using the package of ggplot2 (Wickham, 2009; R Core Team, 2014).

Heterologous protein production in *E. coli*

Signal peptide prediction was performed using SignalP 5.0 (http://www.cbs.dtu.dk/services/SignalP/). The coding region for the mature Mgx1LysM protein was amplified from *Z. tritici* IPO323 genomic cDNA using primers *Mgx1LysM*-cDNA-F/ R (Table S1) and cloned into the pETSUMO vector and transformed as pETSUMO-Mgx1LysM into *E. coli* strain Origami for heterologous protein production as fusion protein with a 6×His-SUMO affinity-tag. *Mgx1LysM* expression was induced with 0.2 mM isopropyl β-D-1-thiogalactopyranoside (IPTG) at 28°C overnight. Next, *E. coli* cells were harvested by centrifugation at 3,800 g for one hour and resuspended in 20 mL cell lysis buffer (50 mM Tris-HCl pH 8.5, 150 mM NaCl, 2 mL glycerol, 120 mg lysozyme, 40 mg deoxycholic acid, 1.25 mg DNase I and 1 protease inhibitor pill) and incubated at 4°C for two hours with stirring, and centrifuged at 20,000 g for one hour. The resulting cleared supernatant was immediately placed on ice and subjected to further purification.

The His60 Ni Superflow Resin (Clontech, California, USA) was used for Mgx1LysM purification and first equilibrated with wash buffer (50 mM Na_2HPO_4, 150 mM NaCl, 10 mM imidazole, pH 8.0) after which the protein preparation was loaded on the column. The target protein was eluted with elution buffer (50 mM Na_2HPO_4, 150 mM NaCl, 300 mM imidazole, pH 8.0), and purity of the elution was tested on an SDS-PAGE gel followed by Coomassie Brilliant Blue (CBB) staining. The 6×His-SUMO affinity-tag was cleaved with the SUMO Protease ULP1 during overnight dialysis against 200 mM NaCl. Non-cleaved Mgx1LysM fusion protein was removed using His60 Ni Superflow resin, and the flow-through with cleaved Mgx1LysM was adjusted to the required concentration.

Chitin binding assay

E. coli-produced proteins were adjusted to a concentration of 30 μg/mL in chitin binding buffer (50 mM Tris PH 8.0, 150 mM NaCl) and 800 μL of protein solution was incubated with 50 μL of magnetic chitin beads, or 5 mg of crab shell chitin, cellulose or xylan in a rotary shaker at 4°C for 6h. The insoluble fraction was pelleted by centrifuging at 13,500 g for 5 min and resuspend in 100 μL demineralized water. Supernatants were collected into Microcon Ultracel YM-10 tubes (Merck, Darmstadt, Germany) and concentrated a volume of approximately 100 μL. For each of the insoluble carbohydrates, 30 μL of the pellet solution and the concentrated supernatant was incubated with 10 μL of SDS-PAGE protein loading buffer (4×; 200 mM Tris-HCl, pH 6.5, 0.4 M dithiothreitol, 8% sodium dodecyl sulfate, 6 mM bromophenol blue, 40% glycerol) and incubated at 95°C for 10 min. Samples were loaded into an SDS-PAGE gel followed by CBB staining.

Hyphal protection against chitinase hydrolysis

Trichoderma viride conidiospores were harvested from five-day-old potato dextrose agar (PDA; OXOID, Basingstoke, United Kingdom), washed with sterile water, and adjusted to a concentration of 10^6 spores/mL with potato dextrose broth (PDB; Becton Dickinson, Maryland, USA). Conidiospore suspensions were dispensed into a 96-well microtiter plate in aliquots of 50 μL and incubated at room temperature overnight. Effector proteins were added to a final concentration of 10 μM, and after 2 h of incubation 3 μL of chitinase from *Clostridium thermocellum* (Creative Enzymes, New York, USA) was added into the appropriate wells. As control, sterile water was added. All treatments were further incubated for 4 h and hyphal growth was inspected with a Nikon H600L microscope.

Reactive oxygen species measurement

Reactive oxygen species (ROS) production measurements were performed using three *Nicotiana benthamiana* leaf discs (Ø = 0.5 cm) per treatment, which were collected from two-week-old *N. benthamiana* plants, placed into a 96-well microtiter plate, and rinsed with 200 μL demineralized water. After 24 hours the water was replaced by 50 μL fresh demineralized water and the plate was

incubated for another hours at room temperature. Meanwhile, mixtures of $(GlcNAc)_6$ (IsoSep AB, Tullinge, Sweden) and effector proteins were incubated for two hours. In total, 20 µL of $(GlcNAc)_6$ was added in a final concentration of 10 µM to trigger ROS production in the absence or presence of 100 µL of effector protein in a final concentration of 50 µM in measuring solution containing 100 µM L-012 substrate (FUJIFILM, Neuss, Germany) and 40 µg/mL horseradish peroxidase (Sigma-Aldrich, Missouri, USA). Chemiluminescence measurements were taken every minute over 30 min in a CLARIOstar microplate reader (BMG LABTECH, Ortenberg, Germany).

Agrobacterium tumefaciens-mediated *Z. tritici* transformation

To generate *Mgx1LysM* deletion mutants, approximately 1.0 kb upstream and 1.2 kb downstream fragments of *Mgx1LysM* were amplified from genomic DNA of *Z. tritici* IPO323 using primer pairs *Mgx1LysM*-userL-F/R and *Mgx1LysM*-userR-F/R (Table S1) and the amplicons were cloned into vector pRF-NU2 as previously described (Frandsen et al, 2008). The resulting deletion construct was transformed into *Z. tritici* mutant *Δku70* and the previously generated *ΔMg1LysM*, *ΔMg3LysM* and *ΔMg1-ΔMg3* to generate double- and triple-gene deletion mutants. In short, minimal medium (MM) and induction medium (IM) were prepared at a pH of 7.0 and *Z. tritici* conidiospores were collected, washed and adjusted to a final concentration of 10^7 spores/mL. Transformation plates were incubated at 16°C in dark for two to three weeks. Putative transformants were transferred to PDA plates supplemented with 200 µg/mL cefotaxime and 25 µg/mL nourseothricin (Sigma-Aldrich, Missouri, USA) and absence of *Mgx1LysM* was confirmed with PCR using the gene-specific primers *Mgx1LysM*-F/*Mgx1LysM*-R and the primer pair with NAT-F as the forward primer that targets the nourseothricin cassette and the reverse primer *Mgx1LysM*-out-R targeting the downstream fragment of *Mgx1LysM* (Table S1).

Z. tritici inoculations on wheat

For all inoculation assays, the wheat cultivar "Riband" was used. *Z. tritici* wild-type strain IPO323 and the mutants were grown either on yeast extract peptone dextrose (YPD; 10 g yeast extract/L, 20 g peptone/L, 20 g dextrose and 15 g agar/L) or in yeast glucose medium (YGM; 10 g yeast extract/L, 30 g glucose/L) supplemented with appropriate antibiotics at 16°C with orbital shaking (100 rpm) for at least five days to obtain yeast-like conidiospores that were used for plant inoculation. To this end, conidiospores were collected by centrifuging the suspensions at 2,000 g for 5 min and adjustment to a final concentration of 10^7 spores/mL with 0.5% Tween 20 for inoculation by brushing on adaxial and abaxial sides of primary leaves of 11-day-old wheat plants. The inoculated plants were covered in a plastic tent for two days to secure high humidity, after which the tent was opened in one-side.

Fungal biomass was measured with real-time PCR using a C1000 Touch™ Thermal Cycler (Bio-Rad, California, USA) with the *Z. tritici*-specific β-*tubulin* primers *Ztβtubulin*-F/R in combination with primers *TaCDC*-F/R that target the constitutively expressed cell division

control gene of wheat (Table S1). Relative fungal biomass was calculated with the $E^{-\Delta Ct}$ method and boxplots were made with RStudio using the package of ggplot2 (Wickham, 2009; R Core Team, 2014).

ACKNOWLEDGEMENTS

H. Tian acknowledges receipt of a PhD fellowship from the China Scholarship Council (CSC). Work in the laboratory of B.P.H.J.Thomma is supported by the Research Council Earth and Life Sciences (ALW) of the Netherlands Organization of Scientific Research (NWO) and by the Deutsche Forschungsgemeinschaft (DFG, German Research Foundation) under Germany's Excellence Strategy – EXC 2048/1 – Project ID: 390686111.

SUPPLEMENTARY DATA

TABLE S1 | Primers used in this study.

Primer name	Sequences
Mgx1LysM-userL-F	GGTCTTAAUAGAAAGGGCACTATTCAACAAGC
Mgx1LysM-userL-R	GGCATTAAUATACCATGCTGCCGAAGTTGAA
Mgx1LysM-userR-F	GGACTTAAUAAGGCGAAGCTCTTGAAAACTGG
Mgx1LysM-userR-R	GGGTTTAAUATCCAATCTTCACGTACCCGGTTTC
Mgx1LysM-F	CACGCCACGAAGACGATACCAT
Mgx1LysM-R	TTCAAGAGCTTCGCCTTTGGG
NAT-F	GTCACCAACGTCAACGCACCG
Mgx1LysM-out-R	ATCGGCGCTGTACAGAAATATGCATA
Mgx1LysM-cDNA-F	GGTGGTGAATTCCAGAACAACGCACAGTGTCG
Mgx1LysM-cDNA-R	GGTGGTGCGGCCGCTTATTATCAGCTGACATGTTTCTTCAAG
TaCDC-F	CAAATACGCCATCAGGGAGAACATC
TaCDC-R	CGCTGCCGAAACCACGAGAC
Ztβtubulin-F	AACGGTCGTTACCTCACCTG
Ztβtubulin-R	ACGTTGTTCGGAATCCACTC

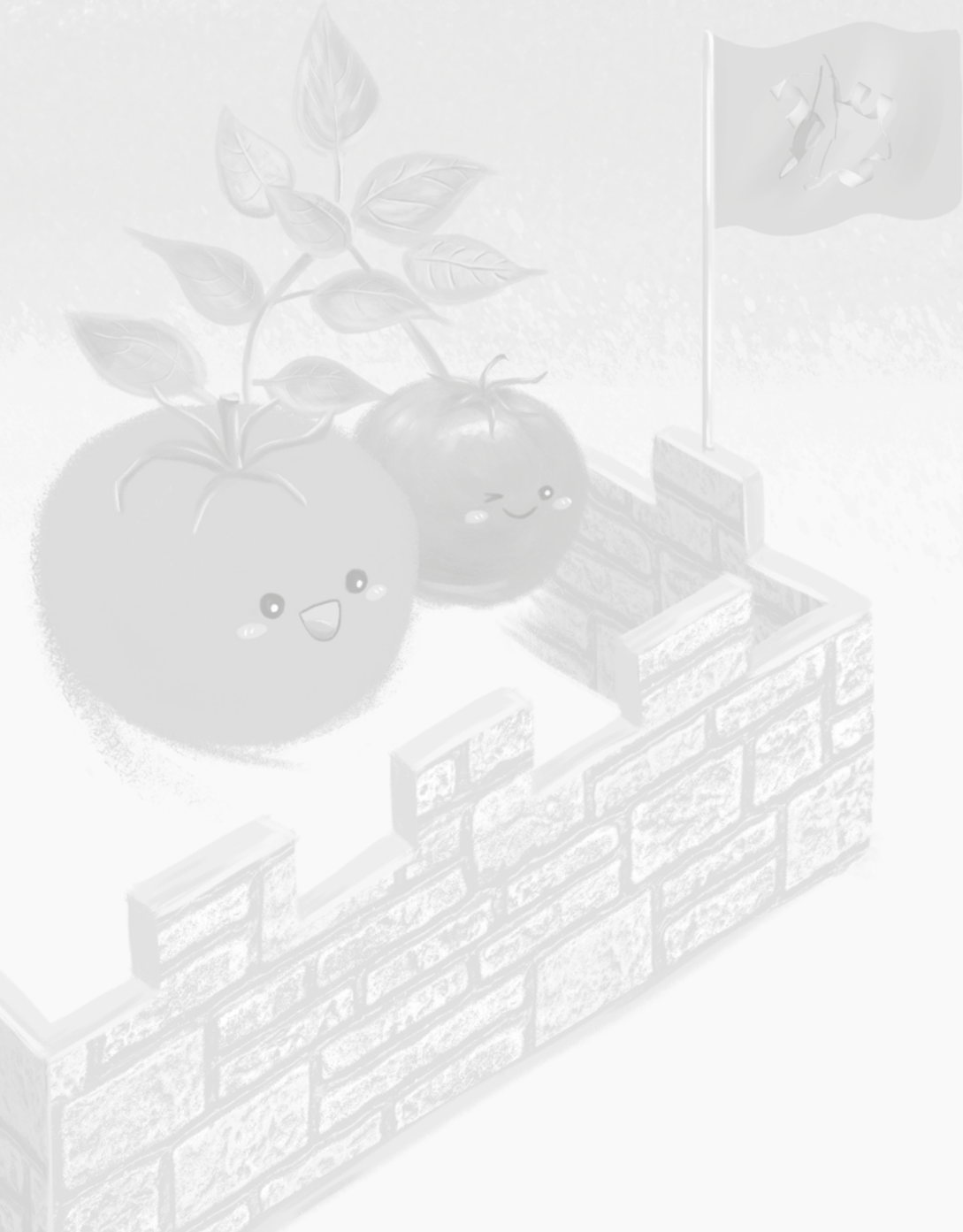

Chapter 6

A secreted LysM effector protects fungal hyphae through chitin-dependent homodimer polymerization

Andrea Sánchez-Vallet[1,2,‡], Hui Tian[1,‡], Luis Rodriguez-Moreno[1,‡,†], Dirk-Jan Valkenburg[1], Raspudin Saleem-Batcha[3,§], Stephan Wawra[4], Anja Kombrink[1], Leonie Verhage[1], Ronnie de Jonge[1,f], H. Peter van Esse[1,ø], Alga Zuccaro[4], Daniel Croll[5], Jeroen R. Mesters[3,+,*] and Bart P.H.J. Thomma[1,4,+,*]

[1] Laboratory of Phytopathology, Wageningen University& Research, Droevendaalsesteeg 1, 6708 PB Wageningen, The Netherlands.
[2] Plant Pathology Group, Institute of Integrative Biology, ETH Zurich, Zurich, Switzerland.
[3] Institute of Biochemistry, Center for Structural and Cell Biology in Medicine, University of Lübeck, Ratzeburger Allee 160, 23538 Lübeck, Germany.
[4] University of Cologne, Botanical Institute, Cluster of Excellence on Plant Sciences (CEPLAS), 50674 Cologne, Germany.
[5] Institute of Biology, University of Neuchâtel, Rue Emile-Argand 11, CH-2000 Neuchâtel, Switzerland.

This chapter has been accepted as:

Sánchez-Vallet A, Tian H, Rodriguez-Moreno L, Valkenburg D-J, Saleem-Batcha R, Wawra S, Kombrink A, Verhage L, de Jonge R, van Esse HP, et al (2020) A secreted LysM effector protects fungal hyphae through chitin-dependent homodimer polymerization. PLoS Pathog **16**: 1–21.

ABSTRACT

Plants trigger immune responses upon recognition of fungal cell wall chitin, followed by the release of various antimicrobials, including chitinase enzymes that hydrolyze chitin. In turn, many fungal pathogens secrete LysM effectors that prevent chitin recognition by the host through scavenging of chitin oligomers. We previously showed that intrachain LysM dimerization of the *Cladosporium fulvum* effector Ecp6 confers an ultrahigh-affinity binding groove that competitively sequesters chitin oligomers from host immune receptors. Additionally, particular LysM effectors are found to protect fungal hyphae against chitinase hydrolysis during host colonization. However, the molecular basis for the protection of fungal cell walls against hydrolysis remained unclear. Here, we determined a crystal structure of the single LysM domain-containing effector Mg1LysM of the wheat pathogen *Zymoseptoria tritici* and reveal that Mg1LysM is involved in the formation of two kinds of dimers; a chitin-dependent dimer as well as a chitin-independent homodimer. In this manner, Mg1LysM gains the capacity to form a supramolecular structure by chitin-induced oligomerization of chitin-independent Mg1LysM homodimers, a property that confers protection to fungal cell walls against host chitinases.

INTRODUCTION

Fungi constitute an evolutionarily and ecologically diverse group of microorganisms that are characterized by the presence of chitin, an *N*-acetyl-D-glucosamine (GlcNAc) homopolymer, in their cell walls. In addition to providing strength, shape, rigidity and protection against environmental hazards, chitin is also a well-known inducer of plant immune responses (Boller, 1995; Sánchez-Vallet et al, 2015; Shibuya et al, 1993). A major mechanism of plant defense against fungal invasion includes the secretion of microbial cell wall-degrading enzymes that include chitin-degrading enzymes, known as chitinases, to hinder fungal pathogen ingress (Schlumbaum et al, 1986; van Loon et al, 2006). Plant chitinases are diverse in nature, and grouped into six different classes that belong to glycosyl hydrolase families 18 and 19 (Adrangi & Faramarzi, 2013; Hamid et al, 2013). Although many chitinases are specifically produced upon pathogen invasion, others are constitutively expressed (van Loon et al, 2006).

Chitin hydrolysis on the one hand inhibits fungal growth, and on the other hand releases chitooligosacharides (Kasprzewska, 2003; Liu et al, 2014) that are recognized by cell surface receptors of host cells to mount an appropriate immune response (Rovenich et al, 2016; Sánchez-Vallet et al, 2015). In plants, chitin is recognized in the extracellular space through membrane-exposed Lysin motif (LysM)-containing receptor molecules (Kaku et al, 2006; Liu et al, 2012; Miya et al, 2007; Shibuya et al, 1993). In turn, many successful fungal pathogens have evolved effector molecules that either protect their cell walls against plant chitinases or prevent or perturb the elicitation of chitin-triggered host immunity (De Jonge et al, 2010; Marshall et al, 2011; Ökmen et al, 2018; Rovenich et al, 2016; Sánchez-Vallet et al, 2015).

Since decades, the interaction between the foliar fungal pathogen *Cladosporium fulvum* and its only host tomato has been studied to unravel the role of pathogen virulence and host defense mechanisms, including mechanisms that revolve around chitin (de Wit, 2016). After leaf penetration, *C. fulvum* secretes an arsenal of apoplastic effector proteins, including the chitin-binding effector proteins Avr4, which protects fungal hyphae against hydrolysis by plant chitinases (van den Burg et al, 2006; Van Esse et al, 2007), and Ecp6, which perturbs the activation of chitin-triggered host immunity (De Jonge et al, 2010; Sánchez-Vallet et al, 2013). Whereas Avr4 binds chitin through an invertebrate chitin-binding domain (Kohler et al, 2016, van den Burg et al, 2004), Ecp6 utilizes LysM domains for chitin binding (De Jonge et al, 2010; Sánchez-Vallet et al, 2013). Previous biochemical analysis revealed that Avr4 monomers require a stretch of at least three exposed GlcNAc residues for binding, and positive allosteric interactions among Avr4 molecules occur during chitin binding to facilitate the shielding of cell wall chitin against host chitinases (van den Burg et al, 2004). Based on X-ray crystallography it was recently shown that two Avr4 molecules interact through their chitohexaose ligand to form a three-dimensional molecular sandwich that encapsulates two chitohexaose molecules within the dimeric assembly (Hurlburt et al, 2018). A crystal structure of Ecp6 revealed chitin-induced dimerization of two of the three LysM domains, resulting in the formation of an ultrahigh affinity (pM) chitin-binding groove, conferring the capacity to outcompete plant receptors for chitin binding (Sánchez-

Vallet et al, 2013). Interestingly, whereas Avr4 homologs are found in other, *C. fulvum*-related, Dothideomycete plant pathogens (Stergiopoulos et al, 2010), LysM effectors are widespread in the fungal kingdom (Bolton et al, 2008; De Jonge & Thomma, 2009; Kombrink & Thomma, 2013). In several plant pathogenic fungi, including the Dothideomycete *Zymoseptoria tritici* and the Sodariomycetes *Magnaporthe oryzae*, *Colletotrichum higginsianum* and *Verticillium dahliae*, LysM effectors have been shown to contribute to virulence through chitin binding (Kombrink et al, 2017; Marshall et al, 2011; Mentlak et al, 2012; Takahara et al, 2016).

The LysM effectors Mg1LysM and Mg3LysM, with one and three LysM domains, respectively, have been characterized from the Septoria tritici blotch pathogen of wheat, *Z. tritici* (Marshall et al, 2011). Functional characterization has revealed that Mg3LysM can suppress chitin-induced immunity in a similar fashion as *C. fulvum* Ecp6. Surprisingly, in contrast to Ecp6 and similar to Avr4, Mg3LysM was additionally shown to have the ability to protect fungal hyphae against chitinase hydrolysis. As expected, based on the presence of a single LysM domain only, a role in suppression of chitin-triggered immunity could not be demonstrated for Mg1LysM (Marshall et al, 2011). Intriguingly, however, Mg1LysM was characterized as a functional homolog of Avr4 that protects hyphae against hydrolysis by host chitinases (Marshall et al, 2011). In order to understand how a LysM effector that is composed from little more than only a single LysM domain is able to confer protection of cell wall chitin from hydrolysis by plant enzymes, we aimed to obtain a crystal structure of the *Z. tritici* effector Mg1LysM in this study. Surprisingly, we discovered that Mg1LysM has the ability to simultaneously undergo ligand-mediated dimerization as well as ligand-independent homodimerization, allowing the formation of a contiguous oligomeric structure that anchors to the fungal cell wall through chitin to confer its protection ability.

RESULTS

Crystal structure of Mg1LysM reveals ligand-dependent and -independent intermolecular dimerization

In order to understand LysM effector functionality, and particularly how Mg1LysM is able to protect chitin against chitinase hydrolysis, the crystal structure of Mg1LysM was determined. To this end, Mg1LysM was heterologously produced in the yeast *Pichia pastoris* and purified based on the presence of a His-FLAG affinity tag. The large Mg1LysM crystals that were finally obtained by micro-seeding techniques (Bergfors, 2003) belonged to the space group *P 61 2 2*. Some crystals were soaked with the Ta_6Br_{14} cluster and initial phases were determined by the single-wavelength anomalous dispersion technique (SAD; Table 1). The initial phases were further improved with the help of an I3C soaked crystal. A native dataset was finally refined to a resolution of 2.41 Å with an Rwork and Rfree of 17.96% and 22.03%, respectively (Table 1). The structure model comprises in total four copies of the complete mature protein sequence except for the first amino acid after the signal peptide for chains A to C and the first two amino acids after the signal peptide for chain D, and one carbohydrate molecule per asymmetric unit (a.u.).

TABLE 1 | Data collection and refinement statistics.

	Native	Derivative-1 (SAD) $(Ta_6Br_{12})^{2+}$	Derivative-2 (SIRAS) (I3C)
Data collection statistics			
Beamline		BL14.1 - BESSY	
Wavelength (Å)	0.91841	1.24845	1.88313
Space group		$P6_122$	
Cell dimensions a, b, c (Å)	119.4, 119.4, 157.7	119.5, 119.5, 157.6	119.3, 119.3, 157.3
Resolution (Å)	49.12–2.41 (2.54–2.41)	26.97–2.96 (3.12–2.96)	39.37–5.00 (5.27–5.00)
R_{sym} [#] (%)	8.3 (50.4)	7.8 (20.1)	12.9 (20.7)
I / σI [§]	18.0 (4.5)	28.2 (11.5)	17.6 (17.3)
Completeness (%)	92.1 (100)	91.5 (100)	99.8 (100)
Redundancy	10.7 (10.7)	17.6 (16.3)	19.1 (19.9)
Anomalous completeness (%)	-	91.4 (100)	100 (100)
Anomalous multiplicity	-	9.5 (8.6)	11.1 (11.0)
Phasing statistics			
Figure of Merit (FOM)	-	0.57	0.36
Map Skew	-	1.40	0.03
Correlation of local RMS density	-	0.92	0.60
Correlation Coefficient (CC)	-	0.56	0.27
Refinement statistics			
Resolution (Å)	2.41	-	-
No. of reflections (total / free)	24,112 / 1,219	-	-
R_{work} / R_{free} [†] (%)	17.96 / 22.03	-	-
No. of atoms / average B-factor			
Overall	2,595 / 55.2	-	-
Protein	2,419 / 55.6	-	-
Ligand	43 / 53.7	-	-
R.m.s. deviations bond lengths (Å)	0.010	-	-
R.m.s. deviations bond angles (°)	1.195	-	-
Ramachandran plot (% favored / % outliers)	95.8 / 0.0	-	-
MolProbity (clash- & overall score)	6.42 / 1.65	-	-

The values in the parentheses refer to the highest resolution shell.

[#] $R_{sym} = (\Sigma|I_{hkl} - \langle I_{hkl}\rangle|) / (\Sigma I_{hkl})$, where the average intensity $\langle I_{hkl}\rangle$ is taken over all symmetry equivalent measurements and I_{hkl} is the measured intensity for any given reflection.

[§] $I/\sigma I$ is the mean reflection intensity divided by the estimated error.

[†] $R_{work} = ||F_o| - |F_c|| / |F_o|$, where F_o and F_c are the observed and calculated structure factor amplitudes, respectively. R_{free} is equivalent to R_{work} but calculated for 5% of the reflections chosen at random and omitted from the refinement process.

As expected, the tertiary structure of the LysM domain of an Mg1LysM monomer is similar to that of previously described LysM domains (Bateman & Bycroft, 2000; Bielnicki et al, 2006; Bozsoki et al, 2017; Koharudin et al, 2011; Liu et al, 2012; Sánchez-Vallet et al, 2013) with a conserved βααβ-fold in which the antiparallel β-sheet lies adjacent to two α-helices (Fig. 1 and Fig. S1). The compact LysM structure is stabilized by two disulfide bridges between Cys^{44} and Cys^{78}, and between Cys^{13} and Cys^{70} (Fig. 1 and Fig. S1). In addition to the single LysM domain, Mg1LysM comprises a relatively long N-terminal tail that contains a short β-strand (Fig. 1).

The four Mg1LysM monomers within the a.u. form two pairs of homodimers that are each very tightly packed. The large homodimerization interface that occurs between two monomers was calculated to be 1113 Å2 using PISA (Protein Interfaces, Surfaces and Assemblies; http://www.ebi.ac.uk/pdbe/prot_int/pistart.html) (Krissinel & Henrick, 2007) and is stabilized by a total of 25 hydrogen bonds between residues of each of the monomers. In addition, the crystal structure revealed that the N-terminal 12 amino acid tails of the homodimer run anti-parallel and form a small but stable β-sheet (^{5}ITI^{7} of each chain) that is stabilized by clustering of all four isoleucine side-chain residues and by threonine-threonine sidechain hydrogen bonding, potentially strengthening the homodimer (Fig. 1). The latter hypothesis is further supported by the formation of two additional salt bridges formed between Arg^{2} of one subunit and Asp^{12} of the other one (Fig. 1). The root mean square deviations (rmsd) between the Cα atoms of the two homodimers of the a.u. is 0.267 Å as calculated with Lsqkab of the CCP4 suite (Winn, et al, 2011).

Surprisingly, when determining the crystal structure for the *C. fulvum* LysM effector Ecp6 in the absence of exogenously added chitin we found a chitin tetramer in a large interdomain groove between two of the three intrachain LysM domains that appeared to constitute an ultra-high affinity binding site, while no chitin binding was observed to the remaining, third LysM domain of Ecp6 (Sánchez-Vallet et al, 2013). Unexpectedly, the calculated $2|F_0| - |F_c|$ electron density map of the Mg1LysM crystal structure assembly similarly revealed well-defined electron density for a single chitin trimer bound to one monomer of the a.u. only (Fig. S2). Inspection of the crystal packing interactions unveiled the presence of a chitin binding pocket formed between two Mg1LysM protomers of neighbouring homodimers (Fig. 1). Since protein purification and crystallization was performed without exogenous addition of chitin in this case as well, we concluded that the chitin once more was derived from the cell wall of the heterologous protein production host *P. pastoris*. Potentially, this finding indicates that Mg1LysM displays an increased affinity for chitin (low micromolar range) when compared with other, single-acting, LysM domains. The chitin binding site is formed by the loops between the first β-strand and the first α-helix and between the second α-helix and the second β-strand of Mg1LysM, encompassing the residues ^{26}GDTLT^{30} and ^{56}NRI^{58} that are conserved in many other LysM domains including those of Ecp6 (Sánchez-Vallet et al, 2013) (Fig. S1). Remarkably, besides the ligand-independent Mg1LysM homodimerization described above, the crystal structure revealed that chitin induces a dimerization of homodimers and, consequently, that a chitin-binding groove is formed by two LysM domains from two independent protomers (Fig. 1; Fig. 2). In addition to the amino acids

that are in direct contact with the chitin trimer, the ligand-induced dimerization is strengthened by several hydrogen bonds that occur between residues from the two protomers involved. One salt bridge between residues K^{31} and D^{54} of the different protomers stabilizes the binding of the single chitin molecule and adds further strength to the dimerization, resulting in a tight binding pocket in which the chitin trimer is strongly bound (Fig. 2). Arguably, we would expect an increased chitin-binding affinity of Mg1LysM when compared with a single-acting LysM domain, which can explain in turn why the chitin remained adhered to the Mg1LysM protein during the protein purification procedure.

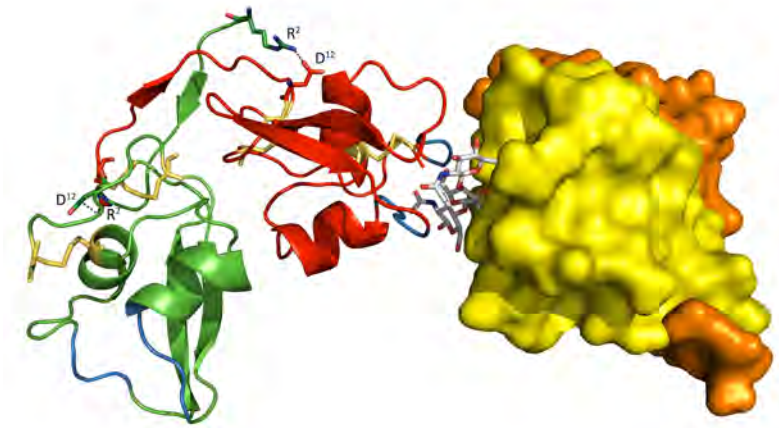

FIGURE 1 | Overall crystal structure of the *Zymoseptoria tritici* effector Mg1LysM. Crystal structure model in which a dimer of two Mg1LysM homodimers is shown, with each of the Mg1LysM molecules in a different colour (orange, yellow, red and green). While the two monomers that form a ligand-independent homodimer on the right are represented as a surface model, the two monomers that form a ligand-independent homodimer on the left are represented by ribbons with the (putative) chitin binding sites indicated in blue and the disulfide bridges as yellow sticks. The chitin trimer that mediates the dimerization of two ligand-independent Mg1LysM homodimers is depicted by grey sticks. The two salt bridges between R^2 and D^{12} in the dimer interface on the left are indicated with grey discontinuous lines.

In order to confirm the chitin-binding activity and determine the Mg1LysM chitin-binding affinity, a polysaccharide affinity precipitation assay and isothermal titration calorimetry (ITC) analysis were used, respectively. Since the crystal structure revealed that a portion of the Mg1LysM binding sites were occupied by chitin in the *P. pastoris*-produced Mg1LysM preparation, we pursued production of Mg1LysM in the bacterium *Escherichia coli* as a heterologous system that is devoid of chitin, in order to obtain chitin-free protein. The precipitation assay confirmed the binding of Mg1LysM to chitin and not to other insoluble polysaccharides (Marshall et al. 2011; Fig. S3). Subsequent ITC analysis based on chitohexaose $(GlcNAc)_6$ titration revealed that this protein preparation bound chitin with a binding affinity of 4.36 μM (Fig. 3). As previously demonstrated (Sanchez-Vallet et al. 2013), *P. pastoris*-produced Ecp6 monomers bind chitin with a stoichiometry of 1:1 (Fig. S3). In contrast, a stoichiometry of 1:2 was observed (n = 0.504) for Mg1LysM based on a single-binding-site model, analogous to the observation that two Mg1LysM

protomers originating from two Mg1LysM homodimers bind a single chitin trimer as disclosed in the crystal structure model. Obviously, this ratio also implies a polymerisation reaction in solution upon addition of the ligand chitohexaose. Thus, this finding can be interpreted as an independent confirmation of the ligand-induced Mg1LysM polymerisation as observed in the crystal structure.

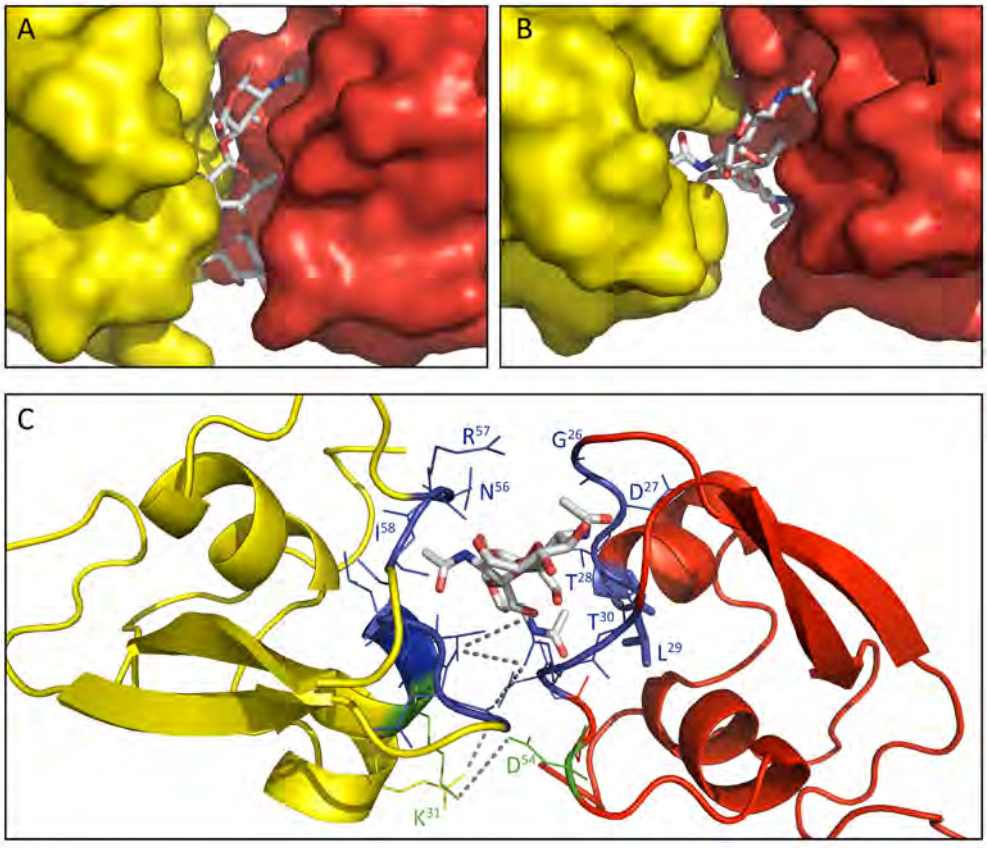

FIGURE 2 | The chitin binding groove formed by two Mg1LysM protomers. (A) A chitin trimer $(GlcNAc)_3$, displayed as grey sticks, was identified in a binding pocket formed by two Mg1LysM protomers (indicated in yellow and red, respectively). (B) Representation of the binding pocket from the top. (C) Detail of the chitin binding site. The amino acids involved in direct chitin trimer binding (^{26}GDTLT^{30} and ^{56}NRI^{58}) are represented with blue sticks and labelled. In addition, K^{31} and D^{54} (represented in green) of the two different Mg1LysM protomers form a salt bridge that tightly closes the binding pocket. Grey discontinuous lines represent the salt bridge and the hydrogen bonds between the protomers.

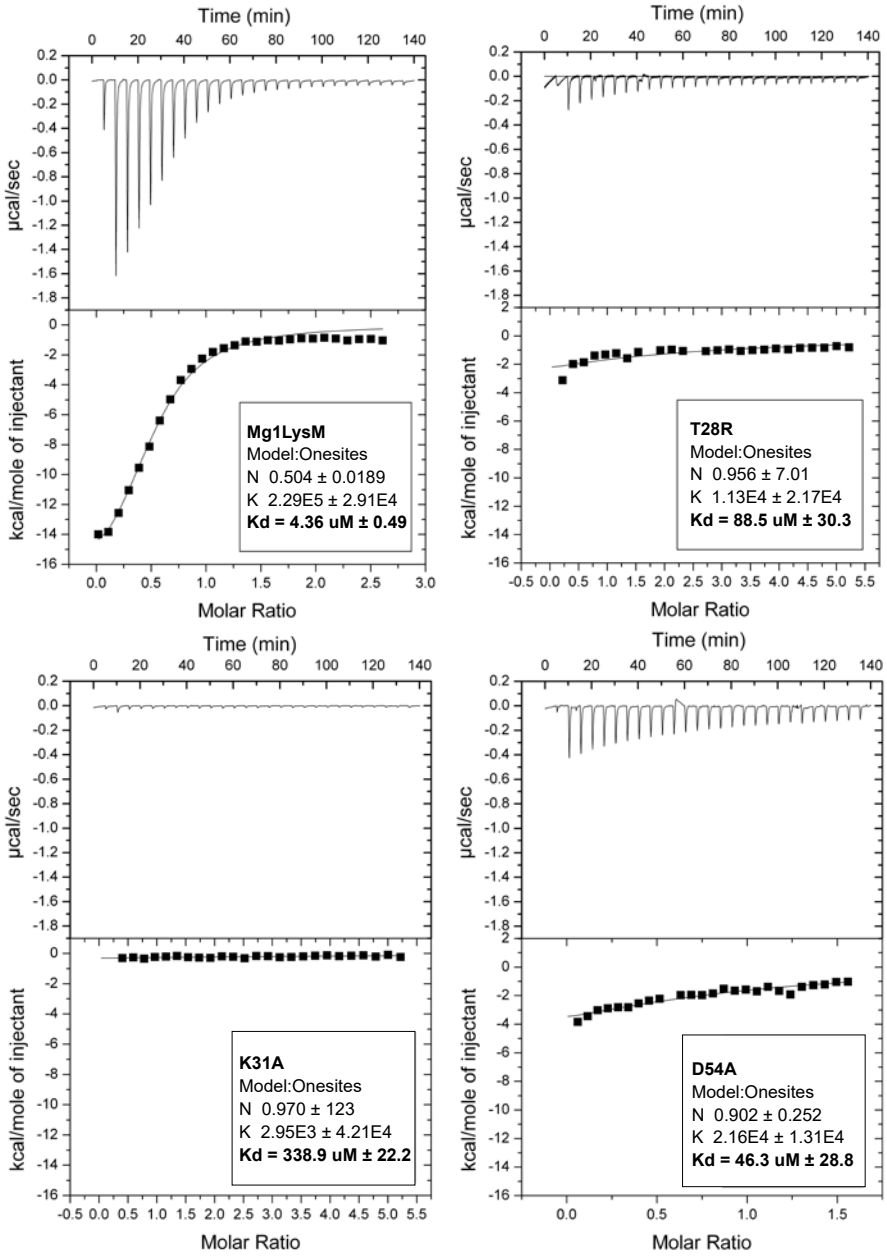

FIGURE 3 | Two Mg1LysM protomers bind a single chitin hexamer with high affinity. Isothermal titration calorimetry of $(GlcNAc)_6$ binding by wild-type Mg1LysM produced in *E. coli*, and the mutants $T^{28}R$, $K^{31}A$ and $D^{54}A$. The dissociation constant (K_d) and the stoichiometry (N) of the interactions are indicated.

Mg1LysM sequence conservation in a world-wide collection of *Z. tritici* isolates

In order to evaluate Mg1LysM conservation in *Z. tritici*, the occurrence of sequence polymorphisms was evaluated in a collection of 149 isolates from four different populations collected in Switzerland, Australia, Israel and the USA (Hartmann et al, 2017). This analysis revealed that the Mg1LysM protein sequence is highly conserved (Table S1). Only five non-synonymous mutations were identified in the full length Mg1LysM protein, three of which were previously identified (Marshall et al, 2011). Interestingly, none of these non-synonymous SNPs localized within the signal peptide, the homodimerization surface, the chitin-binding groove or concerned the residues involved in disulfide or salt bridge formation (Fig. 4A), pointing towards the relevance of these sites for the functionality of Mg1LysM. To test the impact of these polymorphisms on chitin binding, we heterologously produced two allelic variants of Mg1LysM in *E. coli*, namely the variants from the *Z. tritici* isolates ST99-CH1E4 and ST99-CH3F4 that, collectively, carry the five non-synonymous mutations (Fig. 4C; Table S1). Whereas both strains share the polymorphisms N3Q and Q34K, strain ST99-CH1E4 additionally carries R24Q, while strain ST99-CH3F4 additionally carries the polymorphisms R48K and Q20T (Fig. 4C; Table S1). Interestingly, a polysaccharide affinity precipitation assay revealed that, like the wild-type protein Mg1LysM, the two variants Mg1LysM_1E4 and Mg1LysM_3F4 still bind chitin (Fig. 4D), suggesting that the allelic variants have retained their biological activity.

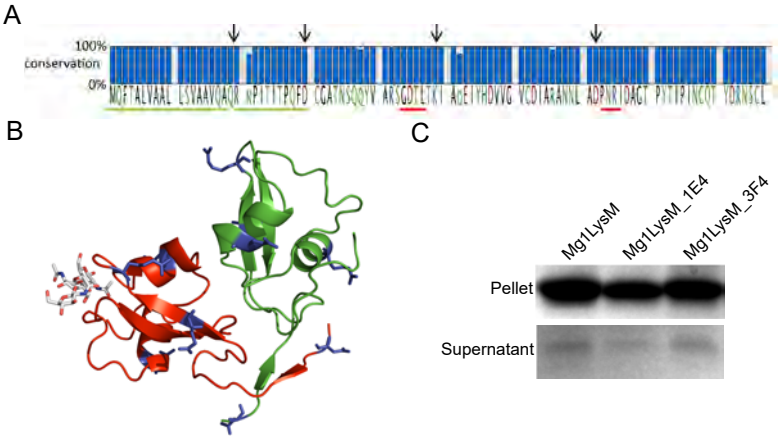

FIGURE 4 | Mg1LysM sequence polymorphisms in *Z. tritici*. (A) Five non-synonymous SNPs were identified in 149 *Z. tritici* strains from four different populations. Arrows indicate the position of the residues involved in the formation of salt bridges, while green underlining indicates the signal peptide and red underlining the chitin-binding loops. Red and green underlines indicate the signal peptide and the chitin binding sites, respectively. (B) While the mutations (shown in blue sticks) do not co-localize but occur dispersed over the Mg1LysM protein, none of them is in the chitin-binding site or in the (homo-)dimerization surface. (C) Mg1LysM and the two allelic variants Mg1LysM_1E4 and Mg1LysM-3F4 bind insoluble chitin. All proteins were heterologously produced in *E. coli* and incubated with chitin for 6 hours. After centrifugation, pellets and supernatants were analysed on polyacrylamide gel followed by CBB staining.

Chitin-induced Mg1LysM polymerization is crucial for protection of hyphae against the hydrolytic activity of plant chitinases

We previously showed that Mg1LysM is able to protect chitin against chitinase hydrolysis (Marshall et al., 2011). Localization experiments making use of BODIPY-labelled Mg1LysM protein exogenously applied to *Trichoderma viride*, a fungal species that exposes cell wall chitin during growth *in vitro*, revealed that Mg1LysM binds to fungal cell walls (Fig. 5A). Next, we attempted to evaluate the contribution of the ligand-independent Mg1LysM homodimerization to hyphal protection against chitinases. To this end, we pursued to produce an Mg1LysM mutant that lacked the 12-amino acid tail that is, besides the large protomer-protomer interface, responsible for ligand-independent homodimerization. Unfortunately, production of this mutant in the heterologous host *P. pastoris* was not successful as hardly any protein could be detected. The protein is apparently degraded either due to exposure of the hydrophobic residues (V40 and I68) located at the centre of the large (1113 Å2) homodimerization interface, or homodimerization is stringently required for proper folding of the protein.

Subsequently, we evaluated the role of chitin-induced Mg1LysM homodimerization in the protection of fungal hyphae against chitinases by generating three mutant proteins. The T^{28} residue that makes direct contact with the chitin substrate in the binding site that was previously shown to be essential for chitin binding in the *C. fulvum* LysM effector Ecp6 was substituted by arginine. In addition, the two residues involved in the formation of the intermolecular salt bridge near the chitin binding site (K^{31} and D^{54}) were substituted by alanines, respectively. In order to obtain chitin-free proteins, production in *E. coli* was pursued.

Based on previous findings for Ecp6 (Sánchez-Vallet et al, 2013), we predicted that the $T^{28}R$ mutant was incapable of binding chitin, but the chitin binding capacity of the mutants impaired in the intermolecular salt bridge formation remained to be elucidated (Sánchez-Vallet et al, 2013). ITC analysis with the mutant $T^{28}R$ revealed a significantly reduced binding affinity of 88.5 μM, which is twenty times weaker when compared with wild-type Mg1LysM protein produced in *E. coli* (4.36 μM; Fig. 3). However, also the binding affinity of the mutants $K^{31}A$ and $D^{54}A$ decreased, to 338.9 μM and 46.3 μM, respectively (Fig. 3). Furthermore, besides a lower chitin-binding capacity, the stoichiometry calculated for the mutants $K^{31}A$ and $D^{54}A$ changed from 1:2 as observed for the wild-type Mg1LysM protein to 1:1. This finding implies that a single monomer of $K^{31}A$ or $D^{54}A$ binds a single chitohexaose in solution, whereas a single chitohexaose is bound by two wild-type Mg1LysM protomers, supporting the hypothesis that the chitin-induced dimerization is impaired in $K^{31}A$ and $D^{54}A$ by disruption of the intermolecular salt bridge (Fig. 3).

Subsequently, we tested the ability of the Mg1LysM mutants to protect fungal hyphae against the hydrolytic activity of plant chitinases. To this end, spores of *Fusarium oxysporum* and *Trichoderma viride* were germinated, incubated with a plant extract containing hydrolytic enzymes including chitinases, and supplemented with wild-type or mutant Mg1LysM. As expected, wild-type Mg1LysM protein produced in *E. coli* prevented the hydrolysis of hyphae of *Fusarium oxysporum* f. sp. *lycopersici* (Fig. 5B) and *Trichoderma viride* (Fig. S4). Furthermore,

mutant $T^{28}R$ that is mutated in the substrate-binding loop did not protect *F. oxysporum* and *T. viride* hyphae against these hydrolytic enzymes (Fig. 5B and Fig. S4), confirming that chitin-binding of Mg1LysM is required to confer protection of cell walls against hydrolysis by plant enzymes. Considering the even lower chitin-binding activity, it is not surprising that also mutant $K^{31}A$ did not protect cellwalls against enzymatic hydrolysis. However, also mutant $D^{54}A$ no longer protected cell walls, suggesting that a ten-fold reduction of chitin-binding affinity is sufficient to disrupt the protective activity of Mg1LysM. Unfortunately, based on these findings it is impossible to determine the contribution of the dimerization to the protection activity of Mg1LysM.

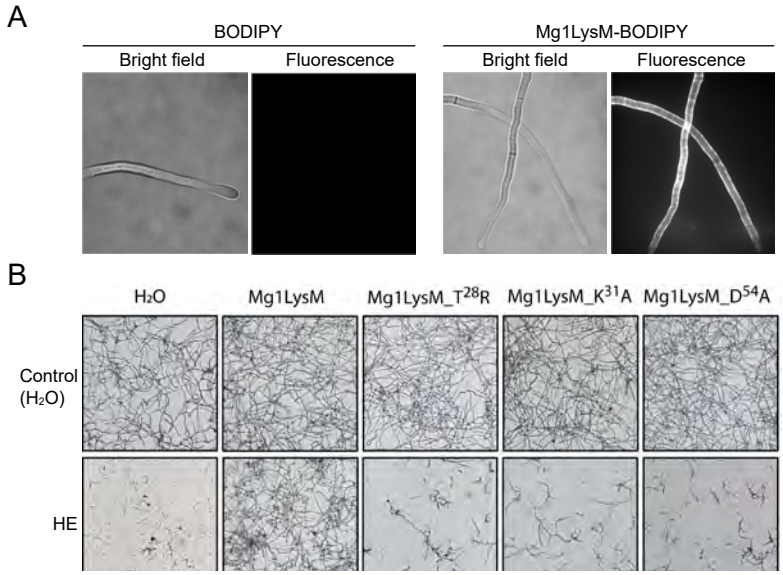

FIGURE 5 | Mg1LysM mutants are impaired in protection against chitinases. (A) *Trichoderma viride* incubated with Mg1LysM with the amine-reactive fluorescent dye BODIPY, or with BODIPY only as a control,for 4 hours and bright field and fluorescence microscopy pictures are shown. (B) Microscopic pictures of *Fusarium oxysporum* f. sp. *lycopersici* grown *in vitro* in the absence or presence of wild-type or mutant Mg1LysM, 4 hours after addition of tomato hydrolytic enzymes (HE) that include chitinases, or water as control.

We previously determined that LysM effector Ecp6 has two sites that bind chitin with 1:1 stoichiometry, one with ultra-high affinity (k_d = 280 pM) and one in the range with which Mg1LysM binds chitin (k_d = 1.70 μM) (Bateman & Bycroft, 2000; Bielnicki et al, 2006; Bozsoki et al, 2017; Koharudin et al, 2011; Liu et al, 2012; Sánchez-Vallet et al, 2013), but both of which bind chitin with higher affinity than Mg1LysM. Intriguingly, Ecp6 fails to protect hyphae against hydrolysis by chitinases (De Jonge et al, 2010; Sánchez-Vallet et al, 2013). Nevertheless, localization experiments making use of constitutive expression of C-terminally GFP-tagged Ecp6 in *Verticillium dahliae*, and of BODIPY-labelled Ecp6 protein exogenously applied to *Botrytis cinerea*, two fungal species that expose chitin on their cell walls during growth *in vitro*,

revealed that Ecp6 can bind to fungal cell walls (Fig. S5) in a similar fashion as *Cladosporium fulvum* effector protein Avr4 that protects fungal cell walls against hydrolysis by chitin binding through an invertebrate chitin-binding domain (van den Burg et al, 2006; Van Esse et al, 2007). These findings suggest that binding of a LysM effector to cell wall chitin with high affinity is not sufficient to mediate protection against hydrolytic enzymes. Moreover, from these observations we infer that chitin-induced dimerization of Mg1LysM may be crucial for hyphal protection against plant enzymatic hydrolysis.

Considering that Mg1LysM homodimers possess two chitin-binding sites on opposite sides of the protein complex (Fig. 1), combined with the observed chitin-induced dimerization that may be responsible for the protective activity, we hypothesized that Mg1LysM will form highly oligomeric super-complexes in which ligand-independent Mg1LysM homodimers dimerize on both ends in a chitin-dependent manner (Fig. 6A). Moreover, we hypothesized that LysM effectors that do not protect hyphae against chitinase hydrolysis would not display such oligomerisation. To test these hypotheses, we first assessed whether we could alter the particle size distribution of Mg1LysM in solutions by adding chitohexaose. Using dynamic light scattering (DLS) we observed that, upon chitin addition at a molar ratio of 1:2 the radius distribution of Mg1LysM particles shifted from around 10 nm in the absence of chitin to 100 nm in the presence of chitin. Moreover, further increase of the chitin concentration to a 1:5 ratio induced a strong signal appearing at 100 μM, demonstrating clear ligand-induced polymerisation of Mg1LysM protein to large protein complexes. Next, we assessed the effect of chitohexaose on the distribution of Ecp6 particles in solution. Interestingly, although the addition of chitohexaose smoothened the Ecp6 particle size distribution, suggesting the stabilization of Ecp6 molecules, chitin addition did not lead to an increased particle size. Thus, in contrast to Mg1LysM, Ecp6 does not display chitin-induced polymerization.

To confirm our observations with respect to the chitin-induced polymerization of Mg1LysM, we pursued an independent validation of our observations. To this end, we reasoned that if Mg1LysM indeed polymerizes in the presence of chitin, we should ultimately be able to precipitate such polymeric complexes during centrifugation into a pellet, whereas such a pellet cannot occur in case polymerization does not take place. Thus, we incubated Mg1LysM overnight with chitohexaose and subsequently centrifuged the sample at 20,000 g in the presence of 0.002% methylene blue to visualize the protein. A clear pellet appeared when Mg1LysM was incubated with chitin, but not in the control treatment where no chitin was added to the Mg1LysM protein, nor in the control treatment with chitohexaose only in the absence of Mg1LysM (Fig. 7). Collectively, these data confirm the occurrence of chitin-induced Mg1LysM effector polymers. In contrast, similar treatments of Ecp6 with chitin did not result in a pellet after centrifugation, confirming that Ecp6 does not undergo chitin-induced polymerization (Fig. 7).

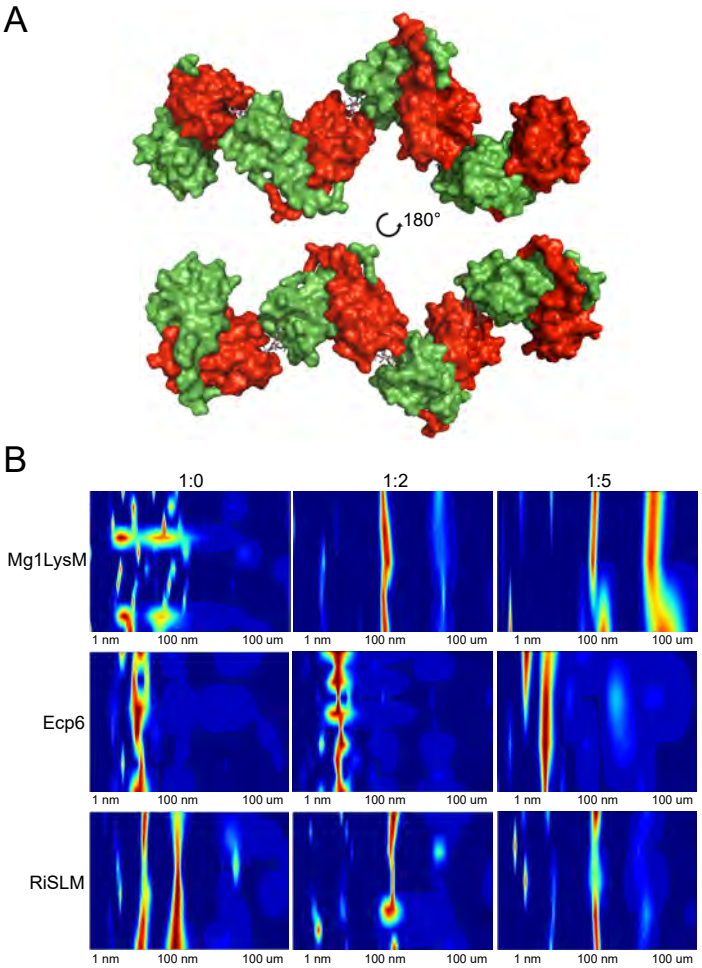

FIGURE 6 | Chitin-induced polymerization of Mg1LysM homodimers. (A) Model inferred from the crystal structure of Mg1LysM in which a continuous structure of Mg1LysM homodimers and chitin is formed. Alternating chitin molecules (in grey sticks) and Mg1LysM homodimers (in red and green), each of them with two chitin-binding sites, are shown. (B) Dynamic light scattering (DLS) heat maps of Mg1LysM,*C. fulvum* Ecp6 and RiSLM treated with chitohexaose in molar ratios of 1:0, 1:2 and 1:5 (protein: chitohexaose), respectively. The particle size distribution is indicated as a Color scale ranging from blue (lowest amount) to red (highest amount) for a particle size range of 1 nm to 100 um.

Recently, it was demonstrated that the arbuscular mycorrhizal (AM) fungus *Rhizophagus irregularis* secretes the LysM effector RiSLM to facilitate its mutualistic symbiosis (Zeng et al., 2020). Interestingly, like Mg1LysM, RiSLM was shown to be composed of a single LysM only, and furthermore to protect hyphae against hydrolysis by chitinases. Thus, we used RiSLM to test whether chitin-induced polymerisation is restricted to Mg1LysM only, or similarly occurs for RiSLM as well. Interestingly, like with Mg1LysM, a chitin-induced particle size shift was observed in the DLS assay with RiSLM (Fig. 6B). Moreover, upon overnight incubation of

RiSLM with chitohexaose a clear pellet could be obtained after centrifugation, demonstrating that polymerization occurred (Fig. 7).

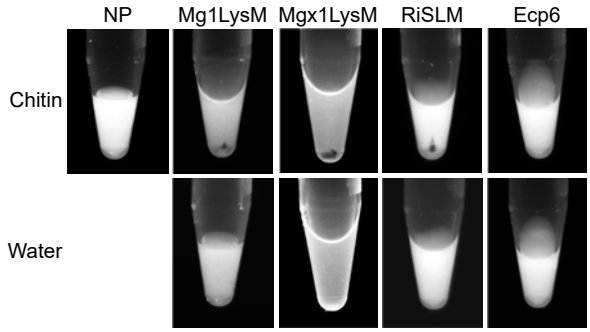

FIGURE 7 | Chitin-induced polymerization of Mg1LysM, Mgx1LysM and RiSLM. Effector proteins were incubated with chitohexaose (chitin) or water as control. After overnight incubation, methylene blue was added and protein solutions were centrifuged, resulting in protein pellets as a consequence of polymerization for Mg1LysM, Mgx1LysM and RiSLM, but not for Ecp6. NP is the 'no protein' sample with chitin in the absence of LysM effector protein.

In Chapter 5, we demonstrated that *Z. tritici* produces a third, previously disregarded, LysM effector that was designated Mgx1LysM. Like Mg1LysM, also Mgx1LysM contains only one LysM, binds chitin, suppresses chitin-induced plant immunity and protects hyphal growth against chitinase hydrolysis (Chapter 5). Therefore, we assessed whether Mgx1LysM undergoes chitin-induced polymerization in the centrifugation assay. Indeed, like Mg1LysM and RiSLM, a clear pellet was observed upon incubation with chitohexaose and subsequent centrifugation (Fig. 7). Collectively, these data suggest that chitin-induced polymerization is a common phenomenon that occurs not only with Mg1LysM, but also with other LysM effectors that contain only one LysM and protect fungal hyphae.

DISCUSSION

Studies on many plant pathogenic fungi have shown that the perception of microbial cell wall-derived glycans by plant hosts plays a central role in microbe–host interactions (Rovenich et al, 2016). Among these glycans, fungal cell wall chitin has emerged as one of the most potent fungal elicitors of host immune responses (Rovenich et al, 2016; Sánchez-Vallet et al, 2015). The widespread glycan perception capacity in plants has spurred the evolution of various fungal strategies to evade glycan perception (Rovenich et al, 2016; Sánchez-Vallet et al, 2015). Many fungal pathogens secrete LysM effectors to perturb the induction of chitin-triggered immunity. Structural analysis of the *C. fulvum* LysM effector Ecp6 has revealed that this activity could be attributed to the presence of an ultra-high chitin binding affinity site in the LysM effector protein that is established by intramolecular LysM domain dimerization (Sánchez-Vallet et al,

2013). However, some LysM effectors rather, or additionally, are able to prevent the hydrolysis of fungal cell wall chitin by plant chitinases. Moreover, functional characterization of Mg1LysM, a LysM effector that is merely composed of a single LysM domain and a few additional amino acids, suggested that the ability to protect cell walls is conferred simply by the chitin-binding ability of the LysM domain (Marshall et al, 2011). Yet, the observation that various other LysM effectors, including *C. fulvum* Ecp6, *M. oryzae* Slp1 and *C. higginsianum* ELP1 and ELP2, are not able to protect hyphae challenged this hypothesis (De Jonge et al, 2010; Mentlak et al, 2012; Takahara et al, 2016). Thus, the mechanism by which some LysM effectors are able to protect fungal cell walls remained to be characterized. The crystal structure model that was generated in this study has revealed that Mg1LysM is able to undergo chitin-mediated dimerization such that a chitin molecule is deeply buried in the protein dimer. Nevertheless, the structure of the dimer allows a chitin chain to protrude into the solvent on either side of the binding groove, such that it is conceivable that the dimer can be formed on long-chain chitin polymers of any length, including polymeric cell wall chitin. In addition to several noncovalent bounds between the two Mg1LysM protomers and between the protein and the chitin, a salt bridge between the two Mg1LysM protomers strengthens the chitin-binding affinity and thus supports the chitin-induced dimerization by stabilizing the chitin binding groove. Arguably, it is this particular trait that confers the ability to protect hyphae against plant chitinases, as disruption of the ion bond in the $K^{31}A$ mutant abolished hyphal protection and chitin binding by itself is not sufficient to confer cell wall protection. The crystal structure further revealed that Mg1LysM undergoes ligand-independent homodimerization whereby a large dimerization interface of two Mg1LysM monomers is stabilized by several noncovalent bounds and further strengthened by two salt bridges between the interlaced N-terminal regions of the protein. Despite various efforts, we have not been able to produce monomeric Mg1LysM protein, suggesting that ligand-independent homodimerization is required for proper folding of the protein. Consequently, Mg1LysM homodimers are released and possess two chitin-binding sites on opposite sides of the protein (Fig. 1). Combined with the observed chitin-induced dimerization, we postulate that this provides Mg1LysM with the ability to form highly oligomeric super-complexes in the fungal cell wall, in which ligand-independent Mg1LysM homodimers dimerize on both ends in a chitin-dependent manner, leading to the formation of a contiguous structure throughout the cell wall (Fig. 6A). Indeed, a chitin-inducible shift in particle size could be demonstrated for Mg1LysM in DLS experiments, confirming the occurrence of polymerisation, whereas such shift was not observed for Ecp6. Moreover, overnight incubation of Mg1LysM with chitohexaose led to the formation of polymers that could be pelleted during centrifugation, demonstrating that the polymers grew to relatively large particles. Also this phenomenon was not observed for Ecp6. Intriguingly, the recently characterized additional *Z. tritici* LysM effector Mgx1LysM (Chapter 5) and *R. irregularis* RiSLM (Zeng et al., 2020) that, like Mg1LysM, comprise a single LysM only and protect hyphae against chitinases, similarly possess the ability to polymerize in a chitin-dependent manner, suggesting that polymerization into polymeric super-complexes in the fungal cell wall is a common phenomenon among LysM effectors that protect fungal hyphae. Possibly, it is such contiguous structure that provides steric

hindrance that renders fungal cell wall chitin inaccessible to chitinase enzymes. Thus, both ligand-independent homodimerization as well as ligand-induced dimerization of Mg1LysM appear to be required for its cell wall protective function. Accordingly, residues shaping these regions are fully conserved in all Mg1LysM isoforms that have been identified to date.

MATERIALS AND METHODS

Protein production and purification

Mg1LysM was previously produced in *Pichia pastoris* strain GS115 as described (Marshall et al, 2011). Purification was performed by gel filtration chromatography (Superdex 75: GE Healthcare, Chicago, IL, US) in 20 mM HEPES, pH 7.0, and 50 mM NaCl. *P. pastoris* produced protein (6-10 mg/mL) was used for protein crystallization. *Escherichia coli* protein production was performed using pET-SUMO (Thermo Fisher, Waltham, MA, USA). Mg1LysM was cloned into pGEM-T (Promega, Madison, WI, US) using specific primers (Table S1). Mutants were obtained by PCR using overlapping primers with the corresponding mismatch (Table 2) followed by digestion of the template by *Dpn*I. For the cloning of ST99_CH3F4 and ST99_CH1E4 versions of Mg1LysM, the sequence was commercially synthesized (Eurofins Genomics, Ebersberg, Germany). After digestion of the resulting vector with *Sac*I and *Hind*III (Promega, Madison, WI, US), Mg1LysM was cloned in the final vector pET-SUMO. The expression system *E. coli* ORIGAMI (DE3, Merck, Darmstadt, Germany) cells was used to express the protein following the manufacturer's instructions. Transformants were selected and grown in Luria broth (LB) medium until an optical density of 0.8 at 600 nm was reached. Protein production was induced with the addition of 0.05 mM Isopropyl β-D-1-thiogalactopyranoside (IPTG) at 28°C. Cells were harvested by centrifugation ~20 h after induction, the cell pellets were dissolved and lysed using lysozyme from chicken egg (Sigma-Aldrich, St. Louis, MO, US) and the 6xHis-SUMO tagged proteins were purified from the soluble protein fraction after centrifugation using an Ni^{2+}-NTA Superflow column (Qiagen, Venlo, Netherlands). Next, purified proteins were incubated with the SUMO protease ULP1 from *Saccharomyces cerevisiae* (Thermo Fisher, Waltham, MA, USA), dialysed over night against 200 mM NaCl at 4°C, and again passed through a Ni^{2+}-NTA Superflow column. Native proteins were finally dialysed against 50 mM NaH_2PO_4, 300 mM NaCl at pH 8.0, concentrated to 0.6 mg/mL over Amicon ultracentrifugal filter units (Sigma-Aldrich, St. Louis, MO, USA) and used for subsequent assays. RiSLM was produced as described previously (Zeng et al., 2020).

Crystallization conditions and structure determination

First crystal hits with 1,4-dioxane as the reservoir solution were obtained overnight in a small initial vapor-diffusion crystallization screening campaign using the Phoenix robot (Art Robbins Instrument LLC, Sunnyvale, CA, USA) with 96-well Intelli Plates (Dunn Labortechnik GmbH, Asbach, Germany) and several different commercial screens (Hampton Research, Aliso Viejo,

CA, USA; Molecular Dimensions, Newmarket, Suffolk, UK) (Newman et al, 2005). Conditions were further optimized and useful crystals were finally obtained by micro-seeding techniques using 0.1 M sodium citrate pH 5.6, 5%-20% PEG4000 and 5% isopropanol as the reservoir solution (Bergfors, 2003). 0.2 M sodium acetate pH 4.6 with 20% ethylene glycol was used as the crystal cryo-buffer. Several crystals were soaked with either I3C (Jena Bioscience GmbH, Jena, Germany), 2 mM in cryo-buffer, quick soak, or Ta_6Br_{14} (Jena Bioscience GmbH, Jena, Germany), 1 mM in cryo-buffer, 1 hr soak, brief wash and prolonged back soak. X-ray diffraction data were collected on BL14.1 at the BESSY II electron storage ring operated by the Helmholz-Zentrum Berlin (Gerlach et al, 2016). Using the Phenix AutoSol wizard (Adams et al, 2010), initial phases were obtained from the $Ta_6Br_{12}^{2-}$ derivatized crystals by single-wavelength anomalous dispersion techniques (SAD) that were improved by phase information from the I3C derivatized crystals by single isomorphous replacement with anomalous scattering (SIRAS).

The structure was refined using *REFMAC*5 (Murshudov et al, 2011) and phenix (Adams et al, 2010) and manually built using *Coot* (Emsley et al, 2010). All figures showing structural representations were prepared with the program *PyMOL* (The PyMOL Molecular Graphics System, Version 2.0 Schrödinger, LLC, DeLano Scientific, Palo Alto, CA, USA]. The quality of the final model was validated with *MolProbity* (Chen et al, 2010). Refinement and phasing statistics are summarized in Table 1.

Chitinase-protection assay

In-vitro chitinase protection assays were performed as described previously (van den Burg et al, 2004). Essentially, ~10^3 conidiospores of *Fusarium oxysporum* f. sp. *lycopersici* or *Trichoderma viride* were incubated overnight at room temperature in 40 µL of half-strength potato dextrose broth (PDB; Becton Dickinson, Franklin Lakes, NJ, USA) in a 96-well microtiter plate. Subsequently, wild-type or mutant Mg1LysM protein was added at a final concentration of 20 µM. After a 2 h incubation period, 10 µL of tomato extract containing hydrolytic enzymes was added (van den Burg et al, 2004). Fungal growth was assessed microscopically after 4 h of incubation at room temperature.

Polysaccharide precipitation assay

The polysaccharide precipitation assay was performed as described (Marshall et al, 2011). 800 µL of Mg1LysM (30 µg/mL) was incubated with 50 µL of chitin beads (NEB, Massachusetts, USA), 10 mg shrimp chitin, chitosan, cellulose or xylan (all from Sigma-ALRICH, Missouri, USA) for 6 h at 4°C. The insoluble fraction was pelleted by centrifugation (13,000 g, 5 min), resuspended in 100 µL of water and incubated at 95°C for 10 minutes. The supernatant was concentrated using Microcon Ultracel YM-10 tubes (Merck, Darmstadt, Germany) to 80 µL, incubated at 95°C for 10 minutes with 30 µL of protein loading buffer (4×). The presence of proteins in pellet and supernatant was examined on a Mini-PROTEAN TGX Stain-Free Gel (Bio-Rad, California, USA) followed by Coomassie brilliant blue staining.

Isothermal titration calorimetry

Isothermal titration calorimetry (ITC) experiments were performed at 20°C following standard procedures using a Microcal VP-ITC calorimeter (GE Healthcare, Chicago, IL, US). The *E. coli*-produced wild-type Mg1LysM (20 μM) and the mutants $T^{28}R$ (15 μM), $K^{31}A$ (30 μM) and $D^{54}A$ (30 μM) were titrated with a single injection of 2 μL, followed by 26 injections of 10 μL of $(GlcNAc)_6$ (Isosep AB, Tullinge, Sweden) at 200 μM. Ecp6 (15 μM) was titrated with $(GlcNAc)_6$ at 400 μM. Before the experiment, all proteins were dialyzed against 20 mM of sodium chloride, pH 7.0. Chitohexaose (Megazyme, Wicklow, Ireland) was freshly dissolved in the dialysis buffer. Data were analyzed using Origin (OriginLab, Northampton, MA, USA) and fitted to a one-binding-site model. Before and after the experiment protein samples were analysed on SDS-PAGE gel and stained with Coomassie brilliant blue.

Dynamic light scattering (DLS) measurements

Mg1LysM, RiSLM and Ecp6 were dialyzed overnight against water, and subsequently incubated with 0.01% Triton X-100 for 4 hours to improve protein solubility. Next, chitohexaose (Megazyme, Wicklow, Ireland) was added in a molar ratio of 1:0, 1:2 and 1:5 (protein:chitin) and incubated overnight. Particle size distribution was measured by a SpectroSize 300 (Xtal Concepts, Hamburg, Germany).

Polymerization assay

Mg1LysM and Ecp6 were adjusted to a concentration of 400 μM and 100 μL of each protein was incubated with 100 μL of 4 mM chitohexaose (Megazyme, Wicklow, Ireland), or 100 μL water as control, at room temperature overnight. Similarly, 100 μL of Mgx1LysM (570 μM) and RiSLM (600 μM) were incubated with 80 μL and 75 μL of 4 mM chitohexaose (Megazyme, Wicklow, Ireland), respectively, or water as control in a total volume of 200 μL. The next day, 2 μL of 0.2% methylene blue (Sigma-Aldrich, Missouri, USA) was added and incubated for 10 min after which protein solutions were centrifuged at 20,000 g for 15 min. Photos were taken with a ChemiDoc MP system (Bio-Rad, California, USA) with custom setting for RFP.

Localisation of Mg1LysM and Ecp6

Labelling of effector proteins with BODIPY TMR-X amine reactive probe (Invitrogen, Carlsbad, CA, USA) was performed as described previously (van den Burg et al, 2006; Van Esse et al, 2007). For localisation assay of Mg1LysM, conidiospores of *Trichoderma viride* were harvested from five-day-old potato dextrose agar (PDA) plates and adjusted to 10^6 conidiospores/mL with half-strength PDB. The conidiospore solution was pipetted into a 96-well microtiter plate in aliquots of 50 μL and the plate was incubated overnight at room temperature for germination. The next day, BODIPY-labeled Mg1LysM was applied at a final concentration of 8 μM and incubated for 4 hrs at room temperature in the dark. Microscopic analysis was performed using a Nikon Eclipse Ti microscope using a 100× Plan apo oil immersion objective (NA 1.4) and a 561 nm laserline. Pictures were processed and analysed with ImageJ (http://rsbweb.nih.gov/ij/).

For localisation study of Ecp6, conidiospores of a *V. dahliae* transformant were grown in a few micro liters of PDB on a glass slide with coverslip. To prevent the samples from drying out, the slides were mounted on top of moistened tissue in an empty pipette box with water on the bottom. After approximately 6 hr of growth at room temperature, the slides were used for localization studies. Conidiospores of *Botrytis cinerea* were harvested and germinated overnight in PDB at room temperature. BODIPY-labeled proteins were applied at a concentration of 4 μM and incubated for 2-3 hrs at room temperature in the dark. The localisation studies were performed using a Nikon eclipse 90i UV microscope and NIS-Elements AR 2.3 software (Nikon Instruments Inc., Melville, USA).

Assembly and alignment of *Mg1LysM* sequences

Illumina whole-genome sequencing data from a global collection of *Z. tritici* isolates was used to extract *Mg1LysM* sequences (Hartmann & Croll, 2017). We used the SPAdes assembler version 3.6.2 (Bankevich et al, 2012) to generate *de-novo* genome assemblies. The SPAdes pipeline includes the BayesHammer read error correction module to build contigs in a stepwise procedure based on increasing k-mer lengths. We defined the k-mer range as 21, 35, 49, 63 and 77. We used the "—careful" option to reduce mismatches and indel errors in the assembly. Polished assemblies were then used to retrieve the contigs containing *Mg1LysM* orthologs based on blastn (Camacho et al, 2009). High-confidence sequence matches were extracted with samtools (Li et al, 2009) from each draft assembly and aligned using MAFFT version 7.305b (Katoh & Standley, 2013) using the --auto option and 1,000 iterative refinement cycles. Alignments were processed using JalView (Waterhouse et al, 2009) and CLC Genomic Workbench 9 (Qiagen, Venlo, Netherlands).

Accession codes

All whole-genome sequencing data is accessible on the Nucleotide Short Read Archive (accession numbers PRJNA327615 and PRJNA178194). The atomic coordinates and experimental structure factors were deposited with the Protein Data Bank under accession code 6Q40.

ACKNOWLEDGEMENTS

Work in the laboratory of B.P.H.J.T. is supported by the Research Council Earth and Life Sciences (ALW) of the Netherlands Organization of Scientific Research (NWO). We thank Kiki Kots for providing help with confocol microscopy. The funders had no role in study design, data collection and analysis, decision to publish, or preparation of the manuscript. The authors acknowledge support from the partners of the European Research Area Network for Coordinating Action in Plant Sciences (ERA-CAPS) consortium "SIPIS".

AUTHOR CONTRIBUTIONS

ASV, JRM, BPHJT conceived the study; ASV, HT, LRM, RdJ, HPvE designed experiments; ASV, HT, LRM, DJV, RSB, SW, AK, LV, DC performed experiments; RdJ, HPvE, AZ analyzed data; ASV, HT, LRM, JRM, BPHJT wrote the manuscript; JRM, BPHJT supervised the project; all authors discussed the results and contributed to the final manuscript.

SUPPLEMENTARY DATA

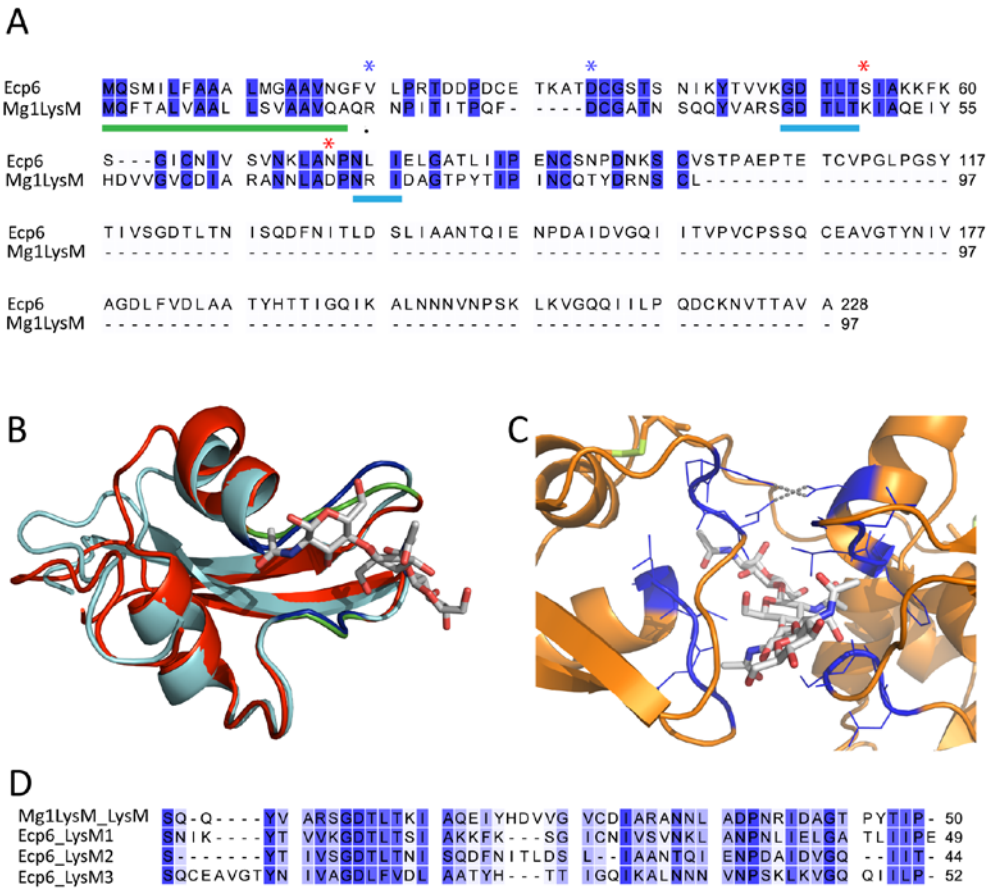

FIGURE S1 | Protein alignment of Ecp6 and Mg1LysM. (A) Protein sequence alignment of Ecp6 and Mg1LysM. The two chitin binding loops of Mg1LysM are indicated with a blue line and the signal peptide with a green line. Red and blue asterisks indicate the position of the residues involved in the formation of salt bridges in the binding groove and in the dimerization surface, respectively. (B) Structural alignment of the LysM1 domain from Ecp6 (in blue) and the LysM domain from Mg1LysM (in red). The chitin trimer is shown in grey sticks. The chitin binding loops are shown in dark blue and green for LysM1 and for Mg1LysM, respectively. (C) Chitin binding pocket formed by LysM1 and LysM3 of Ecp6. In orange ribbons, a single molecule of Ecp6 is shown. The residues involved in chitin binding are shown as blue sticks. Hydrogen bonds between the two LysM domains are shown in grey. (D) Protein sequence alignment of the LysM domains of Ecp6 and Mg1LysM.

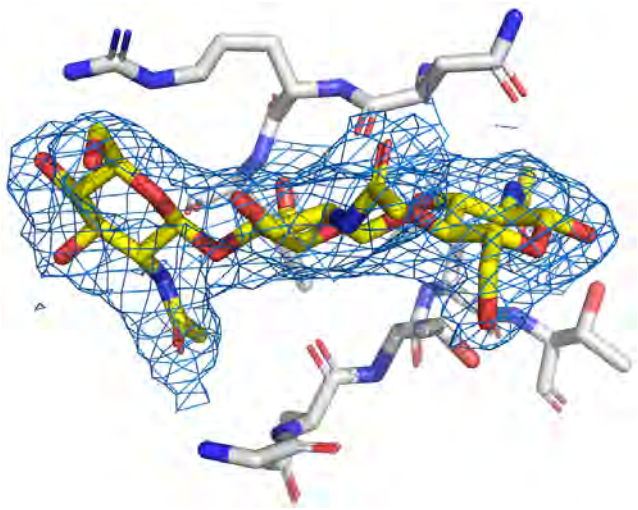

FIGURE S2 | $2|F_0| - |F_c|$ map. $2|F_0| - |F_c|$ electron density map around the chitin trimer (carbon atoms coloured yellow) is contoured at 1 sigma above the mean. Amino acids of the chitin binding motif ([26]GDTLT[30] and [56]NRI[58]) are represented as sticks (carbon atoms coloured light-grey).

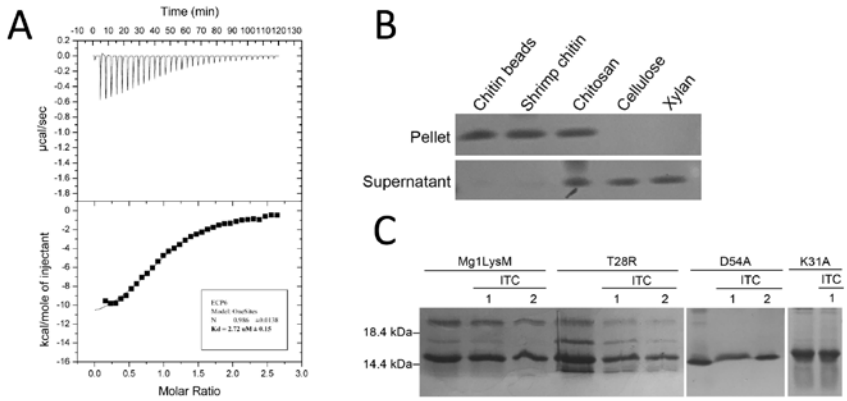

FIGURE S3 | (A) Isothermal titration calorimetry of $(GlcNAc)_6$ binding by Ecp6 produced in *P. pastoris*. (B) Mg1LysM protein binds to insoluble chitin, but not to other carbohydrates. The purified Mg1LysM protein produced in *E. coli* was incubated with chitin beads, the insoluble carbohydrates shrimp chitin, chitosan, cellulose and xylan and centrifuged. Both the pellet and the supernatant were analyzed on protein gels. (C) Coomassie Brilliant Blue stained gel of Mg1LysM and mutant proteins before and after ITC assay. 1 and 2 indicate two independent ITC measurements.

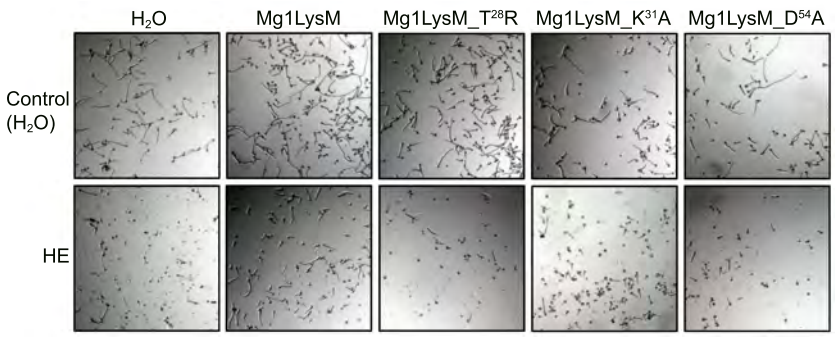

FIGURE S4 | Mg1LysM mutants are impaired in protection of *Trichoderma viride* against chitinases. Microscopic pictures of *Trichoderma viride* grown *in vitro* in the absence or presence of wild-type or mutant Mg1LysM, 4 hours after addition of tomato hydrolytic enzymes (HE) that include chitinases, or water as control.

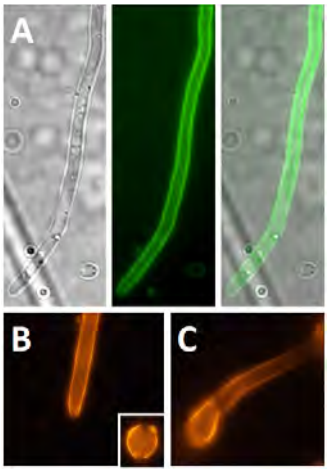

FIGURE S5 | *C. fulvum* LysM effector Ecp6 protein localizes to fungal cell walls. (A) Brightfield image (left), fluorescence image (middle) and the overlay image (right) of a hypha from an *Ecp6-GFP* transformant of *Verticillium dahliae*. The chitin-binding *C. fulvum* LysM effector Ecp6 (B) and chitin-binding effector Avr4 (C) that carries an invertebrate chitin-binding domain were labeled with the amine-reactive fluorescent dye BODIPY and incubated with *Botrytis cinerea* spores for 2-3 hours and observed with fluorescence microscopy.

TABLE S1 | Primers used in this study for cloning Mg1LysM and its mutants.

Primer	Sequence
Mg1LysM-pETSUMO-F	GCGCGCGAGCTCCAGCGGAATCCAATCACCATC
Mg1LysM-pETSUMO-R	GCGCGCAAGCTTctaTTAGAGGCAGCTGTTGCGGTCG
Mg1LysM-T28R-F	CGTCGCGCGCAGTGGAGACCGACTCACCAAGATCGCCC
Mg1LysM-T28R-R	CTTGGGCGATCTTGGTGAGTCGGTCTCCACTGCGCGCGACG
Mg1LysM-K31A-F	GGAGACACCCTCACCGCGATCGC
Mg1LysM-K31A-R	ATTTCTTGGGCGATCGCGGTGAG
Mg1LysM-D54A-F	CGAACAACCTGGCCGCCCCAAA
Mg1LysM-D54A-R	TCGATCCTGTTTGGGGCGGCCA

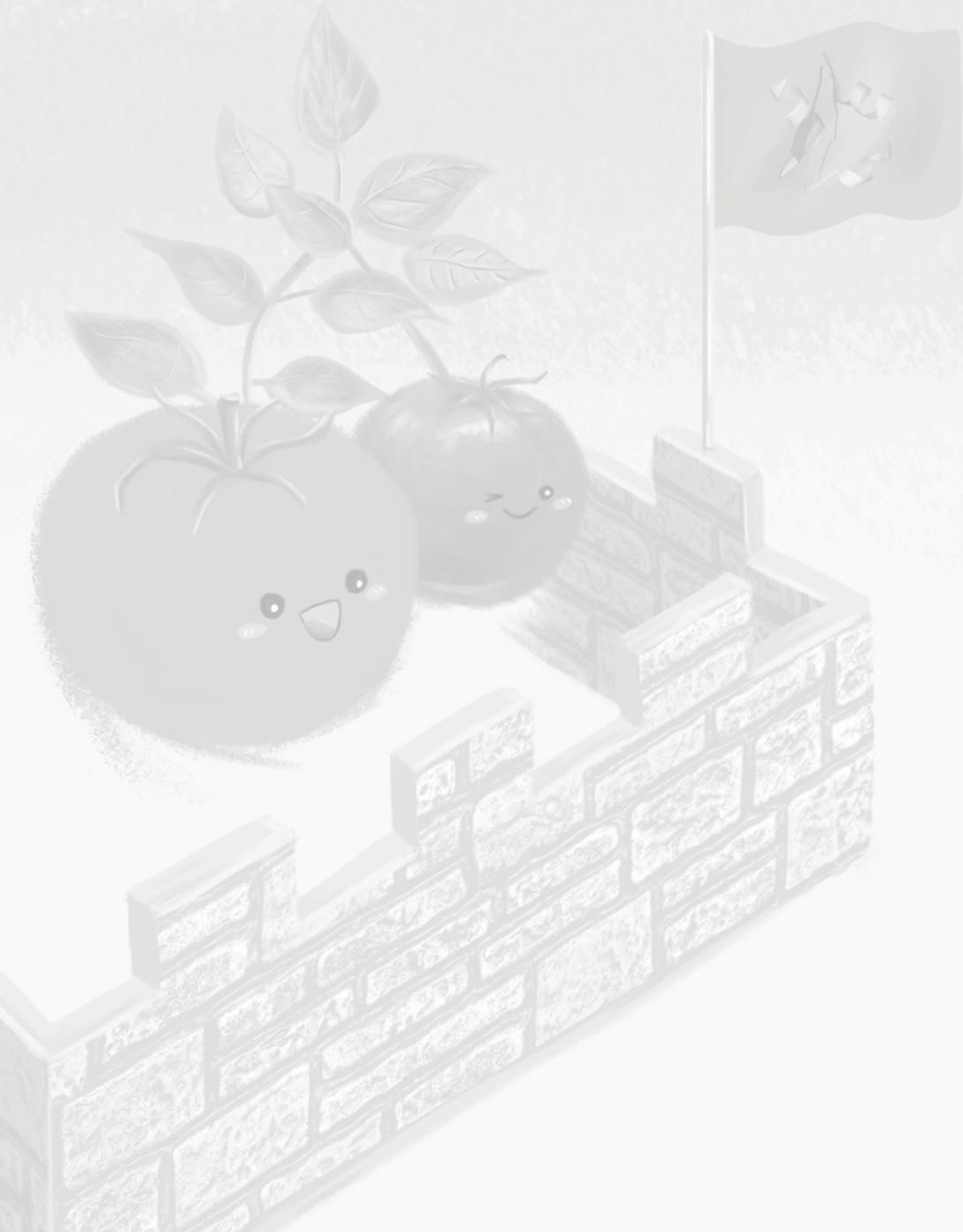

Chapter 7

General Discussion

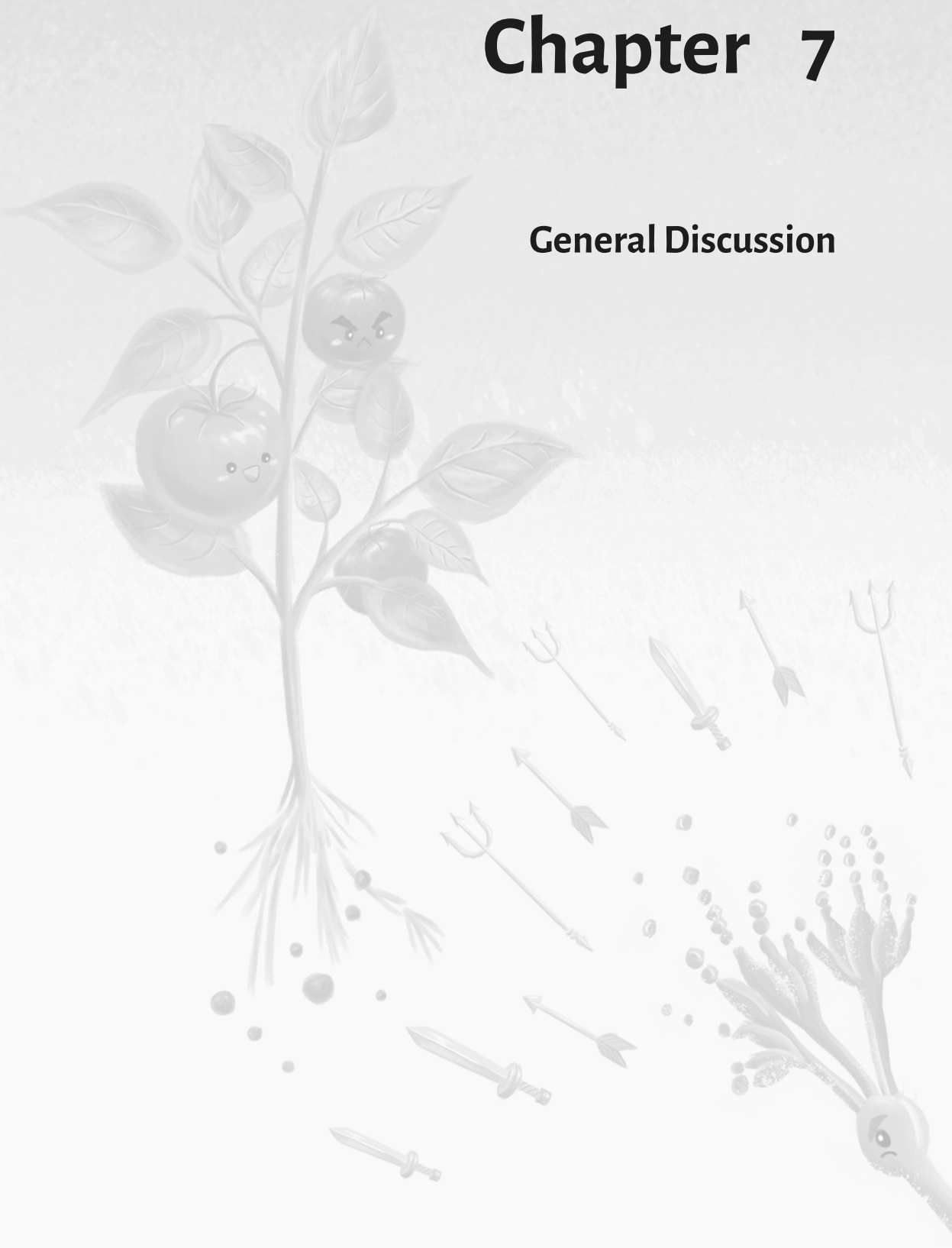

INTRODUCTION

According to the oldest microfossils, life on earth emerged at least 3,800 million years ago (Mojzsis et al., 1996; Nutman et al., 2016). However, it was not until the 17th century, when the first microscope was invented by Antonie van Leeuwenhoek, that cells were found to be the smallest unit of living matter. Through the evolution of life, unicellular organisms such as bacteria and archaea evolved into eukaryotic cells, which evolved into multicellular organisms that are composed of different types of cells that perform different functions in turn (Bonner, 1974; Bell, 1997; Kaiser, 2001; Bonner, 2012; West et al., 2015). The cells of many of these organisms, irrespective whether they are unicellular or multicellular, carry a cell wall; a complex and dynamic layer outside of the cell membrane that is mainly composed of carbohydrates. The composition of these cell walls differs drastically between species, and within the same organism cell wall compositions may differ between cell types and developmental stages (Cosgrove et al., 2005; De Lorenzo et al., 2019).

Whereas some organisms are autotrophic, others are heterotrophic and somehow depend on other organisms to complete their life cycle (May and Anderson, 1990; Kawaguchi and Minamisawa, 2010). Some of these heterotrophs establish symbioses that range from mutualistic to parasitic depending on whether the host organism benefits or suffers from the interaction, respectively (Bogitsh et al., 2019; Hirsch et al., 2004). In order to defend themselves against parasitic organisms, hosts need to detect the presence of potentially harmful invaders. To this end, they typically detect the presence of non-self molecules or modified-self molecules that may arise as a consequence of parasite attack. In case of interactions between plants and pathogenic microbes, the first intimate contact often takes place in the apoplast, the space between plant cells that forms a compartment that is hostile to microbial invaders due to the presence of hydrolytic enzymes that include chitinases and glucanases. These hydrolytic enzymes not only disrupt microbial cell wall integrity, and are thus detrimental to microbial growth and proliferation, but also release cell wall components, such as chitin and glucan oligomers, that can serve as invasion patterns (IPs) in turn; molecules that betray microbial invasion to the host because they are recognized by a broad range of cell surface-localized pattern recognition receptors (PRRs) that activate a wide array of immune responses (Cook et al., 2015). Often, these responses are sufficient to arrest microbial ingress.

Fungi are a group of eukaryotic organisms with a heterotrophic life style that are known as principal decomposers in ecological systems and that form their own kingdom of life. Besides saprotrophs, they include symbionts of plants, animals, or other fungi, including parasites. Fungal cell walls are complex and dynamic matrices that play essential roles in cell viability, morphogenesis, and pathogenesis (Gow et al., 2017; Hopke et al., 2018). In contrast to plant cell walls, fungal cell walls contain chitin, an unbranched long-chain β-(1,4)-linked homopolymer of *N*-acetylglucosamine (GlcNAc) that, after cellulose, is considered to be the second most abundant polysaccharide in nature as, besides in fungal cell walls, chitin occurs in the exoskeletons of arthropods, nematode eggshells and pharynx, cephalopod beaks, and fish and lissamphibian scales. As plants are devoid of chitin, they evolved chitin perception systems to detect fungal invaders (Sanchez-Vallet et al., 2015; Fesel and Zuccaro, 2016; Rovenich et al., 2016). The characterized

PRRs that perceive chitin thus far all contain extracellular lysin motifs (LysMs); carbohydrate-binding moieties that were named after the bacterial autolysins in which they were first identified (Buist et al., 2008). These PRRs can be further divided into LysM receptor-like kinases (LysM-RLKs) and LysM receptor-like proteins (LysM-RLPs) based on whether they contain a cytoplasmic kinase domain (Altenbach and Robatzek, 2007; Boller and Felix, 2009; Gust et al., 2012; Rovenich et al., 2016). However, successful fungal pathogens evolved ways to overcome chitin-induced plant immunity, including the secretion of effector proteins that contain LysM domains; so-called LysM effectors (Kombrink et al., 2013; Sanchez-Vallet et al., 2015).

Although the importance of chitin in interactions between pathogenic fungi and host plants is well established, the mechanistic details of chitin perception by plant hosts was largely limited to two plant species: Arabidopsis (*Arabidopsis thaliana*) and rice (*Oryza sativa*). Furthermore, mechanistic understanding of the functioning of LysM effectors was mostly built on Ecp6 of the leaf mould fungus *Cladosporium fulvum* that has tomato as its sole host and that, consequently, does not infect Arabidopsis or rice. The research in this thesis aimed to reveal on how chitin-induced immune responses are activated in tomato, and deepen our understanding of the mechanisms by which LysM effectors confer their functions by further studying *C. fulvum* Ecp6, but also by studying the LysM effector complement of the wheat pathogen *Zymoseptoria tritici*. In this chapter, I will discuss the main findings of this thesis research and, in a broader perspective, how these contribute to our understanding of the mechanisms underlying the activation of chitin-triggered immunity in plants and the strategies that fungi of various nature evolved to overcome chitin-induced plant immunity.

Tomato chitin receptors and the assembly of receptor complexes

It has become evident that within the same plant several chitin receptors can operate, belonging either to the LysM-RLKs or the LysM-RLPs, and that assemble into dynamic receptor complexes upon chitin perception, the composition of which may depend on its localization (Miya et al., 2007; Faulkner et al., 2013; Cao et al., 2014; Cheval et al., 2020). For example, in Arabidopsis, the LysM-RLK AtLYK5 binds chitin with high affinity and acts as the primary chitin receptor (Cao et al., 2014). However, its close homolog AtLYK4 displays partially redundant activities and appears to regulate chitin signalling as well, as only *lyk4lyk5* double mutants completely lose chitin responsiveness (Wan et al., 2012; Cao et al., 2014). Since AtLYK5 contains a catalytically inactive kinase domain, it requires another RLK with an active kinase domain to confer appropriate signals across the plasma membrane. Indeed, the chitin-binding LysM-RLK AtCERK1 was shown to associate with AtLYK5 upon chitin perception, leading to a heteromeric receptor complex that is essential for chitin signalling (Miya et al., 2007; Wan et al., 2008; Petutschnig et al., 2010; Liu et al., 2012b; Cao et al., 2014). Additionally, AtLYK4 is also recruited by the AtLYK5-AtCERK1 receptor complex, serving as a scaffold protein to stabilize the receptor complex, thus enhancing chitin signal transduction in Arabidopsis (Xue et al., 2019).

Besides the three LysM-RLKs, AtLYK4, AtLYK5 and AtCERK1, also the LysM-RLP AtLYM2 plays a role in chitin signalling. Although this receptor generally does not seem to act on the cell membrane, it was shown to mediate molecular fluxes in response to chitin in an AtCERK1-independent manner in plasmodesmata (Faulkner et al., 2013; Narusaka et al., 2013). Although the regulation of these molecular fluxes furthermore requires both AtLYK4 and AtLYK5, only AtLYM2 and AtLYK4 could be detected in the plasmodesmal plasma membrane (Cheval et al., 2020). Collectively, these findings underpin the occurrence of differentially composed chitin receptor complexes at different cellular locations in Arabidopsis.

The study of chitin receptor complexes in rice has revealed similarities and differences when compared with Arabidopsis. In both plant species CERK1 plays a central role. However, rice OsCERK1 is recruited in a chitin-dependent manner by the LysM-RLP OsCEBiP which acts as primary chitin receptor (Kaku et al., 2006; Shimizu et al., 2010; Hayafune et al., 2014). Besides formation of the OsCEBiP-OsCERK1 complex, two additional LysM-RLPs, OsLYP4 and OsLYP6, were characterized to mediate chitin signalling in conjunction with OsCERK1, independent from OsCEBiP (Liu et al., 2012a; Ao et al., 2014; Miyata et al., 2014). Thus, the assembly of different chitin receptor complexes also occurs in rice.

Based on observations in Arabidopsis and rice, we hypothesized that LysM-containing receptors are similarly required for chitin perception in tomato (*Solanum lycopersicum*). Therefore, affinity purification based on chitin-binding was performed using tomato microsomal proteins, revealing two candidate receptor proteins that, indeed, contain extracellular LysMs and that were named SlLYK4 and SlCEBiP according to their homologs in Arabidopsis and rice, respectively (Chapter 2). Whereas a critical role in mediating chitin signaling could be attributed to SlLYK4 in our experiments, evidence for such a role of SlCEBiP remained ambiguous as we could not convincingly demonstrate that the corresponding CRISPR-Cas9 mutant was a genuine loss-of-function mutant (Chapter 2). Although the affinity purification can be taken as a first line of evidence for their functionality as genuine chitin receptor, further evidence is required to claim that particularly SlLYK4 is a true chitin receptor. To this end, the extracellular domain of SlLYK4 can be expressed and subjected to a quantitative chitin binding assay, for instance based on isothermal titration calorimetry (ITC), to determine its binding affinity.

Like its homologs AtLYK4 and AtLYK5, SlLYK4 contains an inactive kinase domain. Thus, in order to confer chitin signaling, SlLYK4 needs to recruit another RLK that carries a functional kinase domain to form a functional receptor complex. However, besides SlCEBiP that lacks an intracellular domain, no other proteins were co-purified, suggesting that a potential RLK-type co-receptor does not bind chitin directly, or only with low affinity. Considering the role of AtCERK1 and OsCERK1 as co-receptor in chitin receptor complexes of Arabidopsis and rice, respectively (Shimizu et al., 2010; Liu et al., 2012b; Cao et al., 2014), its tomato homolog SlLYK1 may play such role as it contains an active kinase domain. Moreover, SlLYK1 has previously been demonstrated to act in mediating tomato

chitin signaling (Liao et al., 2018). However, a physical association between SlLYK4 and SlLYK1, as similarly demonstrated for AtLYK5 and AtCERK1 or OsCEBiP and OsCERK1, remains to be demonstrated.

Considering the existence of receptor complexes of different compositions in Arabidopsis as well as in rice, it is still possible that also SlCEBiP is involved in chitin perception or signaling, besides SlLYK4 and SlLYK1 (Shimizu et al., 2010; Liu et al., 2012b; Hayafune et al., 2014; Cao et al., 2014; Cheval et al., 2020). To assess this possibility, verified loss-of-function mutants of *SlCEBiP* need to be generated and investigated. To provide more evidence for differential composition of receptor complexes in tomato, the extracellular domains of SlLYK4, SlCEBiP and SlLYK1 can be heterologously produced and subjected to co-immunoprecipitation (co-IP) assays in the presence and absence of chitin. Furthermore, co-IP upon *in planta* expression of full-length protein can be pursued, but also other types of assays such as Förster resonance energy transfer-fluorescence lifetime imaging (FRET-FLIM) analysis. Collectively, these experiments should reveal the nature of tomato chitin receptor complexes in more detail.

LysM receptors mediate mutualistic symbioses

Besides chitin, plant LysM-containing receptors play essential roles in perceiving chitin derivatives such as lipochitooligosaccharides (LCOs), molecules with a chitin backbone that generally consists of four or five residues and an acyl chain attached to the non-reducing terminal GlcNAc that are known to act as Nod factors, rhizobial signal molecules that are essential for the initiation of a symbiosis with legume plants (Gough, 2003; Gust et al., 2012). Similarly, arbuscular mycorrhizal (AM) fungi secrete LCOs that are known as Myc factors in combination with chitooligosaccharides (COs) to initiate their symbiosis (Gust et al., 2012; Liang et al., 2014; Limpens et al., 2015; Feng et al., 2019). The perception of Nod or Myc factors in various plant species involves receptor complexes with LysM-RLKs (Gough, 2003; Maillet et al., 2011; Genre et al., 2013; Liang et al., 2014; Zipfel and Oldroyd, 2017). For example, in *Lotus japonicus*, the LysM-RLKs NFR1 and NFR5 are essential for Nod factor recognition during the interaction with *Mesorhizobium loti* bacteria (Madsen et al., 2003; Radutoiu et al., 2003; Broghammer et al., 2012). Similarly, in *Medicago truncatula*, the LysM-RLK MtNFP is responsible for Nod factor recognition and forms a receptor complex with the NFR1 ortholog MtLYK3 (Amor et al., 2003; Arrighi et al., 2006; Pietraszewska-Bogiel et al., 2013). Interestingly, LjNFR5 and MtNFP possess no active intracellular kinase domain, suggesting that LjNFR1 and MtLYK3, respectively, confer downstream signalling (Limpens et al., 2015). Interestingly, although rhizobium symbiosis is generally considered to be unique for legume plants, an exception has been discovered in the non-legume plant *Parasponia andersonii* that is able to engage in rhizobial symbiosis, and in which the LysM-RLK PaNFP was found be essential not only for rhizobial, but also for AM symbiotic, interactions (Op den Camp et al., 2011).

When compared with Nod factor perception, significantly less is known with respect to recognition of Myc factors. In rice, OsCERK1 was shown to act in the establishment of symbiosis with the AM fungus *R. irregularis* in an OsCEBiP-independent manner (Miyata et al., 2014; Zhang et al., 2015). This observation demonstrates that OsCERK1 has a dual functionality in microbial interactions, namely OsCEBiP-dependent establishment of immune responses against pathogens, and OsCEBiP-independent establishment of mutualistic symbiosis. Also tomato LysM-RLKs have been implicated in AM symbiosis, as SlLYK10 and SlLYK12 were shown to be required for mycorrhizal colonization (Buendia et al., 2016; Liao et al., 2018). Phylogenetic analysis suggests that SlLYK10 is the ortholog of MtNFP that, like AtLYK4 and AtLYK5, contains an inactive kinase whereas SlLYK12 belongs to the LYK subfamily that contains proteins with predicted active kinase including AtCERK1 (Arrighi etal., 2006; Buendia et al., 2016). Therefore, it is tempting to speculate that SlLYK10 may associate with SlLYK12 in a receptor complex that mediates AM symbiosis in tomato.

How fungal LysM effectors perturb chitin-induced plant immunity

As plants developed sophisticated perception systems to detect fungal cell wall chitin in order to mount immune responses, fungal pathogens have to employ strategies to counteract chitin-triggered host responses. Some fungal pathogens can convert chitin to chitosan, which acts as a much weaker elicitor in many plant species, by deacetylation (EI Gueddari et al., 2002; Gao et al., 2019). An alternative strategy is the secretion of polysaccharides, such as alpha-1,3-glucan, to mask cell wall chitin and prevent chitin hydrolysis, release and recognition (Fujikawa et al., 2009; Fujikawa et al., 2012). Besides these strategies, fungi typically secrete effectors to interfere with host immune responses (Rovenich et al., 2014). Particularly, many fungi are thought to employ LysM effectors as these effectors are widely distributed in the fungal kingdom (de Jonge and Thomma, 2009; Sánchez-Vallet et al, 2015; Rovenich et al, 2016). Since the functional analysis of the first LysM effector little over a decade ago (Bolton et al., 2008; de Jonge et al., 2010), an increasing number of these effectors has been functionally characterized in various fungal species (Table 1).

During the colonization of tomato, the leaf mould pathogen *Cladosporium fulvum* secretes the LysM effector Ecp6 that carries three LysMs. Ecp6 binds chitin with ultra-high affinity and greatly contributes to fungal virulence (Table 1) (Bolton et al., 2008; de Jonge et al., 2010; Sanchez-Vallet et al., 2013). A crystal structure of Ecp6 revealed that two of its three LysM domains, namely LysM1 and LysM3, undergo chitin-induced intermolecular dimerization, thus establishing a chitin binding groove with picomolar affinity (Sanchez-Vallet et al., 2013). This affinity is significantly higher than that of plant receptors that bind chitin in the low micromolar range (Iizasa et al., 2010; Liu et al., 2012b; Cao et al., 2014), which inspired the hypothesis that Ecp6 sequesters chitin molecules from host receptors to prevent the activation of chitin-triggered plant immunity. However, whether the chitin binding capacity

of the remaining LysM2 of Ecp6 at μM affinity is relevant for the virulence function of Ecp6 remained unknown. In Chapter 3, we demonstrated not only that LysM2 contributes to the virulence function of Ecp6, but also that this LysM operates through the suppression of chitin responsive gene expression. Furthermore, in this chapter we provided evidence for the potential occurrence of physical interactions between Ecp6 and plant chitin receptors. This may suggest that, besides through sequestration, Ecp6 perturbs chitin triggered immunity through interference in receptor complex assembly or functioning. Interestingly, the physical interaction mediated by LysM2 was found to occur in a chitin-independent manner. Considering the relatively low affinity for chitin, chitin-independent interference with receptor complexes may prevent out-competition by receptor monomers. However, also the composite LysM1-LysM3 binding groove seems to contribute to the interaction of Ecp6 with host receptors, albeit in a chitin-dependent manner and with a much smaller contribution. This may suggest that Ecp6 is able to bind to the same chitin molecule that is already bound by a receptor monomer to prevent further receptor complex formation (Fig. 1). Thus, the data presented in Chapter 3 may suggest that *C. fulvum* Ecp6 possesses dual functionality, as it not only outcompetes plant receptors for chitin binding, but also interacts with chitin receptor proteins, possibly to prevent the assembly of a functional receptor complex or interfere with activation of chitin-induced immunity. In turn, also these interactions with receptors may be established through two mechanisms; chitin-independent interactions through LysM2 and chitin-dependent interactions through the composite LysM1-LysM3 binding groove. It needs to be acknowledged that the data presented in Chapter 3 do not provide evidence to solidify hypotheses as, first of all, evidence for the interaction between Ecp6 and host receptors *in planta* has not been provided. To this end co-IP upon *in planta* expression of Ecp6 and full-length receptor proteins can be pursued, but also e.g. FRET-FLIM analysis. Furthermore, we have not provided evidence for a physiological role of the interaction of Ecp6 with host receptors in the undermining of immune responses. To this end, perturbation of chitin-induced immune responses such as *WRKY* gene expression, calcium fluxes, and AtCERK1 or mitogen-associated protein (MAP) kinase phosphorylation could be tested in tomato upon treatment with the Ecp6 variant carrying a mutation in LysM3 that disrupt the ultra-high affinity binding site, thus assessing the perturbation potential of Ecp6 in absence of chitin sequestration conferred by the composite LysM-LysM3 binding site. Additionally, other LysM effectors that suppress chitin-triggered immunity but cannot outcompete host receptors for chitin binding can be utilized, such as *R. irregulare* RiSLM or *Z. tritici* Mg1LysM and Mgx1LysM that contain only a single LysM.

TABLE 1 | Diverse contributions of effectors that target chitin-triggered immunity in interactions between plants and fungi.

Effector	Chitin-binding domain (#)	Fungal species	Type of interaction with plants	Host plant	Hyphal protection
Mg1LysM	LysM (1)	*Zymoseptoria tritici*	Pathogenic	Wheat	✓
Mgx1LysM	LysM (1)	*Zymoseptoria tritici*	Pathogenic	Wheat	✓
Mg3LysM	LysM (3)	*Zymoseptoria tritici*	Pathogenic	Wheat	✓
RiSLM	LysM (1)	*Rhizophagus irregularis*	Mutualistic	Broad host range	✓
MoSlp1	LysM (2)	*Magnaporthe oryzae*	Pathogenic	Rice	✗
Vd2LysM	LysM (2)	*Verticillium dahliae*	Pathogenic	Broad host range	✓
ChElp1	LysM (2)	*Colletotrichum higginsianum*	Pathogenic	Brassicaceae	✗
ChElp2	LysM (2)	*Colletotrichum higginsianum*	Pathogenic	Brassicaceae	✗
RsLysM	LysM (2)	*Rhizotonia solani*	Pathogenic	Broad host range	✗
Ecp6	LysM (3)	*Cladosporium fulvum*	Pathogenic	Tomato	✗
Tal6	LysM (7)	*Trichoderma atroviride*	Mutualistic, biocontrol	Broad host range	✓
Avr4	CBM14 (1)	*Cladosporium fulvum*	Pathogenic	Tomato	✓
VnaChtBP	CBM18 (1)	*Verticillium nonalfalfae*	Pathogenic	Tree of heaven, hop, kiwifruit, spinach and few Solanaceae	✓
MpChi	--	*Moniliophthora perniciosa*	Pathogenic	Mostly tropical plants	✗
MrChi	--	*Moniliophthora roreri*	Pathogenic	Malvaceae	✗
PDA1	✗	*Verticillium dahliae*	Pathogenic	Broad host range	?
Fv-cmp	✗	*Fusarium verticillioides*	Pathogenic	Maize	?
Bz-cmps	✗	*Bipolaris zeicola*	Pathogenic	Maize, sorghum and apple	?
Stm-cmp	✗	*Stenocarpella maydis*	Pathogenic	Maize and canes	?
FoMep1	✗	*F. oxysporum* f. sp. lycopersici	Pathogenic	Tomato	?
FoSep1	✗	*F. oxysporum* f. sp. lycopersici	Pathogenic	Tomato	?
UmFly1	✗	*Ustilago maydis*	Pathogenic	Maize and teosinte	?

? = not tested, n.a. = does not apply

Suppression of immunity	Chitinase inactivation	Chitin receptor interaction	Demonstrated contribution to Virulence on plants	Reference
✓	?	?	✓	(Marshall, et al., 2011; Chapter 5)
✓	?	?	✓	(Chapter 5)
✓	?	?	✓	(Marshall et al., 2011)
✓	?	?	✓	(Zeng et al., 2019)
✓	?	?	✓	(Mentlak et al., 2012)
✓	?	?	✓	(Kombrink et al., 2017)
✓	?	?	✓	(Takahara et al., 2016)
✓	?	?	✓	(Takahara et al., 2016)
✓	?	?	✓	(Dolfors et al., 2019)
✓	?	✓	✓	(Bolton et al., 2008; de Jonge et al., 2010; Chapter 3)
✓	?	?	n.a.	(Seidl-Seiboth et al., 2013; Romero-Contreras et al., 2019)
✗	?	?	✓	(van den Burg et al., 2006; van Esse et al., 2007)
✓	?	?	✗	(Volk et al., 2019)
✓	?	?	✓	(Fiorin et al., 2018)
✓	?	?	✓	(Fiorin et al., 2018)
?	?	?	✓	(Gao et al., 2019)
?	✓	?	?	(Naumann et al., 2011)
?	✓	?	?	(Naumann, 2009)
?	✓	?	?	(Naumann, 2009)
?	✓	?	✓	(Jashni et al., 2015)
?	✓	?	✓	(Jashni et al., 2015)
?	✓	?	✓	(Okmen et al., 2018)

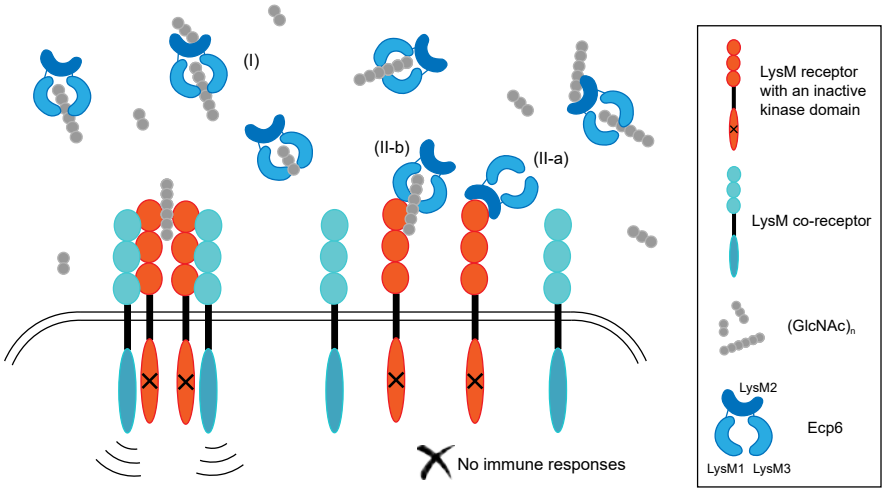

FIGURE 1 | Proposed dual functionality of *C. fulvum* Ecp6 in suppression of chitin-triggered immunity. The tomato leaf mould pathogen *C. fulvum* secretes a LysM effector with three LysMs, Ecp6, to suppress the activation of chitin-induced plant immunity via: (I) sequestration of chitin fragments with pM affinity, thus outcompeting plant LysM-containing immune receptors for chitin binding, and via (II) perturbation of the assembly of LysM-containing immune receptor complexes that activate downstream signalling by: (II-a) direct binding of LysM2 of Ecp6 interferes to LysM domains of the immune receptor, and by (II-b) binding of the composite LysM1-LysM3 chitin binding site of Ecp6 to a chitin fragment that is bound by a LysM-containing immune receptor to prevent the assembly of functional immune complexes.

Functional diversification of LysM effectors

The genome of the wheat-specific pathogen *Zymoseptoria tritici* encodes three LysM effectors: Mg1LysM and Mgx1LysM (previously named MgxLysM) that contain only one LysM, and Mg3LysM that contains three LysMs (Marshall et al., 2011). It was previously shown that although Mg1LysM and Mg3LysM both bind chitin, only Mg3LysM suppressed chitin-induced immunity and, accordingly, contributed to *Z. tritici* virulence on wheat (Marshall et al., 2011). However, additionally, both Mg1LysM and Mg3LysM were shown to protect fungal hyphae against hydrolysis by plant chitinases (de Jonge et al., 2010; Marshall et al., 2011). The mechanism underlying hyphal protection was investigated by pursuing a three-dimensional structure of Mg1LysM (Chapter 6). Based on the crystal structure, it was shown that Mg1LysM can form a supramolecular structure by chitin-induced polymerization of chitin-independent Mg1LysM homodimers, which shields cell wall chitin from host chitinases in turn (Chapter 6). Intriguingly, RiSLM of the AM fungus *Rhizophagus irregularis* that carries a single LysM only (Zeng et al., 2020), was similarly shown to be able to polymerize in the presence of chitin, while *C. fulvum* Ecp6 that lacks the protective ability did not, suggesting that the ability to polymerize in the presence of chitin is crucial for the ability to protect fungal hyphae against enzymatic hydrolysis. This hypothesis was further confirmed by the observation that Mgx1LysM, a novel LysM effector of *Z. tritici* of which a detailed functional characterization is described in Chapter 5 of this thesis

and that acts fully redundantly with Mg1LysM, polymerizes in the presence of chitin (Chapter 6) and displays the ability to protect fungal hyphae against hydrolysis. Thus, all LysM effectors that are composed of a single LysM characterized to date protect fungal hyphae and have the ability to polymerize. Whether this mechanism is also utilized by LysM effectors that protect fungal hyphae and that carry more than a single LysM, such as *V. dahliae* Vd2LysM or *Z. tritici* Mg3LysM, remains to be addressed. However, it will take more sophisticated assays than polymerization assays in the presence of chitin to investigate this. Finally, it needs to be acknowledged that the ability to protect fungal hyphae is a trait that is shared by some, but not all, LysM effectors as, besides *C. fulvum* Ecp6, also the LysM effectors Slp1 from the rice blast pathogen *Magnaporthe oryzae* and Elp1 and Elp2 from the Brassicaceae anthracnose pathogen *Colletotrichum higginsianum* that all contain two LysMs do not protect fungal hyphae against chitinase hydrolysis (Mentlak et al., 2012; Takahara et al., 2016).

We have also demonstrated that all three *Z. tritici* effectors are capable of suppressing chitin-induced plant immunity (Marshall et a., 2011; Chapter 5). Given the high degree of homology to Ecp6, Mg3LysM is likely to supress immunity in a similar fashion, including chitin sequestration (Sanchez-Vallet et al., 2013) and possibly receptor complex perturbation (Chapter 3). However, it presently remains enigmatic how Mg1LysM and Mgx1LysM, as well as *R. irregulare* RiSLM, suppress chitin-triggered immunity. Possibly, like displayed by Ecp6 besides sequestration, these effectors have the ability to perturb the assembly of functional chitin receptor complexes that are crucial for successful activation of chitin-triggered immunity.

Protection of hyphae against chitinases is also displayed by Tal6 of the plant-associated endophyte and mycoparasite *Trichoderma atroviride* that contains seven LysMs. Besides protection of hyphal growth against chitinase hydrolysis and suppression of plant immune responses Tal6 is claimed to increase the antagonistic capacity of *T. atroviride* towards *Rhizoctonia solani* on plant hosts, leading to increased plant weight, stem and root length (Table 1; Romero-Contreras et al., 2019). Although the mechanism how Tal6 confers host protection remains to be addressed, these findings seem to point towards further functional diversification of fungal LysM effectors.

LysM effectors with two LysMs also display chitin-mediated polymerization

Whereas the polymerization of LysM effectors composed of a single LysM in the presence of chitin correlates with their ability to protect hyphae, such correlation is not observed for LysM effectors composed of two LysMs, some of which protect hyphae (e.g. Vd2LysM) while others do not (e.g. MoSlp1, ChElp1, ChElp2) (Table 1; Mentlak et al., 2012; Takahara et al., 2016; Kombrink et al., 2017). How these LysM effectors bind chitin remained elusive since no three-dimensional structure has been available. Therefore, in chapter 4 we aimed to reveal the chitin-binding mechanism of such LysM effectors by pursuing X-ray crystallography, but our efforts failed. However, the lack of crystal growth inspired the hypothesis that the LysMs of these effectors undergo chitin-induced intermolecular dimerization, ultimately leading to polymerisation in the presence of chitin. The subsequently conducted DLS measurements on ChElp2 in the presence

of chitin and the centrifugation assays to assess polymer formation of ChElp2, MoSlp1 and Vd2LysM in the presence of chitin strongly supported this hypothesis (Chapter 4). However, since both MoSlp1 and ChElp2 display the ability to polymerize despite not being able to protect fungal hyphae, it cannot be concluded that the ability to polymerize in the presence of chitin is sufficient for a LysM effector to protect hyphae against chitinase hydrolysis.

Fungal employment of chitin-binding effector proteins that lack LysMs

Despite the wide occurrence of LysM effectors in the fungal kingdom, fungi evolved other types of effectors to interfere with chitin-triggered immunity in their host plants. Accordingly, these effectors contain other types of carbohydrate-binding motifs (CBMs) than LysMs. For instance, *C. fulvum* employs the Avr4 effector carries an invertebrate chitin binding domain (CBM14; PF01607) to shields its hyphae against hydrolytic enzymes in a fashion like the LysM effectors of *Z. tritici* (Table 1) (van de Burg et al., 2006; van Esse et al., 2007). This observation fits with the observation that *C. fulvum* Ecp6 does not possess the ability to protect fungal hyphae and also with the observation that, despite being a close relative of *C. fulvum* within the *Mycosphaerellaceae*, *Z. tritici* contains no Avr4 homolog (de Jonge et al., 2010; Marshall et al., 2011). Another type of effector that interferes with chitin-triggered immunity is found in the cacao pathogenic fungus *Moniliophthora perniciosa* that evolved the inactive chitinase MpChi that belongs to plant chitinase glycoside hydrolase 18 family (GH18) to sequester cell wall-derived chitin fragments with high affinity (nM) (Table 1; Fiorin et al., 2018). Interestingly, it appears that this strategy is also employed by the cacao pathogen *Moniliophthora roreri* that similarly secretes a functionally equivalent inactive chitinase MrChi to sequester chitin molecules (Table 1; Fiorin et al., 2018). Another example is provided by the effector protein VnaChtBP of the xylem-invading vascular wilt pathogen of hop (*Humulus lupulus*), *Verticillium nonalfalfae*, that was shown to bind chitin through a CBM18 domain (PF00187) that is also known as chitin binding 1 and found in various plant and fungal proteins that bind GlcNAc (Wright et al. 1991). Like the LysM effectors of *Z. tritici*, this effector protects fungal hyphae against hydrolysis by plant chitinases and suppresses chitin-induced ROS bursts (Table 1; Volk et al., 2019). Finally, from the soil-borne fungus *Verticillium dahliae* the secreted polysaccharide deacetylase PDA1 was characterized to facilitate fungal virulence through direct deacetylation of chitin oligomers, converting them to chitosan that serves as a much weaker elicitor (Gao et al., 2019).

Besides these fungal effectors that shield, sequester or modify chitin molecules, effectors that directly target chitinase activity have also been characterized. Chitinases are widely distributed in the plant kingdom and can be grouped into six classes that belong to glycosyl hydrolase families 18 and 19 (GH18 and GH19) (Li and Greene, 2010; Grover, 2012). Based on their protein sequence, GH18 chitinases are divided into classes III and V, and GH19 chitinases into classes I, II, and IV (Santos et al., 2008; Ohnuma et al. 2011; Ohnuma et al. 2012). Class I, IV and V chitinases all contain a chitin-binding domain (CBD) that is absent in class II and III chitinases. Furthermore, while class I chitinases localize to vacuole, most of other chitinases are extracellular, residing in

apoplast (Neuhaus et al. 1991; Wubben et al. 1992). It has been demonstrated that some fungi employ effector proteins to inhibit chitinase activity. For example, the maize pathogens *Fusarium verticillioides*, *Bipolaris zeicola* and *Stenocarpella maydis* secrete chitinase-modifying proteins (cmps) to truncate class IV chitinases at different sites of their amino termini, thus inactivating the chitinases (Naumann et al. 2009; Naumann and Wicklow 2010; Naumann 2011). A similar strategy is employed by the fungal maize pathogen *Ustilago maydis* that secretes the fungalysin UmFly1 to protect hyphal growth through cleavage of maize chitinases (Table 1; Okmen et al., 2018). Furthermore, the tomato vascular wilt pathogen *Fusarium oxysporum* f. sp. lycopersici secretes a metalloprotease as well as a serine protease to target the tomato chitinases SlChi1 and SlChi13 to remove the chitin-binding domain from the N-termini of these chitinases, leading to inactivity (Jashni et al., 2015), a mechanism that is similarly exploited by *V. dahliae* and *Botrytis cinerea* (Jashni et al., 2015). Thus, besides LysM effectors, successful fungal pathogens evolved other types of effectors to deregulate chitin-induced host immunity by modifying or shielding cell wall chitin or sequestering fragments thereof, or by inactivating plant chitinases. All these findings underpin the importance of chitin as an IP in diverse interactions between plants and fungi.

Other major cell wall polysaccharides that act as IP

Fungal cell walls possess β-glucan that cross-linked to chitin as major polysaccharide, which mainly comprises branched β-1,3-glucan and β-1,6-glucan that are also major constituents of oomycete cell walls (Aimanianda et al., 2009; Latgé, 2010; Melida et al., 2013; Yoshimi et al., 2016). β-glucan acts as an IP that activates plant immunity (Fesel and Zuccaro, 2016), although the mechanism of its perception and signalling in plants remains largely unknown. The first characterized receptor recognizing β-glucan is the soybean β-glucan elicitor binding protein (GEBP) that perceives the released glucan from cell walls of *Phytophthora megasperma* by soybean glucanases to activate immune responses (Umemoto et al., 1997). Interestingly, GEBP localizes to plasma membrane but contains no intracellular signalling domain, suggesting that it probably is a co-receptor to mediate glucan-activated immunity (Umemoto et al., 1997). To this end it is interesting to note that AtCERK1 was shown to be involved in β-glucan signalling in Arabidopsis, possibly as immune co-receptor (Melida et al., 2018). It has been demonstrated that the immune responses upon perception of β-glucans of different lengths vary among plant species, and that the degree of polymerization plays an essential role in the recognition of long-chain β-glucans (Wanke et al., 2020). In contrast to the CERK1-dependent β-glucan recognition in Arabidopsis, the perception of long-chain β-1,3-glucans in *N. benthamiana* and rice is CERK1-independent, implicating different β-glucan receptor systems in different plant species (Wanke et al., 2020).

To avoid β-glucan-triggered immunity, some pathogenic fungi as well as oomycetes evolved various strategies, such as the secretion of α-1,3-glucan to mask β-glucan (Fujikawa et al., 2012) and secretion of effector proteins to perturb the functioning of plant glucanases that release glucan fragments from microbial cell walls. For instance, the oomycete soybean pathogen *Phytophthora sojae* produces glucanase inhibitor proteins (GIPs) to inhibit the enzymatic activity of endo-1,3-

glucanases to prevent the liberation of β-glucan from its cell walls (Rose et al., 2002; Bishop et al., 2005). A similar GIP activity has been reported for the fungal pathogen *Colletotrichum lindemuthianum* to inhibit an endo-β-1,3-glucanase in bean leaves (Albersheim and Valent 1974). Besides direct inhibition of glucanase activity by effectors, the hemibiotrophic pathogen *Colletotrichum graminicola* overcomes glucan-induced maize (*Zea mays*) immunity by repressing the expression of *KRE5* and *KRE6* that encode key enzymes involved in β-1,6-glucan synthesis to reduce β-1,6-glucan exposure (Yoshimi et al., 2017).

Although bacterial cell walls do not contain chitin, they do contain β-glucans (Rahar et al., 2011). Besides, a major and conserved bacterial cell wall constituent that acts as an IP is peptidoglycan, a heteropolymer that is composed of alternating residues of β-1,4-linked *N*-acetylglucosamine (GlcNAc) and *N*-acetylmuramic acid (MurNAc) with oligopeptides linked to the lactic acid residue of MurNA (Gust et al., 2007; Vollmer et al., 2008; Mesnage et al., 2014). Receptor complexes that are composed of LysM-RLKs and LysM-RLPs have been characterized to play an essential role in peptidoglycan recognition. In Arabidopsis, AtCERK1 was shown to associate with the LysM-RLPs AtLYM1 and AtLYM3 to mediate peptidoglycan signalling (Willmann et al., 2011). Similarly, OsCERK1 was shown to be involved in peptidoglycan recognition in receptor complexes with the LysM-RLPs OsLYP4 and OsLYP6 in rice (Liu et al., 2012; Ao et al., 2014; Hayafune et al., 2014). Thus, it appears that CERK1 plays dual role in the activation of immune responses upon recognition of not only fungal chitin but also bacterial peptidoglycan. Intriguingly, the bacterial pathogen *Pseudomonas syringae* pv. tomato DC3000 evolved to inject the type-III effector AvrPtoB into Arabidopsis cells to inactivate CERK1. AvrPtoB is an E3-ligase that ubiquitinates the CERK1 kinase domain and thus targets CERK1 for degradation, leading to the suppression of peptidoglycan-induced immunity and thus to support of bacterial colonization (Gimenez-Ibanez et al., 2009).

Concluding remarks

The above-described chitin, Myc factors and Nod factors, β-glucans and peptidoglycan are the most well-characterized microbial cell wall polysaccharides that act as IPs. Besides these, more cell wall components are recognized by plants, such as fungal COs, cyclic β-glucans (Pettolino et al., 2009; Feng et al., 2019) and bacterial lipopolysaccharides (LPS) (Wang and Quinn, 2010; Erbs and Newman, 2012), and probably many more remain to be discovered. Therefore, microbial cell walls can be considered a rich source of IPs, some of which are not only perceived by plants, but also by human and animal immune systems (Ariizumi et al., 2000; Kumar et al., 2009; Bozza et al., 2009; Brown, 2011; Rosadini and Kagan, 2017). The complexity of the role of polysaccharides in the interactions between microbes and their hosts is much larger than we appreciate thus far. Furthermore, it should be considered that the vast majority of microbes do not live as pure cultures of dispersed single cells, but rather live and grow at interfaces to form polymicrobial aggregated structures such as biofilms, in which the microbes embed themselves in a matrix of hydrated extracellular polymeric substances (EPS) that are mainly composed of polysaccharides,

proteins, nucleic acids and lipids (Wingender et al., 1999; Flemming and Wingender, 2010; Lin et al., 2017; Kavanaugh et al., 2019). Many components of EPS play a significant role to facilitate the initial steps of the colonization on abiotic and biotic surfaces by planktonic cells, and protect the microbes not only from harsh environments, but also from host defences during infection (Flemming et al., 2007; Flemming and Wingender, 2010; Kavanaugh et al., 2019; Ravaioli et al., 2020). However, in turn, components involved in biofilms may serve as new IPs. For instance, it has been shown that acyl homoserine lactones, a class of quorum sensing signals produced by bacteria to switch to a biofilm lifestyle, triggers systemic defence responses in tomato (Von Bodman et al., 2003; Schuhegger et al., 2006). Thus, various other, less well-characterized microbial cell wall constituents as well as secreted compounds such as polysaccharides and extracellular DNA are molecules that are potentially recognized by hosts. Further research, making use of state-of-the-art technologies to address glycobiology should help to increase our understanding and appreciation of sugars in host-microbe interactions.

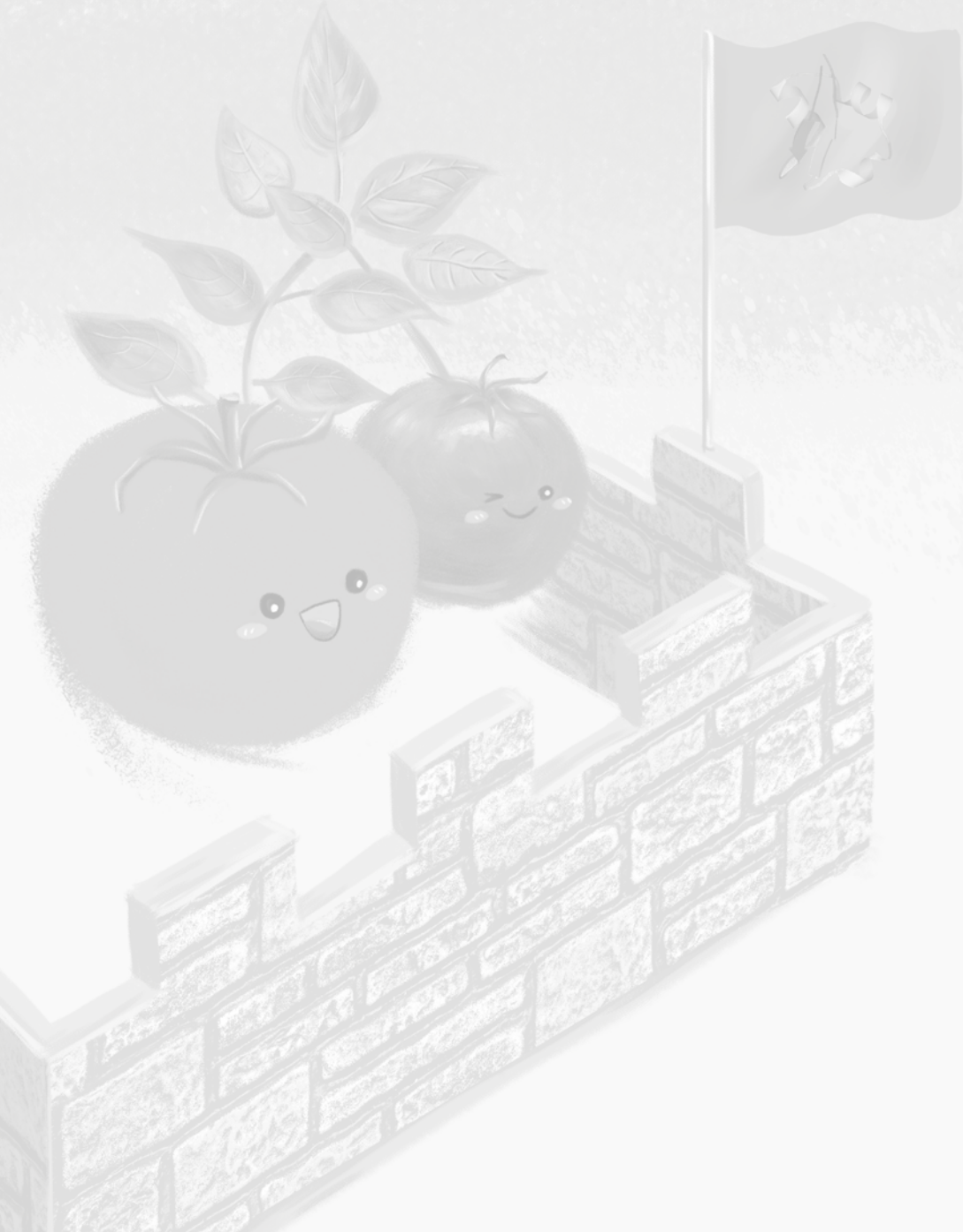

References

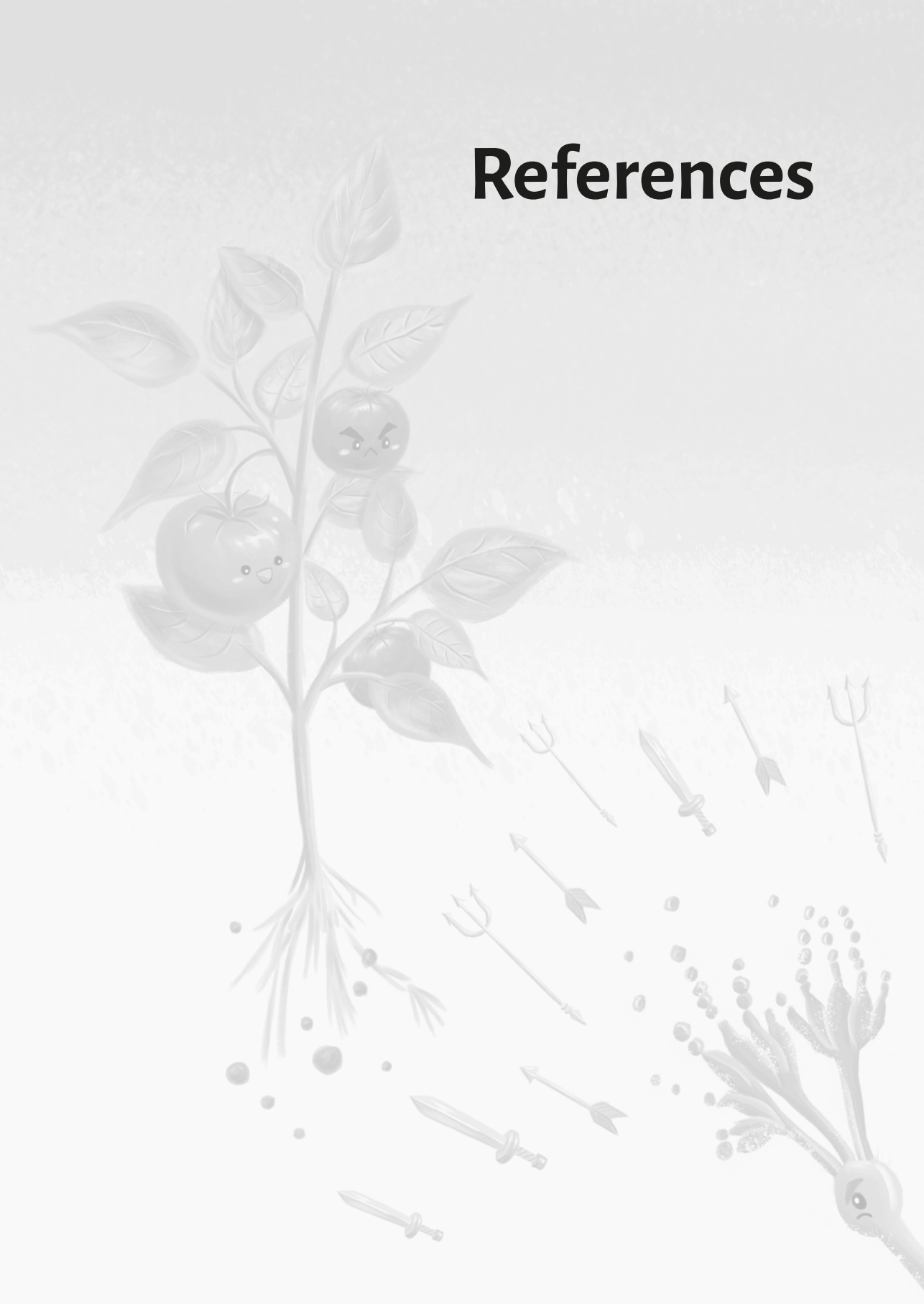

Adams, P.D., Afonine, P.V., Bunkóczi, G., Chen, V.B., Davis, I.W., Echols, N., Headd, J.J., Hung, L-W., Kapral, G.J., Grosse-Kunstleve, R.W. (2010) PHENIX: a comprehensive Python-based system for macromolecular structure solution. Acta Crystallogr D 66: 213-221.

Adrangi, S. and Faramarzi, M.A. (2013) From bacteria to human: a journey into the world of chitinases. Biotechnol. Adv. 31: 1786-1795.

Aimanianda, V., Clavaud, C., Simenel, C., Fontaine, T., Delepierre, M. and Latge, J.P. (2009) Cell wall beta-(1,6)-glucan of Saccharomyces cerevisiae: structural characterization and in situ synthesis. J. Biol. Chem. 284: 13401-13412.

Akamatsu, A., Wong, H.L., Fujiwara, M., Okuda, J., Nishide, K., Uno, K., Imai, K., Umemura, K., Kawasaki, T., Kawano, Y., et al. (2013) An OsCEBiP/OsCERK1-OsRacGEF1-OsRac1 module is an essential early component of chitin-induced rice immunity. Cell Host & Microbe 13: 465-476.

Akcapinar, G.B., Kappel, L., Sezerman, O.U. and Seidl-Seiboth, V. (2015) Molecular diversity of LysM carbohydrate-binding motifs in fungi. Curr. Genet. 61: 103-113.

Aktar, M.W., Sengupta, D. and Chowdhury, A. (2009) Impact of pesticides use in agriculture: their benefits and hazards. Interdiscip Toxicol 2: 1-12.

Albersheim, P. and Valent, B.S. (1974) Host-pathogen interactions. VII. Plant pathogens secrete proteins which inhibit enzymes of the host capable of attacking the pathogen 53: 684-687.

Altenbach, D. and Robatzek, S. (2007) Pattern recognition receptors: from the cell surface to intracellular dynamics. Mol Plant Microbe Interact 20: 1031-1039.

Amor, B.B., Shaw, S.L., Oldroyd, G.E., Maillet, F., Penmetsa, R.V., Cook, D., Long, S.R., Denarie, J. and Gough, C. (2003) The NFP locus of *Medicago truncatula* controls an early step of Nod factor signal transduction upstream of a rapid calcium flux and root hair deformation. Plant J. 34: 495-506.

Antolin-Llovera, M., Petutsching, E.K., Ried, M.K., Lipka, V., Nurnberger, T., Robatzek, S. and Parniske, M. (2014) Knowing your friends and foes--plant receptor-like kinases as initiators of symbiosis or defence. New Phytol. 204: 791-802.

Antolin-Llovera, M., Ried, M.K., Binder, A. and Parniske, M. (2012) Receptor kinase signaling pathways in plant-microbe interactions. Annu. Rev. Phytopathol. 50: 451-473.

Ao, Y., Li, Z., Feng, D., Xiong, F., Liu, J., Li, J.F., Wang, M., Wang, J., Liu, B. and Wang, H.B. (2014) OsCERK1 and OsRLCK176 play important roles in peptidoglycan and chitin signaling in rice innate immunity. Plant J. 80: 1072-1084.

Arrighi, J.F., Barre, A., Ben Amor, B., Bersoult, A., Soriano, L.C., Mirabella, R., de Carvalho-Niebel, F., Journet, E.P., Gherardi, M., Huguet, T., et al. (2006) The *Medicago truncatula* lysine motif-receptor-like kinase gene family includes NFP and new nodule-expressed genes. Plant Physiol. 142: 265-279.

Ayers, A.R., Valent, B., Ebel, J. and Albersheim, P. (1976) Host-pathogen interactions: XI. Composition and structure of wall-released elicitor fractions. Plant Physiol. 57: 766-774.

Baker, H.M., Day, C.L., Norris, G.E. and Baker, E.N. (1994) Enzymatic deglycosylation as a tool for crystallization of mammalian binding proteins. Acta crystallogr D 50: 380-384.

Bankevich, A., Nurk, S., Antipov, D., Gurevich, A.A., Dvorkin, M., Kulikov, A.S., Lesin, V.M., Nikolenko, S.I., Pham, S. and Prjibelski, A.D. (2012) SPAdes: a new genome assembly algorithm and its applications to single-cell sequencing. J Comput. Biol. 19: 455-477.

Bartesaghi, A., Merk, A., Banerjee, S., Matthies, D., Wu, X., Milne, J.L. and Subramaniam, S. (2015) 2.2 A resolution cryo-EM structure of beta-galactosidase in complex with a cell-permeant inhibitor. Science 348: 1147-1151.

Bateman, A. and Bycroft, M. (2000) The structure of a LysM domain from *E. coli* membrane-bound lytic murein transglycosylase D (MltD). J. Mol. Biol. 299: 1113-1119.

Baureithel, K., Felix, G. and Boller, T. (1994) Specific, high affinity binding of chitin fragments to tomato cells and membranes. Competitive inhibition of binding by derivatives of chitooligosaccharides and a Nod factor of Rhizobium. J. Biol. Chem. 269: 17931-17938.

Beliveau, C., Potvin, C., Trudel, J., Asselin, A. and Bellemare, G. (1991) Cloning, sequencing, and expression in Escherichia coli of a *Streptococcus faecalis* autolysin. J. Bacteriol. 173: 5619-5623.

Bell, G. (1997) Size and complexity among multicellular organisms. Biol. J. Linn. Soc. 60: 345-363.

Bergfors, T. (2003) Seeds to crystals. J. Struct. Biol. 142: 66-76.

Bhat, R.G. and Subbarao, K.V. (1999) Host Range Specificity in *Verticillium dahliae*. Phytopathology 89: 1218-1225.

Bielnicki, J., Devedjiev, Y., Derewenda, U., Dauter, Z., Joachimiak, A. and Derewenda, Z.S. (2006) *B. subtilis* ykuD protein at 2.0 A resolution: insights into the structure and function of a novel, ubiquitous family of bacterial enzymes. Proteins 62: 144-151.

Bishop, J.G., Ripoll, D.R., Bashir, S., Damasceno, C.M., Seeds, J.D. and Rose, J.K. (2005) Selection on Glycine beta-1,3-endoglucanase genes differentially inhibited by a *Phytophthora* glucanase inhibitor protein. Genetics 169: 1009-1019.

Bogitsh, B.J., Carter, C.E. and Oeltmann, T.N. (2019) Symbiosis and Parasitism. Human Parasitology: 1-14.

Boller, T. (1995) Chemoperception of microbial signals in plant cells. Annu. Rev. Plant Biol. 46: 189-214.

Boller, T. and Felix, G. (2009) A renaissance of elicitors: perception of microbe-associated molecular patterns and danger signals by pattern-recognition receptors. Annu. Rev. Plant Biol. 60: 379-406.

Bolton, M.D., van Esse, H.P., Vossen, J.H., de Jonge, R., Stergiopoulos, I., Stulemeijer, I.J., van den Berg, G.C., Borras-Hidalgo, O., Dekker, H.L., de Koster, C.G., et al. (2008) The novel *Cladosporium fulvum* lysin motif effector Ecp6 is a virulence factor with orthologues in other fungal species. Mol. Microbiol. 69: 119-136.

Bonfante, P. and Genre, A. (2010) Mechanisms underlying beneficial plant-fungus interactions in mycorrhizal symbiosis. Nature Communications 1: 48.

Bonner J.T. (1974) On development-the biology of form. Cambridge, MA: Harvard Univ. Press. 80–109.

Bourke, P.M.A. (1964) Emergence of potato blight, 1843-46. Nature 203: 805-808.

Bowman, S.M. and Free, S.J. (2006) The structure and synthesis of the fungal cell wall. Bioessays 28: 799-808.

Bozsoki, Z., Cheng, J., Feng, F., Gysel, K., Vinther, M., Andersen, K.R., Oldroyd, G., Blaise, M., Radutoiu, S. and Stougaard, J. (2017) Receptor-mediated chitin perception in legume roots is functionally separable from Nod factor perception. Proc Natl Acad Sci USA 114: E8118-E8127.

Bozza, S., Clavaud, C., Giovannini, G., Fontaine, T., Beauvais, A., Sarfati, J., D'Angelo, C., Perruccio, K., Bonifazi, P., Zagarella, S., et al. (2009) Immune sensing of *Aspergillus fumigatus* proteins, glycolipids, and polysaccharides and the impact on Th immunity and vaccination. J. Immunol. 183: 2407-2414.

Braun, V. (2015) Bacterial cell wall research in Tubingen: a brief historical account. Int. J. Med. Microbiol. 305: 178-182.

Broghammer, A., Krusell, L., Blaise, M., Sauer, J., Sullivan, J.T., Maolanon, N., Vinther, M., Lorentzen, A., Madsen, E.B., Jensen, K.J., et al. (2012) Legume receptors perceive the rhizobial lipochitin oligosaccharide signal molecules by direct binding. Proc Natl Acad Sci USA 109: 13859-13864.

Brooks, C., Nekrasov, V., Lippman, Z.B. and Van Eck, J. (2014) Efficient gene editing in tomato in the first generation using the clustered regularly interspaced short palindromic repeats/CRISPR-associated9 system. Plant Physiol. 166: 1292-1297.

Brown, G.D. (2011) Innate antifungal immunity: the key role of phagocytes. Annu. Rev. Immunol. 29: 1-21.

Brule, D., Villano, C., Davies, L.J., Trda, L., Claverie, J., Heloir, M.C., Chiltz, A., Adrian, M., Darblade, B., Tornero, P., et al. (2019) The grapevine (*Vitis vinifera*) LysM receptor kinases VvLYK1-1 and VvLYK1-2 mediate chitooligosaccharide-triggered immunity. Plant Biotechnol J 17 (4): 812-825.

Buendia, L., Girardin, A., Wang, T., Cottret, L. and Lefebvre, B. (2018) LysM receptor-Like kinase and LysM receptor-like protein families: An update on phylogeny and functional characterization. Front Plant Sci 9: 1531.

Buendia, L., Wang, T., Girardin, A. and Lefebvre, B. (2016) The LysM receptor-like kinase SlLYK10 regulates the arbuscular mycorrhizal symbiosis in tomato. New Phytol. 210: 184-195.

Buist, G., Kok, J., Leenhouts, K.J., Dabrowska, M., Venema, G. and Haandrikman, A.J. (1995) Molecular cloning and nucleotide sequence of the gene encoding the major peptidoglycan hydrolase of Lactococcus lactis, a muramidase needed for cell separation. J. Bacteriol. 177: 1554-1563.

Buist, G., Steen, A., Kok, J. and Kuipers, O.P. (2008) LysM, a widely distributed protein motif for binding to (peptido) glycans. Mol. Microbiol. 68: 838-847.

Camacho, C., Coulouris, G., Avagyan, V., Ma, N., Papadopoulos, J., Bealer, K., Madden, T.L. (2009) BLAST+: architecture and applications. BMC Bioinformatics 10: 421.

Cao, Y., Liang, Y., Tanaka, K., Nguyen, C.T., Jedrzejczak, R.P., Joachimiak, A. and Stacey, G. (2014) The kinase LYK5 is a major chitin receptor in Arabidopsis and forms a chitin-induced complex with related kinase CERK1. Elife 3: e03766.

Carolan, K., Helps, J., van den Berg, F., Bain, R., Paveley, N. and van den Bosch, F. (2017) Extending the durability of cultivar resistance by limiting epidemic growth rates. Proc Biol Sci 284.

Cen, K., Li, B., Lu, Y., Zhang, S. and Wang, C. (2017) Divergent LysM effectors contribute to the virulence of *Beauveria bassiana* by evasion of insect immune defenses. PLOS pathog. 13: e1006604.

Chari, R., Yeo, N.C., Chavez, A. and Church, G.M. (2017) sgRNA Scorer 2.0: A Species-Independent Model To Predict CRISPR/Cas9 Activity. ACS Synth Biol 6: 902-904.

Chayen, N.E. and Saridakis, E. (2008) Protein crystallization: from purified protein to diffraction-quality crystal. Nat. Methods 5: 147-153.

Chen, V.B., Arendall, W.B., Headd, J.J., Keedy, D.A., Immormino, R.M., Kapral, G.J., Murray, L.W., Richardson, J.S., Richardson, D.C. (2010) MolProbity: all-atom structure validation for macromolecular crystallography. Acta Crystallogr D 66: 12-21.

Cheng, Y., Glaeser, R.M. and Nogales, E. (2017) How Cryo-EM became so hot. Cell 171: 1229-1231.

Cheval, C., Samwald, S., Johnston, M.G., de Keijzer, J., Breakspear, A., Liu, X., Bellandi, A., Kadota, Y., Zipfel, C. and Faulkner, C. (2020) Chitin perception in plasmodesmata characterizes submembrane immune-signaling specificity in plants. Proc Natl Acad Sci USA 117: 9621-9629.

Chisholm, S.T., Coaker, G., Day, B. and Staskawicz, B.J. (2006) Host-microbe interactions: shaping the evolution of the plant immune response. Cell 124: 803-814.

Cook, D.E., Mesarich, C.H. and Thomma, B.P. (2015) Understanding plant immunity as a surveillance system to detect invasion. Annu. Rev. Phytopathol. 53: 541-563.

Cord-Landwehr, S., Melcher, R. L., Kolkenbrock, S., & Moerschbacher, B. M. (2016). A chitin deacetylase from the endophytic fungus *Pestalotiopsis* sp. efficiently inactivates the elicitor activity of chitin oligomers in rice cells. Scientific reports 6: 38018.

Cosgrove, D.J. (2005) Growth of the plant cell wall. Nat. Rev. Mol. Cell Biol. 6: 850-861.

Dallery, J.F., Zimmer, M., Halder, V., Suliman, M., Pigne, S., Le Goff, G., Gianniou, D.D., Trougakos, I.P., Ouazzani, J., Gasperini, D., et al. (2020) Inhibition of jasmonate-mediated plant defences by the fungal metabolite higginsianin B. J. Exp. Bot. 71: 2910-2921.

Damalas, C.A. and Eleftherohorinos, I.G. (2011) Pesticide exposure, safety issues, and risk assessment indicators. Int J Environ Res Public Health 8: 1402-1419.

Damm, U., O'Connell, R.J., Groenewald, J.Z. and Crous, P.W. (2014) The *Colletotrichum* d*estructivum* species complex - hemibiotrophic pathogens of forage and field crops. Stud Mycol 79: 49-84.

Davis, S.J., Puklavec, M.J., Ashford, D.A., Harlos, K., Jones, E.Y., Stuart, D.I. and Williams, A.F. (1993) Expression of soluble recombinant glycoproteins with predefined glycosylation: application to the crystallization of the T-cell glycoprotein CD2. Protein engineering 6: 229-232.

de Jonge, R., Bolton, M.D. and Thomma, B.P. (2011) How filamentous pathogens co-opt plants: the ins and outs of fungal effectors. Curr. Opin. Plant Biol. 14: 400-406.

de Jonge, R., Peter van Esse, H., Kombrink, A., Shinya, T., Desaki, Y., Bours, R., van der Krol, S., Shibuya, N., Joosten, M.H.A.J. and Thomma, B.P.H.J. (2010) Conserved fungal LysM effector Ecp6 prevents chitin-triggered immunity in plants. Science 329: 953-955.

de Jonge, R. and Thomma, B.P. (2009) Fungal LysM effectors: extinguishers of host immunity? Trends Microbiol. 17: 151-157.

De Jonge, R., Van Esse, H.P., Kombrink, A., Shinya, T., Desaki, Y., Bours, R., Van Der Krol, S., Shibuya, N., Joosten, M.H. and Thomma, B.P. (2010) Conserved fungal LysM effector Ecp6 prevents chitin-triggered immunity in plants. Science 329: 953-955.

De Lorenzo, G., Ferrari, S., Giovannoni, M., Mattei, B. and Cervone, F. (2019) Cell wall traits that influence plant development, immunity, and bioconversion. Plant J. 97: 134-147.

Delaux, P.M., Sejalon-Delmas, N., Becard, G. and Ane, J.M. (2013) Evolution of the plant-microbe symbiotic 'toolkit'. Trends Plant Sci. 18: 298-304.

DeLano, W.L. (2009) The PyMOL Molecular Graphics System; DeLano Scientific: San Carlos, CA, 2002.

De Mita, S., Streng, A., Bisseling, T. and Geurts, R. (2014) Evolution of a symbiotic receptor through gene duplications in the legume-rhizobium mutualism. New Phytol 201 (3): 961-972.

Dereeper, A., Guignon, V., Blanc, G., Audic, S., Buffet, S., Chevenet, F., Dufayard, J.F., Guindon, S., Lefort, V., Lescot, M., et al. (2008) Phylogeny.fr: robust phylogenetic analysis for the non-specialist. Nucleic Acids Res. 36: W465-469.

Desaki, Y., Kohari, M., Shibuya, N. and Kaku, H. (2018) MAMP-triggered plant immunity mediated by the LysM-receptor kinase CERK1. Journal of General Plant Pathology 85: 1-11.

Desaki, Y., Miyata, K., Suzuki, M., Shibuya, N. and Kaku, H. (2018) Plant immunity and symbiosis signaling mediated by LysM receptors. Innate Immun 24: 92-100.

Dessau, M.A. and Modis, Y. (2011) Protein crystallization for X-ray crystallography. J Vis Exp. 16: 2285

de Wit, P.J. (2016) *Cladosporium fulvum* effectors: weapons in the arms race with tomato. Annu. Rev. Phytopathol. 54: 1-23.

Dickman, M.B. and de Figueiredo, P. (2013) Death be not proud--cell death control in plant fungal interactions. PLoS Path. 9: e1003542.

Dierks, K., Meyer, A., Einspahr, H. and Betzel, C. (2008) Dynamic light scattering in protein crystallization droplets, adaptations for analysis and optimization of crystallization processes. Cryst. Growth Des. 8: 1628–1634.

Dodds, P.N. and Rathjen, J.P. (2010) Plant immunity: towards an integrated view of plant-pathogen interactions. Nat. Rev. Genet. 11: 539-548.

Doench, J.G., Fusi, N., Sullender, M., Hegde, M., Vaimberg, E.W., Donovan, K.F., Smith, I., Tothova, Z., Wilen, C., Orchard, R., et al. (2016) Optimized sgRNA design to maximize activity and minimize off-target effects of CRISPR-Cas9. Nat. Biotechnol. 34: 184-191.

Dolfors, F., Holmquist, L., Dixelius, C. and Tzelepis, G. (2019) A LysM effector protein from the basidiomycete *Rhizoctonia solani* contributes to virulence through suppression of chitin-triggered immunity. Mol. Genet. Genomics 294: 1211-1218.

Dow, M., Newman, M.A. and von Roepenack, E. (2000) The induction and modulation of plant defense responses by bacterial lipopolysaccharides. Annu. Rev. Phytopathol. 38: 241-261.

Duncan, K.E. and Howard, R.J. (2000) Cytological analysis of wheat infection by the leaf blotch pathogen *Mycosphaerella graminicola*. Mycol. Res. 104: 1074-1082.

El Gueddari, N.E., Rauchhaus, U., Moerschbacher, B.M. and Deising, H.B. (2002) Developmentally regulated conversion of surface-exposed chitin to chitosan in cell walls of plant pathogenic fungi. New Phytol. 156: 103–112.

Elmlund, D., Le, S.N. and Elmlund, H. (2017) High-resolution cryo-EM: the nuts and bolts. Curr. Opin. Struct. Biol. 46: 1-6.

Emsley, P., Lohkamp, B., Scott, W.G. and Cowtan, K. (2010) Features and development of Coot. Acta Crystallogr D 66: 486-501.

Engler, C., Kandzia, R. and Marillonnet, S. (2008) A one pot, one step, precision cloning method with high throughput capability. PLoS One 3: e3647.

Erbs, G. and Newman, M.A. (2012) The role of lipopolysaccharide and peptidoglycan, two glycosylated bacterial microbe-associated molecular patterns (MAMPs), in plant innate immunity. Mol. Plant Pathol. 13: 95-104.

Erbs, G., Silipo, A., Aslam, S., De Castro, C., Liparoti, V., Flagiello, A., Pucci, P., Lanzetta, R., Parrilli, M., Molinaro, A., et al. (2008) Peptidoglycan and muropeptides from pathogens Agrobacterium and Xanthomonas elicit plant innate immunity: structure and activity. Chem. Biol. 15: 438-448.

Erwig, J., Ghareeb, H., Kopischke, M., Hacke, R., Matei, A., Petutschnig, E. and Lipka, V. (2017) Chitin-induced and CHITIN ELICITOR RECEPTOR KINASE1 (CERK1) phosphorylation-dependent endocytosis of Arabidopsis thaliana LYSIN MOTIF-CONTAINING RECEPTOR-LIKE KINASE5 (LYK5). New Phytol. 215: 382-396.

Eyal, Z. (1999) The Septoria tritici and Stagonospora nodorum blotch diseases of wheat. Eur. J. Plant Pathol. 105: 13.

Faulkner, C., Petutschnig, E., Benitez-Alfonso, Y., Beck, M., Robatzek, S., Lipka, V. and Maule, A.J. (2013) LYM2-dependent chitin perception limits molecular flux via plasmodesmata. Proc Natl Acad Sci USA 110: 9166-9170.

Felix, G., Baureithel, K. and Boller, T. (1998) Desensitization of the perception system for chitin fragments in tomato cells. Plant Physiol. 117: 643-650.

Felix, G., Duran, J.D., Volko, S. and Boller, T. (1999) Plants have a sensitive perception system for the most conserved domain of bacterial flagellin. The Plant journal : for cell and molecular biology 18: 265-276.

Felix, G., Regenass, M. and Boller, M. (1993) Specific perception of subnanomolar concentrations of chitin fragments by tomato cells induction of extracellular alkalinization, changes in protein phosphorylation, and establishment of a refractory state. Plant J. 4: 10.

Feng, F., Sun, J., Radhakrishnan, G.V., Lee, T., Bozsoki, Z., Fort, S., Gavrin, A., Gysel, K., Thygesen, M.B., Andersen, K.R., et al. (2019) A combination of chitooligosaccharide and lipochitooligosaccharide recognition promotes arbuscular mycorrhizal associations in *Medicago truncatula*. Nat Commun 10: 5047.

Fernandez-Calvino, L., Faulkner, C., Walshaw, J., Saalbach, G., Bayer, E., Benitez-Alfonso, Y. and Maule, A. (2011) Arabidopsis plasmodesmal proteome. PLoS One 6: e18880.

Fesel, P.H. and Zuccaro, A. (2016) beta-glucan: Crucial component of the fungal cell wall and elusive MAMP in plants. Fungal Genet. Biol. 90: 53-60.

Finn, R.D., Attwood, T.K., Babbitt, P.C., Bateman, A., Bork, P., Bridge, A.J., Chang, H.Y., Dosztanyi, Z., El-Gebali, S., Fraser, M., et al. (2017) InterPro in 2017-beyond protein family and domain annotations. Nucleic Acids Res. 45: D190-D199.

Fiorin, G.L., Sanchez-Vallet, A., Thomazella, D.P.T., do Prado, P.F.V., do Nascimento, L.C., Figueira, A.V.O., Thomma, B., Pereira, G.A.G. and Teixeira, P. (2018) Suppression of plant immunity by fungal chitinase-like effectors. Curr. Biol. 28: 3023-3030.

Fisher, M.C., Henk, D.A., Briggs, C.J., Brownstein, J.S., Madoff, L.C., McCraw, S.L. and Gurr, S.J. (2012) Emerging fungal threats to animal, plant and ecosystem health. Nature 484: 186-194.

Flemming, H.C., Neu, T.R. and Wozniak, D.J. (2007) The EPS matrix: the "house of biofilm cells". J. Bacteriol. 189: 7945-7947.

Flemming, H.C. and Wingender, J. (2010) The biofilm matrix. Nat. Rev. Microbiol. 8: 623-633.

Flor, H.H. (1971) Current status of the gene-for-gene concept. Annual Reviews 9: 22.

Frandsen, R.J., Andersson, J.A., Kristensen, M.B. and Giese, H. (2008) Efficient four fragment cloning for the construction of vectors for targeted gene replacement in filamentous fungi. BMC Mol. Biol. 9: 70.

Free, S.J. (2013) Fungal cell wall organization and biosynthesis. Adv. Genet. 81: 33-82.

Friesen, T.L., Meinhardt, S.W. and Faris, J.D. (2007) The *Stagonospora nodorum*-wheat pathosystem involves multiple proteinaceous host-selective toxins and corresponding host sensitivity genes that interact in an inverse gene-for-gene manner. Plant J. 51: 681-692.

Froussart, E., Bonneau, J., Franche, C. and Bogusz, D. (2016) Recent advances in actinorhizal symbiosis signaling. Plant Mol. Biol. 90: 613-622.

Fujikawa, T., Kuga, Y., Yano, S., Yoshimi, A., Tachiki, T., Abe, K. and Nishimura, M. (2009) Dynamics of cell wall components of *Magnaporthe grisea* during infectious structure development. Mol. Microbiol. 73: 553-570.

Fujikawa, T., Sakaguchi, A., Nishizawa, Y., Kouzai, Y., Minami, E., Yano, S., Koga, H., Meshi, T. and Nishimura, M. (2012) Surface alpha-1,3-glucan facilitates fungal stealth infection by interfering with innate immunity in plants. PLoS Path. 8: e1002882.

Gao, F., Zhang, B.-S., Zhao, J.-H., Huang, J.-F., Jia, P.-S., Wang, S., Zhang, J., Zhou, J.-M. and Guo, H.-S. (2019) Deacetylation of chitin oligomers increases virulence in soil-borne fungal pathogens. Nat. Plants 5: 1167-1176.

Garvey, K.J., Saedi, M.S. and Ito, J. (1986) Nucleotide sequence of Bacillus phage phi 29 genes 14 and 15: homology of gene 15 with other phage lysozymes. Nucleic Acids Res. 14: 10001-10008.

Genre, A., Chabaud, M., Balzergue, C., Puech-Pages, V., Novero, M., Rey, T., Fournier, J., Rochange, S., Becard, G., Bonfante, P., et al. (2013) Short-chain chitin oligomers from arbuscular mycorrhizal fungi trigger nuclear Ca^{2+} spiking in *Medicago truncatula* roots and their production is enhanced by strigolactone. New Phytol. 198: 190-202.

Gerlach, M., Mueller, U. and Weiss, M.S. (2016) The MX beamlines BL14. 1-3 at BESSY II. JLSRF 2: 47.

Gherbi, H., Markmann, K., Svistoonoff, S., Estevan, J., Autran, D., Giczey, G., Auguy, F., Peret, B., Laplaze, L., Franche, C., et al. (2008) SymRK defines a common genetic basis for plant root endosymbioses with arbuscular mycorrhiza fungi, rhizobia, and Frankiabacteria. Proc Natl Acad Sci USA 105: 4928-4932.

Gibelin-Viala, C., Amblard, E., Puech-Pages, V., Bonhomme, M., Garcia, M., Bascaules-Bedin, A., Fliegmann, J., Wen, J., Mysore, K.S., le Signor, C., et al. (2019) The *Medicago truncatula* LysM receptor-like kinase LYK9 plays a dual role in immunity and the arbuscular mycorrhizal symbiosis. New Phytol. 223: 1516-1529.

Gimenez-Ibanez, S., Hann, D.R., Ntoukakis, V., Petutschnig, E., Lipka, V. and Rathjen, J.P. (2009) AvrPtoB targets the LysM receptor kinase CERK1 to promote bacterial virulence on plants. Curr. Biol. 19: 423-429.

Gomez-Gomez, L. and Boller, T. (2000) FLS2: an LRR receptor-like kinase involved in the perception of the bacterial elicitor flagellin in Arabidopsis. Mol. Cell 5: 1003-1011.

Gough, C. (2003) Rhizobium symbiosis: insight into Nod factor receptors. Curr. Biol. 13: R973-975.

Gough, C., Cottret, L., Lefebvre, B. and Bono, J.J. (2018) Evolutionary history of plant LysM receptor proteins related to root endosymbiosis. Front Plant Sci 9: 923.

Gow, N.A.R., Latge, J.P. and Munro, C.A. (2017) The fungal cell wall: Structure, biosynthesis, and function. Microbiol Spectr. 5

Grover, A. (2012) Plant chitinases: genetic diversity and physiological roles. Crit. Rev. Plant Sci. 31: 57-73.

Gu, Z., Liu, T., Ding, B., Li, F., Wang, Q., Qian, S., Ye, F., Chen, T., Yang, Y., Wang, J., et al. (2017) Two lysin-motif receptor kinases, Gh-LYK1 and Gh-LYK2, contribute to resistance against Verticillium wilt in upland cotton. Front Plant Sci 8: 2133.

Gust, A.A., Willmann, R., Desaki, Y., Grabherr, H.M. and Nurnberger, T. (2012) Plant LysM proteins: modules mediating symbiosis and immunity. Trends Plant Sci. 17: 495-502.

Haltiwanger, R.S. and Lowe, J.B. (2004) Role of glycosylation in development. Annu. Rev. Biochem. 73: 491-537.

Hammond-Kosack, K.E. and Jones, J.D. (1996) Resistance gene-dependent plant defense responses. Plant Cell 8: 1773-1791.

Hamid, R., Khan, M.A., Ahmad, M., Ahmad, M.M., Abdin, M.Z., Musarrat, J. and Javed, S. (2013) Chitinases: an update. J. Pharm. Bioallied Sci. 5: 21-29.

Hartmann, F.E. and Croll, D. (2017) Distinct trajectories of massive recent gene gains and losses in populations of a microbial eukaryotic pathogen. Mol. Biol. Evol. 34: 2808-2822.

Hartmann, F.E., Sánchez-Vallet, A., McDonald, B.A., Croll, D. (2017) A fungal wheat pathogen evolved host specialization by extensive chromosomal rearrangements. ISME J. 11: 1189-1204.

Hawkins, N.J., Bass, C., Dixon, A. and Neve, P. (2018) The evolutionary origins of pesticide resistance. Biol. Rev. Camb. Philos. Soc.

Hayafune, M., Berisio, R., Marchetti, R., Silipo, A., Kayama, M., Desaki, Y., Arima, S., Squeglia, F., Ruggiero, A., Tokuyasu, K., et al. (2014) Chitin-induced activation of immune signaling by the rice receptor CEBiP relies on a unique sandwich-type dimerization. Proc Natl Acad Sci USA 111: E404-413.

Hirsch, A.M. (2004) Plant-microbe symbioses: A continuum from commensalism to parasitism. Symbiosis 37: 1-3.

Hirt, H. (1997) Multiple roles of MAP kinases in plant signal transduction. Trends Plant Sci. 2: 11-15.

Hopke, A., Brown, A.J.P., Hall, R.A. and Wheeler, R.T. (2018) Dynamic fungal cell wall architecture in stress adaptation and immune evasion. Trends Microbiol. 26: 284-295.

Houterman, P.M., Cornelissen, B.J. and Rep, M. (2008) Suppression of plant resistance gene-based immunity by a fungal effector. PLoS pathog. 4: e1000061.

Huibers, R.P., Loonen, A.E., Gao, D., Van den Ackerveken, G., Visser, R.G. and Bai, Y. (2013) Powdery mildew resistance in tomato by impairment of SlPMR4 and SlDMR1. PLoS One 8: e67467.

Hurlburt, N.K., Chen, L-H., Stergiopoulos, I. and Fisher, A.J. (2018) Structure of the *Cladosporium fulvum* Avr4 effector in complex with (GlcNAc) 6 reveals the ligand-binding mechanism and uncouples its intrinsic function from recognition by the Cf-4 resistance protein. PLoS Pathog. 14: e1007263.

Iizasa, E., Mitsutomi, M. and Nagano, Y. (2010) Direct binding of a plant LysM receptor-like kinase, LysM RLK1/CERK1, to chitin in vitro. J. Biol. Chem. 285: 2996-3004.

Ito, Y., Kaku, H. and Shibuya, N. (1997) Identification of a high-affinity binding protein for N-acetylchitooligosaccharide elicitor in the plasma membrane of suspension-cultured rice cells by affinity labeling. Plant J. 12: 10.

Jashni, M.K., Dols, I.H., Iida, Y., Boeren, S., Beenen, H.G., Mehrabi, R., Collemare, J. and de Wit, P.J. (2015) Synergistic action of a metalloprotease and a serine protease from *Fusarium oxysporum* f. sp. lycopersici cleaves chitin-binding tomato chitinases, reduces their antifungal activity, and enhances fungal virulence. Mol Plant Microbe Interact. 28: 996-1008.

Jing, H.C., Lovell, D., Gutteridge, R., Jenk, D., Kornyukhin, D., Mitrofanova, O.P., Kema, G.H. and Hammond-Kosack, K.E. (2008) Phenotypic and genetic analysis of the *Triticum monococcum-Mycosphaerella graminicola* interaction. New Phytol. 179: 1121-1132.

Jones, J.D. and Dangl, J.L. (2006) The plant immune system. Nature 444: 323-329.

Joris, B., Englebert, S., Chu, C.P., Kariyama, R., Daneo-Moore, L., Shockman, G.D. and Ghuysen, J.M. (1992) Modular design of the Enterococcus hirae muramidase-2 and *Streptococcus faecalis* autolysin. FEMS Microbiol. Lett. 70: 257-264.

Kaiser, D. (2001) Building a multicellular organism. Annu. Rev. Genet. 35: 103-123.

Kaku, H., Nishizawa, Y., Ishii-Minami, N., Akimoto-Tomiyama, C., Dohmae, N., Takio, K., Minami, E. and Shibuya, N. (2006) Plant cells recognize chitin fragments for defense signaling through a plasma membrane receptor. Proc Natl Acad Sci USA 103: 11086-11091.

Kasprzewska, A. (2003) Plant chitinases-regulation and function. Cell. Mol. Biol. Lett. 8: 809-824.

Katoh, K. and Standley, D.M. (2013) MAFFT multiple sequence alignment software version 7: improvements in performance and usability. Mol. Biol. Evol. 30: 772-780.

Kavanaugh, J.S., Flack, C.E., Lister, J., Ricker, E.B., Ibberson, C.B., Jenul, C., Moormeier, D.E., Delmain, E.A., Bayles, K.W. and Horswill, A.R. (2019) Identification of extracellular DNA-binding proteins in the biofilm matrix. mBio 10.

Kawaguchi, M. and Minamisawa, K. (2010) Plant-microbe communications for symbiosis. Plant Cell Physiol. 51: 1377-1380.

Kelley, L.A., Mezulis, S., Yates, C.M., Wass, M.N. and Sternberg, M.J.E. (2015) The Phyre2 web portal for protein modeling, prediction and analysis. Nat. Protoc. 10: 845-858.

Kema, G.H., Verstappen, E.C. and Waalwijk, C. (2000) Avirulence in the wheat septoria tritici leaf blotch fungus *Mycosphaerella graminicola* is controlled by a single locus. Mol Plant Microbe Interact. 13: 1375-1379.

Kettles, G.J. and Kanyuka, K. (2016) Dissecting the molecular interactions between wheat and the fungal pathogen *Zymoseptoria tritici*. Front Plant Sci 7: 508.

Koharudin, L.M., Viscomi, A.R., Montanini, B., Kershaw, M.J., Talbot, N.J., Ottonello, S. and Gronenborn, A.M. (2011) Structure-function analysis of a CVNH-LysM lectin expressed during plant infection by the rice blast fungus *Magnaporthe oryzae*. Structure 19: 662-674.

Kohler, A.C., Chen, L-H., Hurlburt, N., Salvucci, A., Schwessinger, B., Fisher, A.J. and Stergiopoulos, I. (2016) Structural analysis of an Avr4 effector ortholog offers insight into chitin-binding and recognition by the Cf-4 receptor. Plant Cell 28: 1945-1965.

Kombrink, A., Rovenich, H., Shi-Kunne, X., Rojas-Padilla, E., van den Berg, G.C., Domazakis, E., de Jonge, R., Valkenburg, D.J., Sanchez-Vallet, A., Seidl, M.F., et al. (2017) *Verticillium dahliae* LysM effectors differentially contribute to virulence on plant hosts. Mol. Plant Pathol. 18: 596-608.

Kombrink, A., Sanchez-Vallet, A. and Thomma, B.P.H.J. (2011) The role of chitin detection in plant-pathogen interactions. Microbes Infect. 13: 1168-1176.

Kombrink, A. and Thomma, B.P.H.J. (2013) LysM effectors: secreted proteins supporting fungal life. PLoS pathog. 9: e1003769.

Kumar, H., Kawai, T. and Akira, S. (2009) Toll-like receptors and innate immunity. Biochem. Biophys. Res. Commun. 388: 621-625.

Krissinel, E. and Henrick, K. (2007) Inference of macromolecular assemblies from crystalline state. J. Mol. Biol. 372: 774-797.

Lanfranco, L., Fiorilli, V. and Gutjahr, C. (2018) Partner communication and role of nutrients in the arbuscular mycorrhizal symbiosis. New Phytol. 220: 1031-1046.

Latge, J.P. (2007) The cell wall: a carbohydrate armour for the fungal cell. Mol. Microbiol. 66: 279-290.

Latge, J.P. (2010) Tasting the fungal cell wall. Cell. Microbiol. 12: 863-872.

Lee, W.S., Rudd, J.J., Hammond-Kosack, K.E. and Kanyuka, K. (2014) *Mycosphaerella graminicola* LysM effector-mediated stealth pathogenesis subverts recognition through both CERK1 and CEBiP homologues in wheat. Mol Plant Microbe Interact 27: 236-243.

Lenardon, M.D., Munro, C.A. and Gow, N.A. (2010) Chitin synthesis and fungal pathogenesis. Curr. Opin. Microbiol. 13: 416-423.

Lewis, D.H. (1973) Concepts in fungal nutrition and the origin of biotrophy. Biological Reviews 48: 261-278.

Li, H. and Greene, L.H. (2010) Sequence and structural analysis of the chitinase insertion domain reveals two conserved motifs involved in chitin-binding. PLoS One 5: e8654.

Liang, G., Zhang, H., Lou, D. and Yu, D. (2016) Selection of highly efficient sgRNAs for CRISPR/Cas9-based plant genome editing. Sci Rep 6: 21451.

Liang, Y., Toth, K., Cao, Y., Tanaka, K., Espinoza, C. and Stacey, G. (2014) Lipochitooligosaccharide recognition: an ancient story. New Phytol. 204: 289-296.

Liao, D., Sun, X., Wang, N., Song, F. and Liang, Y. (2018) Tomato LysM Receptor-like kinase SlLYK12 is involved in arbuscular mycorrhizal symbiosis. Front. Plant Sci. 9: 1004.

Liebrand, T.W., Smit, P., Abd-El-Haliem, A., de Jonge, R., Cordewener, J.H., America, A.H., Sklenar, J., Jones, A.M., Robatzek, S., Thomma, B.P., et al. (2012) Endoplasmic reticulum-quality control chaperones facilitate the biogenesis of Cf receptor-like proteins involved in pathogen resistance of tomato. Plant Physiol. 159: 1819-1833.

Limpens, E. and Bisseling, T. (2003) Signaling in symbiosis. Curr. Opin. Plant Biol. 6: 343-350.

Limpens, E., Franken, C., Smit, P., Willemse, J., Bisseling, T. and Geurts, R. (2003) LysM domain receptor kinases regulating rhizobial Nod factor-induced infection. Science 302: 630-633.

Limpens, E., van Zeijl, A. and Geurts, R. (2015) Lipochitooligosaccharides modulate plant host immunity to enable endosymbioses. Annu. Rev. Phytopathol. 53: 311-334.

Lin, S., Yang, L., Chen, G., Li, B., Chen, D., Li, L. and Xu, Z. (2017) Pathogenic features and characteristics of food borne pathogens biofilm: Biomass, viability and matrix. Microb. Pathog. 111: 285-291.

Liu, B., Li, J.F., Ao, Y., Qu, J., Li, Z., Su, J., Zhang, Y., Liu, J., Feng, D., Qi, K., et al. (2012) Lysin motif-containing proteins LYP4 and LYP6 play dual roles in peptidoglycan and chitin perception in rice innate immunity. Plant Cell 24: 3406-3419.

Li, H., Handsaker, B., Wysoker, A., Fennell, T., Ruan, J., Homer, N., Marth, G., Abecasis, G. and Durbin, R. (2009) The sequence alignment/map format and SAMtools. Bioinformatics 25: 2078-2079.

Liu, S., Wang, J., Han, Z., Gong, X., Zhang, H. and Chai, J. (2016) Molecular mechanism for fungal cell wall recognition by rice chitin receptor OsCEBiP. Structure 24: 1192-1200.

Liu, T., Liu, Z., Song, C., Hu, Y., Han, Z., She, J., Fan, F., Wang, J., Jin, C., Chang, J., et al. (2012) Chitin-induced dimerization activates a plant immune receptor. Science 336: 1160-1164.

Liu, T., Chen, L., Ma, Q., Shen, X. and Yang, Q. (2014) Structural insights into chitinolytic enzymes and inhibition mechanisms of selective inhibitors. Curr. Pharm. Des. 20: 754-770.

Liu, Y., Schiff, M. and Dinesh-Kumar, S.P. (2002) Virus-induced gene silencing in tomato. Plant J. 31: 777-786.

Livak, K.J. and Schmittgen, T.D. (2001) Analysis of relative gene expression data using real-time quantitative PCR and the 2(-Delta Delta C(T)) Method. Methods 25: 402-408.

Lohmann, G.V., Shimoda, Y., Nielsen, M.W., Jorgensen, F.G., Grossmann, C., Sandal, N., Sorensen, K., Thirup, S., Madsen, L.H., Tabata, S., et al. (2010) Evolution and regulation of the *Lotus japonicus* LysM receptor gene family. Mol. Plant Microbe Interact. 23: 510-521.

Lorber, B., Fischer, F., Bailly, M., Roy, H. and Kern, D. (2012) Protein analysis by dynamic light scattering: methods and techniques for students. Biochem Mol Biol Educ. 40: 372-382.

Low, P.S. and Merida, J.R. (1996) The oxidative burst in plant defense: Function and signal transduction. Physiol. Plant 96: 533-542.

Lyumkis, D. (2019) Challenges and opportunities in cryo-EM single-particle analysis. J. Biol. Chem. 294: 5181-5197.

Madsen, E.B., Madsen, L.H., Radutoiu, S., Olbryt, M., Rakwalska, M., Szczyglowski, K., Sato, S., Kaneko, T., Tabata, S., Sandal, N., et al. (2003) A receptor kinase gene of the LysM type is involved in legume perception of rhizobial signals. Nature 425: 637-640.

Maillet, F., Poinsot, V., Andre, O., Puech-Pages, V., Haouy, A., Gueunier, M., Cromer, L., Giraudet, D., Formey, D., Niebel, A., et al. (2011) Fungal lipochitooligosaccharide symbiotic signals in arbuscular mycorrhiza. Nature 469: 58-63.

Margineanu, A., Chan, J.J., Kelly, D.J., Warren, S.C., Flatters, D., Kumar, S., Katan, M., Dunsby, C.W. and French, P.M. (2016) Screening for protein-protein interactions using Forster resonance energy transfer (FRET) and fluorescence lifetime imaging microscopy (FLIM). Sci Rep 6: 28186.

Marshall, R., Kombrink, A., Motteram, J., Loza-Reyes, E., Lucas, J., Hammond-Kosack, K.E., Thomma, B.P.H.J. and Rudd, J.J. (2011) Analysis of two in planta expressed LysM effector homologs from the fungus *Mycosphaerella graminicola* reveals novel functional properties and varying contributions to virulence on wheat. Plant Physiol. 156: 756-769.

Martins, M., Uppuluri, P., Thomas, D.P., Cleary, I.A., Henriques, M., Lopez-Ribot, J.L. and Oliveira, R. (2010) Presence of extracellular DNA in the *Candida albicans* biofilm matrix and its contribution to biofilms. Mycopathologia 169: 323-331.

May, R. and Anderson, R. (1990) Parasite—host coevolution. Parasitology 100: 89-101.

Murshudov, G.N., Skubák, P., Lebedev, A.A., Pannu, N.S., Steiner, R.A., Nicholls, R.A., Winn, M.D., Long, F. and Vagin, A.A. (2011) REFMAC5 for the refinement of macromolecular crystal structures. Acta Crystallogr D 67: 355-367.

McPherson, A. and Cudney, B. (2006) Searching for silver bullets: an alternative strategy for crystallizing macromolecules. J Struct Biol. 156: 387-406.

McPherson, A. and Gavira, J.A. (2014) Introduction to protein crystallization. Acta Crystallogr F Struct Biol Commun. 70: 2-20.

McPherson, A., Nguyen, C., Cudney, R. and Larson, S.B. (2011) The role of small molecule additives and chemical modification in protein crystallization. Cryst. Growth Des. 11: 1469-1474.

Melida, H., Sandoval-Sierra, J.V., Dieguez-Uribeondo, J. and Bulone, V. (2013) Analyses of extracellular carbohydrates in oomycetes unveil the existence of three different cell wall types. Eukaryot. Cell 12: 194-203.

Melida, H., Sopena-Torres, S., Bacete, L., Garrido-Arandia, M., Jorda, L., Lopez, G., Munoz-Barrios, A., Pacios, L.F. and Molina, A. (2018) Non-branched beta-1,3-glucan oligosaccharides trigger immune responses in Arabidopsis. Plant J. 93: 34-49.

Meng, F. and Kurgan, L. (2016) DFLpred: High-throughput prediction of disordered flexible linker regions in protein sequences. Bioinformatics 32: i341-i350.

Mentlak, T.A., Kombrink, A., Shinya, T., Ryder, L.S., Otomo, I., Saitoh, H., Terauchi, R., Nishizawa, Y., Shibuya, N., Thomma, B.P., et al. (2012) Effector-mediated suppression of chitin-triggered immunity by *Magnaporthe oryzae* is necessary for rice blast disease. Plant Cell 24: 322-335.

Mesnage, S., Dellarole, M., Baxter, N.J., Rouget, J.B., Dimitrov, J.D., Wang, N., Fujimoto, Y., Hounslow, A.M., Lacroix-Desmazes, S., Fukase, K., et al. (2014) Molecular basis for bacterial peptidoglycan recognition by LysM domains. Nat Commun. 5: 4269.

Mirzadi Gohari, A., Ware, S.B., Wittenberg, A.H., Mehrabi, R., Ben M'Barek, S., Verstappen, E.C., van der Lee, T.A., Robert, O., Schouten, H.J., de Wit, P.P., et al. (2015) Effector discovery in the fungal wheat pathogen *Zymoseptoria tritici*. Mol. Plant Pathol. 16: 931-945.

Miya, A., Albert, P., Shinya, T., Desaki, Y., Ichimura, K., Shirasu, K., Narusaka, Y., Kawakami, N., Kaku, H. and Shibuya, N. (2007) CERK1, a LysM receptor kinase, is essential for chitin elicitor signaling in Arabidopsis. Proc Natl Acad Sci USA 104: 19613-19618.

Miyata, K., Kozaki, T., Kouzai, Y., Ozawa, K., Ishii, K., Asamizu, E., Okabe, Y., Umehara, Y., Miyamoto, A., Kobae, Y., et al. (2014) The bifunctional plant receptor, OsCERK1, regulates both chitin-triggered immunity and arbuscular mycorrhizal symbiosis in rice. Plant Cell Physiol. 55: 1864-1872.

Mojzsis, S.J., Arrhenius, G., McKeegan, K.D., Harrison, T.M., Nutman, A.P. and Friend, C.R. (1996) Evidence for life on Earth before 3,800 million years ago. Nature 384: 55-59.

Moremen, K.W., Tiemeyer, M. and Nairn, A.V. (2012) Vertebrate protein glycosylation: diversity, synthesis and function. Nat. Rev. Mol. Cell Biol. 13: 448-462.

Murakami, E., Cheng, J., Gysel, K., Bozsoki, Z., Kawaharada, Y., Hjuler, C.T., Sorensen, K.K., Tao, K., Kelly, S., Venice, F., et al. (2018) Epidermal LysM receptor ensures robust symbiotic signalling in *Lotus japonicus*. Elife 7: e33506.

Murata, K. and Wolf, M. (2018) Cryo-electron microscopy for structural analysis of dynamic biological macromolecules. Biochim Biophys Acta Gen Subj 1862: 324-334.

Nagashima, Y., von Schaewen, A. and Koiwa, H. (2018) Function of N-glycosylation in plants. Plant Sci. 274: 70-79.

Nakagawa, T., Kaku, H., Shimoda, Y., Sugiyama, A., Shimamura, M., Takanashi, K., Yazaki, K., Aoki, T., Shibuya, N. and Kouchi, H. (2011) From defense to symbiosis: limited alterations in the kinase domain of LysM receptor-like kinases are crucial for evolution of legume-Rhizobium symbiosis. Plant J. 65: 169-180.

Narusaka, Y., Shinya, T., Narusaka, M., Motoyama, N., Shimada, H., Murakami, K. and Shibuya, N. (2013) Presence of LYM2 dependent but CERK1 independent disease resistance in Arabidopsis. Plant Signal Behav. 8: e25345.

Naumann, T.A. (2011) Modification of recombinant maize ChitA chitinase by fungal chitinase-modifying proteins. Mol. Plant Pathol. 12: 365-372.

Naumann, T.A. and Wicklow, D.T. (2013) Chitinase modifying proteins from phylogenetically distinct lineages of Brassica pathogens. Physiol. Mol. Plant Pathol. 82: 1-9.

Naumann, T.A., Wicklow, D.T. and Price, N.P. (2011) Identification of a chitinase-modifying protein from *Fusarium verticillioides*: truncation of a host resistance protein by a fungalysin metalloprotease. J. Biol. Chem. 286: 35358-35366.

Neuhaus, J.M., Sticher, L., Meins, F.J. and Boller, T. (1991) A short C-terminal sequence is necessary and sufficient for the targeting of chitinases to the plant vacuole. Proc Natl Acad Sci USA 88: 10362-10366.

Newman, J., Egan, D., Walter, T.S., Meged, R., Berry, I., Ben Jelloul, M., Sussman, J.L., Stuart, D.I. and Perrakis, A. (2005) Towards rationalization of crystallization screening for small-to medium-sized academic laboratories: the PACT/JCSG+ strategy. Acta Crystallogr. D 61: 1426-1431.

Niesen, FH, Koch, A, Lenski, U, Harttig, U, Roske, Y, Heinemann, U, et al. (2008) An approach to quality management in structural biology: biophysical selection of proteins for successful crystallization. J Struct Biol. 162: 451-459.

Nogales, E. (2018) Cryo-EM. Curr. Biol. 28: R1127-R1128.

Nutman, A.P., Bennett, V.C., Friend, C.R., Van Kranendonk, M.J. and Chivas, A.R. (2016) Rapid emergence of life shown by discovery of 3,700-million-year-old microbial structures. Nature 537: 535-538.

Oerke, E.C. and Dehne, H.W. (2004) Safeguarding production—losses in major crops and the role of crop protection. Crop Protect. 23: 275-285.

Okada, M., Matsumura, M. and Shibuya, N. (2001) Identification of a high-affinity binding protein for N-acetylchitooligosaccharide elicitor in the plasma membrane from rice leaf and root cells. J. Plant Physiol. 158: 121-124.

Ökmen, B., Kemmerich, B., Hilbig, D., Wemhöner, R., Aschenbroich, J., Perrar, A., Huesgen, P.F., **Schipper, K. and Doehlemann, G.** (2018) Dual function of a secreted fungalysin metalloprotease in *Ustilago maydis*. New Phytol. 220: 249-261.

Olah, B., Briere, C., Becard, G., Denarie, J. and Gough, C. (2005) Nod factors and a diffusible factor from arbuscular mycorrhizal fungi stimulate lateral root formation in *Medicago truncatula* via the DMI1/DMI2 signalling pathway. Plant J. 44: 195-207.

Oldroyd, G.E. (2013) Speak, friend, and enter: signalling systems that promote beneficial symbiotic associations in plants. Nat. Rev. Microbiol. 11: 252-263.

Oliveira-Garcia, E. and Deising, H.B. (2016) Attenuation of PAMP-triggered immunity in maize requires down-regulation of the key beta-1,6-glucan synthesis genes KRE5 and KRE6 in biotrophic hyphae of *Colletotrichum graminicola*. Plant J. 87: 355-375.

Op den Camp, R., Streng, A., De Mita, S., Cao, Q., Polone, E., Liu, W., Ammiraju, J.S., Kudrna, D., Wing, R., Untergasser, A., et al. (2011) LysM-type mycorrhizal receptor recruited for rhizobium symbiosis in nonlegume *Parasponia*. Science 331: 909-912.

Oyeleye, A. and Normi, Y.M. (2018) Chitinase: diversity, limitations, and trends in engineering for suitable applications. Biosci Rep 38: BSR2018032300.

Pan, C., Ye, L., Qin, L., Liu, X., He, Y., Wang, J., Chen, L. and Lu, G. (2016) CRISPR/Cas9-mediated efficient and heritable targeted mutagenesis in tomato plants in the first and later generations. Sci Rep 6: 24765.

Parniske, M. (2004) Molecular genetics of the arbuscular mycorrhizal symbiosis. Curr Opin Plant Biol. 7: 414-421.

Peccoud, J., Weber, E., Engler, C., Gruetzner, R., Werner, S. and Marillonnet, S. (2011) A modular cloning system for standardized assembly of multigene constructs. PLoS ONE 6: e16765.

Pekarsky, A., Veiter, L., Rajamanickam, V., Herwig, C., Grunwald-Gruber, C., Altmann, F. and Spadiut, O. (2018) Production of a recombinant peroxidase in different glyco-engineered *Pichia pastoris* strains: a morphological and physiological comparison. Microb Cell Fact. 17: 183.

Pennisi, E. (2010) Armed and dangerous. Science 327: 804-805.

Petersen, T.N., Brunak, S., von Heijne, G. and Nielsen, H. (2011) SignalP 4.0: discriminating signal peptides from transmembrane regions. Nat. Methods 8: 785-786.

Petutschnig, E.K., Jones, A.M., Serazetdinova, L., Lipka, U. and Lipka, V. (2010) The lysin motif receptor-like kinase (LysM-RLK) CERK1 is a major chitin-binding protein in *Arabidopsis thaliana* and subject to chitin-induced phosphorylation. J. Biol. Chem. 285: 28902-28911.

Petutschnig, E.K., Stolze, M., Lipka, U., Kopischke, M., Horlacher, J., Valerius, O., Rozhon, W., Gust, A.A., Kemmerling, B., Poppenberger, B., et al. (2014) A novel Arabidopsis CHITIN ELICITOR RECEPTOR KINASE 1 (CERK1) mutant with enhanced pathogen-induced cell death and altered receptor processing. New Phytol. 204: 955-967.

Pietraszewska-Bogiel, A., Lefebvre, B., Koini, M.A., Klaus-Heisen, D., Takken, F.L., Geurts, R., Cullimore, J.V. and Gadella, T.W. (2013) Interaction of *Medicago truncatula* lysin motif receptor-like kinases, NFP and LYK3, produced in *Nicotiana benthamiana* induces defence-like responses. PLoS One 8: e65055.

Pnini-Cohen, S., Zilberstein, A., Schuster, S., Sharon, A. and Eyal, Z. (2000) Elucidation of Septoria tritici x wheat interactions using GUS-expressing isolates. Phytopathology 90: 297-304.

Price, W.N., 2nd, Chen, Y., Handelman, S.K., Neely, H., Manor, P., Karlin, R., Nair, R., Liu, J., Baran, M., Everett, J., et al. (2009) Understanding the physical properties that control protein crystallization by analysis of large-scale experimental data. Nat. Biotechnol. 27: 51-57.

Proteau, A., Shi, R. and Cygler, M. (2010) Application of dynamic light scattering in protein crystallization. Curr Protoc Protein Sci Chapter 17: Unit 17 10.

Raetz, C.R. and Whitfield, C. (2002) Lipopolysaccharide endotoxins. Annu. Rev. Biochem. 71: 635-700.

Radkov, A.D., Hsu, Y.P., Booher, G. and VanNieuwenhze, M.S. (2018) Imaging bacterial cell wall biosynthesis. Annu. Rev. Biochem. 87: 991-1014.

Radutoiu, S., Madsen, L.H., Madsen, E.B., Felle, H.H., Umehara, Y., Gronlund, M., Sato, S., Nakamura, Y., Tabata, S., Sandal, N., et al. (2003) Plant recognition of symbiotic bacteria requires two LysM receptor-like kinases. Nature 425: 585-592.

Radutoiu, S., Madsen, L.H., Madsen, E.B., Jurkiewicz, A., Fukai, E., Quistgaard, E.M., Albrektsen, A.S., James, E.K., Thirup, S. and Stougaard, J. (2007) LysM domains mediate lipochitin-oligosaccharide recognition and Nfr genes extend the symbiotic host range. EMBO J. 26: 3923-3935.

Rahar, S., Swami, G., Nagpal, N., Nagpal, M. A., & Singh, G. S. (2011). Preparation, characterization, and biological properties of β-glucans. J Adv Pharm Technol Res. 2: 94–103.

Ran, F.A., Hsu, P.D., Lin, C.Y., Gootenberg, J.S., Konermann, S., Trevino, A.E., Scott, D.A., Inoue, A., Matoba, S., Zhang, Y., et al. (2013) Double nicking by RNA-guided CRISPR Cas9 for enhanced genome editing specificity. Cell 154: 1380-1389.

Rosadini, C.V. and Kagan, J.C. (2017) Early innate immune responses to bacterial LPS. Curr. Opin. Immunol. 44: 14-19.

Ravaioli, S., Campoccia, D., Speziale, P., Pietrocola, G., Zatorska, B., Maso, A., Presterl, E., Montanaro, L. and Arciola, C.R. (2020) Various biofilm matrices of the emerging pathogen *Staphylococcus lugdunensis*: exopolysaccharides, proteins, eDNA and their correlation with biofilm mass. Biofouling 36: 86-100.

Ren, Y.Y. and West, C.A. (1992) Elicitation of diterpene biosynthesis in rice (*Oryza sativa* L.) by chitin. Plant Physiol. 99: 1169-1178.

Rey, T., Nars, A., Bonhomme, M., Bottin, A., Huguet, S., Balzergue, S., Jardinaud, M.F., Bono, J.J., Cullimore, J., Dumas, B., et al. (2013) NFP, a LysM protein controlling Nod factor perception, also intervenes in *Medicago truncatula* resistance to pathogens. New Phytol. 198: 875-886.

Richards, S. and Rose, L.E. (2019) The evolutionary history of LysM-RLKs (LYKs/LYRs) in wild tomatoes. BMC Evol. Biol. 19: 141.

Ride, J.P. and Barber, M.S. (1990) Purification and characterization of multiple forms of endochitinase from wheat leaves. Plant Sci. 71: 185-197.

Ristaino, J.B. (2002) Tracking historic migrations of the Irish potato famine pathogen, Phytophthora infestans. Microb. Infect. 4: 1369-1377.

Roeder, A., Kirschning, C.J., Rupec, R.A., Schaller, M., Weindl, G. and Korting, H.C. (2004) Toll-like receptors as key mediators in innate antifungal immunity. Med. Mycol. 42: 485-498.

Rodriguez-Moreno, L., Ebert, M.K., Bolton, M.D. and Thomma, B.P.H.J. (2018) Tools of the crook- infection strategies of fungal plant pathogens. Plant J. 93: 664-674.

Rodriguez-Moreno, L., Song, Y. and Thomma, B.P. (2017) Transfer and engineering of immune receptors to improve recognition capacities in crops. Curr. Opin. Plant Biol. 38: 42-49.

Romani, L. (2011) Immunity to fungal infections. Nat. Rev. Immunol. 11: 275-288.

Romero-Contreras, Y.J., Ramirez-Valdespino, C.A., Guzman-Guzman, P., Macias-Segoviano, J.I., Villagomez-Castro, J.C. and Olmedo-Monfil, V. (2019) Tal6 From *Trichoderma atroviride* is a LysM effector involved in mycoparasitism and plant association. Front Microbiol. 10: 2231.

Rooney., H.C.E., Klooster., J.W.v.t., Hoorn., R.A.L.v.d., Joosten., M.H.A.J., Jones., J.D.G. and Wit, P.J.G.M.d. (2005) Cladosporium Avr2 inhibits tomato Rcr3 protease required for Cf-2–dependent disease resistance. Science 308: 1783-1786.

Rose, J.K., Ham, K.S., Darvill, A.G. and Albersheim, P. (2002) Molecular cloning and characterization of glucanase inhibitor proteins: coevolution of a counterdefense mechanism by plant pathogens. Plant Cell 14: 1329-1345.

Rovenich, H., Boshoven, J.C. and Thomma, B.P.H.J. (2014) Filamentous pathogen effector functions: of pathogens, hosts and microbiomes. Curr. Opin. Plant Biol. 20: 96-103.

Rovenich, H., Zuccaro, A. and Thomma, B.P. (2016) Convergent evolution of filamentous microbes towards evasion of glycan-triggered immunity. New Phytol. 212: 896-901.

Roy, A., Kucukural, A. and Zhang, Y. (2010) I-TASSER: a unified platform for automated protein structure and function prediction. Nat. Protocol 5: 725-738.

Rudd, J.J., Kanyuka, K., Hassani-Pak, K., Derbyshire, M., Andongabo, A., Devonshire, J., Lysenko, A., Saqi, M., Desai, N.M., Powers, S.J., et al. (2015) Transcriptome and metabolite profiling of the infection cycle of *Zymoseptoria tritici* on wheat reveals a biphasic interaction with plant immunity involving differential pathogen chromosomal contributions and a variation on the hemibiotrophic lifestyle definition. Plant Physiol. 167: 1158-1185.

Rudd, J.J., Keon, J. and Hammond-Kosack, K.E. (2008) The wheat mitogen-activated protein kinases TaMPK3 and TaMPK6 are differentially regulated at multiple levels during compatible disease interactions with *Mycosphaerella graminicola*. Plant Physiol. 147: 802-815.

Saintenac, C., Lee, W.S., Cambon, F., Rudd, J.J., King, R.C., Marande, W., Powers, S.J., Berges, H., Phillips, A.L., Uauy, C., et al. (2018) Wheat receptor-kinase-like protein Stb6 controls gene-for-gene resistance to fungal pathogen *Zymoseptoria tritici*. Nat. Genet. 50: 368-374.

Sanchez-Rangel, D., Sanchez-Nieto, S. and Plasencia, J. (2012) Fumonisin B1, a toxin produced by Fusarium verticillioides, modulates maize beta-1,3-glucanase activities involved in defense response. Planta 235: 965-978.

Sánchez-Vallet A, Tian H, Rodriguez-Moreno L, Valkenburg D-J, Saleem-Batcha R, Wawra S, Kombrink A, Verhage L, de Jonge R, van Esse HP, et al (2020) A secreted LysM effector protects fungal hyphae through chitin-dependent homodimer polymerization. PLoS Pathog **16**: 1–21.

Sanchez-Vallet, A., Mesters, J.R. and Thomma, B.P.H.J. (2015) The battle for chitin recognition in plant-microbe interactions. FEMS Microbiol. Rev. 39: 171-183.

Sanchez-Vallet, A., Saleem-Batcha, R., Kombrink, A., Hansen, G., Valkenburg, D.J., Thomma, B.P.H.J. and Mesters, J.R. (2013) Fungal effector Ecp6 outcompetes host immune receptor for chitin binding through intrachain LysM dimerization. Elife 2: e00790.

Sanson, K.R., Hanna, R.E., Hegde, M., Donovan, K.F., Strand, C., Sullender, M.E., Vaimberg, E.W., Goodale, A., Root, D.E., Piccioni, F., et al. (2018) Optimized libraries for CRISPR-Cas9 genetic screens with multiple modalities. Nat Commun. 9: 5416.

Santhanam, P. (2012) Random insertional mutagenesis in fungal genomes to identify virulence factors. Methods Mol. Biol. 835: 509-517.

Sanz-Martin, J.M., Pacheco-Arjona, J.R., Bello-Rico, V., Vargas, W.A., Monod, M., Diaz-Minguez, J.M., Thon, M.R. and Sukno, S.A. (2016) A highly conserved metalloprotease effector enhances virulence in the maize anthracnose fungus *Colletotrichum graminicola*. Mol. Plant Pathol. 17: 1048-1062.

Sauter, C., D. Ng, J., Lorber, B., Keith, G., Brion, P., Hosseini, M.W., Lehn, J.M. and Giege, R. (1999) Additives for the crystallization of proteins and nucleic acids. J. Cryst. Growth 196: 365-376.

Savary, S., Ficke, A., Aubertot, J.-N. and Hollier, C. (2012) Crop losses due to diseases and their implications for global food production losses and food security. Food Security 4: 519-537.

Schloffel, M.A., Kasbauer, C. and Gust, A.A. (2019) Interplay of plant glycan hydrolases and LysM proteins in plant-Bacteria interactions. Int. J. Med. Microbiol. 309: 252-257.

Schlumbaum, A., Mauch, F., Vögeli, U. and Boller, T. (1986) Plant chitinases are potent inhibitors of fungal growth. Nature 324: 365-367.

Schmitz, A.M., Pawlowska, T.E. and Harrison, M.J. (2019) A short LysM protein with high molecular diversity from an arbuscular mycorrhizal fungus, *Rhizophagus irregularis*. Mycoscience 60: 63-70.

Schrodinger, LLC (2015) The PyMOL molecular graphics system, Version 1.8.

Schuhegger, R., Ihring, A., Gantner, S., Bahnweg, G., Knappe, C., Vogg, G., Hutzler, P., Schmid, M., Van Breusegem, F., Eberl, L., et al. (2006) Induction of systemic resistance in tomato by N-acyl-L-homoserine lactone-producing rhizosphere bacteria. Plant Cell Environ. 29: 909-918.

Seidl-Seiboth, V., Zach, S., Frischmann, A., Spadiut, O., Dietzsch, C., Herwig, C., Ruth, C., Rodler, A., Jungbauer, A. and Kubicek, C.P. (2013) Spore germination of *Trichoderma atroviride* is inhibited by its LysM protein TAL6. FEBS J. 280: 1226-1236.

Shibuya, N., Kaku, H., Kuchitsu, K. and Maliarik, M.J. (1993) Identification of a novel high-affinity binding site for N-acetylchitooligosaccharide elicitor in the membrane fraction from suspension-cultured rice cells. FEBS Lett. 329: 75-78.

Shibuya, N. and Minami, E. (2001) Oligosaccharide signalling for defence responses in plant. Physiol. Mol. Plant Pathol. 59: 223-233.

Shimizu, T., Nakano, T., Takamizawa, D., Desaki, Y., Ishii-Minami, N., Nishizawa, Y., Minami, E., Okada, K., Yamane, H., Kaku, H., et al. (2010) Two LysM receptor molecules, CEBiP and OsCERK1, cooperatively regulate chitin elicitor signaling in rice. Plant J. 64: 204-214.

Shinya, T., Motoyama, N., Ikeda, A., Wada, M., Kamiya, K., Hayafune, M., Kaku, H. and Shibuya, N. (2012) Functional characterization of CEBiP and CERK1 homologs in Arabidopsis and rice reveals the presence of different chitin receptor systems in plants. Plant Cell Physiol. 53: 1696-1706.

Shinya, T., Nakagawa, T., Kaku, H. and Shibuya, N. (2015) Chitin-mediated plant-fungal interactions: catching, hiding and handshaking. Curr. Opin. Plant Biol. 26: 64-71.

Shiu, S.H. and Bleecker, A.B. (2001) Plant receptor-like kinase gene family: diversity, function, and signaling. Sci. Signal 2001: re22.

Skarina, T., Xu, X., Evdokimova, E. and Savchenko, A. (2014) High-throughput crystallization screening. Methods Mol. Biol. 1140: 159-168.

Sorensen, W., Smith, E., Smith, J. and Carton, Y. (2008) Charles V. Riley, France, and Phylloxera. Am. Entomol. 54: 134-149.

Spaink, H.P. (2004) Specific recognition of bacteria by plant LysM domain receptor kinases. Trends Microbiol. 12: 201-204.

Spitzer, J. (2017) Emergence of life on earth: A physicochemical jigsaw puzzle. J. Mol. Evol. 84: 1-7.

Steen, A., Buist, G., Leenhouts, K.J., El Khattabi, M., Grijpstra, F., Zomer, A.L., Venema, G., Kuipers, O.P. and Kok, J. (2003) Cell wall attachment of a widely distributed peptidoglycan binding domain is hindered by cell wall constituents. J. Biol. Chem. 278: 23874-23881.

Stemmer, M., Thumberger, T., Del Sol Keyer, M., Wittbrodt, J. and Mateo, J.L. (2015) CCTop: An Intuitive, Flexible and Reliable CRISPR/Cas9 Target Prediction Tool. PLoS One 10: e0124633.

Stergiopoulos, I., van den Burg, H.A., Okmen, B., Beenen, H.G., van Liere, S., Kema, G.H. and de Wit, P.J. (2010) Tomato Cf resistance proteins mediate recognition of cognate homologous effectors from fungi pathogenic on dicots and monocots. Proc Natl Acad Sci USA 107: 7610-7615.

Strange, R.N. and Scott, P.R. (2005) Plant disease: a threat to global food security. Annu. Rev. Phytopathol. 43: 83-116.

Takahara, H., Hacquard, S., Kombrink, A., Hughes, H.B., Halder, V., Robin, G.P., Hiruma, K., Neumann, U., Shinya, T., Kombrink, E., et al. (2016) *Colletotrichum higginsianum* extracellular LysM proteins play dual roles in appressorial function and suppression of chitin-triggered plant immunity. New Phytol. 211: 1323-1337.

Takahara, H., Hacquard, S., Kombrink, A., Hughes, H.B., Halder, V., Robin, G.P., Hiruma, K., Neumann, U., Shinya, T., Kombrink, E., et al. (2016) *Colletotrichum higginsianum* extracellular LysM proteins play dual roles in appressorial function and suppression of chitin-triggered plant immunity. New Phytol. 211: 1323-1337.

Tanaka, S., Ichikawa, A., Yamada, K., Tsuji, G., Nishiuchi, T., Mori, M., Koga, H., Nishizawa, Y., O'Connell, R. and Kubo, Y. (2010) HvCEBiP, a gene homologous to rice chitin receptor CEBiP, contributes to basal resistance of barley to *Magnaporthe oryzae*. BMC Plant Biol. 10: 288.

Tang, D., Wang, G. and Zhou, J.M. (2017) Receptor kinases in plant-pathogen interactions: more than pattern recognition. Plant Cell 29: 618-637.

Tang, J., Sun, Y., Han, Z. and Shi, W. (2019) An illustration of optimal selected glycosidase for N-glycoproteins deglycosylation and crystallization. Int J Biol Macromol 122: 265-271.

Teng, P.S., Shane, W.W. and MacKenzie, D.R. (1984) Crop losses due to plant pathogens. Crit. Rev. Plant Sci. 2: 21-47.

Thomma, B.P., HP, V.A.N.E., Crous, P.W. and PJ, D.E.W. (2005) *Cladosporium fulvum* (syn. Passalora fulva), a highly specialized plant pathogen as a model for functional studies on plant pathogenic Mycosphaerellaceae. Mol. Plant Pathol. 6: 379-393.

Thomma, B.P., Nurnberger, T. and Joosten, M.H. (2011) Of PAMPs and effectors: the blurred PTI-ETI dichotomy. Plant Cell 23: 4-15.

Tomato Genome, C. (2012) The tomato genome sequence provides insights into fleshy fruit evolution. Nature 485: 635-641.

Torriani, S.F., Melichar, J.P., Mills, C., Pain, N., Sierotzki, H. and Courbot, M. (2015) *Zymoseptoria tritici*: A major threat to wheat production, integrated approaches to control. Fungal Genet. Biol. 79: 8-12.

Umemoto, N., Kakitani, M., Iwamatsu, A., Yoshikawa, M., Yamaoka, N. and Ishida, I. (1997) The structure and function of a soybean beta-glucan-elicitor-binding protein. Proc Natl Acad Sci USA 94: 1029-1034.

Van Esse, H.P., Bolton, M.D., Stergiopoulos, I., de Wit, P.J. and Thomma, B.P. (2007) The chitin-binding *Cladosporium fulvum* effector protein Avr4 is a virulence factor. MPMI 20: 1092-1101.

Van den Ackerveken, G.F., Van Kan, J.A., Joosten, M.H., Muisers, J.M., Verbakel, H.M. and De Wit, P.J. (1993) Characterization of two putative pathogenicity genes of the fungal tomato pathogen *Cladosporium fulvum*. Mol. Plant Microbe Interact. 6: 210-215.

van den Burg, H.A., Harrison, S.J., Joosten, M.H., Vervoort, J. and de Wit, P.J. (2006) *Cladosporium fulvum* Avr4 protects fungal cell walls against hydrolysis by plant chitinases accumulating during infection. Mol. Plant Microbe Interact. 19: 1420-1430.

van den Burg, H.A., Spronk, C.A., Boeren, S., Kennedy, M.A., Vissers, J.P., Vuister, G.W., de Wit, P.J. and Vervoort, J. (2004) Binding of the AVR4 elicitor of *Cladosporium fulvum* to chitotriose units is facilitated by positive allosteric protein-protein interactions. J. Biol. Chem. 279: 16786-16796.

Van der Hoorn, R.A., Laurent, F., Roth, R. and De Wit, P.J. (2000) Agroinfiltration is a versatile tool that facilitates comparative analyses of Avr9/Cf-9-induced and Avr4/Cf-4-induced necrosis. Mol. Plant Microbe Interact. 13: 439-446.

van Esse, H.P., Bolton, M.D., Stergiopoulos, I., de Wit, P.J. and Thomma, B.P. (2007) The chitin-binding *Cladosporium fulvum* effector protein Avr4 is a virulence factor. Mol. Plant Microbe Interact. 20: 1092-1101.

Van Holle, S. and Van Damme, E.J.M. (2018) Signaling through plant lectins: modulation of plant immunity and beyond. Biochem. Soc. Trans. 46: 217-233.

van Loon, L.C., Rep, M. and Pieterse, C.M. (2006) Significance of inducible defense-related proteins in infected plants. Annu. Rev. Phytopathol. 44: 135-162.

Velasquez, A.C., Chakravarthy, S. and Martin, G.B. (2009) Virus-induced gene silencing (VIGS) in Nicotiana benthamiana and tomato. J Vis Exp.

Visweswaran, G.R., Leenhouts, K., van Roosmalen, M., Kok, J. and Buist, G. (2014) Exploiting the peptidoglycan-binding motif, LysM, for medical and industrial applications. Appl. Microbiol. Biotechnol. 98: 4331-4345.

Volk, H., Marton, K., Flajsman, M., Radisek, S., Tian, H., Hein, I., Podlipnik, C., Thomma, B., Kosmelj, K., Javornik, B., et al. (2019) Chitin-binding protein of *Verticillium nonalfalfae* disguises fungus from plant chitinases and suppresses chitin-triggered host immunity. Mol. Plant Microbe Interact. 32: 1378-1390.

Vollmer, W., Blanot, D. and de Pedro, M.A. (2008) Peptidoglycan structure and architecture. FEMS Microbiol. Rev. 32: 149-167.

Von Bodman, S.B., Bauer, W.D. and Coplin, D.L. (2003) Quorum sensing in plant-pathogenic bacteria. Annu. Rev. Phytopathol. 41: 455-482.

Wan, J., Tanaka, K., Zhang, X.C., Son, G.H., Brechenmacher, L., Nguyen, T.H. and Stacey, G. (2012) LYK4, a lysin motif receptor-like kinase, is important for chitin signaling and plant innate immunity in Arabidopsis. Plant Physiol. 160: 396-406.

Wan, J., Zhang, X.C., Neece, D., Ramonell, K.M., Clough, S., Kim, S.Y., Stacey, M.G. and Stacey, G. (2008) A LysM receptor-like kinase plays a critical role in chitin signaling and fungal resistance in Arabidopsis. Plant Cell 20: 471-481.

Wang, W., Vinocur, B. and Altman, A. (2003) Plant responses to drought, salinity and extreme temperatures: towards genetic engineering for stress tolerance. Planta 218: 1-14.

Wang, W., Xie, Z.P. and Staehelin, C. (2014) Functional analysis of chimeric lysin motif domain receptors mediating Nod factor-induced defense signaling in *Arabidopsis thaliana* and chitin-induced nodulation signaling in *Lotus japonicus*. Plant J. 78: 56-69.

Wang, X. and Quinn, P.J. (2010) Lipopolysaccharide: Biosynthetic pathway and structure modification. Prog Lipid Res. 49: 97-107.

Waterhouse AM, Procter JB, Martin DMA, Clamp M, Barton GJ (2009) Jalview Version 2—a multiple sequence alignment editor and analysis workbench. Bioinformatics 25: 1189-1191

Wanke, A., Rovenich, H., Schwanke, F., Velte, S., Becker, S., Hehemann, J.H., Wawra, S. and Zuccaro, A. (2020) Plant species-specific recognition of long and short beta-1,3-linked glucans is mediated by different receptor systems. Plant J. Online ahead of print.

West, S.A., Fisher, R.M., Gardner, A. and Kiers, E.T. (2015) Major evolutionary transitions in individuality. Proc Natl Acad Sci USA 112: 10112-10119.

Willmann, R., Lajunen, H.M., Erbs, G., Newman, M.A., Kolb, D., Tsuda, K., Katagiri, F., Fliegmann, J., Bono, J.J., Cullimore, J.V., et al. (2011) Arabidopsis lysin-motif proteins LYM1 LYM3 CERK1 mediate bacterial peptidoglycan sensing and immunity to bacterial infection. Proc Natl Acad Sci USA 108: 19824-19829.

Wilson, R.A. and Talbot, N.J. (2009) Under pressure: investigating the biology of plant infection by *Magnaporthe oryzae*. Nat. Rev. Microbiol. 7: 185-195.

Wingender, J., Neu, T. and Flemming, H.C. (1999) Microbial extracellular polymeric substances. Springer, Heidelberg: 1–19.

Winn MD, Ballard CC, Cowtan KD, Dodson EJ, Emsley P, Evans PR, Keegan RM, Krissinel EB, Leslie AG, McCoy A (2011) Overview of the CCP4 suite and current developments. *Acta Crystallographica Section D* 67: 235-242

Wlodawer, A., Dauter, Z. and Jaskolski, M. (2017) Protein crystallography: methods and protocols. Humana Press 1607: 672.

Xu, C. and Ng, D.T. (2015) Glycosylation-directed quality control of protein folding. Nat. Rev. Mol. Cell Biol. 16: 742-752.

Yamaguchi, K., Yamada, K., Ishikawa, K., Yoshimura, S., Hayashi, N., Uchihashi, K., Ishihama, N., Kishi-Kaboshi, M., Takahashi, A., Tsuge, S., et al. (2013) A receptor-like cytoplasmic kinase targeted by a plant pathogen effector is directly phosphorylated by the chitin receptor and mediates rice immunity. Cell Host & Microbe 13: 347-357.

Yang, J. and Zhang, Y. (2015) I-TASSER server: new development for protein structure and function predictions. Nucleic Acids Res. 43: W174-181.

Yoshimi, A., Miyazawa, K. and Abe, K. (2016) Cell wall structure and biogenesis in Aspergillus species. Biosci Biotechnol Biochem. 80: 1700-1711.

Yoshimi, A., Miyazawa, K. and Abe, K. (2017) Function and biosynthesis of cell wall alpha-1,3-glucan in fungi. J Fungi 3: 63.

Yoshimura, A., Lien, E., Ingalls, R.R., Tuomanen, E., Dziarski, R. and Golenbock, D. (1999) Cutting edge: Recognition of Gram-Positive Bacterial cell wall components by the innate immune system occurs via Toll-like receptor 2. J. Immunol.163: 1-5.

Zeng, L., Velasquez, A.C., Munkvold, K.R., Zhang, J. and Martin, G.B. (2012) A tomato LysM receptor-like kinase promotes immunity and its kinase activity is inhibited by AvrPtoB. Plant J. 69: 92-103.

Zeng, T., Rodriguez-Moreno, L., Mansurkhodzaev, A., Wang, P., van den Berg, W., Gasciolli, V., Cottaz, S., Fort, S., Thomma, B., Bono, J.J., et al. (2020) A lysin motif effector subverts chitin-triggered immunity to facilitate arbuscular mycorrhizal symbiosis. New Phytol. 225: 448-460.

Zhang, H., Zhang, J., Wei, P., Zhang, B., Gou, F., Feng, Z., Mao, Y., Yang, L., Zhang, H., Xu, N., et al. (2014) The CRISPR/Cas9 system produces specific and homozygous targeted gene editing in rice in one generation. Plant Biotechnol. J. 12: 797-807.

Zhang, X., Dong, W., Sun, J., Feng, F., Deng, Y., He, Z., Oldroyd, G.E. and Wang, E. (2015) The receptor kinase CERK1 has dual functions in symbiosis and immunity signalling. Plant J. 81: 258-267.

Zhang, X.C., Wu, X.L., Seth Findley, Wan, J.R., Libault, M., Nguyen, H.T., Cannon, S.B. and Stacey, G. (2007) Molecular evolution of lysin motif-type receptor-like kinases in plants. Plant Physiol. 144: 623–636.

Zhong, Z., Marcel, T.C., Hartmann, F.E., Ma, X., Plissonneau, C., Zala, M., Ducasse, A., Confais, J., Compain, J., Lapalu, N., et al. (2017) A small secreted protein in *Zymoseptoria tritici* is responsible for avirulence on wheat cultivars carrying the Stb6 resistance gene. New Phytol. 214: 619-631.

Zipfel, C. (2008) Pattern-recognition receptors in plant innate immunity. Curr. Opin. Immunol. 20: 10-16.

Zipfel, C., Kunze, G., Chinchilla, D., Caniard, A., Jones, J.D., Boller, T. and Felix, G. (2006) Perception of the bacterial PAMP EF-Tu by the receptor EFR restricts Agrobacterium-mediated transformation. Cell 125: 749-760.

Zipfel, C. and Oldroyd, G.E. (2017) Plant signalling in symbiosis and immunity. Nature 543: 328-336.

Zuker, M. (2003) Mfold web server for nucleic acid folding and hybridization prediction. Nucleic Acids Res. 31: 3406-3415.

Zwiers, L.H. and De Waard, M.A. (2001) Efficient *Agrobacterium tumefaciens*-mediated gene disruption in the phytopathogen *Mycosphaerella graminicola*. Curr. Genet. 39: 388-393.

SUMMARY

Plants possess an innate immune system that recognizes various types of molecules that accurately betray microbial invasion, also known as invasion patterns (IPs), that include microbe-associated molecular patterns (MAMPs). This recognition occurs through invasion pattern receptors (IPRs) that activate a wide range of immune responses that aim to halt microbial infections. In turn, successful microbes secrete effector proteins to deregulate plant immunity. **Chapter 1** introduces the significant role of the major fungal cell wall component, chitin, in the interactions between plants and fungi. On the one hand, this chapter focuses on chitin perception systems that have been characterized in detail in several plant species, while on the other hand the chapter focuses on effector proteins containing lysin motifs (LysM effectors) employed by the tomato leaf mould pathogen *Cladosporium fulvum* and the wheat Septoria tritici blotch pathogen *Zymoseptoria tritici*.

To date, all chitin receptors identified in plants belong to either the LysM-containing receptor-like kinases (LysM-RLKs) or LysM-containing receptor-like proteins (LysM-RLPs). For instance, the Arabidopsis LysM-RLK AtLYK5 binds chitin with high affinity and forms a tripartite receptor complex with two further LysM-RLKs, AtLYK4 and AtCERK1, to initiate chitin signaling. Similarly, the rice chitin perception system is composed of the LysM-RLK OsCERK1 in association with the LysM-RLP OsCEBiP. In **Chapter 2**, by using chitin affinity-purification followed by mass spectrometry we identified two candidate chitin receptor proteins in tomato, the LysM-RLK SlLYK4 and the LysM-RLP SlCEBiP. Silencing of either *SlLYK4* or *SlCEBiP* resulted in significantly impaired chitin responsiveness. Using Clustered Regularly Interspaced Short Palindromic Repeats/Cas9 (CRISPR-Cas9) we generated mutants of both genes and evaluated their role in chitin signalling. While the function of *SlCEBiP* needs further assessment because it presently remains unclear whether the mutant that was generated truly disrupts gene function, *SlLYK4* was found to play an essential role in mediating chitin signal transduction as *SlLYK4* mutants displayed not only greatly compromised chitin-induced immunity but also enhanced susceptibility to *C. fulvum* infection. We propose that SlLYK4 is a crucial component of the chitin receptor complex of tomato.

To overcome the chitin-induced tomato immunity, *C. fulvum* secretes the LysM effector Ecp6 to outcompete immune receptors for chitin binding. Two of its three LysMs undergo intracellular LysM dimerization, thus forming a chitin-binding groove (LysM1-LysM3) with ultra-high substrate affinity that goes beyond the affinity of host receptors. The remaining singular LysM domain of Ecp6, LysM2, also displays the capability to bind chitin, albeit with a relatively low affinity that does not permit to outcompete chitin receptors. **Chapter 3** aims to investigate whether LysM2 contributes to the virulence function of Ecp6 and how it confers such contribution. Inoculation assays with *C. fulvum* transformants that express a suite of *Ecp6* mutants in the various LysMs revealed that LysM2 contributes to *C. fulvum* virulence, probably through suppression of chitin-responsive gene expression. Interestingly, a physical interaction of Ecp6 with Arabidopsis AtLYK5 and with tomato SlLYK4 that was characterized in chapter could been

demonstrated. Moreover, it appears that while LysM2 confers an interaction with these receptors in a chitin-independent manner, the composite LysM1-LysM3 binding groove contributes to the interaction in a chitin-dependent manner. Thus, besides competing with plant immune receptors for chitin binding, Ecp6 may perturb the assembly of functional chitin receptor complexes that are crucial for the activation of chitin-induced immunity.

Many fungal LysM effectors comprise two LysMs, such as MoSlp1 from the rice blast fungus *Magnaporthe oryzae*, Vd2LysM from the broad host range vascular wilt fungus *Verticillium dahliae*, and ChElp1 and ChElp2 from the Brassicaceae anthracnose fungus *Colletotrichum higginsianum*. They all bind chitin, suppress chitin-triggered host immunity and contribute to fungal virulence. **Chapter 4** describes the functional and structural analyses to investigate whether these fungal LysM effectors with two LysMs bind chitin through intramolecular LysM dimerization, like Ecp6, or rather through intermolecular dimerization. As our considerable efforts to obtain a crystal structure of any of these effectors by X-ray crystallography failed since crystal growth did not occur, we hypothesized that these findings could suggest the occurrence of intermolecular chitin binding for these LysM effectors. With DLS measurements and centrifugation assays we were able to confirm that the formation of chitin-induced polymeric complexes for MoSlp1, V2LysM and ChElp2 occurs, potentially mediating the elimination of chitin oligomers at infection sites by precipitation to suppress the activation of chitin-induced plant immunity.

The wheat-specific pathogen *Z. tritici* encodes three LysM effector proteins, Mg1LysM and Mgx1LysM that contain a single LysM, and Mg3LysM that possesses three LysMs. Previously, Mgx1LysM was disregarded as a presumed pseudogene, while Mg1LysM and Mg3LysM were functionally characterized. **Chapter 5** provides evidence to show that *Mgx1LysM* is not a pseudogene and is functional during wheat colonization. We show that Mgx1LysM binds chitin, protects fungal hyphae against chitinase hydrolysis and is able to suppress a chitin-induced ROS burst. Fungal inoculation assays reveal that while Mg3LysM confers a major contribution to *Z. tritici* virulence, also Mg1LysM and Mgx1LysM contribute to virulence, albeit with smaller contributions, and that all LysM effectors display partial functional redundancy. Thus, we show that *Zymoseptoria tritici* utilizes three LysM effectors to disarm chitin-triggered wheat immunity.

In **Chapter 6**, we determined a crystal structure of *Z. tritici* Mg1LysM to try and explain how this LysM effector protects fungal hyphae against chitinase hydrolysis. Intriguingly, the crystal structure revealed the formation of chitin-independent homodimers as well as chitin-induced dimerization of two Mg1LysM protomers. Based on DLS measurements and centrifugation assays in the presence and absence of chitin oligomers, it could be concluded that Mg1LysM forms a chitin-induced supramolecular structure that, anchored to chitin in the cell wall, may prevent hydrolysis by host chitinases. Interestingly, it could be demonstrated that Mgx1LysM, as well as RiSLM from the arbuscular mycorrhizal (AM) fungus *Rhizophagus irregularis* that similarly contains a single LysM, polymerize in the presence of chitin as well, suggesting that they also undergo chitin-induced dimerization of ligand independent homodimers.

Besides chitin, several other cell wall polysaccharides have previously been characterized as invasion pattern, such as β-glucan and bacterial peptidoglycan. **Chapter 7** synthesizes the findings in this thesis and places them into a broader perspective to highlight the importance of chitin as well as other cell wall components in interactions between plants and microbes.

ACKNOWLEDGEMENTS

After a half-year of dreaming to complete my PhD thesis, here I come to the end. Finally, I get to write the acknowledgements section to express my great appreciation to the people who either contributed to the work presented in this book or created a warm atmosphere during my PhD research period. Besides occasional stressful moments, I had a lot of fun over the past five years. I could not have completed my PhD so smoothly without all the help from my lovely supervisors, friends, colleagues and family.

First of all, many thanks to my promotor, **Bart** Thomma. Without your help for my CSC fellowship application, I would not have had the opportunity to even come to the Netherlands as a PhD student. You are a very passionate, enthusiastic and dedicated researcher. I greatly appreciate your honesty and professional advice throughout my entire PhD. I really enjoyed the travels together with you to Lübeck, Rome etc., because all these trips revealed your other sides besides the "serious supervisor" side, which greatly eased my communication with you from my own perspective. I liked all your tips on how to work wisely and efficiently, and enjoy life after work time. Many thanks to my co-promotor, **Jeroen** Mesters. As a biochemist, you enjoy your work so much that you even drew the structure of your favourite amino acid on your mug. I enjoyed all the work- and life-related talks with you and was amazed how wide the range of your knowledge is. Despite the fact that I often needed to chase after you to ask questions (as everybody and even every machine in the group need your help), I learned a lot about protein crystallization during my visits in Lübeck, thank you.

I would like to continue with thanking the people who contributed to or helped with my PhD work. **Hanna**, I was always impressed by the amount of work you were doing and how much you know. Every time after your presentation, I felt the need to go back to my computer, work harder and smarter. You gave me a lot of inspiration when you were in the group (although I believe that you had no idea). **Katharina**, thanks for generating the tomato chitin receptor mutant lines. You will soon have your PhD defence as well and I wish you a lot of success. **Gabriel,** thank you for not only optimizing ChElp2 expression conditions in *E. coli*, but also for all the help you offered whenever I asked. I enjoyed our dinners and talks a lot. **Grardy**, you are a very nice person (although you may come across a little intimidating at first sight ^_^), thanks for all the help with ordering and experiments throughout my PhD. **Xin** (张鑫), thanks for working on the bioinformatics project with me, although the data are not included in this thesis. I wish you all the best and success with your PhD in Utrecht. **Michael**, whenever I had questions, you helped me with great patience. Thanks for all the helpful suggestions and the mental support, especially at the time when Bart was leaving the chair group. **Kiki**, thanks for your kind help with the confocal microscopy during the corona restrictions in Radix. You made the imaging much easier for me. **Luis**, as my supervisor during my first PhD year, thanks for the introduction into the lab. Also thanks to the students I supervised, **Peter** and **Saha**, for the contributions to the work presented in this thesis. I really enjoyed the time when you were around. The interactions with you have significantly improved my teaching skill.

Futher thanks go to my friends who were, or still are, living in the Netherlands. You gave me so many good memories over the past five years. **Shuqing** (叔青), I really enjoyed the time when you were around in the Laboratory of Phytopathology. You are a very honest and funny person, and I miss the times when we worked together, cooked nice food together and visited nice Dutch or European cities together. Happy times always fly by, now you are working in China, got married and have a super cute son. I wish you a lot of success and happiness. **Yingxue** (映雪), when you first contacted me before you came to the Netherlands, I never thought that you would become one of my best friends. It is a pity that your visiting period was only one year, but I greatly enjoyed the time we spent together, even when we were just laying on couch and talking about random things. I wish you a smooth and happy life in Tianjin (China) with your husband and daughter (咘咘). **Xiaoqian** (小倩), thanks for all the nice dinners and game nights that you organized. I (but maybe also half of the Phytopathology people) will always remember that the bowling night you organized in my first year revealed that my alcohol limit is a single bottle of beer at the bowling night you organized in my first year. **Malaika**, you have a great interest in science and are very enthusiastic about the colour pink. Your collection in the lab even includes a pink pipette and a pink fungus on a plate. Thanks for producing and always sharing your super-efficient ULP1 protease, which was much better than the one I ordered commercially. **Sander**, thank you for being a nice friend, you were one of the only few people I immediately felt comfortable with when I just arrived. **Yin** (宋银), thank you for always trying to help, no matter whether it is with work- or life-related issues. You were really like the older brother to all the Chinese PhDs in the group, cooking nice food once a while to satisfy our stomach and planning holiday trips to relax our mind. **Jinling** (金岭) and **Jinbin** (锦斌), thanks for the nice gatherings you organized, and the share of useful information on PhD and life issues. To the current Chinese PhDs in the Laboratory of Phytopathology, **Wen** (黄雯), **Si** (秦思), **Yaohua** (耀华) and **Weizhen** (为镇), thank you all for the nice time we spent together. I wish you all the best for your PhDs.

Thanks also to the remaining PhDs of our shrunken Verticillium group; **Jasper**, you will also have your PhD defense soon and I wish you lots of success; **Edgar** and **Nelia**, thanks for contributing to the warm and stimulating environment; I wish you all the best for the remaining PhD years.

I really want to thank **Bert**: you always took great care of the plants I ordered at Unifarm, making my experimental planning so much easier. Thanks to **Laurens** who always seems to have solutions for my problems in the lab; thank you for being a real life saver. Many thanks to **Ali**, for always solving a wide range of issues I encountered during my PhD; I was always amazed about the amount of details you remember about everyone and everything in the group. **Ester**, thanks for your help with all the ordering before you left Phytopathology and all the warm, distinguishable laughs.

Although I only spent 7-8 months in Lübeck, I met many people who helped me with great kindness and patience. **Linlin** (琳琳), I greatly appreciate all your help with my protein crystallization experiments and my German life. You showed me the correct way to use many lab

devices and even provided me with all the basic Chinses spices for simple cooking so that I would not starve. I wish you a very successful career in Germany. **Hong** (王红), thank you for always sharing stories and nice food with me. It is a pity that our Dutch travel plan became impossible because of the corona virus. I hope we can still have the chance to resume this plan in the near future. Thank you, **Antje,** for showing me how to use the old AKTA system correctly without destroying it, and for lending me a student card so that I could enjoy cheap Mensa food. Many thanks also go to a team of technician ladies, **Doris**, **Silke**, **Angela** and **Susan,** for showing me around in the lab and getting me familiar with the lab regulations.

Special thanks go to my paranymphs Martin and Nick. **Martin**, thanks for all the scientific discussions that always provided me with new ideas and for sharing your jokes that often made me go "huh?.....". You have so much work-related and -unrelated knowledge and are quite good at learning languages. I wish you can complete your PhD thesis soon and have a smooth after-PhD-life. **Nick**, I was always amazed about your passion and dedication to science. You surely did, and will be doing, a very good job. Trust yourself more, in the same fashion as everyone else trusts you. Lucky me that I still can keep learning from you in near future. I enjoyed the time when the three of us were "locked up" in the writing office (escape room), trying to escape from the last stretch of our PhD: thesis writing. We will surely all make it.

To **CSC**, without this fellowship I would not have had the great opportunity to study in the Netherlands. All these years studying abroad made me thinking about the differences between different cultures, making me gradually better at unbiasedly looking at things and learning me the proper way to love my mother country.

Many thanks to my parents, 想对我的父母郑重的说一声谢谢，谢谢你们对我的养育和一直以来对我求学的支持。从小时候起你们就告诉我，只要我愿意读书，无论是生活还是经济上的困难你们都会克服，会确保我能做我自己想做的事。我在荷兰读博士的这几年你们开心的同时也担心着我的生活和安全，我想说我长大了，我会在保护好自己的同时好好生活。也谢谢我的弟弟田乐，你一直都很支持我做的任何决定，也正是有了这些支持，我才能相对安心地去做我想做的事情。

Thanks to Jos, Annelies, Ruud and Frank, thank you all for the Dutch to English one-second-switch whenever I popped in the frame, and inviting me to nearly all the family activities. I truly enjoyed all the talks and visiting different cities with you.

Thanks to Bart, I know you would be more than happy if I omitted your name from this section. However, I decided to thank you here anyway and leave the awkward feeling to yourself. Thank you for all the it-is-not-the-end-of-life pep talks that you gave throughout my PhD years, especially during my Lübeck visits when I was having a lot of frustrations and doubts about my crystallization project, and over the past six months when I was writing this thesis. I believe by now you regret that you did not record any of your pep talks, otherwise you can just hit the "play" button next time. My honest advice to you is, "DO IT" when the next chance comes, I assure you that you will need it during my postdoc time. I really appreciate all your respect and support....

ABOUT THE AUTHOR

Hui Tian (田卉) was born in a small village near Changzhi (长治) city in Shanxi (山西) province of China on 10th December, 1988. As a child growing up in a family that mainly does farm work, she aimed for a career outside of agriculture. However, life often teaches the lesson that "Changes always overrun plans". Thus, after the College Entrance Examination (高考) in 2007, she was admitted to Shenyang Agricultural University in the north of China as a bachelor student in the School of Life Science, where she did a breeding study on silkworm (a special economic animal).

Since then, she has stuck with agricultural studies for higher education. In 2011, she continued her master in Nanjing Agricultural University in the south of China, majoring in the School of Biochemistry and Molecular Biology. While she was working on the two-year master project of "Functional characterization of a small GTPase Rac1 during the interaction between *Verticillium dahliae* and the host plant cotton", she developed an interest in plant-fungus interactions. Therefore, after her master graduation, she wrote a PhD proposal in 2014 together with prof. dr. ir. Bart Thomma and was granted with a fellowship by the Chinese Scholarship council (CSC) .

In 2015, she left China for the first time in her life and came to the Netherlands, joining the Laboratory of Phytopathology, Wageningen University as a PhD student. Under the joint supervision of Bart Thomma and Jeroen Mesters (Institut für Biochemie, Universität zu Lübeck, Germany), she characterizes the functions and structures of LysM proteins during interaction between the leaf mould fungal pathogen *Cladosporium fulvum*, the wheat-specific pathogen *Zymoseptoria tritici* and their host plants. She will soon start a new scientific journey as postdoc in the group of Evolutionary Microbiology, at the University of Cologne.

LIST OF PUBLICATIONS

Tian H[#], Rövenich H[#], Bracuto V[$], Hanika K[$], Petutschnig EK, Valerius O, Ebert MK, van den Berg GCM, Bai YL, Thomma BPHJ. (2020) LysM2 of the *Cladosporium fulvum* effector Ecp6 contributes to virulence through perturbation of plant chitin receptor complex assembly. In preparation.

Sánchez-Vallet A[†], **Tian H**[†], Rodriguez-Moreno L[†], Valkenburg D-J, Saleem-Batcha R, Wawra S, Kombrink A, Verhage L, de Jonge R, van Esse HP, Zuccaro A, Daniel C, Mesters JR[‡], Thomma, BPHJ[‡] (2020) A secreted LysM effector protects fungal hyphae through chitin-dependent homodimer polymerization. PLoS Pathog. 16: 1–21

Tian H, Fiorin GL, Kombrink A, Mesters JR, Thomma BPHJ (2020a) Fungal LysM effectors that comprise two LysM domains bind chitin through intermolecular dimerization. bioRxiv 2020.06.11.146639

Tian H, McKenzie C[*], Rodriguez-Moreno L[*], Berg G van den, Chen H, Rudd J, Mesters J, Thomma BPHJ (2020b) Three LysM effectors of *Zymoseptoria tritici* collectively disarm chitin-triggered plant immunity. Mol. Plant Pathol. in revision

Volk H, Marton K, Flajšman M, Radišek S, **Tian H**, Hein I, Podlipnik Č, Thomma BPHJ, Košmelj K, Javornik B, et al (2019) Chitin-binding protein of *Verticillium nonalfalfae* disguises fungus from plant chitinases and suppresses chitin-triggered host immunity. Mol Plant-Microbe Interact. 32: 1378–1390

[#, $, †, ‡, *] equal contribution

EDUCATION STATEMENT OF THE GRADUATE SCHOOL EXPERIMENTAL PLANT SCIENCES

Issued to: **Hui Tian**
Date: **14 September 2020**
Group: **Laboratory of Phytopathology**
University: **Wageningen University & Research**

1) Start-Up Phase	*date*	*cp*
▶ **First presentation of your project**		
Expression and purification of LysM proteins from plant pathogenic fungi	29 Mar 2016	1,5
▶ **Writing or rewriting a project proposal**		
Structural biology of LysM proteins from fungal pathogens	30 Oct 2015	6,0
▶ **Writing a review or book chapter**		
▶ **MSc courses**		
Subtotal Start-Up Phase		7,5

2) Scientific Exposure	*date*	*cp*
▶ **EPS PhD student days**		
EPS PhD student retreat "Get2gether", Soest, The Netherlands	28-29 Jan 2016	0,6
EPS PhD student retreat "Get2gether", Soest, The Netherlands	11-12 Feb 2019	0,6
▶ **EPS theme symposia**		
EPS theme 2 symposium & Willie Commelin Scholten Day: Interactions between Plants and Biotic Agents, Leiden, The Netherlands	22 Jan 2016	0,3
EPS theme 4 symposium: Genome biology, Wageningen, The Netherlands	16 Dec 2016	0,3
▶ **Lunteren Days and other national platforms**		
Annual meeting "Experimental Plant Science" in Lunteren, The Netherlands	11-12 Apr 2016	0,6
Molecular Genetics meeting, Wageningen, The Netherlands	21 Oct 2016	0,3
Host-Microbe Genetics meeting, Wageningen, The Netherlands	27 Oct 2017	0,3
Annual meeting "Experimental Plant Science" in Lunteren, The Netherlands	10-11 Apr 2017	0,6
Annual meeting "Experimental Plant Science" in Lunteren, The Netherlands	09-10 Apr 2018	0,6
Host-microbe Genetics meeting, Groningen, The Netherlands	26 Oct 2018	0,3
▶ **Seminars (series), workshops and symposia**		
Seminar: Dr. Oliver Hamant, How do plants read their own shape	16 Mar 2016	0,1
Seminar: Dr. Gerben van Ooijen, Clocks across taxa: Conserved cellular timekeeping mechanisms in plants, algae and other eukaryotes	29 May 2017	0,1
Seminar: Dr. Martin Cann, The immune receptor Rx1 remodels chromatin and chromatin interactors in immunity	11 Jul 2017	0,1
Seminar: Dr. Sanjay Kapoor, Regulators of reproductive development in rice	29 Aug 2017	0,1

	Seminar: Dr. Ronald Snijder, Modern domestication of pelargonium in a commercial environment	09 May 2018	0,1
	Seminar: Dr. Bob Schmitz, Epigenomic studies of nature and induced Epipalleles in plants	06 Jun 2018	0,1
	Seminar: Dr. Yan Wang, A leucine-rich repeat receptor-like protein as PAMP receptor recognising XEG1, a Phytophthora glycoside hydrolase 12	10 Sep 2018	0,1
	Seminar: Dr Antonio Di Pietro, Host adaptation in the fungal cross-kingdom pathogen *Fusarium oxysporum*	17 Oct 2018	0,1
	Seminar: Dr. Theo van der Lee, From genomes to function: bioinformatics to disclose the obligate biotrophic soilborne fungus *Synchytrium endobioticum*	18 Jan 2019	0,1
	Seminar: Prof. Wolf Frommer, Logistics: Allocation of carbon and energy for yield and pathogen resistance	17 Jan 2019	0,1
	Seminar: Rays Jiang, Using cutting-edge genomics tools to study host-microbe interactions	05 Jul 2019	0,1
	Seminar: Prof. Elwira Smakowska, An extracellular network of Arabidopsis leucine-rich repeat receptor kinases	09 Dec 2019	0,1
	Seminar: Prof. Dr. Eva Stukenbrock, Causes and consequences of chromosome instability in a fungal plant pathogen	13 Dec 2019	0,1
	Symposium: Prof. Rolf Hilgenfeld 65th birthday & structural symposium, Lübeck, Germany	06 Apr 2019	0,3
▶	**Seminar plus**		
▶	**International symposia and congresses**		
	Specificity in Plant Immunity and Symbiosis (SIPIS), Göttingen, Germay	06 Dec 2016	0,3
	Specificity in Plant Immunity and Symbiosis (SIPIS), Rome, Italy	27 Sep 2018	0,3
	10th European Plant Science Retreat, Utrecht, The Netherlands	03-06 Jul 2018	1,0
	IS-MPMI XVIII congress, Glasgow, UK	14-18 Jul 2019	1,5
	15th European Conference on Fungal Genetics (ECFG), Rome, Italy	17-20 Feb 2020	1,2
▶	**Presentations**		
	Poster: Dual functionality of a fungal LysM effector: substrate sequestration and receptor complex perturbation?, IS-MPMI XVIII congress, Glasgow, UK	15 Jul 2019	1,0
	Oral presentation: Structural identification of four fungal LysM effectors, SIPIS meeting, Göttingen, Germany	06 Dec 2016	1,0
	Oral presentation: Do all LysMs of Ecp6 contribute to the virulence of *Cladosporium fulvum* on tomato?, 10th European Plant Science Retreat, Utrecht, The Netherlands	04 Jul 2018	1,0
	Oral presentation: Functional dissection and structural determination of fungal LysM effectors, SIPIS meeting 2018, Rome, Italy	27 Sep 2018	1,0
	Oral presentation: How LysM-containing proteins determine plant-pathogen interactions: Functional dissection of the *Cladosporium fulvum* LysM effector Ecp6, Host-microbe interaction meeting, Groningen, The Netherlands	26 Oct 2018	1,0
▶	**IAB interview**		
▶	**Excursions**		
	KeyGene visit	12 Sep 2017	0,2
		Subtotal Scientific Exposure	15,6

3) In-Depth Studies	*date*	*cp*
▶ **Advanced scientific courses & workshops**		
Data analyses and visualization in R (for biologist), Wageningen, The Netherlands	12-13 Dec 2016	0,6
Crystallography, Lübeck, Germany	Nov 2017-Mar 2018	1,0
▶ **Journal club**		
▶ **Individual research training**		
Short term scientific mission at Biochemistry Institute in Lübeck University, Germany	01 Apr-01 Jul 2019	3,0
	Subtotal In-Depth Studies	4,6

4) Personal Development	*date*	*cp*
▶ **General skill training courses**		
EPS introduction course, Wageningen, The Netherlands	11 Feb 2016	0,3
PhD Peer Consultation - a powerful tool to tackle PhD challenges, Wageningen, The Netherlands	Apr - Jun 2016	0,6
Interpersonal communication for PhD candidates, Wageningen, The Netherlands	24-25 Nov 2016	0,6
Posters and Pitching, Wageningen, The Netherlands	8 Oct - 5 Nov 2018	1,0
Career Assessment, Wageningen, The Netherlands	27 Aug 2019	0,3
Scientific Writing, Wageningen, The Netherlands	13 Nov - 18 Dec 2019	1,8
▶ **Organisation of meetings, PhD courses or outreach activities**		
▶ **Membership of EPS PhD Council**		
	Subtotal Personal Development	4,6

TOTAL NUMBER OF CREDIT POINTS*	**32,3**

Herewith the Graduate School declares that the PhD candidate has complied with the educational requirements set by the Educational Committee of EPS with a minimum total of 30 ECTS credits.

** A credit represents a normative study load of 28 hours of study.*

Hui Tian was financially supported by a PhD fellowship from the China Scholarship Council (CSC). The work was carried out in the Laboratory of Phytopathology of Wageningen University & Research in the Netherlands, and in the Institute of Biochemistry of the University of Lübeck in Germany.

Cover design: Jiali Wang (王佳丽)
Layout design: Iliana Boshoven-Gkini | AgileColor.com
Printed: GVO drukkers & vormgever B.V. Ede (NL) | gvo.nl